Salem Nuclear Generating Station Units 1 and 2
Docket Nos. 50-272 and 50-311
Generic Letter 2004-02
Updated Supplemental Response for Salem

Executive Summary

The resolution to Generic Letter (GL) 2004-02 necessitated the replacement of the existing containment sump strainers, which had a surface area of approximately 85 ft^2 and a mesh size of 1/8-inch. The replacement sump strainers for Salem Unit 1 and 2, provided by Control Components Incorporated (CCI), have filtering surface areas of 4,854 ft^2 and 4,656 ft^2 respectively. The strainers for both Salem Units have 1/12-inch (nominal) perforations. In addition, a 9-inch tall debris interceptor with a 4-inch horizontal lip extending in the upstream direction has been installed around the front and sides of the strainer module train to hinder debris transport to the strainer. The debris interceptors consist of grating with perforated plate (mesh size = 1/8 inch) attached to the downstream side of the grating.

The replacement strainers are designed such that the maximum head loss experienced with the worst-case debris and chemical precipitate load combination is less than the limiting hydraulic allowable head loss and less than the structural limit of the strainer. The strainer head loss margin is the limiting margin between the NPSH margin and the strainer structural margin. The minimum head loss margin accounts for an increase in the NPSH required due to a void fraction at the pump inlet. The maximum void fraction at the pump inlet was less than 0.6% by volume for all scenarios. The minimum strainer head loss margin for single pump operation is approximately 1.6 feet for Unit 1 and approximately 1.1 feet for Unit 2, and occurs during cold leg recirculation for Unit 1 and hot leg recirculation for Unit 2. The maximum flow rates for single train operation are 5,110 gpm for Salem Unit 1 and 4,980 gpm for Salem Unit 2. The minimum strainer head loss margin for two-pump operation is approximately 6.5 feet for Unit 1 and approximately 1.2 feet for Unit 2, and occurs during containment spray recirculation for both units. The maximum two-train operation flow rate is 8,826 gpm for both Units, although 8,850 gpm is conservatively used in the design.

The limiting head loss for both one and two pump operation occurs at high sump temperatures prior to chemical precipitation and assumes that the containment pressure is considered equal to the vapor pressure of the water in the sump.

Salem submitted a License Amendment Request (LAR) that was approved by the NRC on November 15, 2007, in order to credit the partial pressure of air initially in containment, which is used in the determination of the NPSH margin at lower sump temperatures. The strainers are also designed such that the head loss is less than the structural limit for all conditions.

Chemical effects bench top testing was performed by Enercon for Salem. This testing determined that minimal or no chemical precipitates would form in the post-LOCA containment sump at temperatures greater than 110°F. Similarly, the Argonne aluminum solubility functions predict that precipitates will not form at sump temperatures greater than 122°F. However, the temperature at which chemical precipitates form has been conservatively increased to 160 °F in the head loss and NPSH calculations.

The replacement strainers have a minimum analytically determined submergence of 3-5/16 inches during recirculation based on the minimum flood level and the height of the installed strainers. This is a conservative value based on a level instrument uncertainty of 1 inch, which is 0.25 inches greater than the actual uncertainty (see below). This value was conservatively reduced to 3 inches for strainer design and testing while the minimum as-built submergence was conservatively used to assess the potential for vortexing. Testing and analysis have shown that vortexing will not occur under maximum flow conditions for both a clean and debris-laden strainer.

PSEG has installed two new level switches in each Salem Unit, although the existing level indicators are also still in use. The new level switches have an accuracy of ±0.75 inches and are more accurate than the existing level indicators; thus providing a more accurate indication of the containment flood level. These level switches alert the control room operator when sufficient containment sump level has been achieved to support initiation of cold leg recirculation.

The minimum flood level calculation considered the hold up of water due to blockage of the refueling cavity drain and loss of water into the reactor cavity. The calculation shows that concurrent flooding of these areas is not a credible condition and that the reactor cavity holds up more water than the refueling cavity. Therefore, the calculation conservatively considered flooding of the reactor cavity, along with the following items:

- Hold-up of water in upper areas of containment
- Hold-up of water in the reactor cavity
- Minimum water volume transferred from RWST
- Hold-up of water in the containment atmosphere (spray droplets and vapor)
- Water condensed on containment heat sinks
- Water to fill initially empty piping (e.g. Containment Spray System (CSS) piping)

PSEG modified three of four wire mesh doors and folding gates in the stairwell near the accumulators for both Salem Units. The modifications replaced wire mesh with bars spaced at least 9 inches apart in the bottom 3 feet of the doors/gates. The wire mesh was removed to prevent water hold-up in the inner annulus. The bars were added to the bottom of the doors/gates to meet radiation protection personnel safety requirements. However, the door/gate nearest to the strainer module was not modified in either Salem Unit because blockage of these doorways would result in a more tortuous path for debris, thus potentially reducing the overall debris transport.

CCI performed debris bypass tests for the Salem replacement strainers. Design basis debris bypass tests were performed in 2005, 2006, and 2008. The particulate debris bypass tests were performed in 2005 and used the large scale test loop. Fiber bypass testing performed in 2006 used a one-sided test strainer module in the multi-functional test loop (MFTL), while the 2008 fiber bypass tests used a more prototypical two-sided test strainer module in the MFTL with a prototypical strainer submergence and flow based on the Salem strainer installation.

CCI performed head loss tests for the Salem replacement strainers both with and without chemical precipitates. Design basis thin bed effect head loss tests and head loss tests with chemical effects were performed in 2008. The design basis head loss tests used a prototypical two-sided test strainer module in the MFTL with a prototypical strainer submergence and flow based on the Salem strainer installation.

Non-design basis chemical effects head loss tests were performed using precipitates generated in the test loop while the design basis chemical effects head loss tests were performed using precipitates generated using the Westinghouse particulate generator method described in WCAP-16530-NP in which precipitates are generated outside the test loop. The maximum head loss in the design basis chemical effects head loss tests occurred after the initial addition of chemical precipitates but prior to the formation of bore holes. Despite the addition of the majority of chemical precipitate after the initial addition, the head loss never increased beyond the maximum head loss prior to bore hole formation. The tests used in-flume agitation (as necessary) to ensure that the majority of debris transported to the strainer module (i.e. near field effects were not credited).

As part of the resolution to Generic Letter 2004-02, PSEG removed all calcium silicate insulation in Salem Unit 1 and 2 from containment areas which could be impacted by a LOCA jet. Also, Min K insulation was replaced wherever possible. Transco Reflective metallic insulation was used at most of the locations. However, in some cases NUKON was used to replace both calcium silicate and Min K due to accessibility concerns. In all cases, the added reflective metallic insulation, NUKON and the remaining Min-K insulation were accounted for in the Debris Generation Calculation.

PSEG implemented a number of programmatic controls to assess and control the introduction of potential debris sources to containment. The programmatic controls include requirements related to coatings, containment housekeeping, materiel condition, and modifications.

The design debris load is determined based on the deterministic methodology for debris generation and transport outlined in Nuclear Energy Institute NEI 04-07 and its associated NRC Safety Evaluation (SE). The baseline guidance is used with some analytical refinements (e.g., Computational Fluid Dynamics (CFD)). The methodology based on plant specific testing is listed below.

- A reduced zone of influence (ZOI) for qualified epoxy coatings is used in the debris generation calculation based on the testing performed by Westinghouse documented in WCAP-16568-P. The ZOI used for qualified epoxy coatings is 4D, which was justified by the testing. This reduced ZOI was accepted by the NRC in an April 6, 2010, letter to the NEI.

- PSEG performed plant specific fiber erosion testing at Fauske and Associates Incorporated (FAI) for the primary types of fiber insulation in containment, NUKON and Kaowool. This testing used a nominal flume velocity of 0.7 ft/s, which is approximately equal to the maximum velocity in the post-LOCA sump pool and greater than the flow velocity in 98% of the post LOCA sump pool. The testing indicated that conservative 30-day erosion fractions for NUKON and Kaowool would be 20% and 15%, respectively. The design debris load is based on these 30-day erosion fractions.

The debris generation calculation determined separate debris loads for Salem Unit 1 and 2. The Salem Unit 2 debris load has been determined based on the containment configuration following the Spring 2008 outage, when the steam generators were replaced and insulated with Transco RMI. The NRC approved an extension request for this approach on August 11, 2006.

The break locations analyzed are on the primary piping and are chosen to maximize the quantity and types of debris transported to the strainer. The design fiber, RMI, and particulate debris load is typically less than the debris load used for subsequent analyses and testing. Justification is provided for subsequent analyses and testing utilizing non-bounding debris loads.

In addition, while a Salem Unit 2 plant walkdown indicated a latent debris load of only 33 lbm, a latent debris load of 200 lbm is included in the design debris load for both Salem Units. The debris transport calculation determined that the area of foreign materials such as labels, tapes, placards, etc., is 573 ft^2 for Unit 1 and 525 ft^2 for Unit 2; however, for conservatism, the strainer design is based on a foreign material area of 667 ft^2 which corresponds to a sacrificial area of 500 ft^2 when crediting overlap.

The debris transport calculation utilized CFD analysis performed using FLUENT to determine which debris would transport to the installed strainers. This analysis contained the following conservatisms:

- Plant specific erosion rates are determined based on a flow velocity of 0.7 ft/s. This velocity is greater than the flow velocity in 98% of the post LOCA sump pool.
- Design debris load is not time dependent; it is based on a 30-day eroded fiber fraction
- No debris retention in upper containment credited (for debris generated in lower containment)
- Debris retention of small debris on grating is not credited
- Transport is based on containment incipient tumbling velocities not bulk transport velocities
- All debris in the active portion of the sump pool is transported to the debris interceptor or the strainer, even though there are some areas of the sump pool where debris would stall.

The Salem Unit 1 and 2 quantities of dissolved chemicals in the post-LOCA sump as well as the quantity of precipitates, which form due to the dissolved chemicals, were determined based on a mission time of 30 days and the methodology provided in WCAP-16530-NP. The methodology utilized in this calculation did not deviate from that approved by the NRC in the SE for WCAP-16530-NP. In addition, none of the refinements outlined in WCAP-16785-NP were used.

The chemical effects analysis maximized the amount of material dissolution in the sump pool. The containment spray duration was modeled as 30 days, which leads to conservative dissolution quantities for non-submerged material. The insulation, submerged aluminum metal and paint, and exposed concrete quantities used in the chemical effects analysis are all bounding.

The ECCS components and systems that are required to operate and pass debris-laden fluid during the recirculation phase of recovery from a postulated LOCA have been identified and have been evaluated for blockage and wear from debris that could pass through the installed strainers.

The ECCS equipment at Salem will remain capable of passing sufficient flow to the reactor to adequately cool the core following a postulated LOCA. The downstream component wear evaluation was performed using the guidance provided in WCAP-16406-P, Revision 1, and its associated NRC SE. The downstream wear evaluation is the same for Salem Unit 1 and 2 and uses inputs which envelope both units.

The in-vessel downstream effects analysis for Salem is consistent with the methodology from Revision 2 of WCAP-16793-NP, "Evaluation of Long-Term Cooling Considering Particulate, Fibrous, and Chemical Debris in the Recirculating Fluid." Salem meets the acceptance criteria set forth in WCAP-16793-NP utilizing the existing debris load and strainer testing.

PSEG is in compliance with the requirements of Generic Letter 2004-02 except for the following:

- As discussed in RAI 21 in the NRC letter to PSEG on December 17, 2008, the NRC staff has not yet issued a final safety evaluation (SE) on the Pressurized-Water Reactor Owners Group (PWROG) topical report WCAP-16793-NP. Salem will provide a response within 90 days of the issuance of the final NRC SE on WCAP-16793-NP.

With the completion of the above task both Salem Units will be in complete compliance with the regulatory requirements listed in GL 2004-02.

Salem Nuclear Generating Station Units 1 and 2
Docket Nos. 50-272 and 50-311
Generic Letter 2004-02
Updated Supplemental Response for Salem

Specific Guidance for Review Areas

1. **Overall Compliance:**
Provide information requested in GL 2004-02 Requested Information Item 2(a) regarding compliance with regulations.

GL 2004-02 Requested Information Item 2(a)
Confirmation that the ECCS and CSS recirculation functions under debris loading conditions are or will be in compliance with the regulatory requirements listed in the Applicable Regulatory Requirements section of this GL. This submittal should address the configuration of the plant that will exist once all modifications required for regulatory compliance have been made and this licensing basis has been updated to reflect the results of the analysis described above.

The ECCS and the CSS recirculation functions under debris loading conditions for Salem Units 1 and 2 are in compliance with the regulatory requirements listed in the Applicable Regulatory Requirements section of Generic Letter 2004-02.

The plant modifications developed as corrective actions in response to the issues identified in GL 2004-02 are installed in Salem Units 1 and 2.

As discussed in RAI 21 (Reference A.82), the NRC staff has not yet issued a final safety evaluation (SE) on the Pressurized-Water Reactor Owners Group (PWROG) topical report WCAP-16793-NP, "Evaluation of Long-Term Cooling Considering Particulate, Fibrous, and Chemical Debris in the Recirculating Fluid" (Reference 28). Salem will provide a response within 90 days of the issuance of the final NRC SE on WCAP-16793-NP.

2. **General Description of and Schedule for Corrective actions:**
Provide a general description of actions taken or planned, and dates for each. For actions planned beyond December 31, 2007, reference approved extension requests or explain how regulatory requirements will be met as per Requested Information Item 2(b). (Note: All requests for extension should be submitted to the NRC as soon as the need becomes clear, preferably not later than October 1, 2007.)

During the recirculation phase of a LOCA two Residual Heat Removal (RHR) pumps take suction through separate lines from the containment sump and discharge through separate paths to the Reactor Coolant System (RCS). The RHR pumps direct flow into the reactor, containment spray, high head charging/safety injection (C/SI) pumps and intermediate head pumps (SI).

The following are the changes implemented at Salem Unit 1 and 2.

- PSEG replaced the original strainers. The original containment sump strainer surface area for each Salem Unit was approximately 85 ft^2. The new ECCS containment sump strainer modules installed at Salem Unit 1 and 2 have a surface area of 4,854 ft^2 and 4,656 ft^2 respectively. The new strainers utilize a pocket design consisting of 3430 and 3290 pockets for Units 1 and 2, respectively. See Figure 3f.4.1.5.1-3 for the basic geometry of a typical strainer pocket. The new surface area was selected based on debris load and chemical precipitates, as well as plant layout. In addition to providing a significant increase in strainer surface area, the new strainer design in both Salem Units incorporates a reduction in strainer hole size from an original 1/8 inch nominal to 1/12 inch nominal for the new strainers. The Salem Unit 1 strainers were installed during the Spring 2007 refueling outage (Reference A.31). The Salem Unit 2 strainers were installed during the Fall 2006 refueling outage (Reference A.32).

- PSEG installed a debris interceptor in front of the new strainer modules for both Salem Units. A 9-inch tall debris interceptor is bolted to the front feet of the strainer modules to prevent large debris from reaching the strainer pockets. The debris interceptor is made of grating with bearing bars on 15/16-inch centers and cross bars on 4-inch centers. Attached to the back of the grating is perforated plate with 1/8-inch diameter perforations. The top of the debris interceptor has an overhanging lip that keeps larger debris from lifting off the floor and flowing over the debris interceptor. At the end of the strainer train, the debris interceptor wraps around the side and extends to the containment liner to limit debris transport to the back of the strainers. The Salem Unit 1 debris interceptors were installed during the Spring 2007 refueling outage (Reference A.118). The Salem Unit 2 debris interceptors were installed during the Fall 2006 refueling outage (Reference A.119)

- PSEG installed two new level switches in each Salem Unit. The new level switches have an accuracy of ±0.75 inches and are more accurate than the previously installed level indicators; thus providing a more accurate indication of the post-LOCA containment flood level. These level switches alert the control room operator when sufficient containment sump level has been achieved to support initiation of cold leg recirculation. The Salem Unit 1 and 2 installations of the new level switches were completed during the Spring 2007 (Reference A.31) and Fall 2006 refueling outages (Reference A.32) respectively. The new level switches supplement the existing level switches which are still in service.

- PSEG replaced all the calcium silicate insulation within the ZOI and Min-K insulation was replaced wherever possible (Reference A.29 and A.30). Transco Reflective metallic insulation was used at most of the locations. However, in some cases NUKON was used to replace both calcium silicate and Min K due to accessibility concerns. In all cases, the added Transco RMI, NUKON and the remaining Min-K insulation were accounted for in the Debris Generation Calculation (Reference A.1). The Salem Unit 1 and Salem Unit 2 Min-K insulation replacements were done during the Spring 2007 and Fall 2006 refueling outages, respectively.

- PSEG modified three of four wire mesh doors and folding gates in the stairwell near the accumulators for both Salem Units. The modifications replaced wire mesh with bars spaced at least 9 inches apart in the bottom 3 feet of the doors/gates. The wire mesh was removed to prevent water hold-up in the inner annulus. The bars were added to the bottom of the doors/gates to meet the radiation protection personnel safety requirements. However, the door/gate nearest to the strainer module was not modified in either Salem Unit because blockage of these doorways would result in a more tortuous path for debris, thus potentially reducing the overall debris transport. The Salem Unit 1 doors were modified during the Spring 2007 refueling outage (Reference A.31). The Salem Unit 2 doors were modified during the Fall 2006 refueling outage (Reference A.32).

- PSEG submitted a licensing basis change on August 15, 2007 (Reference A.8) to revise the licensing basis for the Net Positive Suction Head available (NPSHa) methodology for the ECCS and CSS pumps as described in Appendix 3A of the Salem Updated Final Safety Evaluation Report (UFSAR). The NRC approved the request on November 15, 2007 (Reference A.9).

- PSEG replaced the Salem Unit 2 steam generators during the Spring 2008 refueling outage. The new steam generators are insulated with Transco RMI. The previously installed steam generators were insulated with NUKON.

- PSEG revised its administrative procedures (Reference A.36 and A.37) to ensure that potential sources of debris that may be introduced into containment will be assessed for adverse effects on the ECCS and CSS recirculation functions. These programmatic controls include requirements related to coatings, containment housekeeping, materiel condition, and modifications. The procedure revisions were issued on December 18, 2007.

In addition to the above modifications, the following documents have been generated to support close out of the GL 2004-02 actions:

- Debris Generation Calculation (Reference A.1)
- Fiber Erosion and Debris Interceptor Test Report (Reference A.19)
- Debris Transport Calculation (including CFD analysis) (Reference A.2)
- Post-LOCA Chemical Effects Analysis (Reference A.4)
- Minimum Containment Flood Level Calculation (Reference A.21)
- Downstream Effects Flow Clearances Evaluation (Reference A.25)
- Downstream Wear Effects Calculation (Reference A.18)
- Mission Time Evaluation (Reference A.12)
- Minimum Air Pressure Calculation (Reference A.3)
- Latent Debris Walkdown and Evaluation (Reference A.15)
- Strainer Structural/Seismic Analysis (Reference A.55)
- Walkdown for Debris Sources (References A.16 and A.17)
- Post-LOCA Fuel Deposition Analysis (Reference A.13)
- Strainer Fiber Bypass Test Reports (Reference A.83)
- Strainer Chemical Effects Head Loss Test Report (Reference A.75)
- Chemical Effects Bench Top Test Report (Reference A.95)
- Strainer Head Loss Calculation (includes vortex and flashing assessments) (Reference A.77)
- Deaeration Analysis (Reference A.104)
- ECCS Pump NPSH Calculation (Reference A.41)

3. Specific Information Regarding Methodology for Demonstrating Compliance:

3a. Break Selection

The objective of the break selection process is to identify the break size and location that present the greatest challenge to post-accident sump performance.

3a.1) Describe and provide the basis for the break selection criteria used in the evaluation.

Ten breaks were investigated at Salem (for a sketch of the break locations see response under Item 3b.1 and 3b.2). However, two of these breaks were Alternate Methodology breaks as defined in Section 6 of NEI 04-07 (Reference 2) (not shown on the sketch in Section 3b.2), which Salem did not utilize, and therefore, they are not reported in the final debris generation calculation (Reference A.1). The eight remaining breaks are located on the primary piping. The break locations are:

- Three breaks are located on the crossover leg, which has the largest diameter of the primary piping with a 31-inch inner diameter.

- Four breaks are located on the hot leg, which has the next largest diameter of the primary piping with a 29-inch inner diameter.

- One break is located on the cold leg, which has the smallest diameter of the primary piping with a 27.5-inch inner diameter.

The locations of the analyzed breaks were chosen to maximize the amount and types of debris generated. Therefore, breaks were placed near large equipment, specifically the steam generators, reactor coolant pumps, and pressurizer. Finally, breaks were located in areas expected to maximize the transport of debris to the sump strainer.

3a.2) State whether secondary line breaks were considered in the evaluation (e.g., main steam and feedwater lines) and briefly explain why or why not.

Secondary pipe breaks were not considered for this analysis. Based upon a review of the plant UFSAR and Emergency Operating Procedures (EOPs), as described in the debris generation calculation (Reference A.1), a Main Steam Line Break or a Feedwater Line Break will not result in recirculation and, therefore, need not be considered. Additionally, breaks of small lines (less than 2 inches) were not investigated, because they are bounded by the larger breaks.

3a.3) Discuss the basis for reaching the conclusion that the break size(s) and locations chosen present the greatest challenge to post-accident sump performance.

As discussed in Section 3a.1 of this response, breaks were preferentially located near large equipment. Breaks near large equipment not only generate the most insulation debris, but also generate the most particulate debris since support steel coatings comprise most of the particulate debris load generated by the break. Breaks were also conservatively investigated on the largest possible pipes in containment to maximize the debris generation. Additionally, breaks on the largest pipes in containment are most likely to result in the automatic initiation of containment spray, and thus include the debris contribution from containment spray and from local effects at the break. Therefore, breaks on the largest pipes in containment produce the largest and most varied amount of debris types.

These conservative steps ensure the largest amount and mixture of debris types, which presents the greatest challenge to the sump strainer.

3b. Debris Generation/Zone of Influence (ZOI) (excluding coatings)

The objective of the debris generation/ZOI process is to determine, for each postulated break location: (1) the zone within which the break jet forces would be sufficient to damage materials and create debris; and (2) the amount of debris generated by the break jet forces.

3b.1) Describe the methodology used to determine the ZOIs for generating debris. Identify which debris analyses used approved methodology default values. For debris with ZOIs not defined in the guidance report (GR)/safety evaluation (SE), or if using other than default values, discuss method(s) used to determine ZOI and the basis for each.

3b.2) Provide destruction ZOIs and the basis for the ZOIs for each applicable debris constituent.

Following is the response to items 3b.1 and 3b.2.

The bioshield, for both Salem Units, contains four RCS Loops (as shown in Figure 3b-1 for Salem Unit 1). At the basement level, all four loops are open to one another; however, the northern loops (11 or 13) are mostly isolated from the southern loops (12 or 14) by the primary shield wall and other walls, which are not shown in the figure (see References A.46 and A.47).

The walls create three passageways between the northern and southern loops, which range in width from 2 feet 11 inches to 11 feet 5 inches (see References A.48 and A.49). These restrict the break jet thereby limiting the potential for breaks in one pair of loops (i.e., north or south loops) impacting the other pair of loops.

The primary shield wall in particular provides a shadowing effect between the north and south halves of containment, such that a break in one half of containment will not necessarily affect all four loops. Between elevation 100 feet and the bottom of the operating floor (elevation 125 feet), the refueling pool walls separate the north and south halves of containment (see References A.50 and A.51).

Salem Nuclear Generating Station Units 1 and 2
Docket Nos. 50-272 and 50-311
Generic Letter 2004-02
Updated Supplemental Response for Salem

Figure 3b-1: Salem Unit 1 Break Locations

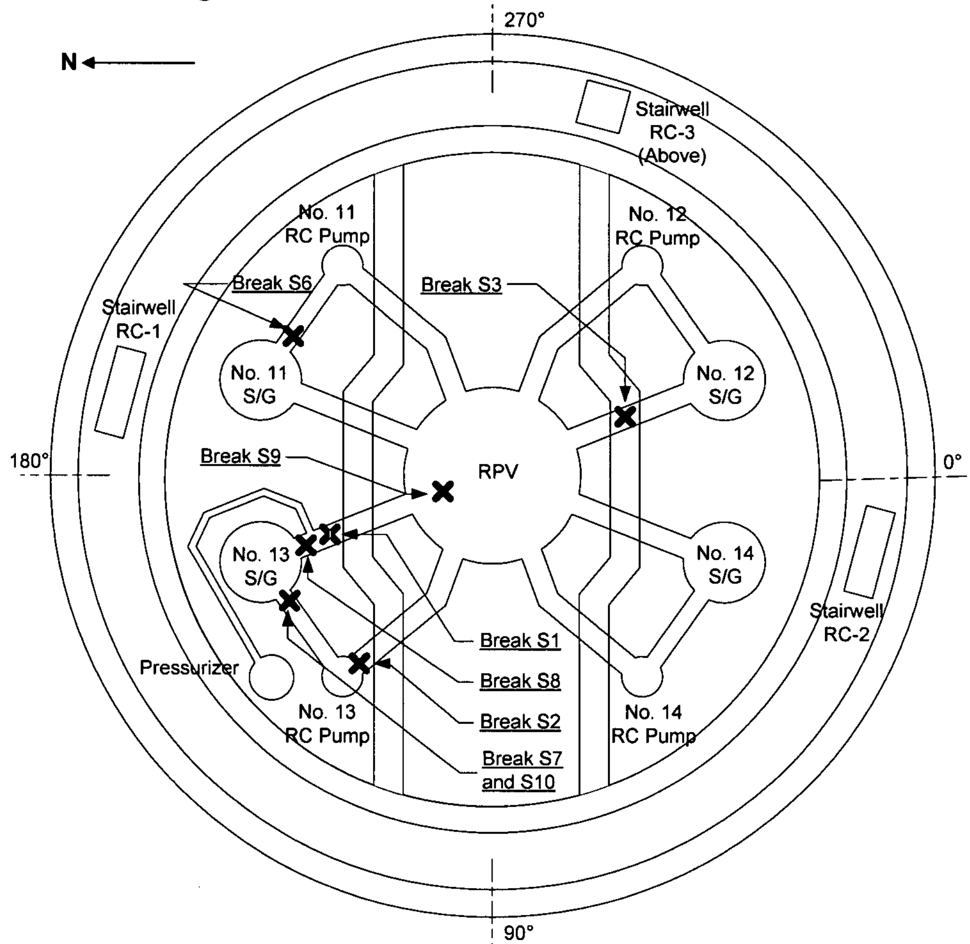

The insulation in containment at Salem consists of jacketed and un-jacketed NUKON fiberglass, anti-sweat fiberglass, Kaowool, Min-K, Metal Reflective Insulation (MRI) and Transco RMI. MRI is labeled as Metal Reflective Insulation on plant insulation drawings and is modeled as Mirror Reflective Metal Insulation.

For MRI, Min-K and all fiber insulation, the modeled ZOI is large enough to encompass all insulation below the operating floor located on at least two of the four RCS loops. MRI and Min-K utilize a ZOI of 28.6D while NUKON (both jacketed and unjacketed), Kaowool, and anti-sweat fiberglass all utilize a ZOI of 17D (Reference A.1). The ZOIs for Min-K and NUKON are consistent with the Min-K and unjacketed NUKON ZOIs provided in the SE for NEI 04-07 (Reference 3); however, the SE does not provide ZOIs for MRI, Kaowool or anti-sweat fiberglass. The use of a 17D ZOI for the NUKON jacketed with stainless steel at Salem is considered conservative.

Metal Reflective Insulation utilizes a ZOI of 28.6D, which is consistent with that for Mirror Reflective Insulation in the SE for NEI 04-07 (Reference 3). This is reasonable and conservative since both types of insulation contain encapsulated stainless steel foil and the ZOI for Mirror insulation is the largest of all tested insulation materials.

Kaowool utilizes the ZOI of 17D for unjacketed NUKON (Reference A.1). Kaowool is either encapsulated or semi-encapsulated with 0.032 inch stainless steel and has a density of 8 lbm/ft^3. In addition, Kaowool is a needled insulation in which the individual fibers are physically interlocked. NUKON is not a needled insulation; instead, individual fibers in NUKON are bound together using a binder/adhesive. Thus, Kaowool is intrinsically stronger than NUKON, especially considering that 30-60% of the NUKON binder burns off when exposed to a hot surface such as a steam generator or pressurizer. Given the stainless steel jacketing on the Kaowool, the intrinsic strength of Kaowool relative to NUKON, as well as as-fabricated density larger than the 2.4 lbm/ft^3 as-fabricated density of NUKON, the use of the NUKON ZOI for Kaowool is considered conservative.

Anti-sweat fiberglass also utilizes the ZOI of 17D for unjacketed NUKON (Reference A.1). The anti-sweat fiberglass is either Owens-Corning Fiberglas or Johns Manville Micro-Lok HP, both of which have as-fabricated densities greater than that of NUKON (2.4 lbm/ft^3). The anti-sweat fiberglass has a volume averaged as-fabricated density of 4.0 lbm/ft^3 (assuming 50% of each type of anti-sweat fiberglass) and is jacketed with 0.016 to 0.020 inch stainless steel. The anti-sweat fiberglass jacketing is secured with 1/2 to 3/4 inch bands spaced approximately 9 inches apart. Owens-Corning Fiberglas is manufactured using the same glass fibers and binder as NUKON, but there are more binding locations than in NUKON as there are more fibers per volume (i.e. higher density). Johns Manville Micro-Lok HP is manufactured using materials similar to Owens-Corning Fiberglas. Therefore, the anti-sweat fiberglass has more intrinsic strength than NUKON. Given the stainless steel jacketing on the anti-sweat fiberglass, the intrinsic strength of anti-sweat fiberglass relative to NUKON, as well as as-fabricated densities larger than the 2.4 lbm/ft^3 as-fabricated density of NUKON, the use of the NUKON ZOI for anti-sweat fiberglass is considered conservative.

In order to perform the calculation of debris generation for MRI, Min-K and all fiber insulation, an inventory of the insulation based on component insulation drawings, piping stress isometrics, piping insulation drawings and piping arrangement drawings is utilized. This inventory is part of the debris generation calculation (Reference A.1). The total amount of each insulation type in each containment

ZOI is found from this inventory. This information is then used to determine the debris total for each insulation type as described in the following paragraphs.

Salem Unit Comparison

The physical layout of the Salem Units, including major equipment types and locations, is the same; however, the insulation types and locations vary. Both Salem Units contain a significant amount of MRI. In Salem Unit 1 the MRI is located on piping and the reactor coolant pumps. In Salem Unit 2 the MRI is located on piping, the reactor coolant pumps, and the pressurizer.

Additionally, the Salem Unit 2 replacement steam generators have Transco RMI insulation. Both Salem Units contain similar amounts of Kaowool and anti-sweat fiberglass insulation located on piping. Min-K insulation is installed in small amounts in a few isolated areas in both Salem Unit 1 and 2. In addition, Min-K insulation is installed on the Unit 2 RCS crossover leg piping (between the steam generators and reactor coolant pumps). The Min-K present in Unit 1 is installed in areas of containment which are unaffected by postulated breaks (except Break S9 which is not bounding), while Unit 2 has Min-K insulation on some piping within the ZOI of the postulated breaks. Debris totals for all insulation types are provided in Table 3b-1a.

Finally, both Salem Units contain NUKON insulation. Salem Unit 1 contains a significant amount of NUKON insulation on the steam generators and pressurizer. With the exception of the bottom hemisphere of the steam generators and pressurizer, this insulation is jacketed. The only NUKON insulation in Salem Unit 2 is located inside hot and cold leg sleeves in the primary shield wall.

Piping Insulation

Anti-sweat fiberglass insulation is located on component cooling (CC) piping inside containment (Reference A.1). The CC piping in the inner annulus is located on piping from Elevation 80 feet to 116 feet (all underneath the operating floor), with the majority on piping from Elevation 88 feet to 116 feet, and the pipe sizes range from 3/4 inch to 3 inches. The CC piping provides cooling to the reactor coolant pump (RCP) and its related components (upper and lower bearing coolers) and generally enters and exits the bioshield near the RCP being served along a relatively direct route. Therefore, anti-sweat fiberglass is distributed relatively evenly among the four primary loops. For any given break (except Break S9, which is not bounding), some anti-sweat fiberglass debris would be generated near the break, while some would be generated far from the break.

The majority (80-90%) of Kaowool insulation within the ZOI of RCS breaks inside containment is located on the piping for the chemical and volume control (CVC) and safety injection (SI) systems (Reference A.1). The pipe sizes on which Kaowool is installed range from 1/2 inch to 14 inches; however, approximately half of the insulation generated by any given break is from piping greater than 6 inches. CVC and SI piping is attached to each of the four primary loops for charging (CVC), RCP seal injection (CVC), cold leg injection (SI), and hot leg injection (SI) functions. Therefore, Kaowool is distributed relatively evenly among the four primary loops. For any given break (except Break S9, which is not bounding), some Kaowool debris would be generated near the break, and some Kaowool debris would be generated far from the break.

For anti-sweat fiberglass and Kaowool insulation on piping, the insulation inventory is utilized to calculate the total amount of that insulation type within the inner annulus. The piping insulation is considered divided evenly among the four primary loops. Therefore, any large break will generate approximately the same amount of debris as any other large break due to the large ZOIs of insulation under consideration. This approach is reasonable since both anti-sweat fiberglass and Kaowool insulation are distributed relatively evenly throughout the inner annulus, as described above.

The containment layout is relatively symmetric (except for the pressurizer and its associated piping). Due to the reactor wall and other walls, a break in one half of containment will not impact the other half for most break locations. For break locations where three loops could be impacted, only a portion of the two loops far from the break is impacted. Therefore, for any given break, the total amount of debris generated is approximately the quantity from two loops. The debris generation calculation assumed that half of the piping is located in each half of containment. For conservatism, to account for any possible differences between the north and south side of containment, the debris load for the side with the break is assumed to contain 20% more debris than the side without the break. This division is approximately equivalent to a 55/45 split between the north and south sides of containment. In addition, the insulation on the pressurizer and associated piping was included for the breaks located on the side of containment with the pressurizer.

Unlike other insulation types (Kaowool, NUKON, Min-K, etc.), MRI insulation consists of thin sheets of metal with air-gaps between them. Therefore, rather than calculating a volume of debris generated, the area of these sheets is calculated. The debris generation calculation (Reference A.1) conservatively considers three layers of these sheets per inch of insulation thickness (11 layers for 3.5 inch thickness, 9 layers for 3.0 inch thickness and 8 layers for 2.5 inch thickness).

The pressurizer surge line, pressurizer spray lines and residual heat removal lines all are insulated with MRI and these lines are all located in the same area of containment, near the pressurizer. Therefore, it would not be conservative to split the insulation debris evenly between the two areas of containment as done for other insulation types. Hence, these debris sources are included in the maximum debris total along with one-half of the remaining MRI insulation in the inner annulus. Also, due to the large ZOI associated with MRI, it is considered possible for a third cold leg to be affected by a break; therefore, a third cold leg is also included in the debris total.

The process for calculating the volume of Min-K insulation differs from all other debris types found on piping. Some Min-K insulation is located on the hot and cold legs inside the sleeves that line the penetrations through the reactor pressure vessel (RPV) cavity. In order for this insulation to become debris and enter the recirculation pool, a break would have to occur inside the RPV cavity, which would result in a much smaller total debris volume due to the truncation of the break jet by the RPV cavity wall. Therefore, this insulation is not included in the maximum debris total for Units 1 and 2.

In Salem Unit 2, Min-K is installed on each of the four crossover legs (between the steam generator and the reactor coolant pump) (Reference A.1). Each crossover leg is surrounded on all sides with lead blankets hung from a frame (using grommets and carabiners) with an open back configuration as depicted in Figure 3b-2.

Figure 3b-2: Lead Blanket Configuration

Three of the four crossover legs are within a ZOI of 28.6D of any break in the RCS piping (the fourth is shielded by the primary shield wall) and only two of the four crossover legs are on the same side of containment as a break as shown in Figure 3b-3. The containment is divided by the refuel pool walls between elevation 100 feet and the bottom of the operating floor at elevation 125 feet.

Figure 3b-3: Unit 2 Reactor Coolant Piping Layout

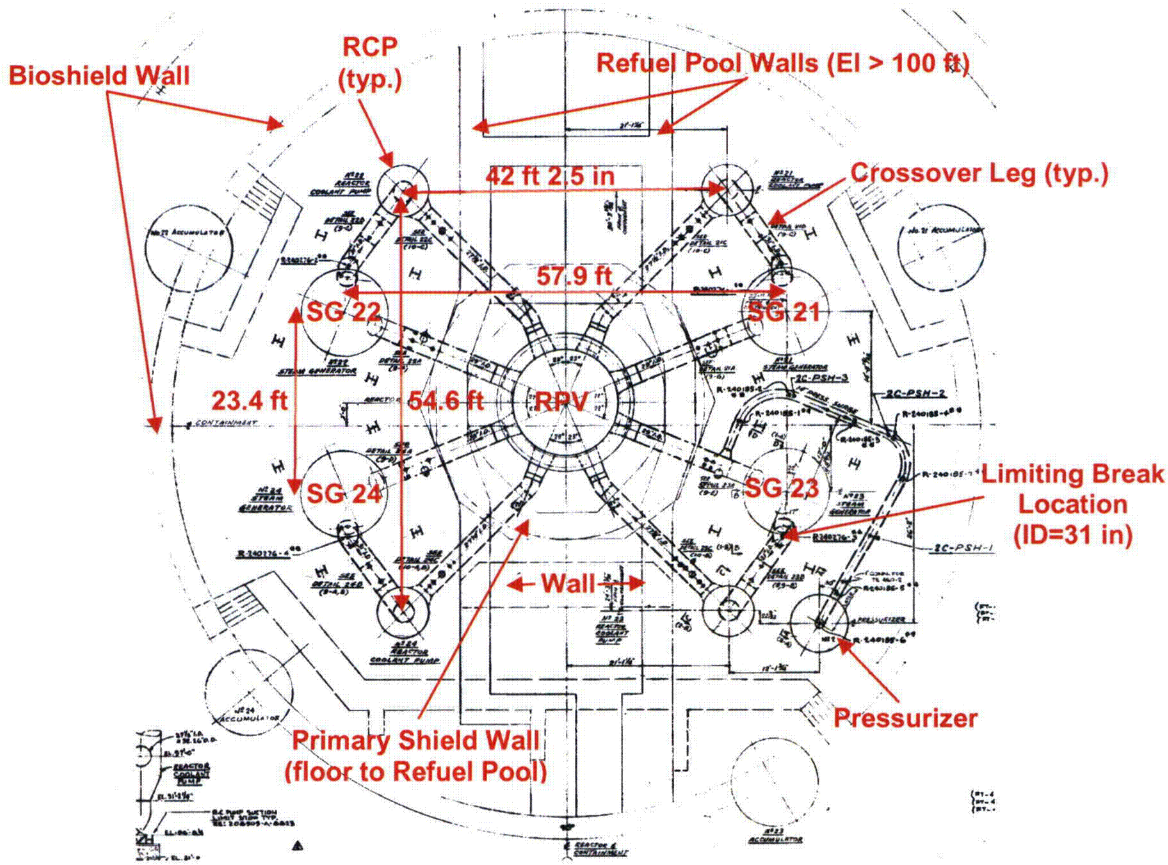

The third crossover leg (on the opposite side of containment from any break) is approximately 18D from the limiting break. The jet pressure at 18D is less than 6 psig (Reference 3). At 18D, it is expected that the lead blankets will either not be damaged or that the grommets could fail, resulting in the blankets falling. In either case, the Min-K on the third crossover leg would not become debris due to the lead blankets surrounding it. In addition, the Min-K on the crossover legs is covered with stainless steel jacketing which protects the insulation. Therefore, for Unit 2 the Min-K insulation on only two crossover legs is considered debris. It should also be noted that the Unit 2 strainer head loss testing included significant margin in the Min-K quantity, as documented in Section 3f.4.1.5.8 of this response.

To illustrate, the Min-K debris generation following a postulated pipe break on the #23 crossover leg (shown as the "Limiting Break" in Figure 3b-3) is outlined below. This break generates the maximum amount of overall insulation debris.

- All the Min-K insulation on the #23 crossover leg is damaged and becomes debris. The lead blankets surrounding the #23 crossover piping will fail.
- All the Min K insulation on the #21 crossover leg is damaged and becomes debris. The lead blankets surrounding the #21 crossover piping will fail.
- The #24 crossover piping is located approximately 18D away from the limiting pipe break. Jet impingement from the break could impact the lead blankets surrounding #24 crossover leg as follows:
  - The blankets could remain in place and not be damaged by jet impingement due to 18D distance from the break. This condition would protect the #24 crossover piping insulation.
  - Due to sufficient momentum transfer from jet impingement, the grommets could fail and the blankets could fall. This would dissipate the remaining energy of the break jet, thereby protecting the #24 crossover leg insulation.
- The Min-K insulation on the #22 crossover leg is not damaged since it is shielded from the break by the primary shield wall.

In the Salem Unit 1 containment, no Min-K is installed within the inner annulus other than that inside the RPV cavity sleeves described above. The Unit 1 crossover legs are insulated with MRI and Transco RMI (conservatively all modeled as MRI in the debris generation analysis).

All debris from insulation on piping is generated below the bottom of the operating floor (Elevation 125 ft).

Equipment Insulation

The following equipment inside the inner annulus is insulated: reactor coolant pumps, steam generators, and the pressurizer. The debris generated due to insulation on each of these components is described below (Reference A.1).

<u>Reactor Coolant Pumps</u>

The reactor coolant pumps (RCPs) in both Salem Units are insulated with MRI and therefore generate equivalent debris amounts in both Salem Units. The RCPs in both Salem Units are insulated with 3-inch thick MRI. The ZOI for MRI is 28.6D, which is large enough that a large break could affect three RCPs. Therefore, the area of MRI covering three of the RCPs is included in the debris total of each break.

Steam Generators and Pressurizer – Salem Unit 1

The shells of the steam generators and pressurizer are insulated with jacketed NUKON while the bottoms of the steam generators and pressurizer are insulated with unjacketed NUKON. However, both the jacketed and unjacketed NUKON insulation are treated the same; i.e. the jacketed NUKON utilizes a ZOI of 17D.

A break in the RCS piping can impact both steam generators on one side of containment as two RCS loops are within a ZOI of 17D. If the break occurs in the half of containment which contains the pressurizer, the pressurizer can also be impacted. All components on the same side of containment as the break are not impacted by all breaks since shadowing due to large equipment (e.g. steam generators) is credited. The ZOI of 17D extends above the bottom of the operating floor (El. 125 ft) and therefore can impact portions of the steam generators and pressurizer which are above the operating floor. However, there are individual openings in the operating floor for the pressurizer and each steam generator. Therefore, the floor will shield part of the upper portion of the steam generator and pressurizer which are not adjacent to the modeled pipe break. Floor shielding is not credited for the steam generator adjacent to the pipe break and debris is generated within the full vertical extent of the ZOI.

The NUKON debris generated in upper and lower containment (above and below the bottom of the operating floor, respectively) is tracked separately to support the debris transport analysis.

The debris generation calculation determined the quantity of debris within concentric sub-shells of the ZOI (e.g. within 7D, from 7D to 8D, etc.). This approach was used in the transport analysis since the debris size distribution within each sub-shell is different, as explained in Section 3c.

Steam Generators and Pressurizer – Salem Unit 2

In Salem Unit 2 the steam generators were replaced during the Spring 2008 outage with new steam generators insulated with Transco RMI (Reference A.14). Since Transco RMI is subject to a relatively small ZOI of 2D, the volume of insulation debris generated on the steam generator is calculated based on its proximity to the postulated breaks.

The shell and hemispherical bottom of the Salem Unit 2 pressurizer are insulated with MRI.

Coatings

Coatings on steel, concrete and equipment in containment were also evaluated. All qualified coatings at Salem are epoxy coatings, which were evaluated for a 4D ZOI. Based upon the results of testing presented in WCAP-16568-P (Reference 22) and accepted by the NRC in 2010 (Reference 39), a 4D ZOI is acceptable. All unqualified coatings (except some on Limitorque valve actuators) are considered to become debris consistent with NEI 04-07 and its associated SER (References 2 and 3). Further discussion of coatings is contained in Section 3h of this response submittal.

No qualified inorganic zinc (IOZ) coatings are utilized inside containment at Salem Units 1 and 2.

Latent Debris and Foreign Materials

As discussed in Section 3d of this response submittal, latent debris and miscellaneous (foreign) materials are also included in the debris generation analysis. The amount of latent debris is calculated from walkdown data in accordance with NEI 02-01 (Reference 20), as reported in the plant walkdown report (Reference A.15). The amount of foreign material debris considered is a conservative maximum, which has been reinforced by walkdowns of both Salem Units (References A.16 and A.17). Further discussion of latent and foreign material debris is presented in the respective sections within this response submittal.

3b.3) Identify if destruction testing was conducted to determine ZOIs. If such testing has not been previously submitted to the NRC for review or information, describe the test procedure and results with reference to the test report(s).

WCAP-16568-P (Reference 22) has been utilized for the determination of the ZOI for qualified coatings. A ZOI of 4D has been used for qualified epoxy coatings. Use of the reduced ZOI for epoxy coatings was accepted by the NRC in 2010 (Reference 39). Applicability of WCAP-16568-P to Salem is discussed in Section 3h.5 of this response.

No qualified inorganic zinc (IOZ) coatings are utilized inside containment at Salem Units 1 and 2.

3b.4) Provide the quantity of each debris type generated for each break location evaluated. If more than four break locations were evaluated, provide data only for the four most limiting locations.

The insulation and coating debris totals for four of the eight breaks analyzed are presented in Tables 3b-1 through 3b-3 (Reference A.1). Breaks S2, S3, S6, and S9 are not presented. Breaks S3 and S6 are the same as Breaks S1 and S7, respectively, except that they are located in RCS loops where the break does not impact the pressurizer; therefore, debris generation totals from Breaks S1 and S7 are bounding. Break S2 is similar to Break S7, but Break S7 is more limiting since it is closer to the pressurizer and steam generators. Break S9 generates minimal debris as it is on a hot leg within the primary shield wall.

Table 3b-1a shows the total amount of insulation debris generated for Breaks S1, S7, S8, and S10, while Table 3b-1b shows the distribution of NUKON debris in each ZOI sub-shell for the limiting Unit 1 pipe break (i.e. Break S1 which results in the greatest quantity of debris on the strainer – see Section 3e.6 of this response). The quantity of debris in ZOI sub-shells was not determined for any other debris types.

The amount of latent and foreign (miscellaneous) debris generated is provided in Section 3d of this response. The bases for coatings debris generation is provided in Section 3h.5 of this response.

Salem Nuclear Generating Station Units 1 and 2
Docket Nos. 50-272 and 50-311
Generic Letter 2004-02
Updated Supplemental Response for Salem

Table 3b-1a: Total Insulation Debris[2]

Debris Type	Units	Break S1	Break S7	Break S8	Break S10
Insulation (U1)					
NUKON (SGs)	[ft^3]	1137.6	690.4	1143.6	851.4
NUKON (Pressurizer)	[ft^3]	222.0	303.0	0(1)	212.2
Kaowool (Piping)	[ft^3]	97	97	97	97
Anti-sweat Fiberglass (Piping)	[ft^3]	48	48	48	48
Min - K	[ft^3]	0	0	0	0
MRI (RC Pumps)	[ft^2]	5510	5510	5510	5510
MRI (Piping)	[ft^2]	27,730	27,730	19,800	27,730
Insulation (U2)					
Kaowool (Piping)	[ft^3]	122	122	122	122
Anti-sweat Fiberglass (Piping)	[ft^3]	50	50	50	50
Min - K (piping)	[ft^3]	17.5	17.5	17.5	17.5
MRI (Pressurizer)	[ft^2]	7180	10,160	0(1)	10,400
MRI (RC Pumps)	[ft^2]	5510	5510	5510	5510
MRI (Piping)	[ft^2]	24,080	24,080	17,400	24,080
Transco RMI (SGs)	[ft^2]	3150	3150	3150	0(1)

Notes:

(1) Component is either outside of the break ZOI or shadowed by a robust barrier or large component (e.g. steam generator) (see Figure 3b-1).

(2) For a sketch of the break locations see Response Sections 3b.1 and 3b.2.

Table 3b-1b: ZOI Sub-Shell Debris Distribution for Unit 1 NUKON (Break S1)

ZOI Sub-Shell	Steam Generator 13			Pressurizer			Steam Generator 11			Sub-total
	Bottom [ft³]	Shell <125 ft [ft³]	Shell >125 ft [ft³]	Bottom [ft³]	Shell <125 ft [ft³]	Shell >125 ft [ft³]	Bottom [ft³]	Shell <125 ft [ft³]	Shell >125 ft [ft³]	[ft³]
0-7D	81.0	153.1	0.0	0.0	0.0	0.0	14.5	2.8	0.0	251.4
7-8D	0.0	40.2	0.0	0.0	0.0	0.0	14.8	20.5	0.0	75.5
8-9D	0.0	37.8	0.0	0.0	0.0	0.0	11.3	26.5	0.0	75.6
9-10D	0.0	36.5	0.0	5.6	3.2	0.0	11.4	33.1	0.0	89.8
10-11D	0.0	35.8	0.0	5.2	15.1	0.0	15.1	45.9	0.0	117.1
11-12D	0.0	27.3	7.9	5.2	24.8	0.0	13.9	88.3	0.0	167.6
12-13D	0.0	12.3	22.6	5.2	44.7	0.0	0.0	54.4	0.0	139.2
13-14D	0.0	0.0	34.7	0.0	34.2	0.0	0.0	31.0	15.8	115.7
14-15D	0.0	0.0	34.8	0.0	16.9	14.2	0.0	19.3	24.0	109.2
15-16D	0.0	0.0	40.9	0.0	12.3	14.0	0.0	17.6	23.6	108.5
16-17D	0.0	0.0	48.8	0.0	2.9	18.5	0.0	3.5	36.4	110.1
Sum*:	81.0	343.0	189.8	21.2	154.1	46.7	81.0	343.0	99.9	**1359.6**

* Summation may not be equal to the sum of the values due to rounding associated with the use of spreadsheets.

Table 3b-2: Qualified Coating Debris (all Epoxy, no IOZ)

Break	**Steel Coatings [ft³]**	**Concrete Floors [ft³]**	**Concrete Walls [ft³]**	**Total Qualified Coatings [ft³]**
S1	3.5	0.0	0.9	4.4
S7	5.3	0.0	0.0	5.3
S8	4.0	0.0	0.5	4.5
S10	5.3	0.8	0.0	6.1

Table 3b-3a: Unit 1 Unqualified Coating Debris

Description	**Area**	**Thickness**	**Volume**
	[ft²]	**[mils]**	**[ft³]**
Polar Crane Upgrade Stencil	2	10.5	0.002
Valve Coatings[1]	various	various	0.48
Aluminum Paint	2750	3	0.6875
Steam Generator Coating	2900	3	0.725
Total			**1.89**

1) Valve coatings consist of both IOZ and epoxy coatings.

Table 3b-3b: Unit 2 Unqualified Coating Debris

Description	Area	Thickness	Volume
	[ft^2]	[mils]	[ft^3]
Polar Crane Upgrade Stencil	2	10.5	0.002
Valve Coatings[1]	various	various	0.48
Aluminum Paint	2900	3	0.725
Total			**1.21**

1) Valve coatings consist of both IOZ and epoxy coatings.

Permanent Lead Shielding Blankets

At Salem Unit 1 and Unit 2, two sets of lead blankets manufactured by LANCS industries are installed around radioactive piping at several locations inside the bioshield area to reduce dose exposure (Reference A.2). Each set of blankets forms a continuous lead curtain around the piping. The blankets are freely hanging with only the top of the blankets secured. The majority of the blankets do not have firm backing (e.g. a wall) behind them. If a LOCA were to occur, a portion of the lead blankets would become debris which could transport to the strainer. The debris types which could be generated are both lead wool and the blanket cover materials, Alpha Maritex 3259-2-SS (inner cover) and 8459-2-SS (outer cover). Lead wool is not considered transportable debris due to its density.

The Air Jet Impact Tests (AJITs) (Reference 23) tested rubberized cloth covered lead blankets, similar to those at Salem, for Boston Edison. In these tests, the lead blankets were installed in a strong back configuration and no lead blanket debris was generated. The air jet surface pressures used, when converted to two-phase jet pressures, correspond to a ZOI of 5.4D. Therefore, the ZOI used for lead blankets is 5.4D. However, small fines are only generated within a ZOI of 2.1D (see Section 3c.4 of this response).

The area of lead blankets within a ZOI of 2.1D is approximately 300 ft^2 for Unit 1 and 335 ft^2 for Unit 2 (Reference A.2 Attachment 8.17). The total area of lead blanket covers within 2.1D is equal to twice the blanket area for both cover materials which corresponds to approximately 600 ft^2 (Unit 1) / 670 ft^2 (Unit 2) of Alpha Maritex 3259-2-SS (inner cover) and 600 ft^2 (Unit 1) / 670 ft^2 (Unit 2) of 8459-2-SS (outer cover). Of the 600 ft^2 (Unit 1) / 670 ft^2 (Unit 2) of Alpha Maritex 3259-2-SS and 8459-2-SS, only 150 ft^2 (Unit 1) / 167.5 ft^2 (Unit 2) of each material is considered the "innermost" cover when determining the size distribution (see Table 3c-7 and lead blanket cover discussion in Section 3c.4).

3b.5) Provide total surface area of all signs, placards, tags, tape, and similar miscellaneous materials in containment

Foreign material debris is discussed in greater detail along with latent debris in Section 3d of this response. The total foreign material debris area found in Salem Unit 1 is 573 ft^2 and in Salem Unit 2 is 525 ft^2.

3c. Debris Characteristics

The objective of the debris characteristics determination process is to establish a conservative debris characteristics profile for use in determining the transportability of debris and its contribution to head loss.

3c.1) Provide the assumed size distribution for each type of debris.

The development of the debris size distributions used for Salem Unit 1 and 2 is discussed below. The size distributions developed and used are as indicated in Tables 3c-1 through 3c-7 (Reference A.2). Coatings are modeled as fines as described in Section 3h.2 of this response.

NUKON

For both jacketed and unjacketed NUKON, a different size distribution is used within each ZOI sub-shell based on the jet pressure within the ZOI sub-shell. The jet pressure within each ZOI sub-shell is determined based on Table I-3 of Appendix I to the SE for NEI 04-07 (Reference 3). For each sub-shell, the jet pressure is considered equal to the pressure at the radius at which the volume of the outer portion of the shell is equal to the volume of the inner portion of the shell; i.e. $r_{jet\_pressure} = [(r_{outer}^3+r_{inner}^3)/2]^{1/3}$. This is slight simplification of the methodology in Appendix II of the SE for NEI 04-07 (Reference 3), but is acceptable since the sub-shells being assessed are relatively small (each shell is only 1D thick). The jet pressure as a function of ZOI is shown in Figure 3c-1 while the jet pressure assigned to each ZOI sub-shell is presented in Table 3c-1.

Figure 3c-1: ZOI as a Function of Jet Pressure

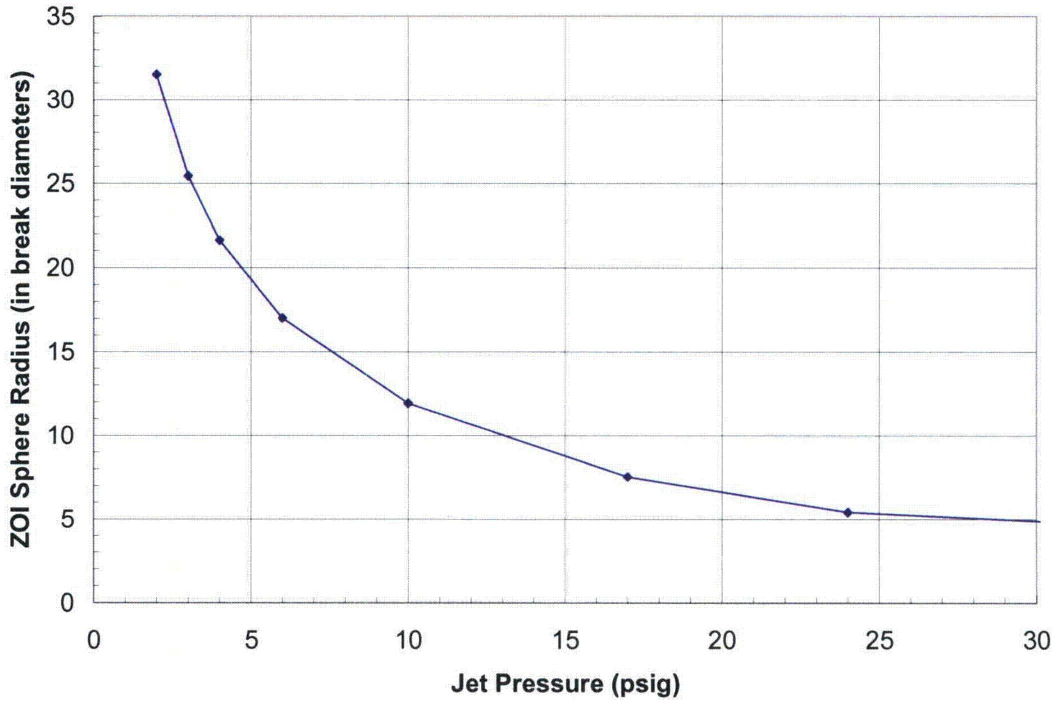

Once a jet pressure is assigned to each sub-shell, the fraction of low density fiberglass (LDFG) debris within the sub-shell which is small fines (fines plus small pieces) is determined based on Figure II-2 of Appendix II to the SE for NEI 04-07 (Reference 3), presented as Figure 3c-2. This data is applicable to NUKON since NUKON is LDFG.

Figure 3c-2: LDFG Small Fines Fraction as Function of Jet Pressure

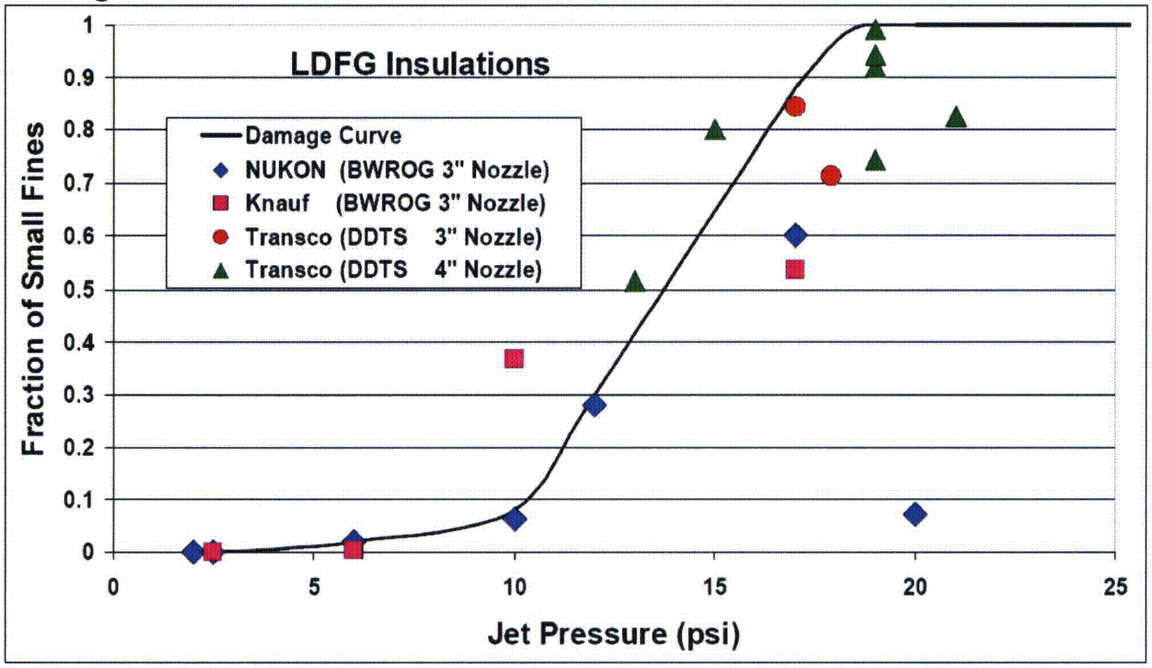

Figure II-2. LDFG Damage Curve for Small Fine Debris

Combining Figures 3c-1 and 3c-2 results in Figure 3c-3 which depicts the fraction of small fines as a function of ZOI.

Figure 3c-3: Fraction of LDFG Small Fines as a Function of ZOI

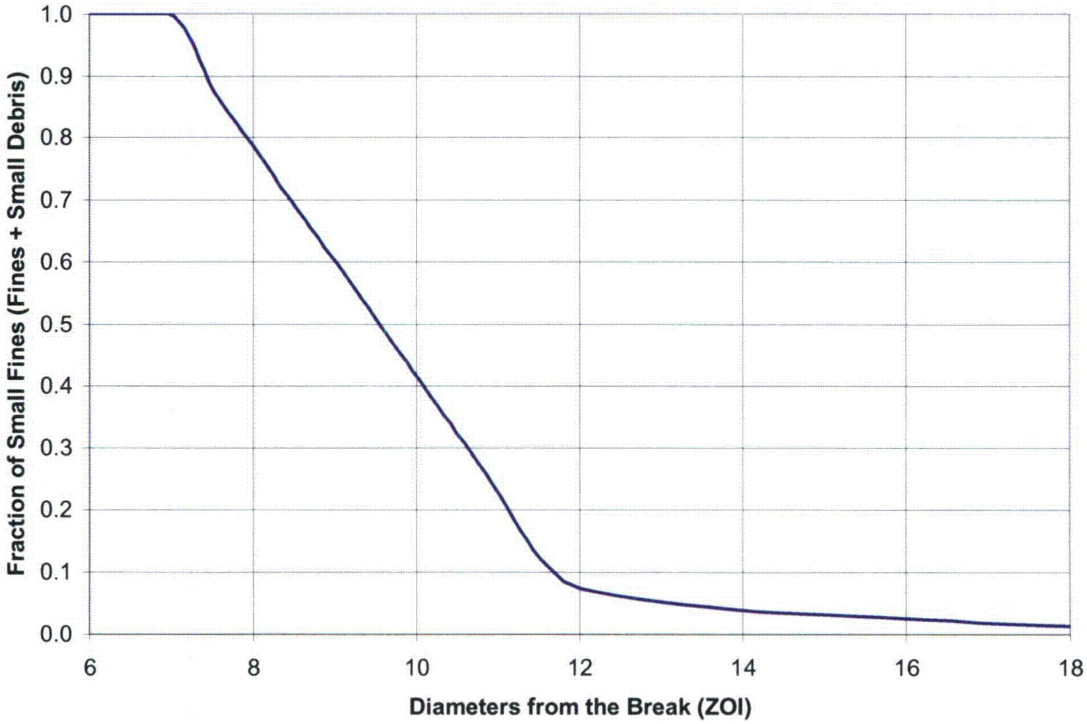

The guidance in Appendix II of the SE for NEI 04-07 (Reference 3) also states that the fraction of unrecoverable debris (i.e. fines) in the Drywell Debris Transport Study (DDTS) ranges from 15 to 25% (an average of 20%). Consistent with the approach for LDFG in the volunteer plant analysis in Appendix VI to the SE for NEI 04-07, all small fines debris are modeled as 20% fines and 80% small pieces.

The fraction of debris which is not small fines consists of both large and intact piece debris since the base wool is enclosed in a durable woven glass fiber fabric. To determine the fraction of the large and intact debris which is intact, data from the Air Jet Impact Tests (AJITs) for both jacketed and unjacketed LDFG (NUKON and Knauf) is used. Data from the tests with insulation jacketed with Sure-Hold Bands is not used. Figure 3c-4 shows the fraction of large and intact debris which is intact.

Figure 3c-4: AJIT Data for Large & Intact LDFG Debris

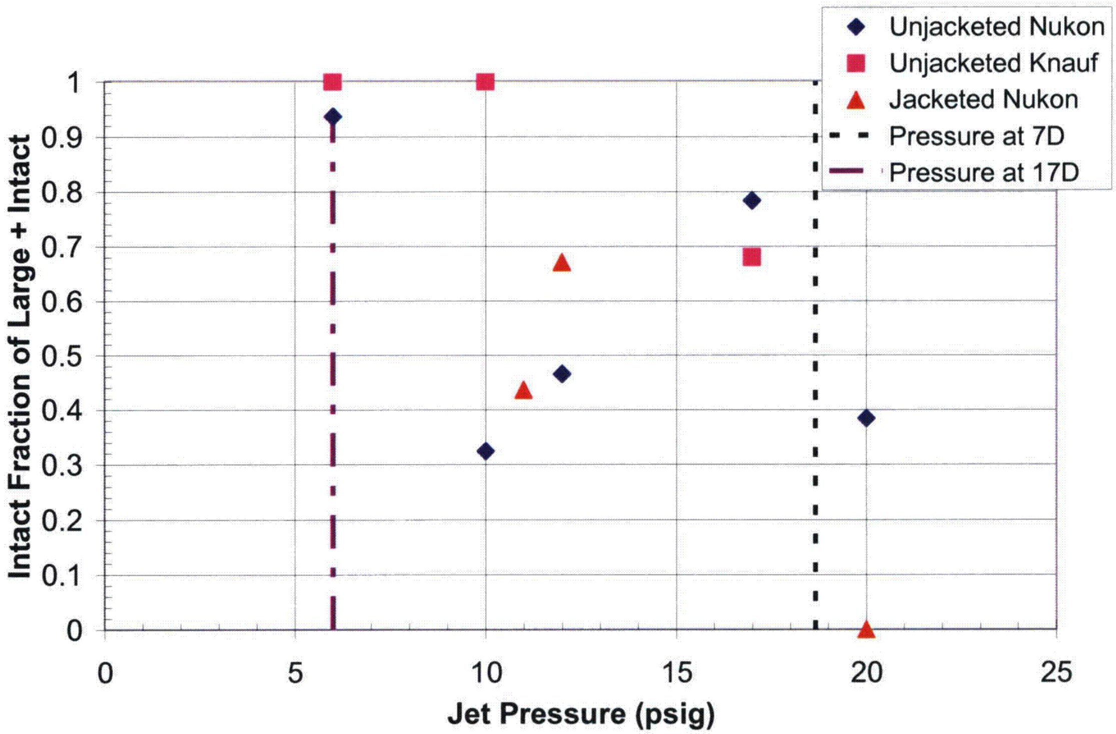

The intact fraction of the large and intact debris is considered to be 50% (note, this is different than 50% of the generated debris being large and intact). This approach is considered acceptable since 6 of the 9 AJIT data points corresponding to ZOIs from 7D to 17D indicate that more than 60% of the large and intact debris is intact with 3 data points indicating that greater than 90% of the large and intact debris is intact. The average intact fraction of large and intact debris for the nine AJIT data points corresponding to ZOIs from 7D to 17D is 70%. Thus, the modeling of 50% of the large and intact debris as large and 50% as intact for ZOIs ranging from 7D to 17D is conservative. This approach is slightly more conservative than that used for LDFG in the volunteer plant analysis in Appendix VI to the SE for NEI 04-07 (Reference 3).

Debris generated from the cloth encasing NUKON basewool to form NUKON blankets is not calculated. This is acceptable since the cloth covering is more robust than the basewool and pieces would not transport in the pool as the cloth is 18 oz/yd^2 and is similar to lead blanket inner covers. Furthermore, if pieces of this cloth did transport, they would likely result in a lower overall strainer head loss as pieces of material often disrupt the formation of homogenous debris beds. In addition, the use of a ZOI of 17D for all NUKON, especially stainless steel jacketed

NUKON, results in the generation of a conservative quantity of transportable fines and erodible small and large debris. The conservatism in the ZOI offsets the small quantity of transportable fines which would be generated from the NUKON cloth covers.

The NUKON size distribution as a function of distance from the break (i.e. ZOI sub-shell) is presented in Table 3c-1.

Table 3c-1: NUKON Size Distribution

ZOI Sub-Shell	ZOI for P_{jet} in D	P_{jet} (psig)	2-Category Size Distribution		4-Category Size Distribution (Fraction within Each ZOI Sub-Shell)			
			Small Fines	Large/ Intact	Fines	Small	Large	Intact
0-7D	< 7.0(1)	> 18.7(1)	1.00	0.00	0.200	0.800	0.000	0.000
7-8D	7.53	16.9	0.87	0.13	0.174	0.696	0.065	0.065
8-9D	8.53	15.4	0.69	0.31	0.138	0.552	0.155	0.155
9-10D	9.53	13.8	0.50	0.50	0.100	0.400	0.250	0.250
10-11D	10.52	12.2	0.32	0.68	0.064	0.256	0.340	0.340
11-12D	11.52	10.6	0.12	0.88	0.024	0.096	0.440	0.440
12-13D	12.52	9.5	0.06	0.94	0.012	0.048	0.470	0.470
13-14D	13.52	8.7	0.04	0.96	0.008	0.032	0.480	0.480
14-15D	14.52	7.9	0.03	0.97	0.006	0.024	0.485	0.485
15-16D	15.52	7.2	0.03	0.97	0.006	0.024	0.485	0.485
16-17D	16.52	6.4	0.02	0.98	0.004	0.016	0.490	0.490

(1) A ZOI of 7D corresponds to a jet pressure of 18.7 psig; however, the small fines fraction is the same for all jet pressures greater than 18.7 psig (corresponding to ZOIs less than 7D).

Since NUKON is modeled with a size distribution which is dependent on the break location relative to the target location, the size distribution for each break modeled is slightly different. The size distribution information in Table 3c-1 is applied to Unit 1 Break S1 and the results are presented in Table 3c-2. A similar approach is used for other breaks.

Table 3c-2a: Unit 1 NUKON Size Distribution Results for Limiting Break S1

ZOI Sub-Shell	Debris Generated Below El. 125 ft.				Debris Generated Above El. 125 ft.			
	Fines (ft^3)	Small (ft^3)	Large (ft^3)	Intact (ft^3)	Fines (ft^3)	Small (ft^3)	Large (ft^3)	Intact (ft^3)
0-7D	50.3	201.2	0.0	0.0	0.0	0.0	0.0	0.0
7-8D	13.1	52.5	4.9	4.9	0.0	0.0	0.0	0.0
8-9D	10.4	41.7	11.7	11.7	0.0	0.0	0.0	0.0
9-10D	9.0	35.9	22.5	22.5	0.0	0.0	0.0	0.0
10-11D	7.5	30.0	39.8	39.8	0.0	0.0	0.0	0.0
11-12D	3.8	15.3	70.2	70.2	0.2	0.8	3.5	3.5
12-13D	1.4	5.6	54.8	54.8	0.3	1.1	10.6	10.6
13-14D	0.5	2.1	31.3	31.3	0.4	1.6	24.2	24.2
14-15D	0.2	0.9	17.5	17.5	0.4	1.8	35.4	35.4
15-16D	0.2	0.7	14.5	14.5	0.5	1.9	38.1	38.1
16-17D	0.0	0.1	3.2	3.2	0.4	1.7	50.8	50.8
Sum*:	96.5	386.0	270.4	270.4	2.2	8.8	162.7	162.7
Fraction:	7.1%	28.4%	19.9%	19.9%	0.2%	0.6%	12.0%	12.0%

* Summation may not be equal to the sum of the values due to rounding associated with the use of spreadsheets.

Table 3c-2b: Unit 1 NUKON Size Distribution Results for Limiting Break S1

Category	Percentage = Debris Fraction Generated Below El. 125 ft + Debris Fraction Generated Above El. 125 ft (Rounded)
Fines	7%
Small Pieces	29%
Large Pieces	32%
Intact Pieces	32%

Metal Reflective Insulation (MRI)

The relative amounts of each size category considered for MRI debris at Salem are presented in Table 3c-3. The size distribution for MRI debris is consistent with Section 3.4.3.3.2 of the NEI Guidance (Reference 2) and based on Figure 3-7 of NUREG/CR-6808 (Reference 18). The figure is generated from data obtained from a test of MRI; therefore, it allows for further refinement of the debris size distribution ascribed to MRI debris at Salem.

The size distribution presented in the figure is approximately 5% fines (1/4-inch and smaller), 70% small pieces (1/4-inch to 4-inch), and 25% large pieces (4-inch and larger). The debris sample from this test is typical of the debris from MRI cassettes nearest the modeled break. Using the size distribution for a cassette nearest the break for the entire MRI ZOI is conservative. Fines that enter the active recirculation pool are considered 100% transportable. Small and large pieces are transported based on velocity data found in various references as discussed in Section 3e.

Table 3c-3: MRI Size Distribution

Category	Category Percentage
Fines (< ½ inch)	5%
Small (½ inch ≤ x < 4 inch)	70%
Large (≥ 4 inch)	25%

Transco RMI

The relative amounts of each size category considered for Transco RMI debris at Salem are presented in Table 3c-4. Transco RMI has a much sturdier encapsulation than MRI, which affects its destruction pressure and thus its size distribution. As specified in Section 3.4.2.2 of the SER, (see Reference 3), the destruction pressure for Transco RMI (114 psi at the distance of 2.0D from the break) is much larger than the destruction pressure for Mirror RMI (2.4 psi at the distance of 28.6D from the break).

Damage to the inner insulation occurs once the protective encapsulation is breached. As the debris generated by higher jet pressures is expected to be more finely fragmented, the percentage of small debris for Transco RMI is expected to be higher than for Mirror RMI. For conservatism, 100% of Transco RMI debris is treated as being fine and small debris. Of the small debris, 10% is considered fine based on the Mirror RMI testing described above since the Mirror testing was meant to be representative of a cassette near the break, such as the Transco RMI cassettes which become debris. In the Mirror RMI testing, ~7% of the fine and small debris was fine based on 5% fines and a total of 75% small and fines; however, the fines fraction is rounded to 10% for conservatism. Fines and small pieces that enter the active recirculation pool are considered 100% transportable. Specifics of debris transport are discussed in Section 3e.

Table 3c-4: Transco RMI Size Distribution

Category	Category Percentage
Fines (< ½ inch)	10%
Small (½ inch ≤ x < 4 inch)	90%
Large (≥ 4 inch)	0%

Kaowool and Anti-Sweat Fiberglass

For NUKON, the SER guidance (Reference 3) endorses a baseline size distribution of 60% fines and small pieces and 40% large and intact pieces. The baseline debris size distribution for NUKON (jacketed or unjacketed) is used for Kaowool and anti-sweat fiberglass. This is considered appropriate since all three insulations are soft fibrous materials and the range of expected densities for Kaowool and anti-sweat fiberglass extends higher than for NUKON, which indicates that they are less likely to fail as small and fine debris when subjected to the same jet pressure. This is due in part to the larger number of contact points between fibers in the higher density materials. Kaowool is a needled insulation, while the anti-sweat fiberglass utilizes binders for adhesion. Kaowool is either encapsulated or semi-encapsulated with 0.032 inch stainless steel and has a density of 8 lbm/ft^3, while anti-sweat fiberglass is jacketed with 0.016 to 0.020 inch stainless steel and has a volume averaged density of 4.0 lbm/ft^3. The anti-sweat fiberglass jacketing is secured with 1/2 to 3/4 inch bands spaced approximately 9 inches apart. Station specific testing has also indicated that Kaowool is much less prone to erosion than NUKON, which indicates Kaowool is more robust and less likely to break into fines from the break jet blast (References A.2 and A.19). Therefore, it is conservative to apply the NUKON size distribution to Kaowool and anti-sweat fiberglass debris.

In addition, Kaowool and anti-sweat fiberglass are distributed relatively evenly among the four RCS loops. Therefore, a portion of the generated debris will be near a given break, while an approximately equal portion will be generated further from the break. Thus, the spatial orientation of the Kaowool and anti-sweat fiberglass lends itself to a baseline size distribution.

Similar to the (non-baseline) NUKON size distribution discussed above, the fines and small pieces are considered 20% fines and 80% small pieces for both Kaowool and anti-sweat fiberglass. This results in 12% (20% x 60%) of the total debris as fines and 48% (80% x 60%) of the total debris as small pieces.

However, the split between large and intact pieces is different for Kaowool and anti-sweat fiberglass. Kaowool is either encapsulated or semi-encapsulated. Therefore, some of the generated debris will be intact and not subject to erosion in the sump pool due to the encapsulation. For this reason, the large and intact pieces of Kaowool are considered 50% large pieces and 50% intact pieces, similar to the (non-baseline) NUKON size distribution discussed above. This results in 20% (50% x 40%) of the total Kaowool debris as large pieces and 20% (50% x 40%) of the total debris as intact pieces.

Unlike Kaowool or NUKON, the anti-sweat fiberglass does not have a protective outer cover. The anti-sweat fiberglass has a paper-based vapor retarder jacket. As this jacket may not retain its integrity in the sump pool, no intact debris is modeled for anti-sweat fiberglass. Thus, 40% of the total anti-sweat fiberglass debris load is large pieces. This approach is conservative in that it does not credit the stainless steel jacketing over the anti-sweat fiberglass resulting in some intact pieces.

The size distributions for Kaowool and anti-sweat fiberglass are presented in Tables 3c-5 and 3c-6, respectively.

Fines that enter the active recirculation pool are considered 100% transportable. Small pieces that enter the active recirculation pool are transported based on velocity data found in various references as discussed in Section 3e.

Table 3c-5: Kaowool Size Distribution

Category	Category Percentage
Fines	12%
Small Pieces	48%
Large Pieces	20%
Intact Pieces	20%

Table 3c-6: Anti-Sweat Fiberglass Size Distribution

Category	Category Percentage
Fines	12%
Small Pieces	48%
Large Pieces	40%
Intact Pieces	0%

Lead Blanket Covers

To determine the size distribution for the lead blanket Alpha Maritex covers, AJIT tests for unjacketed NUKON are utilized. This is conservative since the lead blanket Alpha Maritex covers are more robust than the cloth cover used for NUKON insulation based on the cloth density and weave type. The AJIT tests of unjacketed NUKON indicated that the cover material failed in large or intact pieces for all tests, including tests at surface pressures which correspond to a ZOI of 2.1D (when converted to a two-phase jet pressure). Therefore, all lead blanket cover debris between 2.1D and the ZOI boundary of 5.4D is large or intact pieces. The basis for using a ZOI of 5.4D is provided in Section 3b.4 of this response.

Within a ZOI of 2.1D, fine, small, large, and intact Alpha Maritex cover debris is generated. Based on observations from the Wyle steam jet tests documented in WCAP-16727-NP (Reference 32), only the innermost (i.e. the two cover layers closest to the break) inner and outer Alpha Maritex covers of the blankets closest to the break would become small fines as the covers behind the innermost covers would be shielded by the innermost covers and lead wool. Similarly, all covers in the second set of lead blankets would be shielded by the first set of lead blankets (there are two rows/sets of blankets around radioactive pipes). Similar to the (non-baseline) NUKON size distribution discussed above, the innermost inner and outer covers are 20% fines and 80% small pieces, while the other inner and outer covers are large and intact pieces. This approach is conservative as the lead blanket covers are much more robust than NUKON basewool.

The lead blanket cover size distribution is presented in Table 3c-7.

Table 3c-7: Lead Blanket Cover Size Distribution

Debris Type	Size	Size Distribution	
		0D < ZOI ≤ 2.1D	2.1D < ZOI ≤ 5.4D
Lead Blanket Covers (Innermost Layers - Adjacent to Break)	Fines	20%	0%
	Small Pieces	80%	0%
	Large/Intact Pieces	0%	100%
Lead Blanket Covers (Layers Furthest from the Break)	Fines	0%	0%
	Small Pieces	0%	0%
	Large/Intact Pieces	100%	100%

Min-K

The size distribution for all Min-K insulation is 100% fines. Fines that enter the active recirculation pool are considered 100% transportable.

3c.2) Provide bulk densities (i.e., including voids between the fibers/particles) and material densities (i.e., the density of the microscopic fibers/particles themselves) for fibrous and particulate debris.

NUKON

The bulk density of the NUKON insulation installed at Salem is 2.4 lbm/ft^3 (Reference A.14). This density is used for the sump strainer analyses (References A.2, A.4, A.13, A.18, and A.104) and performance testing (References A.74 and A.89). The fiber material density for NUKON is 159 lbm/ft^3 per Table 3-2 of the NEI Guidance (Reference 2).

Kaowool

Per Table 3-2 of the NEI Guidance (Reference 2) the bulk density of Kaowool insulation ranges from as low as 3.0 lbm/ft^3 to as high as 12 lbm/ft^3. The bulk density of the Kaowool insulation installed at Salem is 8 lbm/ft^3 (Reference A.14). This density is used for the sump strainer analyses (References A.2, A.4, A.13, A.18, and A.104) and performance testing (References A.74 and A.89). The fiber material density for Kaowool is 160-161 lbm/ft^3 per Table 3-2 of the NEI Guidance (Reference 2). A fiber density of 160 lbm/ft^3 is conservatively used when determining equivalent NUKON quantities.

Anti-Sweat Fiberglass

The anti-sweat fiberglass is either Owens-Corning Fiberglas or Johns Manville Micro-Lok HP. The bulk density of Owens-Corning Fiberglas insulation ranges from 3.7-3.9 lbm/ft^3 for the installed insulation thickness (1 inch) on the pipe sizes of interest (1/2 to 3 inch) (Reference A.14). The bulk density of Johns Manville Micro-Lok HP for the same insulation thickness and pipe sizes ranges from 4.0 to 5.1 lbm/ft^3 (Reference A.14). Considering 50% of each type of anti-sweat insulation in containment (Reference A.14), a volume average bulk density of 4.0 lbm/ft^3 is computed (Reference A.1). The fiber material density for Owens-Corning Fiberglas is 159 lbm/ft^3 per Table 3-2 of the NEI Guidance (Reference 2); this density is also applied to Johns Manville Micro-Lok HP since it is made of glass fibers.

The maximum Owens Corning Fiberglas bulk density of 3.9 lbm/ft^3 was used for the sump strainer performance testing (References A.74 and A.89). However, a bulk density of 4.0 lbm/ft^3 is used when determining equivalent NUKON quantities in the debris transport analysis (Reference A.2) as well as in other analyses (References A.4, A.13, A.18, and A.104).

Min-K

Per Table 3-2 of the NEI Guidance (Reference 2) the bulk density of Min-K insulation ranges from as low as 8 lbm/ft^3 to as high as 16 lbm/ft^3. The maximum bulk density of Min-K delivered to Salem based upon supplier data is 16 lbm/ft^3 (Reference A.14), which is used in the analyses (References A.2, A.4, A.13, and A.18) and testing (References A.74 and A.89).

Transco RMI and MRI

Transco RMI and MRI are comprised of thin layers of stainless steel foil. Stainless steel has a density of 490 lbm/ft^3. This density is used for the downstream wear analysis (Reference A.18).

Coatings

The material density for epoxy coatings is 94 lbm/ft^3 per Table 3-3 of the NEI Guidance (Reference 2). The epoxy coating density is also used for the steam generator coatings, which are graphite based modified silicone coatings. The material density for aluminum coatings is 90 lbm/ft^3 per Table 3-3 of the NEI Guidance (Reference 2). The material density for IOZ coatings is 457 lbm/ft^3 per Table 3-3 of the NEI Guidance (Reference 2). Note, all IOZ coatings are unqualified.

3c.3) Provide assumed specific surface areas for fibrous and particulate debris.

Specific Surface Areas for Debris

The specific surface area (S_v) is only used for preliminary analytically determined head loss values across a debris laden sump screen using the correlation given in NUREG/CR-6224. Since the head loss across the installed sump screen is determined via testing, these values are not used in the design basis for Salem. Therefore, these values are not provided as part of this response.

3c.4) Provide the technical basis for any debris characterization assumptions that deviate from NRC-approved guidance.

The debris sources at Salem include insulation, coatings, lead blanket cover material, foreign material, and latent debris. The insulation debris includes fiber (NUKON, anti-sweat fiberglass, Min-K and Kaowool) and stainless steel reflective metallic insulation (Transco RMI and MRI). The characteristics of the insulation and lead blanket cover debris material are discussed in Section 3c.1 of this response and the characteristics of the other debris types (e.g. coatings, foreign and latent materials) are included in sections 3h and 3d respectively of this response. The size distributions used do not deviate from the NRC approved guidance.

3d. Latent Debris
The objective of the latent debris evaluation process is to provide a reasonable approximation of the amount and types of latent debris existing within the containment and its potential impact on sump screen head loss.

3d.1) Provide the methodology used to estimate quantity and composition of latent debris.

3d.2) Provide the basis for assumptions used in the evaluation.

Latent Debris

Latent debris sources are evaluated by containment walkdown as recommended by Section 3.5.2 of the NEI Guidance (Reference 2) and confirmed by the NRC SER (Reference 3). A walkdown of the Salem Unit 2 containment was conducted to determine the appropriate latent debris amount (Reference A.15, Attachment 8.1). The walkdown conforms to the guidance provided in NEI 04-07 (Reference 2) with only minor variations as discussed below.

As shown below, three or more samples were collected for most surface types. The additional samples collected for certain surface types increase the statistical accuracy of the evaluation. Less than three samples were collected for three surface types. Only two samples are available for horizontal HVAC ducting; therefore, the samples collected for horizontal cable trays and horizontal HVAC ducting were combined and used for both categories. Similarly, no samples are available for vertical cable trays; therefore, data from vertical HVAC ducting are used in place of vertical cable tray data. This approach is considered acceptable based on the similarity of the debris on these surfaces. No samples are available for grating; therefore, grating is assumed to have the same latent debris loading as the floor. A listing of the number of each sample type follows.

Number of Samples Collected

Liner 3	HVAC Duct (Vertical) 5
Equipment (Horizontal) 4	Pipe (Horizontal) 3
Equipment (Vertical) 5	Pipe (Vertical) 4
Floor 4	Cable Tray (Horizontal) 3
Wall 5	Cable Tray (Vertical) 0
HVAC Duct (Horizontal) 2	Grating 0

The mass of the samples is accurate to 0.01 grams and is used to determine the latent debris mass distribution (g/ft^2). A statistical analysis of the samples is performed in the calculation of latent debris (Reference A.15). The analysis determines a 90% confidence limit of the mean value for each type of surface based on a normal distribution.

The upper limit of the mean value for each surface type is then applied over the entire surface area of that type throughout containment. This analysis lends further confidence and conservatism to the latent debris mass determination.

Given that the Salem Units are subject to the same housekeeping and closeout procedures, it is reasonable to apply the Salem Unit 2 results to Salem Unit 1. Therefore, a walkdown for Salem Unit 1 was not performed.

The Salem Unit 2 walkdown determined that 33 lb_m (Reference A.15) of latent debris is present in the containment of that Salem Unit; however, for conservatism, 200 lb_m of latent debris is applied to both Salem Units and is considered to be an appropriate maximum value (per Section 3.5.2.2 of NEI 04-07, Reference 2).

Consistent with the NRC SER (Reference 3), 15% of the latent debris load (by mass) is assumed to be fibrous debris and the other 85% (by mass) is treated as particulate debris. Likewise, consistent with the NRC SER (Reference 3), densities of 2.4 lb_m/ft^3 (bulk density) for fibrous debris and 168.6 lbm/ft^3 (2.7 g/cm^3) for particulate debris are used.

As the specific surface area of debris is only relevant for head loss calculations using the correlation in NUREG/CR-6224 (Reference 8) and the strainer head loss is determined experimentally, the specific surface area of latent debris was not determined.

Foreign Materials

Labels, tags, stickers, placards and other miscellaneous or foreign materials are also evaluated via walkdown. A foreign material walkdown was conducted for each Salem Unit. The walkdowns conform to the guidance provided in NEI 02-01 (Reference 20). The results of the walkdowns are reported in the Salem Unit specific walkdown reports (References A.16 and A.17). The walkdowns determined that Salem Units 1 and 2 contain 572 ft^2 and 525 ft^2, respectively, of labels, placards, etc.

Miscellaneous foreign material is also discussed in more detail in the debris transport section of this response (Section 3e).

3d.3) Provide results of the latent debris evaluation, including amount of latent debris types and physical data for latent debris as requested for other debris under c. above.

The amount of latent debris considered for Salem is provided in Table 3d-1. Per section 3.5.2.3 of the SER (Reference 3), 15% of the latent debris (by mass) is considered fibrous with the remainder considered particulate.

Table 3d-1: Latent Debris

Latent Debris	Units	Salem Unit 1	Salem Unit 2
Fiber (15%)	(lb_m)	30	30
Particulate (85%)	(lb_m)	170	170
Total Latent Debris	(lb_m)	200	200

3d.4) Provide amount of sacrificial strainer surface area allotted to miscellaneous latent debris.

In accordance with the SE for NEI 04-07 Section 3.5.2.2.2 (Reference 3), 75% of the calculated area of foreign materials is considered for screen sacrificial area. This reduction accounts for the overlap of foreign materials on the strainer.

A sacrificial area of 500 ft^2 is retained on the strainer surface area for labels, tags, stickers, placards and other miscellaneous or foreign materials (References A.2, A.74, and A.89). This is greater than the recommended 75% of the total foreign material debris area of either Salem Unit, as endorsed by the NEI and NRC guidance documents (References 2 and 3).

Table 3d-2: Foreign Material Debris

Foreign Material Debris	Units	Salem Unit 1	Salem Unit 2
Foreign Material Debris Total	(ft^2)	573	525
Foreign Material Debris (Reduced by 25%)	(ft^2)	430	394
Total Sacrificial Area Retained	(ft^2)	500	500

3e. Debris Transport

The objective of the debris transport evaluation process is to estimate the fraction of debris that would be transported from debris sources within containment to the sump suction strainers.

3e.1) Describe the methodology used to analyze debris transport during the blowdown, washdown, pool-fill-up, and recirculation phases of an accident.

3e.2) Provide the technical basis for assumptions and methods used in the analysis that deviate from the approved guidance.

The debris transport analysis (Reference A.2) for the Salem Units was conducted in accordance with both the NEI Guidance (Reference 2) and its associated NRC SER (Reference 3). As such, each phase of post-LOCA transport is considered: blowdown, washdown, pool fill-up and recirculation. A detailed discussion of each transport phase, including information on its effect on overall debris transport at Salem, is provided in the following paragraphs. The response to both 3e.1 and 3e.2 is contained in the "3e.1" sub-sections below.

Logic trees (Reference A.2) are used to model each phase of post-LOCA debris transport concurrently, and hence determine overall debris transport fractions for each debris type.

3e.1.1 Blowdown Transport

Blowdown transport is the transport of debris immediately following a line break and is due to the break jet. Blowdown is discussed separately for debris generated in lower containment (i.e. below the bottom of the operating floor) and debris generated in upper containment (i.e. above the bottom of the operating floor). The operating floor is at El. 130 feet and is 5 feet thick; therefore the bottom of the operating floor is at El. 125 feet. The approach is applied to generated fiber (NUKON, Kaowool, and anti-sweat fiberglass), particulate (Min-K and qualified coatings), and RMI (MRI and Transco RMI), unless otherwise noted. This approach for debris outside the ZOI is consistent with NEI 04-07 and its associated SE.

<u>Debris Generated in Lower Containment</u>

During blowdown, fiber, particulate, and RMI fine and small debris generated inside the bioshield in lower containment transports to three locations: 1) Out the four bioshield doorways to the "outer annulus" between the bioshield and the containment liner, 2) To upper containment through the openings around the four steam generators and pressurizer, and 3) To the floor inside the bioshield. Since Salem has a two-sided strainer, it is important to determine the fraction of debris which transports to upper containment since the debris in upper containment can transport directly to the back of the strainer. The bioshield has a concrete roof (the operating floor) and the only openings to upper containment are around the steam generators and the pressurizer. Large and intact debris generated inside the bioshield in lower containment transport to the floor.

Fine and small debris readily moves with depressurization air/steam flows; therefore, the flow split between lower and upper containment is needed to compute the blowdown transport fractions for these debris types. To determine steam/air flow fractions to upper and lower containment due to a potential pipe break, area ratios are used as a detailed subdivided thermal-hydraulic analysis of containment is not available. This approach is considered acceptable since the flow split during the initial pressurization of a LOCA event is dominated by the inertial term L/A (length/area). For Salem, the flow split based on the ratio of open areas results in 83% of the flow going to upper containment with the remainder (17%) going out the doors in the bioshield wall to lower containment. This flow split is identical to that which was calculated with the MELCOR code for the volunteer plant for a break in a steam generator cavity (see Figure VI-9 of Appendix VI to the Reference 3). The similarity of the flow split for Salem and the volunteer plant is not completely unexpected as the bioshield at Salem essentially acts as a single large steam generator cavity. Also, it should be noted that the flow split computed is consistent with the free volume split between upper and lower containment: ~75% of the free volume in containment is in upper containment (above the operating floor).

The guidance in the SE for a mostly uncompartmentalized containment such as those at Salem is to transport all debris to the floor. However, Salem has a two-sided strainer and some debris from upper containment may transport directly to the back side of the strainer, bypassing the debris interceptor. In order to account for this effect, 25% of the generated fine and small debris is considered to transport towards the openings around the steam generator and pressurizer during blowdown. This is the blowdown transport fraction given in Reference 3 for fine and small debris for highly compartmentalized containments.

The openings around the steam generator have grating, and the grating will prevent 25% of the small debris transported to the openings from passing through to upper containment based on the Drywell Debris Transport Tests (DDTS, Reference 9). However, there are gaps between the grating and the steam generators and there is no grating in the opening around the pressurizer. Based on the hydraulic resistance (K/A^2) of the flow path through the grating and the open areas, approximately 83% of the flow passes through the grating while 17% of the flow passes through the open area. This effectively results in preventing 20.75% (=0.83*0.25) of small debris from reaching upper containment. Thus, 19.8% of small debris reaches upper containment [=0.25*(1-0.2075)].

The remainder of the fine and small debris which does not transport out the bioshield doorways or to upper containment transports to the floor inside the bioshield.

Thus, during blowdown, fiber, particulate, and RMI debris generated in lower containment is transported along the paths shown in Table 3e.1.1-1. This information is used to determine the debris distribution on the strainer (front vs. back) prior to recirculation.

Table 3e.1.1-1: Blowdown Distribution for Debris Generated in Lower Containment

Debris Type	To Bioshield Doorways	To Upper Containment	To Bioshield Floor
Fines	17%	25%	58%
Small Pieces	17%	19.8%	63.2%
Large Pieces	0%	0%	100%
Intact Pieces	0%	0%	100%

A portion of the fiber and particulate debris (fines and small) entrained in the flow through the doorways in the bioshield will be captured as there is at least one 90° turn/bend at each doorway (see Figure 3e.1.1-1) and condensation will form on the wall surfaces almost immediately after the break. In addition, each doorway has a wire mesh door as shown in Figure 3e.1.1-2 (note, to allow water out of the bioshield, the bottom 3 feet of three of the four doors do not contain wire mesh). Based on the Colorado Engineering Experiment Station, Inc., (CEESI) tests documented in the DDTS (Reference 9), the fraction of fiber debris captured is modeled as 17%. Application of this data to particulate debris is consistent with the overall approach employed in the Volunteer Plant Analysis in Appendix VI to the SE for NEI 04-07 (Reference 3) for Min-K. The bioshield doorways are not subjected to spray due to a concrete slab above the doorways.

This approach is conservative in that it does not credit retention of fine and small fiber and particulate debris on all other wetted, but non-sprayed, surfaces (e.g. the bottom of the operating floor, the inside and outside of the bioshield and primary shield wall above the flood level, and the sides of the refuel pool below El. 125 feet) and structures (e.g. platform gratings, supports, equipment, ductwork, piping, etc.). The area of unsprayed walls and ceilings underneath the operating floor at Salem is greater than 40,000 ft^2.

The debris which transports to the doorways, but is not subject to inertial capture transports to the floor outside the bioshield during blowdown.

Fine and small RMI debris is not subject to inertial capture.

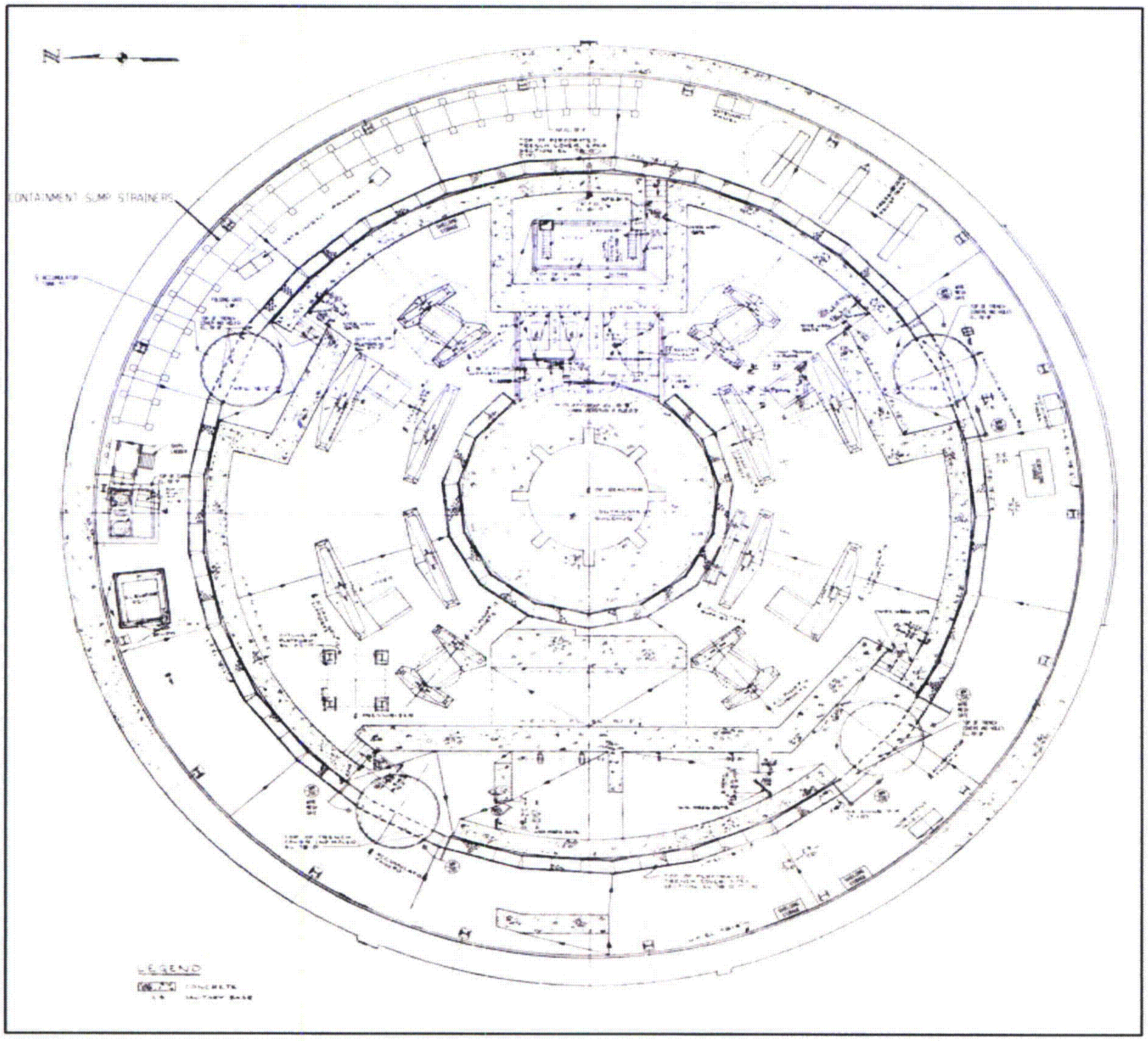

Figure 3.e.1.1-1: Plan View of Containment Basement (Unit 1 shown)

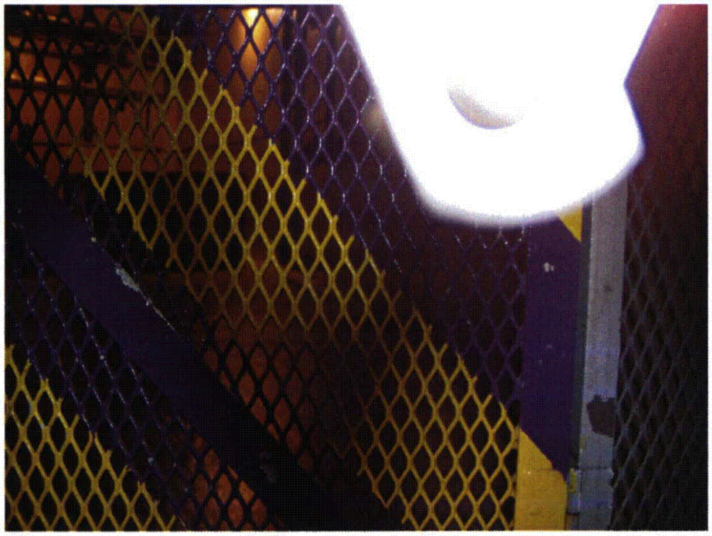

Figure 3e.1.1-2: Wire Mesh Door in Bioshield Doorway

The fiber, particulate, and RMI fine and small debris generated in lower containment which transports to upper containment is modeled as being distributed uniformly throughout upper containment on the operating floor, the steam generator and pressurizer cavities, and the refueling pool. Based on the area of the operating floor, the cavities, and the refueling pool, 72% of the fine and small debris transports to the operating floor. The remainder of fine and small debris transports to the steam generator and pressurizer cavities (13%) and the refueling pool (15%).

Debris Generated in Upper Containment

All debris generated in upper containment (above the bottom of the operating floor) remains in upper containment during blowdown. Fine and small debris are distributed throughout upper containment using the same distribution as for fine and small debris blown into upper containment from lower containment. However, large and intact debris are not distributed throughout upper containment as it is not easily transported in steam/air flows; i.e. it is more likely to fall shortly after being impacted.

Large and intact debris generated in upper containment is all generated within the steam generator or pressurizer cavities. Each steam generator is surrounded by snubber service platforms (grating) at Elevation 125 feet (the bottom of the operating floor) which will prevent large and intact debris generated above this elevation from falling to the floor below (at Elevation 81 feet). Although there is an 8.3 inch gap between the steam generator and the grating, it is assumed that the large and intact debris is blown "up and away" when impacted; i.e. insulation debris will not fall straight down and off the steam generator immediately after being impacted. Each successive section of insulation would impact the next (higher) section of insulation, thus forcing the higher section of insulation outward, over the area with grating.

The opening in the operating floor for the pressurizer does not have grating around it and there is a 13.8 inch gap between the pressurizer and the opening in the operating floor. However, there is a 2 inch curb surrounding the pressurizer opening at Elevation 130 feet 10 inches in the pressurizer cavity. This results in an opening which is approximately 5 feet 10 inches tall (from Elevation 125 feet at the bottom of the operating floor to Elevation 130 feet 10 inches at the top of the curb on the operating floor in the pressurizer cavity). Due to the confined environment in the gap, debris generated between Elevations 125 feet and 130 feet 10 inches is modeled as being transported upwards by the jet pressure in the opening. Once the jet reaches Elevation 130 feet 10 inches, the jet expands outward in the pressurizer cavity, resulting in the large and intact debris being transported away from the pressurizer and into the cavity behind the curb.

In Unit 1, only NUKON debris (from the steam generators and pressurizer) is generated in upper containment. In Unit 2, only MRI debris from the pressurizer is generated in upper containment. However, all Unit 2 MRI debris is modeled as being generated in lower containment for simplicity. This approach is acceptable since MRI is not included in the design basis strainer head loss test debris load (see Section 3f.4.1.5.9.1 of this response).

3e.1.2 Washdown Transport

Washdown transport is the debris transport after the onset of containment spray (CS) and is due to the flow of water from the CS ring headers to the containment sump.

During washdown, debris retained on structures due to inertial capture during blowdown is washed down to the sump pool when subjected to spray. However, debris retained on structures not subject to containment spray does not necessarily transport to the sump pool. The doorways in the bioshield wall (in lower containment) are not sprayed; therefore, the debris captured due to the 90° bend does not all wash down to the sump pool. Based on the volunteer plant analysis (see Table VI-17 of Appendix VI to Reference 3), only 5% of fines and 2% of small debris captured on non-sprayed surfaces is expected to wash down to the sump pool due to condensate drainage. Thus, 95% of fines and 98% of small debris captured on non-sprayed surfaces remains captured during washdown.

Thus, inertial capture due to the 90° bend through the doorways will cause 2.7% [=0.17*0.17*0.95] of the fiber and particulate fines generated in lower containment to be retained on the walls. Similarly, 2.8% [=0.17*0.17*0.98] of the fiber small debris generated in lower containment will be retained on the walls. No particulate small debris is modeled.

Retention of debris by inertial capture results in ~97% of fine and small debris generated in lower containment transporting to the sump pool during blowdown and washdown.

In upper containment, all fine and small fiber, particulate, and RMI debris is transported to the sump pool during washdown. The fine and small debris in the steam generator and pressurizer cavities (13% of debris in upper containment) and refueling pool (15% of debris in upper containment) is all transported to the sump pool in front of the strainer. However, approximately 25% of the operating floor is expected to drain to areas located above and behind the sump strainers (Reference A.2). Conservatively, 25% of the fine and small debris on the operating floor is modeled as transporting to the grating above the strainer and then transporting to the strainer. Although fines would most likely transport with drainage flows, it is unlikely that small pieces would move significantly in the presence of only spray and drainage flow. Since 72% of the fine and small debris in upper containment is on the operating floor, 18% (=0.25*0.72) of the fine and small debris in upper containment is modeled as transporting to the grating over the strainer. No retention of small debris is credited due to the two gratings between the operating floor and the strainer. The remainder (75%) of fine and small debris on the operating floor transports to the sump pool in front of the strainer during washdown. Thus, 82% (=0.72*0.75+0.13+0.15) of fine and small debris in upper containment is returned to the sump pool in front of the strainer. The operating floor contains debris generated both in upper containment and debris generated in lower containment and transported to upper containment during blowdown. The locations of debris deposition in the sump pool and behind the strainer are illustrated in Figure 3e.1.2-1. There are pockets both on the front and back side of the strainer (i.e. it is two-sided).

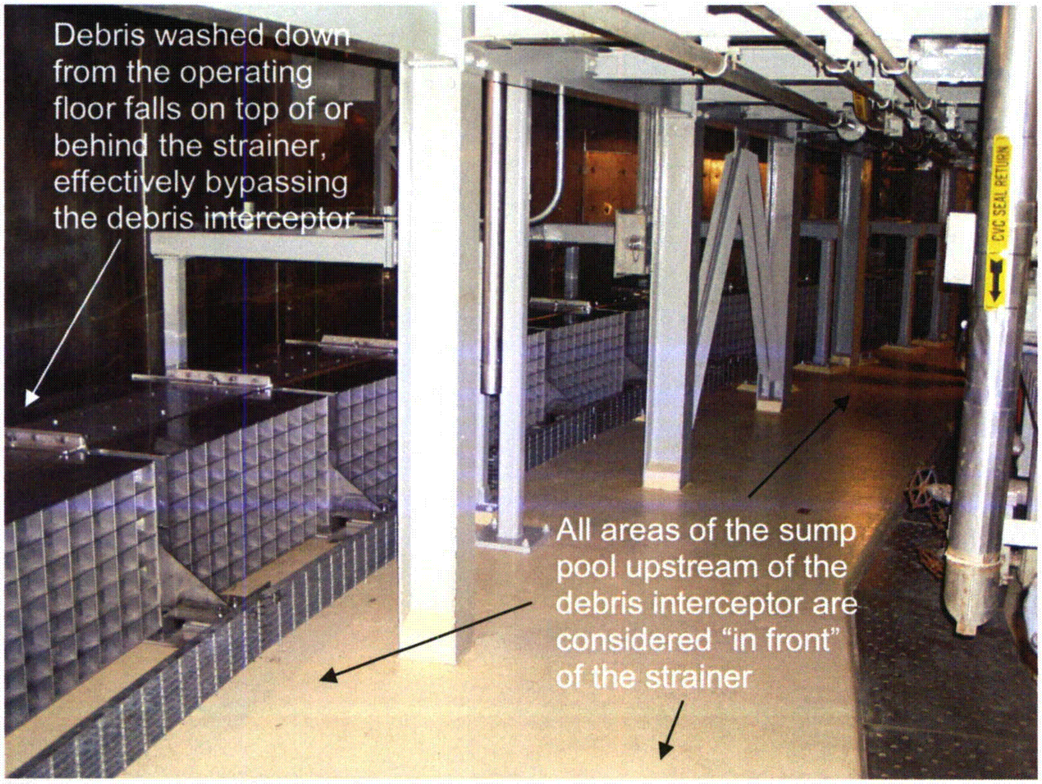

Figure 3e.1.2-1: Unit 2 Strainer Train

Debris transported directly to the strainer during blowdown and washdown may land on top of, in front of or behind the strainer modules. The majority of the grated openings on the operating floor are less than 2.5 feet wide and are 4 inches from the outer wall of containment; therefore, the majority of the debris washed down from upper containment through the grating over the strainer is expected to land behind the strainer. However, there are some obstructions (radiant shields above the strainer) which would cause some of the debris to land on top of the strainers. The distribution of debris transported to the strainer prior to recirculation is shown in Table 3e.1.2-1.

Table 3e.1.2-1: Debris Distribution at Strainer Prior to Recirculation

Unit	Behind Strainer	Top of Strainer
1	75%	25%
2	83%	17%

The large and intact debris generated in upper containment do not transport to the sump pool during washdown. As explained in Section 3e.1.1 of this response, all large and intact debris generated in upper containment remains in its respective cavity (steam generator or pressurizer). The area around the steam generators is surrounded by grating while the area around the pressurizer has a 2 inch curb, both of which are obstructions which prevent large and intact debris from transporting to the sump pool.

Large fiber debris is, however, subject to 1% erosion due to containment spray. Intact debris is not subject to containment spray erosion since the cover on intact debris protects the insulation inside. Based on Appendix VI to the SE (Reference 3), drainage flows (e.g. cascading flows) in upper containment due to containment spray would not lead to significant erosion and the use of 1% erosion is considered acceptable. Also, as demonstrated in the two cross-sectional views of containment in Figure 3e.1.2-2, there are no solid (e.g. concrete) platforms above the operating floor or steam generator/pressurizer cavities which would lead to significant cascading flow onto large debris. The platforms above the operating floor are steel grating around the SGs and pressurizer (not shown in the cross-sections). Although there are some solid steel beams, their area relative to the entire sprayed area of the operating floor is minimal.

Salem Nuclear Generating Station Units 1 and 2
Docket Nos. 50-272 and 50-311
Generic Letter 2004-02
Updated Supplemental Response for Salem

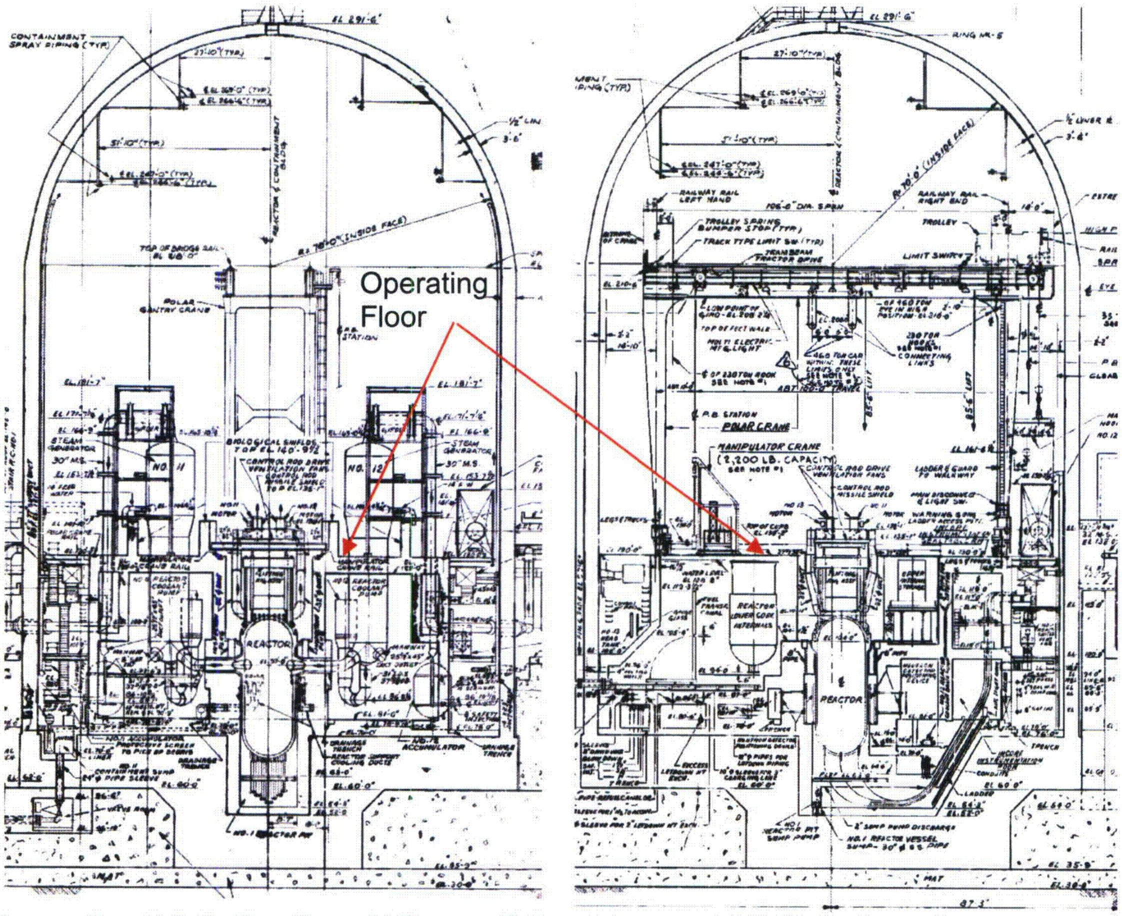

Figure 3.e.1.2-2: Sectional Views of Containment (Unit 1 shown)

Due to washdown transport, all debris in upper containment transports to lower containment except the large and intact debris retained in the steam generator and pressurizer cavities.

3e.1.3 Pool Fill-up Transport

During pool fill-up, all debris on the containment floor inside the bioshield is transported towards the secondary shield wall doorways by the water spilling onto the floor from the break. During this process, some debris is transported to and sequestered in inactive volumes. The following inactive volumes are credited: the elevator pit, the non-emergency sump, the drainage trenches which surround the primary and secondary shields, and the piping connecting the drainage trenches to the non-emergency sump. The total volume of the inactive volumes is approximately 1280 ft^3, which is 7% of the sump pool volume at switchover.

However, the trenches are covered with perforated plate with 13/16 inch holes. Therefore, not all small debris will be able to transport into the trenches based on small debris being as large as 4 inches by 4 inches (Reference 2). For the purposes of this analysis, it is assumed that 20% of the small debris will pass through the perforations, which effectively reduces the trench inactive volume which can be credited for sequestering small debris. This results in the inactive volume for small debris being approximately 480 ft^3, which is 2.6% of the sump volume at switchover.

Based on the inactive volumes discussed above, 7% of fine debris and 2.6% of small debris is sequestered in the inactive volumes. Only fine and small debris which is generated below the operating floor or transported to the sump pool during washdown is sequestered in the inactive volumes. It is reasonable to sequester fine and small debris washed down from upper containment to the sump pool, especially since the quantity of fine and small debris washed down from upper containment to the sump pool which is sequestered in inactive volumes is almost negligible (approximately 0.2% of the Unit 1 Break S1 generated total). Fine and small debris which is initially captured in the bioshield doorways and subsequently washed down to the sump pool is not sequestered in inactive volumes.

Fiber (NUKON, Kaowool, and anti-sweat fiberglass), particulate (Min-K and qualified coatings) and RMI (MRI and Transco RMI) debris are subject to sequestration in the inactive volumes. Unqualified coatings and latent debris are not subject to sequestration since they may not be transported to the sump pool until later in the transient.

Following pool fill-up transport, debris is transported by recirculation, as discussed in the following section.

3e.1.4 Recirculation Transport

Debris in the containment sump pool after blowdown, washdown, and pool fill-up transport is subject to transport by the pool flow present during recirculation.

In accordance with the NEI Guidance and its associated NRC SER (References 2 and 3), all fine debris that transports to the pool and is not sequestered in inactive volumes is assumed to transport to the sump strainer. The transport of small, large and intact pieces of debris during recirculation is dependent on the velocities present in the containment sump pool.

A CFD model developed using FLUENT was utilized to assist with the recirculation evaluation. See Section 3e.3 of this response for further discussion of the CFD model and its use.

NUKON debris transport is investigated and reported in NUREG/CR-6772 (Reference 16) and NUREG/CR-6808 (Reference 18). Transport velocities pertinent to NUKON debris transport at Salem Unit 1 and 2 are taken from these documents. These documents report values at which some debris begins to move and at which a majority begins to move. These values are referred to herein as the "incipient tumbling" and "bulk transport" velocities, respectively. Incipient tumbling velocities are conservatively used for the recirculation transport analysis.

The incipient tumbling velocities used for small and large NUKON are 0.12 ft/s and 0.30 ft/s, respectively. All available small and large NUKON debris in the active pool is considered to transport to the debris interceptors in front of the sump strainer even though more than 45% of the containment sump pool has recirculation velocities less than or equal to 0.12 ft/s and more than 70% of the containment sump pool has recirculation velocities less than or equal to 0.30 ft/s at Salem Unit 1 and 2. NUREG/CR-6772 (Reference 16) also investigates lift-over curb velocities and reports that in order for NUKON debris to transport over a 6-inch curb the pool velocity needs to be greater than or equal 0.34 ft/s.

Plant specific transport testing conducted by Fauske and Associates (Reference A.19) indicates that the appropriate lift-over curb velocity for NUKON debris at Salem is 0.51 ft/s due to the installed debris interceptors. No small or large NUKON debris transports over the debris interceptor, which is described in Section 3e.4 of this response.

Intact NUKON and NUKON jacketing is expected to transport beyond the secondary shield wall doors during pool fill-up and then come to rest, as intact debris and jacketing is not expected to transport at velocities below 0.7 ft/s, and there is no continuous flow path at this velocity between the secondary shield wall doors and the sump strainers.

Recirculation debris transport of anti-sweat fiberglass is modeled using the transport properties for NUKON. This is conservative since anti-sweat fiberglass is made of the same (Owens-Corning Fiberglas) or similar (Johns Manville Micro-Lok HP) glass fibers as NUKON, but in a more compact (dense) form. Therefore anti-sweat fiberglass is less likely to transport than NUKON. However, similar to NUKON, all available small and large anti-sweat fiberglass debris in the active pool is considered to transport to the debris interceptors in front of the sump strainer.

Also, consistent with NUKON, none of the small and large anti-sweat fiberglass debris transports over the debris interceptors.

Kaowool debris transport is also investigated and reported in NUREG/CR-6772 (Reference 16). The minimum incipient tumbling velocity of Kaowool is found to be 0.12 ft/s, which is for large pieces (smaller pieces exhibited a higher incipient tumbling velocity). As for NUKON, all small and large Kaowool debris in the active pool is assumed to transport to the debris interceptors in front of the sump strainer. The lift-over curb velocity for a 6 inch curb for Kaowool reported in NUREG/CR-6772 (Reference 16) is 0.47 ft/s for large pieces and 0.41 ft/s for shredded pieces.

Plant specific transport testing conducted by Fauske and Associates (Reference A.19) indicates that the appropriate lift-over curb velocity for Kaowool debris at Salem Unit 1 and 2 is 0.61 ft/s for very small pieces (smaller than ½ inch by ½ inch) and 0.69 ft/s for other Kaowool pieces due to the installed debris interceptors. No small or large Kaowool debris transports over the debris interceptor, which is described in Section 3e.4 of this response.

Intact Kaowool and Kaowool jacketing is expected to transport beyond the secondary shield wall doors during pool fill-up and then come to rest. Intact debris and jacketing is not expected to transport at velocities below 0.7 ft/s, and there is no continuous flow path of this velocity between the secondary shield wall doors and the sump strainers.

Testing was also performed to determine if NUKON and Kaowool debris is buoyant. The testing indicated that pieces of NUKON and Kaowool readily sink in hot (~200°F) water. The testing is applicable to anti-sweat fiberglass as well due to its similarity to NUKON. Therefore, transport due to floating insulation is not modeled.

RMI debris transport is investigated in NUREG/CR-3616 (Reference 7) and NUREG/CR-6772 (Reference 16). Transport velocities pertinent to RMI debris transport at Salem are taken from these documents. NUREG/CR-3616 (Reference 7) reports transport velocities for multiple sizes of RMI foil debris, but the minimum incipient tumbling velocity reported is 0.20 ft/s. Conservatively, this incipient tumbling velocity is used for small and large debris in the transport analysis. As with NUKON and Kaowool debris, all small and large RMI in the active pool debris is considered to transport to the debris interceptors in front of the sump strainer.

NUREG/CR-6772 determined that the lift-over curb velocity for both ½ inch by ½ inch and 2 inch by 2 inch pieces of RMI is greater than 0.99 ft/s for a 6 inch curb.

No small or large RMI debris transports over the debris interceptor, which is described in Section 3e.4 of this response.

Intact RMI and jacketing is expected to transport beyond the secondary shield wall doors during pool fill-up and then come to rest. Intact RMI and jacketing is not expected to transport at velocities below 0.7 ft/s, and there is no continuous flow path of this velocity between the secondary shield wall door and the sump strainers.

Plant specific fibrous debris erosion values were determined by testing performed by Fauske and Associates (Reference A.19). The Salem erosion testing is described in Section 3e.1.5 of this response.

3e.1.5 Erosion Testing

The discussion of the erosion testing is split into two parts: 1) description of the test set-up and configuration, and 2) data analysis.

3e.1.5.1 Erosion Test Description

Plant specific erosion testing was performed for the two primary types of fiber insulation present at Salem: NUKON and Kaowool. The fiber pieces used in the erosion tests were scissor cut into rectangular pieces with sizes between 1/4 inch and 4 inches, although the erosion data used was based on 1 inch, 2 inch, and 3 inch pieces. All fiber samples were baked prior to the erosion tests to simulate exposure to hot surfaces in containment. The erosion tests focused solely on small piece debris with no large debris included in the tests. Exclusion of large piece debris was conservative, as acknowledged by the NRC in the Salem audit report (Reference A.78).

Based on Section 3c.1 of this response, approximately 1/3 of the NUKON debris generated in lower containment (below El. 125 ft) is larger than that tested in the erosion tests. Anti-sweat fiberglass and Kaowool have similar size distributions to NUKON. Application of the erosion data from small debris to the large debris is clearly very conservative and offsets any non-conservatisms with respect to the method of debris preparation and testing methodology.

For each test, samples of each type of insulation were placed in two stacked wire mesh baskets which extended across the entire width of the flume. The NUKON fiber samples and Kaowool fiber samples were distributed between the two baskets such that the samples only occupied a fraction of the total basket volume and each piece of fiber was directly exposed to the flowing water. Initially, when all the fiber samples were placed in the two baskets, the fraction of the total basket volume occupied by the fiber samples was approximately 20% for NUKON and 35% for Kaowool. As fiber samples were removed to be dried and weighed, the volume occupied by the debris in the two baskets continually decreased. The open nature of the baskets facilitates erosion and removal of eroded debris from the baskets. A turbulence suppressor and flow straightener were located upstream of the fiber samples/baskets.

Erosion data was obtained for various erosion intervals. After each erosion interval, the wet fiber erosion samples were placed on trays, weighed and placed in a drying oven. The oven temperature was maintained at approximately 45 to 50°C while the erosion samples were dried. The samples were periodically removed from the oven and the samples and tray were re-weighed. The erosion samples and tray were then returned to the drying oven for additional drying. This process was continued until the weight of the erosion samples and tray did not change. To determine the long term erosion rates, the same fiber samples were used throughout the tests (i.e. long term erosion rates were obtained using pre-eroded pieces). Thus, the total exposure time of any given fiber sample was equal to the sum of all of the erosion intervals which were used to determine the erosion rate at different times for that fiber sample. To help explain this methodology, the testing chronology for Piece III of 1 inch NUKON is traced in Table 3e.1.5.1-1.

Table 3e.1.5.1-1: Testing Chronology of Piece III of 1 inch NUKON

Test	Erosion Interval for Fiber Sample (hr)	Total Erosion Time for Fiber Sample (hr)	Comments
ER05	4.83	4.83	New 1 inch sample of NUKON (Piece III) placed in flume. Piece removed after 4.83 hrs and dried. Erosion rate computed based on the erosion interval in this test.
ER07	6.08	10.91	Piece III from ER05 placed in flume for 6.08 hrs, resulting in a total erosion time of 10.91 hrs (4.83+6.08). Piece removed after 6.08 hrs and dried. Erosion rate computed based on the erosion interval in this test.
ER08	12.10	23.01	Piece III from ER07 placed in flume for 12.10 hrs, resulting in a total erosion time of 23.01 hrs (10.91+12.10). Piece removed after 12.10 hrs and dried. Erosion rate computed based on the erosion interval in this test.
ER11	192	215.01	Piece III from ER08 placed in flume for 192 hrs, resulting in a total erosion time of 215.01 hrs (23.01+192). Piece removed after 192 hrs and dried. Erosion rate computed based on the erosion interval in this test.
ER11	24	239.01	Piece III from earlier in ER11 placed in flume for and additional 24 hrs, resulting in a total erosion time of 239.01 hrs (215.01+24). Piece removed after 24 hrs and dried. Erosion rate computed based on the erosion interval in this test.

Figures showing the flume and wire mesh baskets are provided below. Note, the capture screen shown in Figures 3e.1.5.1-1 and 3e.1.5.1-2 was not used. These figures also do not show the wire mesh baskets which were used in the tests.

Salem Nuclear Generating Station Units 1 and 2
Docket Nos. 50-272 and 50-311
Generic Letter 2004-02
Updated Supplemental Response for Salem

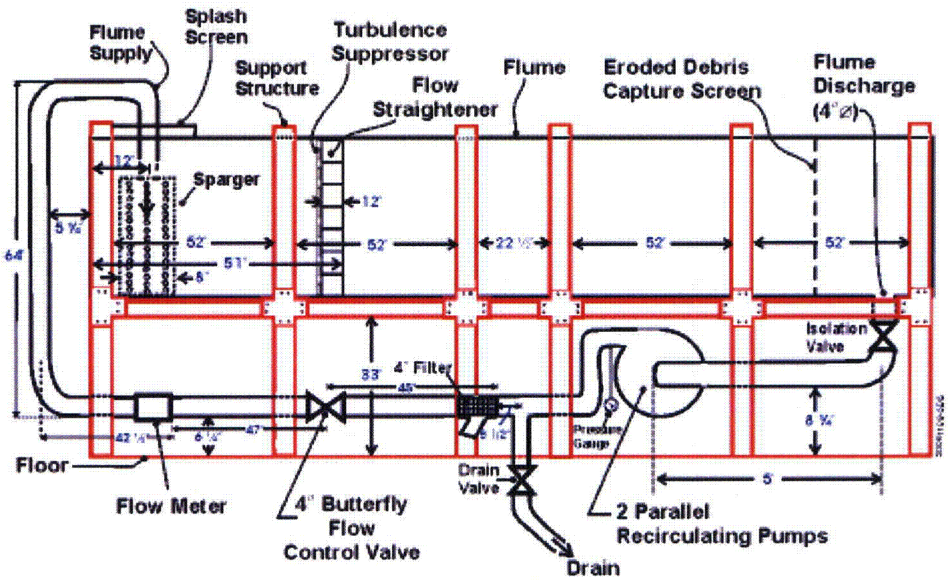

Figure 3e.1.5.1-1: Side View of Flume

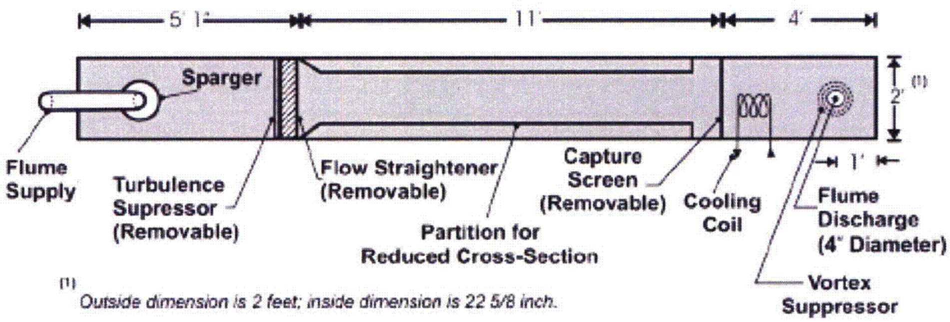

Figure 3e.1.5.1-2: Top View of Flume

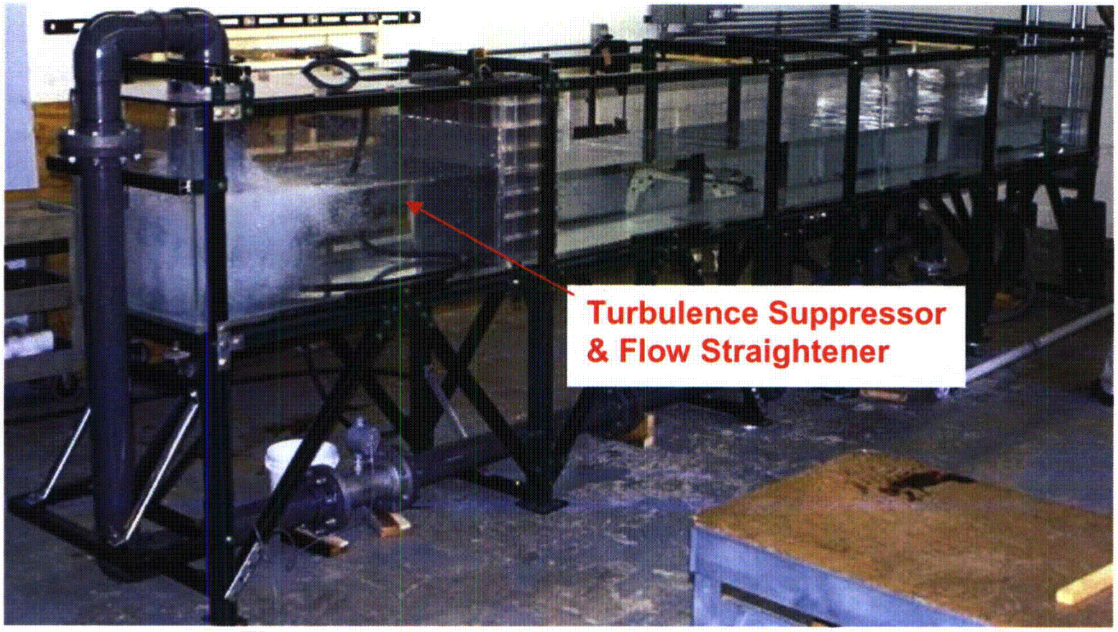

Figure 3e.1.5.1-3: Photo of Test Apparatus

Figure 3e.1.5.1-4: Fiber Samples in Baskets in the Flume During a Test

The majority of erosion test data points were obtained using a nominal flume velocity of 0.72 ft/s, while one set of data points was taken at 0.4 ft/s. The flume velocity of 0.72 ft/s exceeds the incipient tumbling velocity of 0.12 to 0.30 ft/s for small and large NUKON, respectively, by 240% to 600%. In addition, more than 98% of the sump pool experiences velocities less than 0.7 ft/s based on CFD analysis. Similarly, ~82% of the sump pool experiences velocities less than ~0.4 ft/s at 3 inches above the floor. More than 60% of the sump pool experiences velocities less than 0.2 ft/s at 3 inches above the floor. In addition, the velocity experienced near the debris interceptor is less than 0.41 ft/s over 95% of the debris interceptor (the velocity around the debris interceptor is generally less than 0.27 ft/s near the floor). Thus, the velocities used in the erosion tests were clearly conservative for either debris stalled in the sump pool or debris which transports to the debris interceptor but does not lift over the debris interceptor. Velocity contours from the CFD analysis are presented in Figures 3e.1.5.1-5 and 3e.1.5.1-6 and turbulent kinetic energy (TKE) contours are presented in Figures 3e.1.5.1-7 and 3e.1.5.1-8.

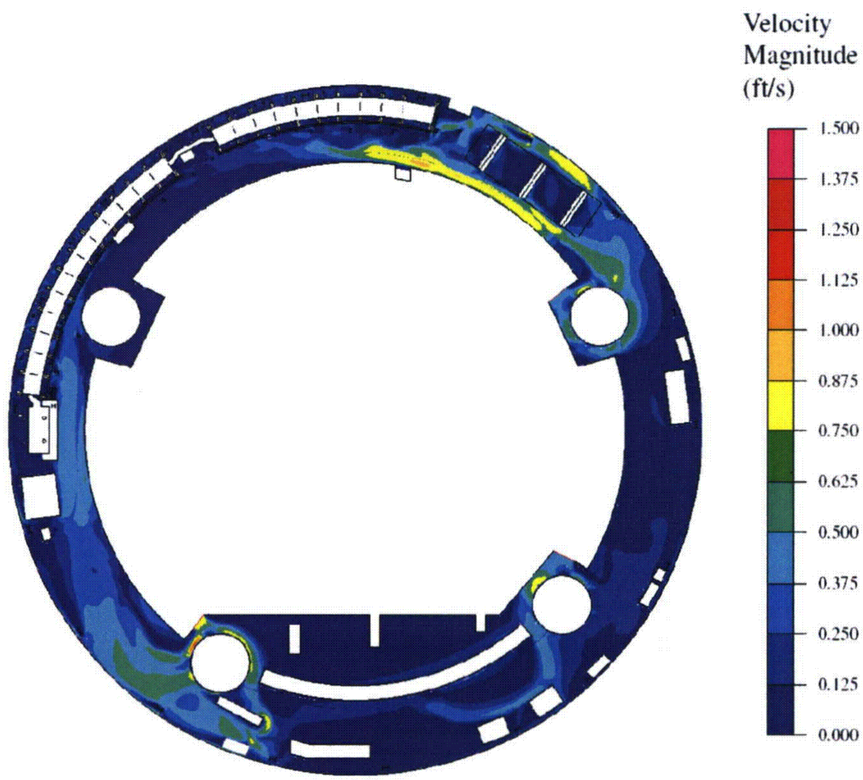

Figure 3e.1.5.1-5: Velocity Magnitude 3 inches Above Floor for 9000 gpm Total Flow

Salem Nuclear Generating Station Units 1 and 2
Docket Nos. 50-272 and 50-311
Generic Letter 2004-02
Updated Supplemental Response for Salem

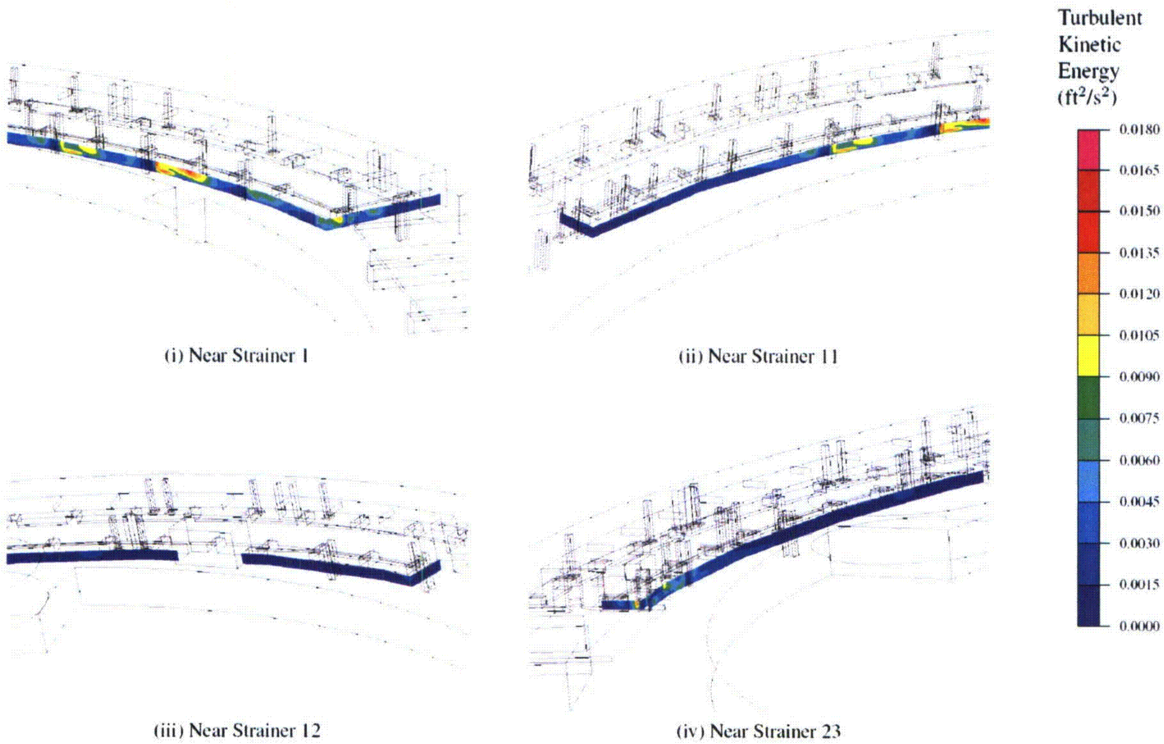

Figure 3e.1.5.1-6: Velocity Contour 12 inches in Front of Debris Interceptor

Salem Nuclear Generating Station Units 1 and 2
Docket Nos. 50-272 and 50-311
Generic Letter 2004-02
Updated Supplemental Response for Salem

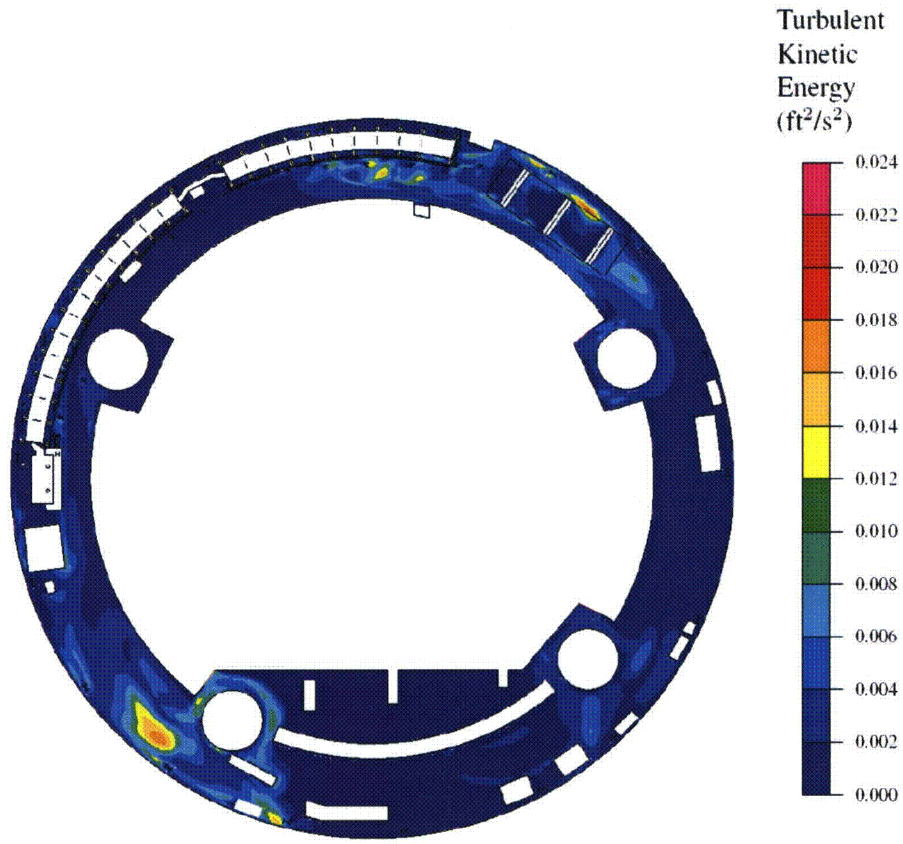

(iii) Entire Containment

Figure 3e.1.5.1-7: TKE 3 inches Above Floor for 9000 gpm Total Flow

Salem Nuclear Generating Station Units 1 and 2
Docket Nos. 50-272 and 50-311
Generic Letter 2004-02
Updated Supplemental Response for Salem

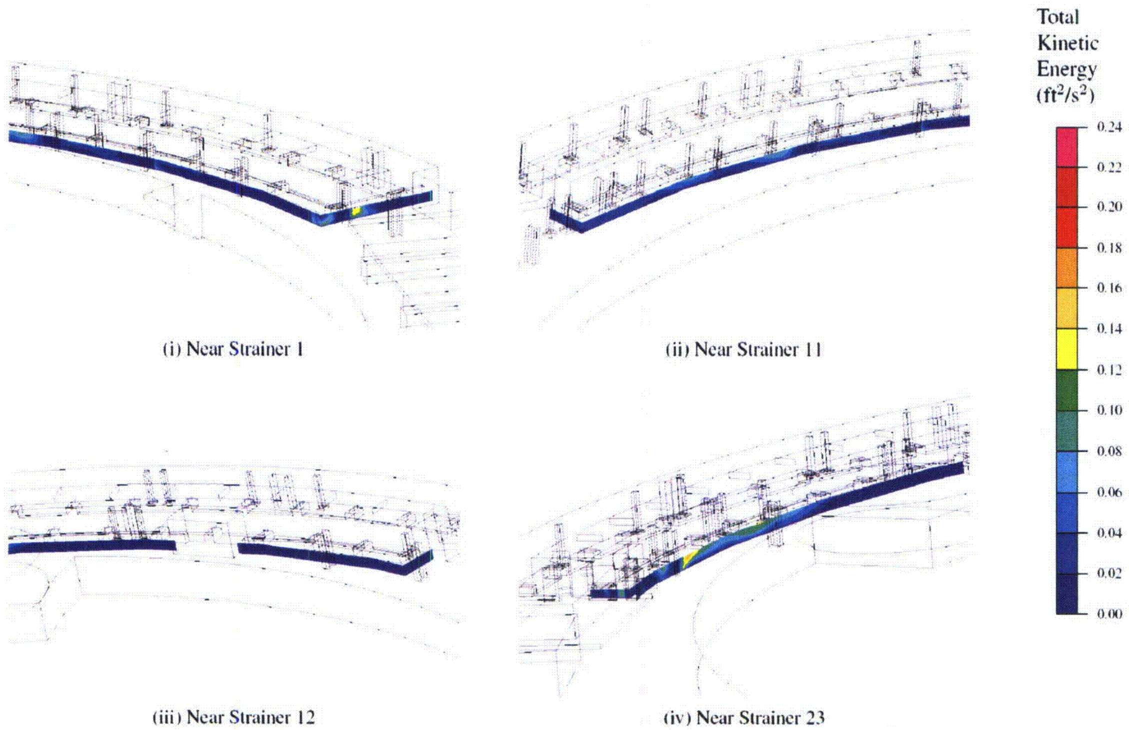

Figure 3e.1.5.1-8: TKE Contour 12 inches in Front of Debris Interceptor

The CFD analysis to determine the flow velocity used in the erosion tests is based on the minimum water level (El. 80 feet 10 inches). In reality, the minimum water level will occur at a single point at the start of the post-LOCA recirculation transient. As the water level rises, the flow velocities in the sump pool will be reduced proportionally. Thus, the fiber which is stalled in the pool or at the debris interceptor will be exposed to lower flow velocities and will erode at a slower rate.

Furthermore, the water height above the fiber samples in the erosion tests was much less than that which would exist in the plant during recirculation. The tests utilized a flume water depth of 11.5 to 14.375 inches. In the plant, the minimum water level is 80 feet 10 inches at recirculation initiation, the maximum floor height is 78 feet 4 inches in the annulus, and the debris interceptor height is approximately 9 inches; thus, there will be a minimum freeboard of 21 inches above the debris interceptor (total water depth of 30 inches).

Although it is possible that the turbulence level (TKE) in the test flume was less than in much of the sump pool due to the turbulence suppressor, it is judged that the conservatism in the velocities used for testing are sufficient to offset the lack of turbulence. Although the chaotic, multi-directional variations in flow most likely do impact the erosion rate, the shear stress on the surface of the erosion samples is also a significant factor and the shear stress on the surface of the fiber samples is related to the flow velocity. The test flow velocity of 0.72 ft/s is almost double the flow velocity in most of the pool. Furthermore, since the fiber samples act as porous obstructions to flow in the flume, the velocity around the edges of the fiber samples in the test is much greater than the bulk velocity of 0.72 ft/s tested. For example, the velocity around a 2 inch fiber piece would be 120% [=12/(12-2)] of the nominal flume velocity in the test (with 12 inches of water) but only 107% [=30/(30-2)] of the nominal pool velocity in the plant (assuming no flow through the fiber pieces).

In addition, Figures 3e.1.5.1-5 and 3e.1.5.1-7 demonstrate that the areas of the sump pool which have the highest turbulence levels also typically have the highest flow velocities. Therefore, it is likely that the debris which would stall in the sump pool (such as that which exits the bioshield from the doorway in the lower right hand corner of containment in the figures) and be subject to erosion would be in areas of the pool with very low TKE and velocities much less than the tested velocity of 0.72 ft/s. The NUKON and Kaowool incipient and bulk tumbling velocities applicable to the Salem sump configuration range from 0.12 to 0.30 ft/s.

It is likely that debris in front of the debris interceptors will be strewn about on the floor over a large distance from the strainer. In this case, most fiber pieces would only be exposed to flowing water on one side (the top) since other fiber pieces would be next to all other sides except the bottom, which would be on the floor. This is conservative in comparison to the fiber pieces in the erosion test in which at least 2 sides (top or bottom and front) of the fiber samples were exposed to flowing water. For fiber samples at the edges of the wire baskets, 3 sides were exposed (top or bottom and front and side). The relatively "open" nature of the volume surrounding the fiber samples in the baskets allowed the fiber samples to move around freely with flow perturbations in the flume. Therefore the fiber samples were more prone to erosion in the basket than fiber pieces would be on the floor of the sump pool or at the debris interceptor where fiber pieces would be more compact and less apt to move around with flow perturbations.

For the above reasons, it is judged that the erosion test flume conservatively modeled the conditions for debris stalled on the floor of the sump pool and debris which would transport to the vicinity of the debris interceptor.

3e.1.5.2 Data Analysis

The details regarding the data reduction and statistical analysis used to compute the 30-day erosion percentages are provided in this section.

The data from the erosion tests performed by FAI was first inspected to ensure that it was appropriate for use. As a result of this inspection, data from several tests was discarded. Data was discarded for two reasons: 1) inaccurate debris collection method and 2) fiber sample delamination during testing. In addition, some data indicated that no erosion had occurred over a given time period. Although plausible, these data points were conservatively not included in the statistical analysis, thus resulting in higher average erosion rates.

For NUKON, a total of 40 data points are used which includes 29 short term data points and 11 long term data points. Of the short term data points, 23 are based on a nominal flow rate of 0.72 ft/s and 6 are based on a nominal flow rate of 0.40 ft/s. This is considered acceptable since the majority of the pool experiences velocities less than 0.41 ft/s, as described above. The inclusion of the lower velocity data results in a slightly lower, although more realistic, short term erosion rate than would result from the use of the high velocity data exclusively. For Kaowool, a total of 24 data points are used which includes 15 short term data points and 9 long term data points. The long versus short term data points are described below.

The data from the erosion tests is analyzed using the t-distribution. This distribution is appropriate for use in experimental scenarios where there is no knowledge of the population average (μ) or variance (σ), which is often the case when working with small sample sets (such as the erosion data). For large sample sizes ($n \geq 30$), the t-distribution does not differ significantly from the standard normal distribution.

Inspection of the data from the erosion tests reveals that the long-term results (those tests lasting longer than approximately 24 hours) for both NUKON and Kaowool can be characterized as normally distributed. This is based on a comparison of the data to the Normal distribution. The short-term results (those tests lasting approximately 24 hours or less) exhibit a more random distribution. This is possibly a result of the sample preparation which causes small fibers to be generated, but which remain on the sample pieces. These small fibers are then washed off the pieces relatively soon after being placed in the test flume, causing a "puff" of fibers to be "eroded." While this phenomenon is not erosion in the strictest sense, it is nonetheless a real phenomenon that would likely occur for jet damaged insulation during and/or shortly after a LOCA; therefore, it is not discounted in this evaluation.

After the "puff" subsides, the erosion mechanism is expected to be constant, i.e. the method of erosion is not expected to change between the short-term tests and the long-term tests. Therefore, it is reasoned that the non-normality of the short-term sample distribution is a matter of the sample size not being sufficiently large to capture the normality of the larger population, rather than a fundamental difference between short and long-term erosion. Thus, it is assumed, based on the normality of the long-term data and the expected similarities between short and long-term erosion, that the short-term test data can also be characterized as normally distributed. Furthermore, given the randomness of the short-term data, a precise means of analysis is not readily available. However, this approach is considered acceptable given the conservatisms integral to this analysis. Thus, the use of the t-distribution for analysis of the short and long-term erosion data is appropriate based on the inspection of the data in comparison to the normal distribution.

Separate analyses are conducted for the data from the short-term tests (t < 27 hours for NUKON and t < 25 hours for Kaowool) and those from the long-term tests (t > 27 hours for NUKON and t > 25 hours for Kaowool). The split between short and long term data was based on the erosion intervals tested. This data may be utilized in a time dependent debris generation analysis, but the results are also combined to give an indication of the total erosion over the course of the entire 30-day recirculation period. The analyses of the short-term and long-term data are conducted similarly and the method of combining the data sets is presented below.

The analyses are begun by determining the sample mean (x) and sample standard deviation (s) using basic statistical equations, given below, where x_i is a data point and n is the number of data points. The data is given in percent per hour.

$$x\ (\%/\text{hr}) = \frac{\sum x_i}{n}$$

$$s\ (\%/\text{hr}) = \sqrt{\frac{\sum (x_i - x)^2}{n-1}}$$

For the long-term data, each data point is then evaluated for statistical validity using the Grubbs test which is outlined in Reference 40. This step is skipped for the short-term data due to the non-normality of that data, as discussed above. Reference 40 provides Critical T values (re-named Critical Z values herein) which, based on the sample size under investigation, provide a means of determining if a data point is an “outlier” or invalid point. If the Z value of a given point (Z_i), calculated using the equation below, is greater than the Critical Z value, that point is likely an outlier and is therefore excluded from the analysis.

$$Z_i = \frac{|x - x_i|}{s}$$

The Critical Z values chosen for the analysis of the erosion data are for a 5% Significance Level, which is analogous to a 5% chance of erroneously discarding a valid data point. Essentially, a 5% Significance Level equates to a 95% confidence that all invalid data points are identified correctly.

A single outlier was found in the Kaowool long-term data and no outliers were found in the NUKON long-term data. Since the outlier was determined to be higher than expected, rather than lower, it was left in the analysis of the population mean and confidence level for conservatism; however, it was excluded from the calculation of the tolerance limit. Since the calculated tolerance limit is not used for anything other than development of Figures 3e.1.5.2-1 and 3e.5.1.2-2, the result of excluding the outlier in this portion of the analysis only highlights the disparity between the outlier data point and the valid data points. Because no outliers were excluded from the calculation of the population mean and confidence interval, the sample mean and standard deviation calculated using all data points are used throughout the analysis. These values of the mean and standard deviation are then used in the determination of the population mean confidence interval and the upper and lower tolerance limits.

Since the exact population mean is unknown, a confidence interval is used to determine the probable population mean. A 90% confidence level is used, meaning that the population mean is expected to be within the determined interval 90% of the time. The confidence interval is determined using the equation below where CL represents the limits of the confidence interval. The t-distribution value ($t_{\alpha/2}$) is determined based on α =0.10 ($\alpha/2$=0.05) where α is 1 minus the confidence level.

$$CL\ (\%/hr) = x \pm \frac{t_{\alpha/2}}{\sqrt{n}} \times s$$

The expected (A = x), minimum (A = minimum CL), and maximum (A = maximum CL) average erosion fraction over a time period is calculated using the equations below. The expected values as well as the upper and lower bounds are computed. Two equations are used since the short and long-term erosion data are evaluated separately. These equations are based on Section III.3.3.3 of Appendix III of the NRC SE for NEI 04-07 (Reference 3).

For short term erosion (up to time t in hours): $ER_{0-t}\,(\%) = 1 - \left(1 - \frac{A}{100}\right)^{t}$

For long term erosion (from time t to 720 hours): $ER_{t-720}\,(\%) = 1 - \left(1 - \frac{A}{100}\right)^{720-t}$

These values are then combined using the following equation to determine the expected, minimum, and maximum total erosion fraction over a 30-day period.

$$ER_{0-720}\,(\%) = ER_{0-t} + (1 - ER_{0-t}) \times ER_{t-720}$$

To further evaluate the quality of the data, a tolerance limit is determined and the sample data is compared to it. Similar to a confidence interval, a tolerance limit provides boundaries within which a value is expected to fall a certain amount of the time. For this analysis, a 95% tolerance limit is calculated with a 95% confidence level; thus, there is a 95% confidence that the tolerance limits bound 95% of the data. The upper tolerance limit (UTL) is determined using the following equation, where k is based on the confidence level and the proportion of measurements bound by the limits. The lower tolerance limit is not computed since analytically it is less than 0 which is not physically possible; thus the lower tolerance limit is not included in Figures 3e.1.5.2-1 and 3e.5.1.2-2.

$$UTL\,(\%/hr) = x + k \times s$$

Unlike a confidence interval, which bounds the population mean, a tolerance limit is intended to bound a percentage of all the data (in this case, 95%). Hence, the fact that the vast majority of the data falls within the tolerance limit boundaries (see Figures 3e.1.5.2-1 and 3e.5.1.2-2) lends further support to the validity of the data.

Based on the statistical analysis, the average erosion rate for NUKON debris is 0.35 ± 0.20 %/hr during the first 27 hours that the NUKON is exposed to flowing water. After 27 hours, the average erosion rate decreases to 0.016 ± 0.005 %/hr. Using this data, it is determined that the average 30-day erosion fraction for small and large piece NUKON debris is 18.4 +7.1/-7.8%. To be conservative, a 30-day erosion fraction of 20%, which is the average 30-day erosion fraction plus 9% margin, is considered acceptable for NUKON debris.

Use of the average erosion values with margin for NUKON rather than the upper bound erosion is judged to be appropriate and reasonable. This approach is consistent with the Drywell Debris Transport Study (NUREG/CR-6369, Reference 9), which states that central estimates (averages) are realistic representations while upper bound values are those which will most likely never be exceeded. Furthermore, this approach is consistent with the overall holistic resolution approach endorsed by the Commission in its Staff Requirements Memorandum dated November 16, 2006 (Reference 41), which states that licensees may use a combination of measures which provide reasonable assurance that long term core cooling is maintained.

Based on the statistical analysis, the average erosion rate for Kaowool debris is 0.11 ± 0.049 %/hr during the first 25 hours that the Kaowool is exposed to flowing water. After 25 hours, the average erosion rate decreases to 0.0028 ± 0.0013 %/hr. Using this data, it is determined that the average 30-day erosion fraction for small and large piece Kaowool debris is 4.6 +2.0/-2.1%. Since the initial "puff" of fibers from the Kaowool samples was not included in the data due to a testing anomaly, a 30-day erosion fraction of 10%, which provides a margin of 52% over the upper confidence limit of 6.6%, is considered acceptable for Kaowool debris.

Fibers used in NUKON are held together with a binder (e.g. adhesive) and are not woven or needled based on discussions with PCI. Some (30-60%) of the binder burns off when exposed to hot surfaces such as the steam generators or pressurizer at Salem. Conversely, Kaowool does not contain any binder/adhesive based on discussions with Thermal Ceramics. Kaowool is manufactured using a needling process in which the fibers are physically interlocked, giving the product its tensile strength. Thus, Kaowool subjected to erosion retains much of its strength whereas NUKON subjected to erosion would be essentially weaker due to the binder burn off. More binding locations along with a physically stronger "binding" of the fibers supports the argument that Kaowool is stronger than NUKON, and therefore is less susceptible to erosion. This conclusion is consistent with the Kaowool and NUKON erosion testing performed.

The erosion data and results of the data analysis are presented in Figures 3e.1.5.2-1 through 3e.1.5.2-4. In each of these plots, the data from individual fiber samples is delineated. The data shown for "other pieces" is for pieces which only showed observable erosion in one interval; i.e. other intervals in the flume did not show observable erosion and therefore are conservatively not included in the erosion analysis. The short term data points are those where the fiber samples were in the flume for less than 27 or 25 hours for NUKON and Kaowool, respectively. The long term data points are those where the fiber samples were in the flume for greater than 27 or 25 hours for NUKON and Kaowool, respectively. The time separating short- and long-term erosion was selected based on the trends shown by the data in Figures 3e.1.5.2-1 and 3e.1.5.2-2.

Figures 3e.1.5.2-1 and 3e.5.1.2-2 show the erosion rate as a function of the time in the flume for NUKON and Kaowool, respectively. From these figures, it is evident that the initial (short-term) erosion rate is much higher than the long-term erosion rate for each fiber piece tested indicating that the erosion rate decreases significantly over time.

In addition, Figures 3e.1.5.2-1 and 3e.5.1.2-2 show the confidence interval (LCL = lower confidence limit, UCL = upper confidence limit), the upper tolerance limit (UTL), and outlier data points. The short and long term average erosion rates used to compute 30-day erosion fractions of 20% and 10% for NUKON and Kaowool, respectively, are also shown. The data supports 20% and 10% 30-day erosion fractions.

Figures 3e.1.5.2-3 and 3e.5.1.2-4 show the cumulative erosion percentage for a given fiber sample as a function of time in the flume / total erosion time. The data in these figures show that the cumulative erosion percentage for each fiber piece increases over time, as expected. In addition, the predicted cumulative erosion percentage based on the erosion rates supporting 30-day erosion fractions of 20% and 10% for NUKON and Kaowool, respectively, is shown in each figure.

Figure 3e.1.5.2-1: NUKON Erosion Rate

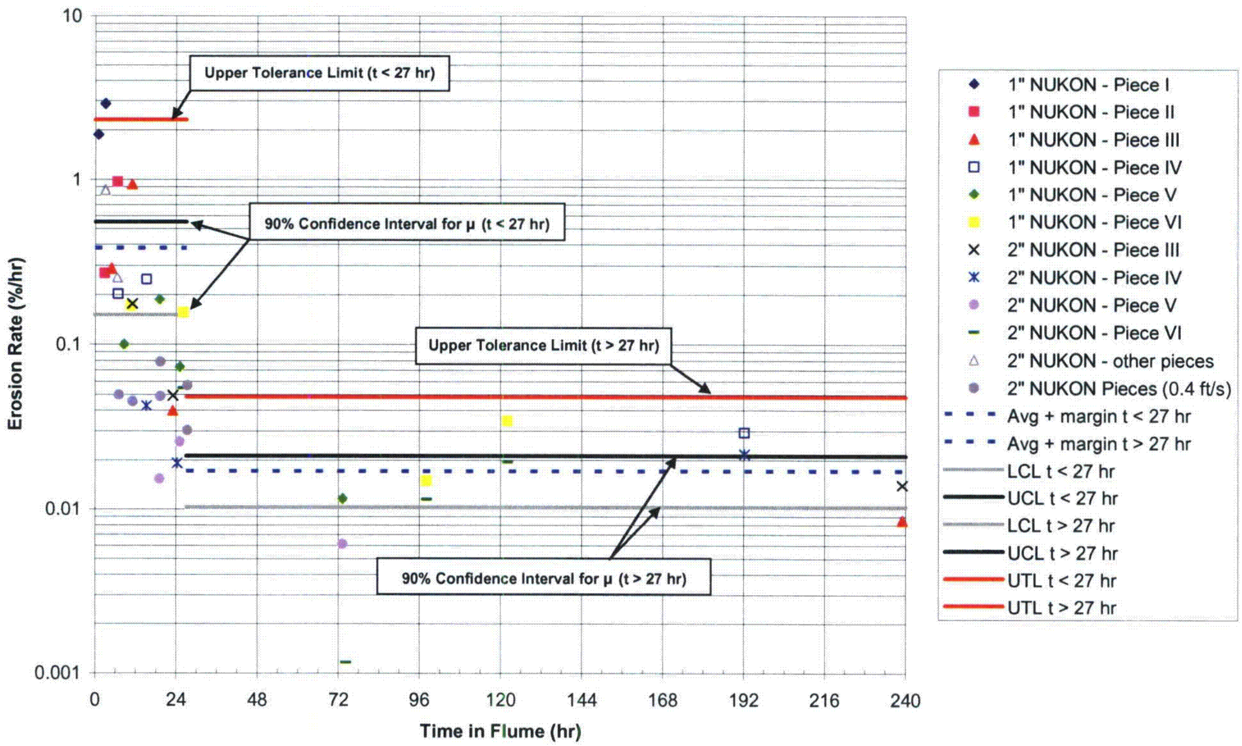

Salem Nuclear Generating Station Units 1 and 2
Docket Nos. 50-272 and 50-311
Generic Letter 2004-02
Updated Supplemental Response for Salem

Figure 3e.1.5.2-2: Kaowool Erosion Rate

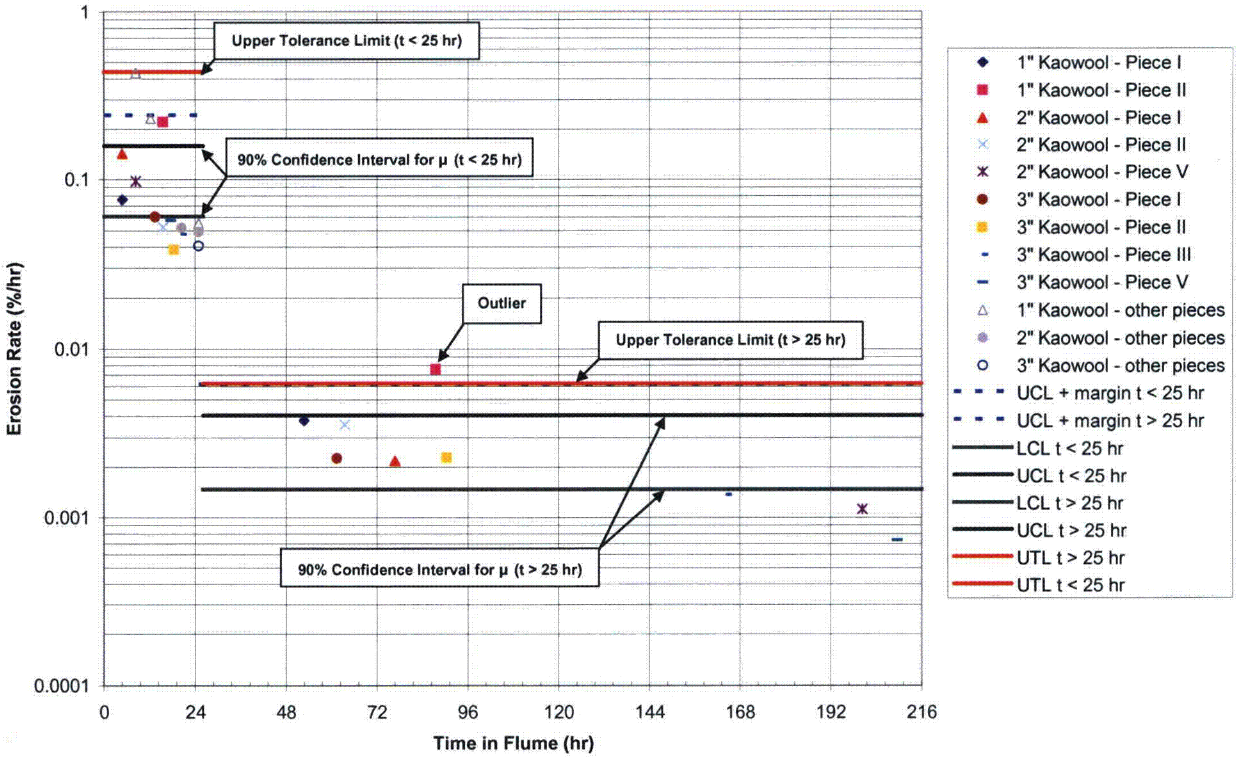

Salem Nuclear Generating Station Units 1 and 2
Docket Nos. 50-272 and 50-311
Generic Letter 2004-02
Updated Supplemental Response for Salem

Figure 3e.1.5.2-3: NUKON Cumulative Erosion - 10 days

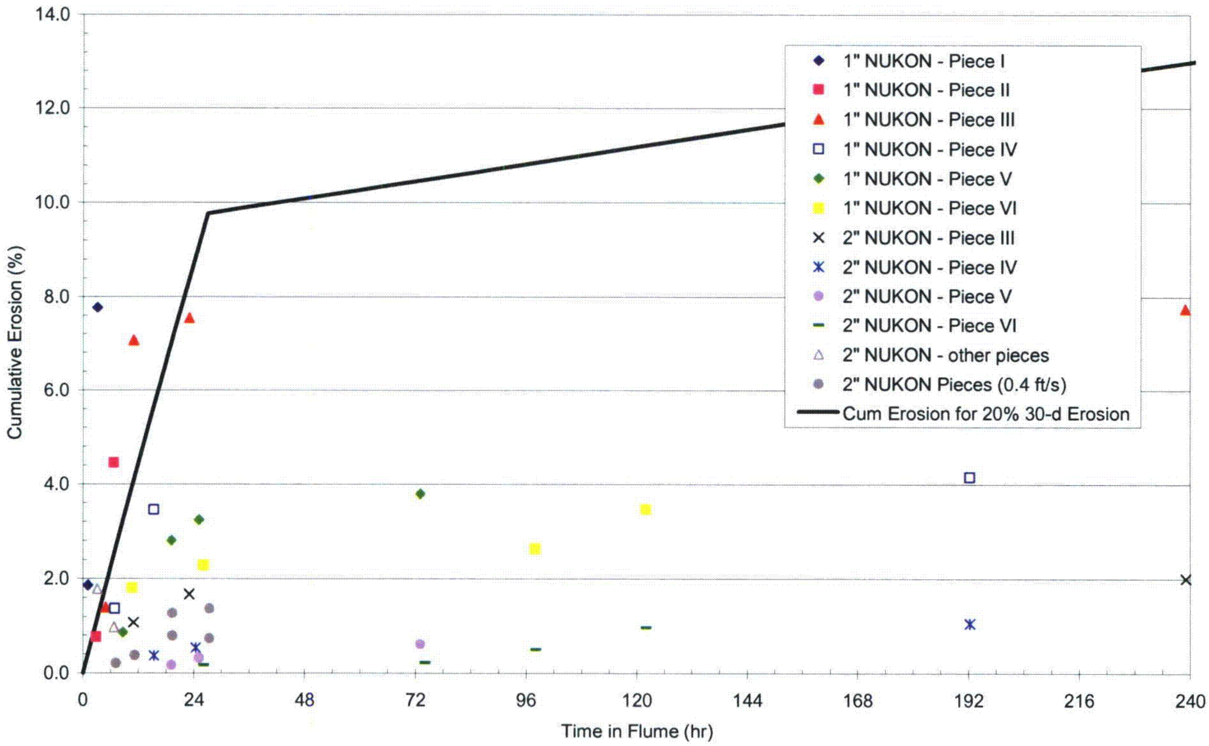

Figure 3e.1.5.2-4: Kaowool Cumulative Erosion - 10 Days

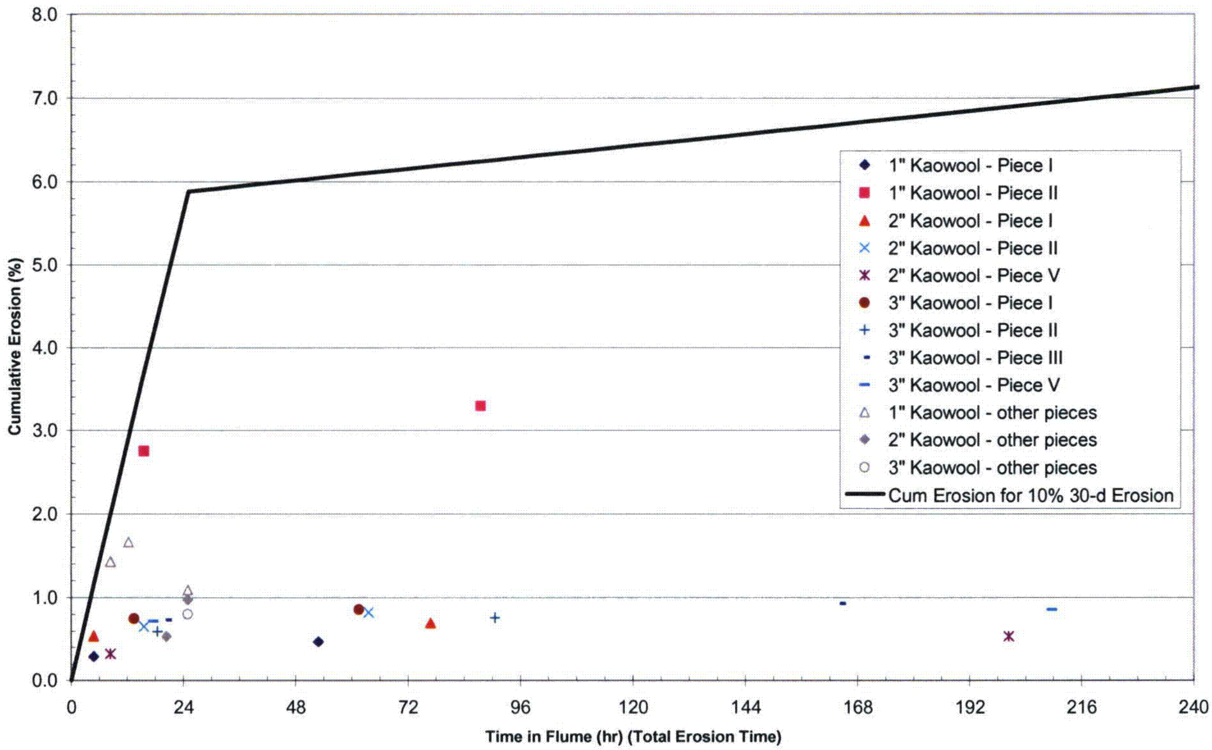

Based on the above data, analysis, and conservatisms intrinsic in the testing, 30-day erosion fractions of 20% and 10% are considered acceptable for NUKON and Kaowool, respectively. This data analysis is consistent with Section 3.5.3.3 of the Salem GL 2004-02 NRC Audit Report (Reference A.78) from the October 2007 on-site audit, in which the 30% and 10% values were independently verified by the NRC as conservatively high. However, based on April 2010 discussions with the NRC, a 30-day erosion fraction of 15% is used for Kaowool. This represents a margin of 127% above the upper confidence limit of 6.6 % determined by testing.

The use of 30-day erosion fractions of 20% and 15% for NUKON and Kaowool is also considered conservative due to the following conservatisms implicit in the testing and overall sump performance analysis.

- All debris in active the pool is conservatively modeled as transporting to the debris interceptor in the transport analysis as opposed to stalling in the pool in low-flow areas of the pool or being retained on structures.

- The 30-day erosion quantity was modeled as arriving at the sump at the onset of recirculation rather than over a 30-day period in the vendor strainer testing. This is conservative since the debris load would be transient and since erosion would most likely be inhibited once chemical precipitates form and deposit on stalled fiber pieces in the pool.
- The design sump flow is maintained for 30-days post-accident.

3e.3) Identify any computational fluid dynamics codes used to compute debris transport fractions during recirculation and summarize the methodology, modeling assumptions, and results.

To assist in the determination of recirculation transport fractions, several CFD simulations were performed using a commercially available software package, FLUENT Version 6.1.22. The use of the program was validated by developing a model of the test apparatus described in NUREG/CR-6773 (Reference 17). The model was then evaluated to ensure that its results closely matched the results reported in NUREG/CR-6773 (Reference 17). FLUENT was found to be in agreement with NUREG/CR-6773.

To gain an understanding of the effect of various parameters on the flow within containment, the following inputs were varied between CFD simulations: flood height, screen design, flow rate through the strainer, flow rate through the break, stairway obstructions, and debris interceptors and containment spray flow.

Two simulations (13 and 14) were used in the evaluation of debris transport. These simulations are representative of the installed strainer modules and the actual containment conditions at the minimum water level following a LOCA. The simulation results include a series of contour plots of velocity and turbulent kinetic energy, plots of flow path lines originating at the break locations and animations of the flow velocities as a function of elevation.

These results were combined with information in the GSI-191 literature and plant specific erosion test results to determine the overall transport fractions for small and large pieces of debris (fines are transportable regardless of pool velocities).

Simulations 13 and 14 of the CFD analysis investigate the installed strainer modules and as-built containment layout. Simulation 14 investigates two-train recirculation, which results in pool velocities higher than Simulation 13, which investigates single train recirculation. Therefore, Simulation 14 is used for the determination of transport fractions.

As stated in Section 3e.1.4 of this response, all debris in the active pool except for intact debris and insulation jacketing, is conservatively considered to transport to the debris interceptors in front of the sump strainer during recirculation. Once reaching the debris interceptors, the CFD analysis is utilized to determine the amount of debris capable of transporting over the interceptors (see Section 3e.4).

3e.4) Provide a summary of, and supporting basis for, any credit taken for debris interceptors.

Debris interceptors are installed at both Salem Unit 1 and 2 around the perimeter of the sump strainers. These debris interceptors are shaped like an upside down "L" with the lip of the interceptor (or the base of the letter "L") facing upstream.

Figure 3e.4-1: Debris Interceptor Installed in Front of Strainer Modules

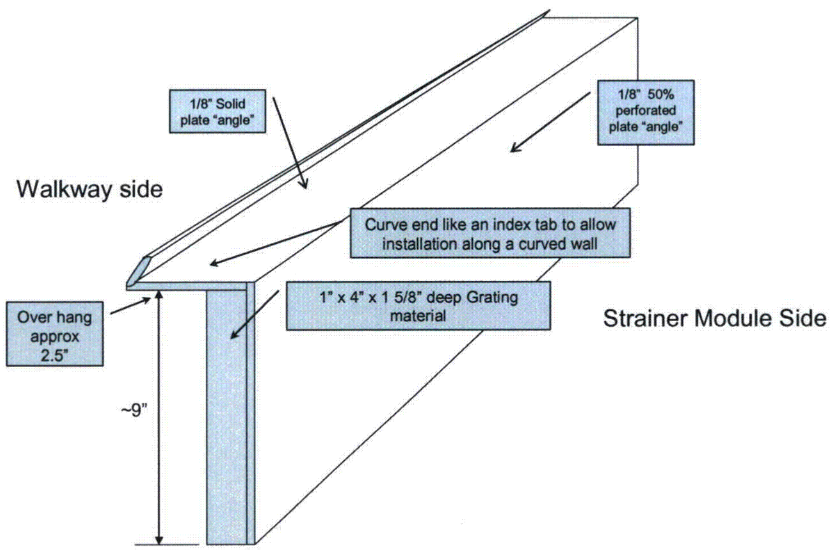

The interceptors stand 9.125-inches high and the lip extends 4-inches upstream (see picture above). They are constructed of grating, perforated plate and solid 11 gauge plate. Plant specific testing conducted by Fauske and Associates (Reference A.19) indicates that the lift-over curb velocities for these interceptors is at least 50% greater than those reported in NUREG/CR-6772 (Reference 16) for a 6-inch curb (Reference A.2). The calculation of debris transport over the debris interceptors is based on the Fauske data whenever possible.

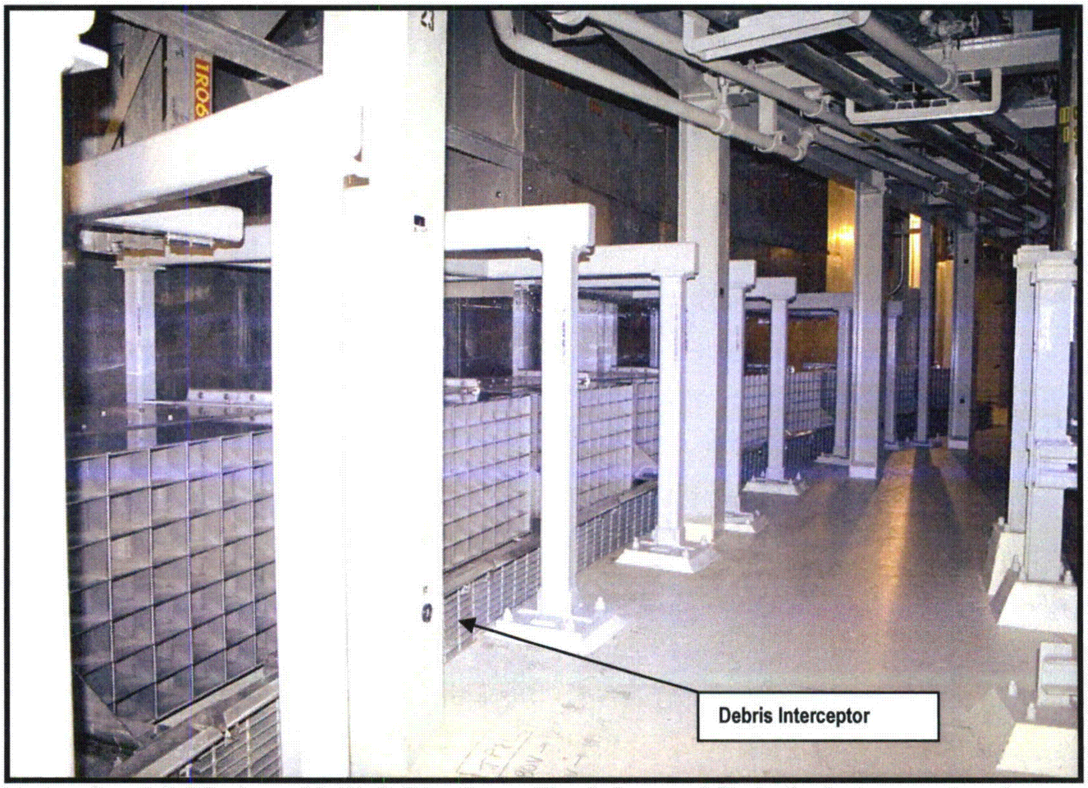

Figure 3e.4-2: Salem Unit 1 Strainer Module and Debris Interceptor Layout

The debris interceptors are not credited for holding up any fine debris. The debris interceptors are credited for holding up small and large pieces of NUKON, Kaowool, anti-sweat fiberglass, Transco RMI, and MRI insulation only. Small and large pieces of NUKON, anti-sweat fiberglass, and Kaowool are subjected to erosion at the debris interceptor as discussed in Section 3e.1.5 of this response.

All fines in the active sump pool are all treated as transporting unimpeded to the sump strainer.

3e.5) State whether fine debris was assumed to settle and provide basis for any settling credited.

In accordance with the NEI Guidance and NRC SER, all fine debris in the active sump pool is modeled as transporting to the strainers.

3e.6) Provide the calculated debris transport fractions and the total quantities of each type of debris transported to the strainers.

The amount of debris determined to transport to the sump strainer for the limiting breaks is provided in Table 3e.6-1. The quantity of NUKON for each of the four potentially limiting breaks is included for Unit 1; Break S1 is the limiting break for NUKON. Similarly, the quantity of coatings for each of the potentially limiting breaks is included for both units; Break S10 is the limiting break for coatings. The MRI and Transco RMI quantity presented is the maximum of the four potentially limiting breaks. The four breaks analyzed are discussed in Section 3b.4 of this response.

Logic trees (Reference A.2) were used in the determination of the overall transport fractions for each debris type. The logic trees include the applicable phases of debris transport discussed herein.

As no small and large piece fibrous debris is expected to lift over the debris interceptor, all fibrous debris which transports to the strainer during recirculation is considered fine debris as described in Sections 3e.1 and 3e.2 of this response. In addition, a small amount of small piece debris transports to the downstream/back side of the strainer during blowdown as shown in Table 3e.6-2.

Table 3e.6-1: Total Debris Generated and Transported to Strainer

Debris Type	Units	Generated Debris	Total Debris Transport	Total Debris Transport Fraction
Insulation (U1)				
NUKON (Break S1)	[ft^3]	1360	232.5	0.17
NUKON (Break S7)	[ft^3]	993	199.3	0.20
NUKON (Break S8)	[ft^3]	1144	211.0	0.18
NUKON (Break S10)	[ft^3]	1064	168.9	0.16
Kaowool	[ft^3]	97	21.5	0.22
Anti-sweat Fiberglass	[ft^3]	48	14.1	0.29
MRI	[ft^2]	33,240	2380	0.07
Insulation (U2)				
Kaowool	[ft^3]	122	27.0	0.22
Anti-sweat Fiberglass	[ft^3]	50	14.7	0.29
Min - K	[ft^3]	17.5	15.9	0.91
MRI	[ft^2]	39,990	2863	0.07
Transco RMI	[ft^2]	3150	395	0.13
Qualified Coatings (U1&U2)				
Break S1	[ft^3]	4.4	4.0	0.91
Break S7	[ft^3]	5.3	4.8	0.91
Break S8	[ft^3]	4.5	4.1	0.91
Break S10	[ft^3]	6.1	5.5	0.91
Unqualified Coatings				
Unit 1	[ft^3]	1.89	1.89	1.0
Unit 2	[ft^3]	1.21	1.21	1.0
Latent Debris[1] (U1 & U2)	[lbm]	200	200	1.0
Lead Blanket Covers				
Unit 1	[ft^2]	1200	54.6	0.046
Unit 2	[ft^2]	1340	61.0	0.046
Foreign Materials[2]				
Labels / Placards (U1)	[ft^2]	573	573	1.0
Labels / Placards (U2)	[ft^2]	525	525	1.0

1) *Latent debris consists of 30 lbm of fiber and 170 lbm of particulate (see Section 3d.3 of this response); this is equivalent to 12.5 ft^3 of fiber and 1.01 ft^3 of particulate based on the bulk densities provided in the SE for NEI 04-07 (Reference 3).*
2) *The quantity presented does not account for overlap on the strainer – see Section 3d.4 of this response.*

As discussed in the debris transport calculation (Reference A.2) and the blowdown and washdown portions of Sections 3e.1 and 3e.2 of this response, some debris transports to the strainer modules prior to the onset of recirculation by transporting to upper containment during blowdown and then to the strainers during washdown.

This transport path results in some of the debris being deposited on top of or behind the strainer modules. The final distribution of debris (on top or behind strainer versus in front of the strainer) is shown in Table 3e.6-2.

Table 3e.6-2: Location of Transported Debris at Strainer

Debris Type	Units	Transport Analysis Values[1]	
		In Front of Strainer	Top/Back of Strainer
Insulation (U1)			
NUKON (Break S1)	[ft^3]	212.4	20.1
NUKON (Break S7)	[ft^3]	176.4	22.9
NUKON (Break S8)	[ft^3]	191.6	19.4
NUKON (Break S10)	[ft^3]	158.0	10.9
Kaowool	[ft^3]	19.3	2.2
Anti-sweat Fiberglass	[ft^3]	13.0	1.1
MRI	[ft^2]	1476	903
Insulation (U2)			
Kaowool	[ft^3]	24.3	2.7
Anti-sweat Fiberglass	[ft^3]	13.6	1.1
Min - K	[ft^3]	15.1	0.8
MRI	[ft^2]	1776	1087
Transco RMI	[ft^2]	280	115
Qualified Coatings (U1&U2)			
Break S1	[ft^3]	3.8	0.2
Break S7	[ft^3]	4.6	0.2
Break S8	[ft^3]	3.9	0.2
Break S10	[ft^3]	5.3	0.3
Unqualified Coatings			
Unit 1	[ft^3]	1.89	0.0
Unit 2	[ft^3]	1.21	0.0
Latent Debris			
Fiber	[ft^3]	12.5	0.0
Particulate	[ft^3]	1.01	0.0
Lead Blanket Covers			
Unit 1	[ft^2]	54.6	0.0
Unit 2	[ft^2]	61.0	0.0
Foreign Materials			
Labels / Placards (U1)	[ft^2]	573	0.0
Labels / Placards (U2)	[ft^2]	525	0.0

Notes:
1) Sum does not necessarily equal the total in Table 3e.6-1 due to truncation.

3f. Head Loss and Vortexing

The objectives of the head loss and vortexing evaluations are to calculate head loss across the sump strainer and to evaluate the susceptibility of the strainer to vortex formation.

3f.1 Provide a schematic diagram of the emergency core cooling system (ECCS) and containment spray systems (CSS).

The following are simplified P&ID drawings associated with the ECCS and CSS. These drawings are included in Attachment 7 to this submittal.

- Drawing 205250-Simp No 1 Salem Unit ECCS Simplified P&ID
- Drawing 205350-Simp No 2 Salem Unit ECCS Simplified P&ID
- Drawing 205234-Simp No 1 Salem Unit Safety Injection Simplified P&ID
- Drawing 205334-Simp No 2 Salem Unit Safety Injection Simplified P&ID
- Drawing 205235-Simp No 1 Salem Unit Containment Spray Simplified P&ID
- Drawing 205335-Simp No 2 Salem Unit Containment Spray Simplified P&ID

3f.2 Provide the minimum submergence of the strainer under small-break loss-of-coolant accident (SBLOCA) and large-break loss-of-coolant accident (LBLOCA) conditions.

Although the discussion is applicable to both SBLOCA and LBLOCA, it is expected that for some SBLOCAs the outflow from the RWST may be low enough that transition to recirculation phase may not be necessary. The plant may be stabilized before the RWST level depletes to the point of having to align the ECCS for recirculation.

The minimum submergence of the strainer for initiation of recirculation phase is 3-5/16 inches (Reference A.6) for both Salem Unit 1 and Salem Unit 2. However, strainer head loss testing conservatively used a 3-inch submergence.

The minimum strainer submergence was conservatively determined using the maximum elevation of the top of the strainer along with the minimum post-LOCA sump water level elevation. The maximum elevation of the top of the strainer is determined as the strainer module height plus the height of the strainer feet off the floor.

The strainer feet are adjustable and are conservatively modeled as fully extended. In addition, the floor in the outer annulus at Salem (where the strainer is located) is sloped upwards from the secondary shield wall to the containment liner (the total rise is 2 inches).

The strainer was conservatively considered to be located at the highest floor elevation, even though the strainer was placed several feet away from the containment liner. The floor elevation at this point is approximately 1 inch lower than at the liner.

3f.3 Provide a summary of the methodology, assumptions and results of the vortexing evaluation. Provide bases for key assumptions.

This section contains a discussion of both the vortexing and deaeration analyses performed for the installed strainers while flashing is discussed in Section 3f.14 of this response. These analyses are documented in the strainer head loss calculation (Reference A.77) and the deaeration calculation (Reference A.104). The analyses show that the void fraction at the RHR pump inlet does not result in adverse operating conditions for all analyzed scenarios.

3f.3.1 Vortexing Analysis

Air ingestion due to vortexing typically takes place where local high water velocities are present. For the installed strainer configuration, vortexing conditions are addressed for the following three scenarios.

1. For a clean strainer, the high flow rates into the module closest to the sump can lead to excessive water velocities through the pockets and may result in the formation of vortices.

2. If the RHR pumps are stopped and then restarted with a debris laden strainer, local deaeration inside the strainer following the pump stop may result in the release of air bubbles downstream of the debris bed. The air bubbles then can rise to the top of the strainer where they produce local clean strainer windows by dislodging small areas of debris. At pump restart, high velocities through the clean strainer windows may occur and may result in the formation of vortices.

3. Local bore holes in a debris laden strainer can lead to high flow rates through these holes, thus inducing high local water velocities which may lead to the formation of vortices.

Each of the above scenarios is assessed in the following subsections.

3f.3.1.1 Vortexing Due to High Velocities Through the Clean Strainer

Generic vortex testing has been performed by the strainer vendor, CCI, in which high rates of flow were forced through four clean strainer pockets under minimal submergence conditions (Reference A.77). The results of these tests defined three regimes of vortex intensity as a function of Froude number and submergence.

- Regime A: More or less stationary limited vortex cones at surface with no air intake into pockets
- Regime B: Infrequent unsteady vortices which cause singular air bubble intake at frequencies of 1 to 5 short-duration vortices within 5 minutes
- Regime C: Frequent unsteady vortices with 2 to 5 vortices within 1 minute, however no air intake that would come close to 1% volume flow.

The three regimes are presented in Figure 3f.3.1.1-1.

Figure 3f.3.1.1-1: Clean Strainer Vortexing Limits

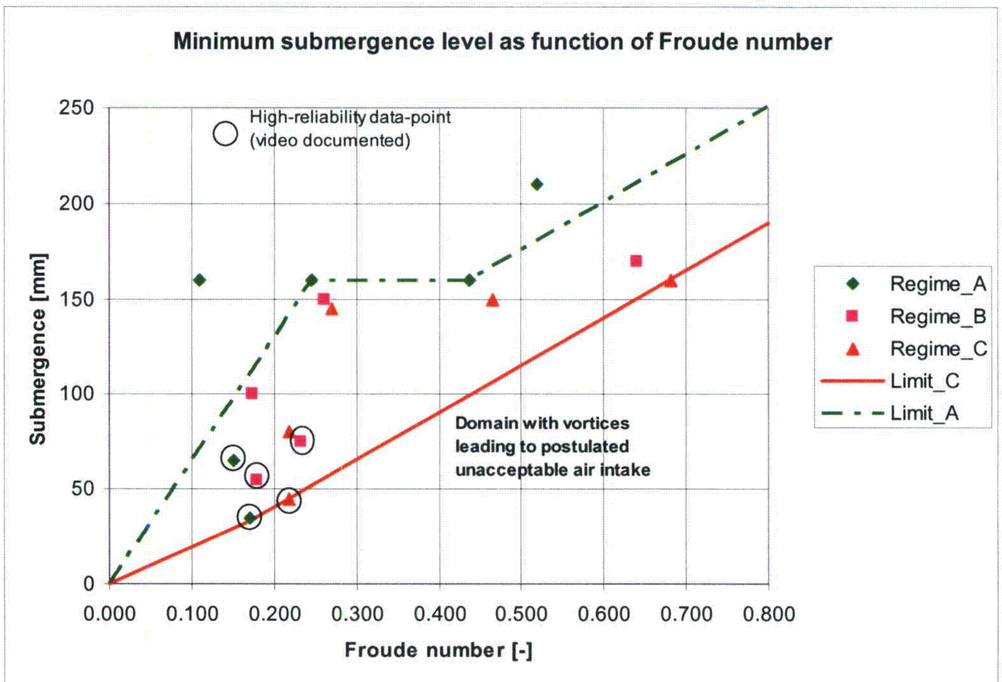

For operation points above the Limit A line, no air ingestion into the screen occurs. For operation points below the Limit C line, unacceptable air ingestion into the screen may occur. In the intermediate region between the two limit lines, intermittent air ingestion into the strainer could occur. For operation points in the intermediate region, the possibility of transporting the ingested air to the pump inlet and the potential impact on NPSH requirements are analyzed.

For Salem, the clean strainers were analyzed for vortexing under both one and two pump operation. When the Salem train of strainer modules is loaded with debris, there is little variation in flow among the modules. However, when the strainers are clean, the majority of the flow is through the module closest to the sump (Reference A.77). The flow rate through the closest one third of the closest module was determined using a modified version of the methodology described in Section 3f.9 of this response in which the head loss in the strainer pockets is dominated by the hydraulic resistance of the perforated plate instead of the debris bed. For the two pump operation at Salem under clean strainer conditions, it was determined that 49% of the flow passes through the closest one third of the closest module to the sump which results in an approach velocity of 0.582 m/s. For one pump operation under clean strainer conditions, the approach velocity for the last one third of a module is 0.328 m/s (Reference A.77). The velocities are based on Unit 2, which is similar to Unit 1 for clean strainer conditions where flow passes primarily through the modules adjacent to the sump.

The design minimum submergence of the Salem strainers is three inches (Reference A.6). Three inches of submergence has been used for the head loss tests and the NPSH calculation. For the clean strainer vortex analysis, the as-built dimensions to the uppermost perforated portions of the top pockets in the module closest to the sump have been used to determine a minimum submergence of 3.78 inches for Unit 1 and a minimum submergence of 3.85 inches for Unit 2 (Reference A.77).

The resulting operating points are plotted against the limit lines from the clean strainer vortex test results in Figure 3f.3.1.1-2. The Froude number (Fr) is computed using

$$Fr = \frac{v^2}{gh}$$

where v is the approach velocity, g is gravity, and h is the submergence.

Figure 3f.3.1.1-2: Clean Strainer Vortex Test Results

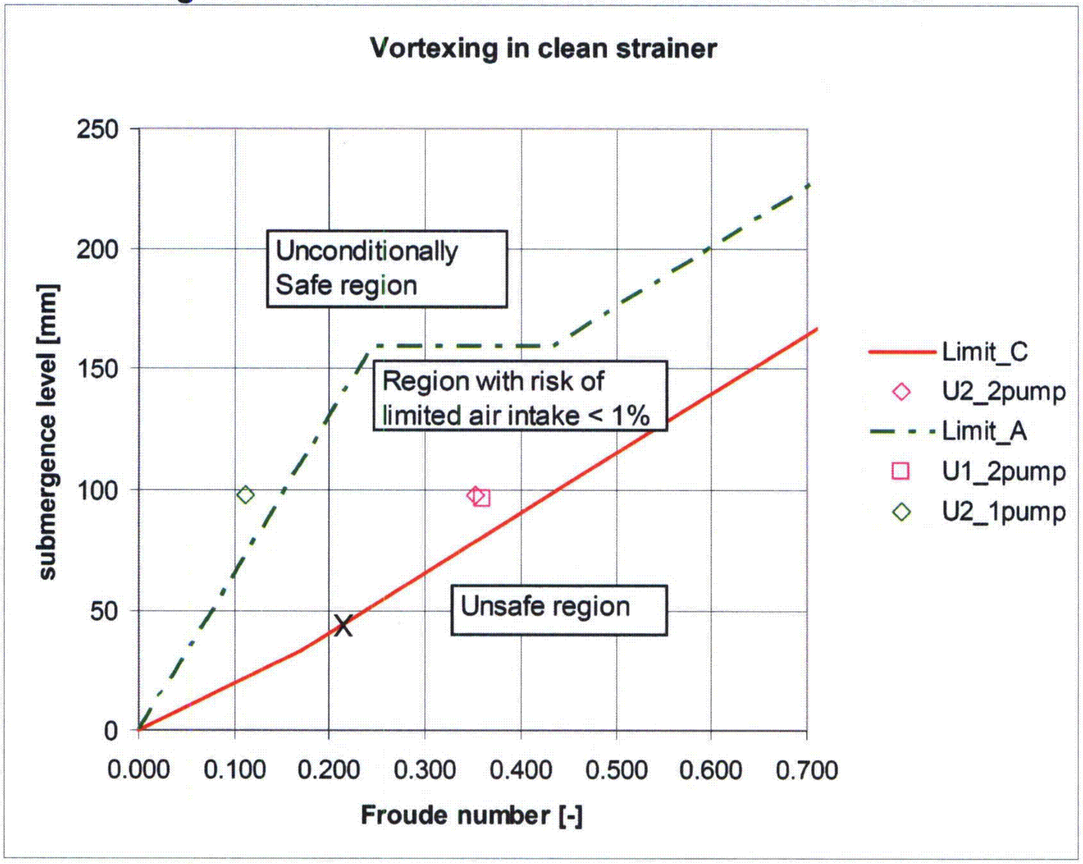

The Salem one pump operation (green diamond) lies in the safe region with no threat of air ingestion into the strainer. The two pump operation points (pink diamond and pink square) lie in the intermediate region where there is the possibility of intermittent air ingestion into the strainer for both Unit 1 and 2.

Video analysis of the vortices formed in the CCI Generic Vortex Tests conducted in January 2008 (Reference A.113) was performed to determine the worst case air ingestion in the intermediate region between the limit lines. The video used for the analysis was:

CCI_vort_test_45mm_45m3h.MOV

The video was used to determine the size of potential vortices which could occur for the clean screen condition (Reference A.77). The size of the vortex relative to the pocket was estimated based on Figure 3f.3.1.1-3. Figure 3f.3.1.1-3 is an image that was taken from a video of a clean screen vortex test whose Froude number (0.218) and submergence (1.8 in) bound the worst case Froude number and submergence at modules nearest the sump pit at Salem. The minimum submergence at Salem is based on the minimum water level at switchover of 80 feet 10 inches, which includes 0.25 inches of margin. The water level then increases from the minimum to over 81 feet 6 inches for the conservative case of a LOCA with full RCS reflood. The water level following switchover is computed using the conservative assumptions outlined in Section 3g.8 of this response.

Figure 3f.3.1.1-3: Vortex in Clean Strainer Pocket

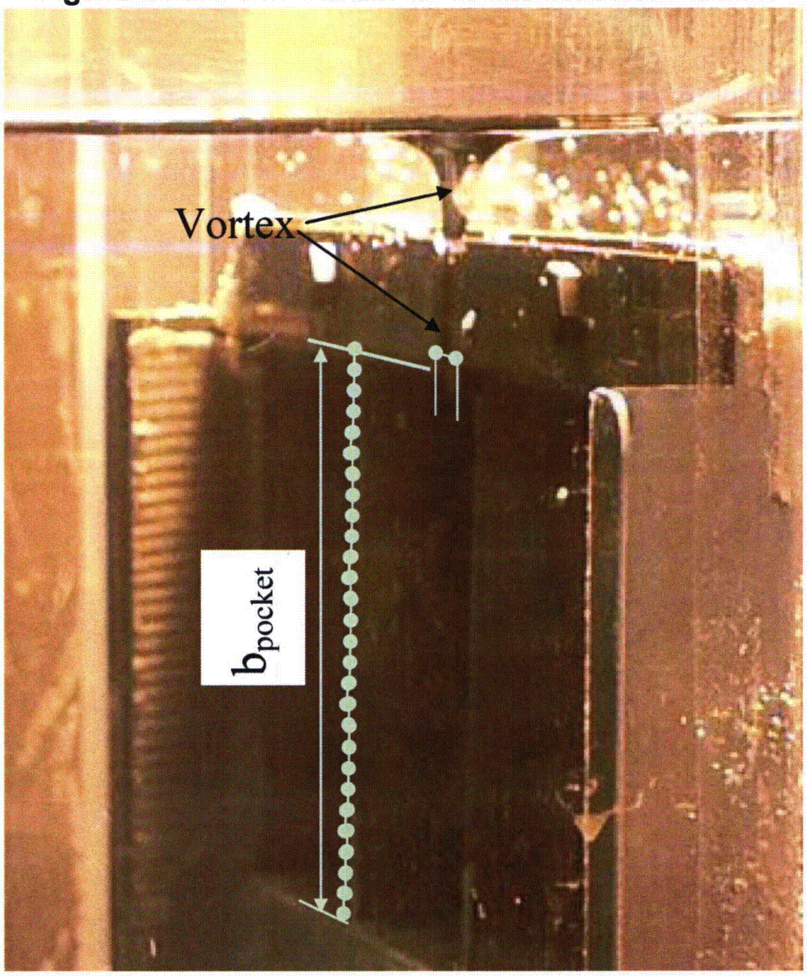

The data point selected for the vortex analysis (explained below) is marked as a black ‘X’ on the red “Limit_C” line used to delineate the unsafe operating region from the operating region with limited air intake in Figure 3f.3.1.1-2. Salem operates in either the unconditionally safe region or in the safe region with limited air intake, as shown by the U1_2pump, U2_1pump, and U2_2pump data points in Figure 3f.3.1.1-2. Vortices such as the one shown in Figure 3f.3.1.1-3 occurred less than 20% of the time, but are conservatively assumed to occur 100% of the time in the vortex analysis.

Based on scaling of the screen shot in Figure 3f.3.1.1-3, the vortex diameter is approximately 1/27th of the height of the pocket. Since the pocket opening is 120 mm tall, the diameter of the vortex is 4.44 mm [=120 mm/27], and the cross sectional area of the vortex is $1.55x10^{-5}$ m^2 [$=\pi d^2/4$].

The air from the vortex is modeled as reaching the velocity of water once it is inside the pocket. Thus, the proportion of air ingested (α_p) is the ratio of the cross section of the vortex to the cross section of the 4 pockets which were used during the tests. The inside of the pocket is 70 mm wide and 109 mm tall. Thus, 0.05% [$=1.55x10^{-5}$ m^2 / (4*0.070 m*0.109 m)] air ingestion by volume is computed.

In addition, water will flow through all rows of the strainer, not just the top row (only the top row of pockets of the test strainer was open during the generic vortex tests). At Salem, each strainer module is 7 rows tall. Thus, the effective air ingestion over the entire height of the strainer is 0.00726% [=0.05%/7].

As stated previously, 49% of the water to the sump flows through the nearest 1/3 of the strainer module nearest the sump pit (e.g. through the first ~3 columns of pockets nearest the sump pit) for the clean strainer scenario. The remaining water (51%) flows through the furthest 2/3 of the module nearest the sump pit and two modules further from the sump pit. The flow through the further portions of the strainer is not susceptible to vortex formation due to the lower velocities through the strainer. The strainer trains have a total of 24 and 23 modules, respectively, for Units 1 and 2; thus, almost no water flows through the modules furthest from the sump pit for the clean strainer condition. Since vortex formation will only occur in the nearest 1/3 of the strainer module near the sump pit, the potential volumetric fraction of air entering the sump pit is 0.00356% [=0.00726%*0.49] (Reference A.77).

The impact of ingesting 3.56 E-3% of air by volume into the pump suction on the required NPSH can be determined using the methodology found in Appendix A of Regulatory Guide 1.82 (Reference 4), which states that the NPSH Required increases at a rate equal to 0.5 times the air ingestion rate in percent volume. For the clean strainer with two pumps operating, the NPSH Required would therefore increase by a factor of 0.00178. For the maximum NPSH Required of 25 feet (see Table 3g-3 of this response), this increase is 0.04 feet. This is negligible when compared to the NPSH margin gained by having no debris on the strainer. This value conservatively neglects the impact of air bubble compression due to the greater static head at the pump inlet. It also neglects potential reabsorption of evolved air into the water although the solubility of air in water increases with increasing pressure, and it is likely that some evolved air will re-dissolve before reaching the pumps.

Therefore, although a small fraction of air by volume may be ingested into the Salem Unit 1 and 2 strainers due to vortexing while the strainers are clean and operating with two pumps, the impact of the ingested air on the NPSH Required is negligible.

Since clean screen vortices occur near the top of the strainer, it is possible that some air could accumulate near the top of the suction box if it is not entrained. The total quantity of air which could accumulate inside the strainer due to clean screen vortexing is less than 0.02 ft^3, which is considered negligible. The potential accumulated air volume is determined based on the time after recirculation that the strainer submergence is low enough to allow vortexing and by utilizing a realistic vortex formation frequency (Reference A.77).

The impact of deaeration due to the clean strainer head loss is bounded by the deaeration analysis presented for a debris laden strainer in Section 3f.3.2 of this response.

3f.3.1.2 Vortexing Due to Pump Stop and Restart

For normal continuous pump suction with debris on the screen, there is a fairly uniform distribution of velocity through the debris bed and this velocity is sufficiently low that it precludes any vortex formation (Reference A.77). However, it has been observed by CCI that if the pump is stopped, air bubbles (trapped in the internal cavities of the strainer) can escape through perforated top cover plates, or through the top pockets. These air bubbles have been observed to create localized "clean strainer windows" in the perforated cover plates. A limited amount of entrapped air bubbles can form during strainer operation due to the head loss across the debris bed and the reduced solubility of air in water at the lower pressure downstream of the debris bed. This deaeration has always been observed and cannot be prevented for any kind of strainers.

CCI has observed that after restarting the pump, these "clean strainer windows" can show localized high velocities. At these locations, vortices have been observed which brought air inside the strainer cavities through the perforated top cover plates. A dedicated test campaign was conducted in order to assess this scenario (Reference A.94). The results of these tests were as follows:

a) No vortexing was observed for any tested flow condition after pump restart for strainers with unperforated cover plates.

b) For strainers with perforated cover plates, vortexing could be observed when a "clean strainer window" was formed. The propensity for vortex formation depended on flow rate, submergence level and window size.

The Salem strainer is provided with unperforated (solid) top covers; i.e. Salem corresponds to configuration a) above (Reference A.77).

Since it is very difficult to compare the above test conditions with the expected Salem conditions for pump stop / restart, Salem specific test sequences were performed with pump stop and restart during the 2008 strainer head loss tests (Reference A.75). No vortex formation was observed for any of these tests. These tests were run with the minimum submergence of 3 inches (Reference A.6) and flow rates scaled to the maximum two pump plant flow rates, thus mirroring plant conditions. See Section 3f.4.1.5 and 3f.4.2.3 of this response for the description and results of the 2008 strainer head loss tests.

Thus, vortex formation due to the stopping and restarting of the pumps will not occur for the Salem sump strainer.

3f.3.1.3 Vortexing Due to High Velocities Through Bore Holes

During the Salem plant specific chemical effects head loss tests performed by the strainer vendor, CCI, bore holes formed in the debris beds when chemical precipitates were present (Reference A.75). A bore hole occurs when the head loss across the debris bed increases to the point that the structural integrity of the debris bed is compromised. At this increased head loss, a localized area of the debris bed collapses (See Figure 3f.4.2.3.4-4). This leads to an area of low hydraulic resistance in the bed and high localized fluid velocities. If these localized high fluid velocities are combined with minimal submergence conditions, vortices could occur.

Direct observation of the formation of a bore hole during the head loss tests was not possible due to the high turbidity of the water immediately after the chemical precipitate additions (Reference A.77). Instead, the formation of the bore holes was indicated by sudden drops in the measured head loss across the debris beds (See Figures 3f.4.2.3.4-1 and 3f.4.2.3.5-1). The ratio of the head loss measured just before the formation of the bore hole to the head loss measured just after the formation of the bore hole is used to determine relative hydraulic resistance of the debris bed with and without the bore hole (Reference A.77). The localized high fluid velocity in the strainer pocket with the bore hole is found by using a modified version of the methodology described in Section 3f.9 of this response by assuming the worst case scenario in which the entire observed drop in head loss was due to the formation of one bore hole in one pocket in the top row of each side of the strainer module closest to the suction box.

Six suspected bore hole formation events indicated by sudden drops in measured head loss from the chemical effects head loss tests were analyzed for the potential for vortex formation (Reference A.77). The conditions found during these bore hole formation events, designated B1 through B6, were compared to the clean strainer vortex test results shown in Figure 3f.3.1.1-2. The minimum submergence used for these comparisons was 11.4 inches based on the results of the minimum containment sump flood level analysis (Reference A.21), and the knowledge that the bore holes did not form until after the existence of chemical precipitates (See Sections 3f.4.2.3.4 and 3f.4.2.3.5 of this response). Since it has been shown that chemical precipitates do not form until after the containment sump cools to a temperature of 160 °F (See Section 3o.1.21d(i) of this response), and since this temperature is not reached until after the RWST has been depleted, the increased submergence of 11.4 inches is justified (Reference A.99). Note, if chemical precipitates are not formed until the containment sump reaches 110°F, as determined by Salem specific benchtop testing (Reference A.95), additional submergence is achieved.

The results of the bore hole vortex analysis can be seen in Figure 3f.3.1.3-1. All bore hole events analyzed fall well above the Limit A line where no air ingestion into the screen occurs. Therefore, there is no risk of formation of harmful vortices due to the formation of bore holes in the strainer debris bed.

Figure 3f.3.1.3-1: Vortexing Risk at Bore Hole Formation

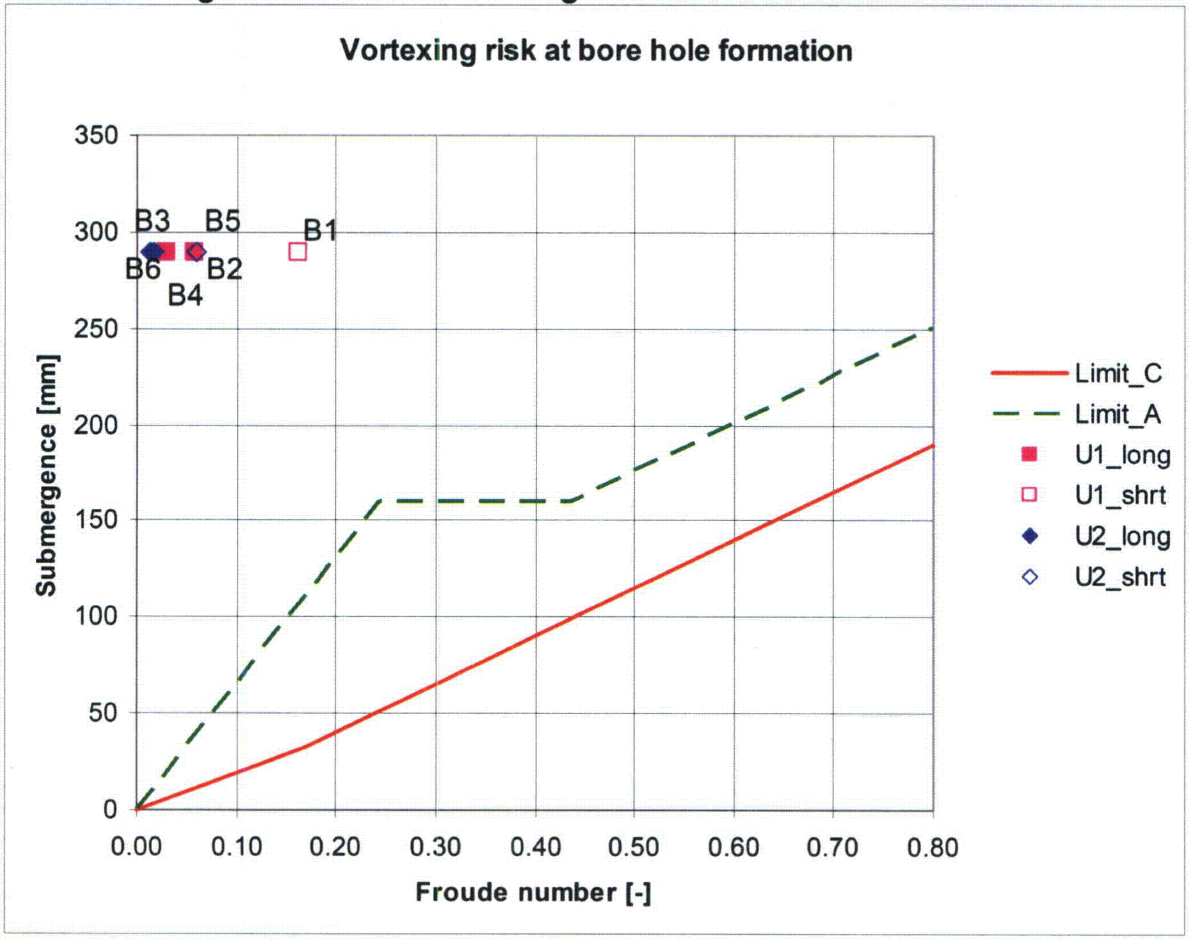

Therefore, based on the analyses presented in Sections 3f.3.1.1 through 3f.3.1.3 of this response, vortexing will not adversely impact the operation of the RHR pumps.

3f.3.2 Deaeration Analysis

Air ingestion downstream of the strainer due to deaeration occurs if air saturated water (i.e. with the maximum amount of dissolved air) enters the strainer and the head loss across the strainer leads to lower air solubility, which results in the release of air in the water downstream of the strainer. This phenomenon is inevitable downstream of the strainer debris bed due to the reduced water pressure.

However, if the pressure of the water increases downstream of the strainer, a portion of the evolved air can be re-dissolved in the water, thus reducing the potential for air ingestion at the pump inlet. Re-dissolution of air could occur where the water column above the pump inlet results in an increased pressure at the pump suction nozzle.

For Salem, the minimum water level elevation is 80.83 feet and the RHR pump centerline elevation is 46.83 feet, resulting in a 34 foot water column (Reference A.77). The maximum suction line loss at the maximum two pump operation flow rate is up to approximately 5 feet (Reference A.41). The suction line loss combined with the strainer structural limit (16.94 feet, Reference A.77) results in a total head loss between the strainer and the pump inlet that is less than the increase in pressure head due to the water column. Thus, a portion of the air which evolves due to the head loss across the strainer will re-dissolve prior to reaching the pumps.

However, re-dissolution of the evolved air due to deaeration is not credited due to the transient behavior of the process. The deaeration analysis is split into two parts. First, an assessment is performed to determine the quantity of air evolved as well as its impact on NPSH. Second, an assessment is performed to determine the ability of the evolved air to form air bubbles at the top of the suction box.

3f.3.2.1 Air Evolution

In order to assess the impact of degasification, a conservative analysis was performed in lieu of demonstrating that evolved air bubbles would dissolve back into solution. The analysis (Reference A.104) determined the quantity of air which would come out of solution as water passed through the debris bed and then determined the void fraction at the pump inlet. The quantity of air which is dissolved in solution and which evolves from solution is computed using Henry's Law. The methodology used is consistent with that employed in the NUREG/CR-6224 Correlation and Deaeration Software Package issued by the NRC in 2005 (Reference 42).

The analysis was performed using both the Double Ended Pump Suction (DEPS) Minimum Safeguards and the DEPS Maximum Safeguards post-LOCA pressure/temperature profiles in order to determine the worst case void fraction. These transient profiles were used to determine the containment pressure and temperature corresponding to a given sump temperature. The sump pool was assumed to be saturated with air. The relative humidity above the sump pool (which impacts the amount of air in solution) was modeled as 100% as would be expected in a post-accident environment at switchover. A transient water level was used wherein the minimum strainer submergence was modeled at the time of switchover, and the water level increased thereafter (as determined in the minimum flood level analysis). In addition, the amount of air evolved was computed separately for each row of pockets (7 rows total) since less air comes out of solution in the lower pockets due to the greater air solubility at higher pressures. The air evolved was tracked separately for each pocket row up to the pump inlet. At the pump inlet, the total void fraction was computed as the average of the void fraction computed based on the air evolved in each individual row. Averaging the individual void fractions is appropriate since the flow from the individual rows will be mixed in the suction piping. For sump temperatures less than 160°F (at which chemical precipitates could be present), the void fraction was conservatively computed based on the top row only due to the potential presence of bore holes.

The analysis conservatively ignored any re-dissolution of the air en route to the pump inlet as stated previously. However, compression was credited for the evolved air bubbles at the pump inlet due to the greater pressure at the pump inlet relative to the pressure immediately downstream of the strainer. The compression is modeled as isothermal since it is gradual, the evolved air bubbles are relatively small (see Section 3f.3.2.2 of this response for bubble sizes), and the surrounding water is at a constant temperature as the fluid flows from the strainer to the pump inlet.

The results of the deaeration analysis are presented in Tables 3f.3.2.1-1 and 3f.3.2.1-2 (Reference A.104). The limiting void fraction is the maximum void fraction calculated for the DEPS Minimum and Maximum Safeguards scenarios.

Salem Nuclear Generating Station Units 1 and 2
Docket Nos. 50-272 and 50-311
Generic Letter 2004-02
Updated Supplemental Response for Salem

Table 3f.3.2.1-1: Unit 1 Limiting Void Fraction at Pump Inlet

Sump Temperature	Void Fraction (α) at Pump Inlet (%)					
	Cold Leg Recirculation		Containment Spray Recirculation		Hot Leg Recirculation	
°F	**1-pump**	**2-pump**	**1-pump**	**2-pump**	**1-pump**	**2-pump**
60.0	0.2038%	0.2979%	0.2014%	0.2996%	0.2026%	0.2979%
70.0	0.1884%	0.2755%	0.1862%	0.2771%	0.1873%	0.2755%
80.0	0.1764%	0.2580%	0.1743%	0.2595%	0.1754%	0.2580%
90.0	0.1673%	0.2447%	0.1653%	0.2461%	0.1663%	0.2447%
100.0	0.1606%	0.2350%	0.1587%	0.2363%	0.1596%	0.2350%
110.0	0.1401%	0.2048%	0.1386%	0.2059%	0.1393%	0.2048%
120.0	0.1246%	0.1821%	0.1234%	0.1830%	0.1240%	0.1821%
130.0	0.1123%	0.1641%	0.1113%	0.1648%	0.1118%	0.1641%
140.0	0.0984%	0.1430%	0.0976%	0.1436%	0.0980%	0.1430%
150.0	0.0885%	0.1291%	0.0879%	0.1296%	0.0882%	0.1291%
159.9	0.0839%	0.1222%	0.0833%	0.1226%	0.0836%	0.1222%
160.0	0.0008%	0.0284%	0.0008%	0.0285%	0.0008%	0.0284%
170.0	0.0007%	0.0267%	0.0007%	0.0268%	0.0007%	0.0267%
180.0	0.0006%	0.0259%	0.0006%	0.0260%	0.0006%	0.0259%
190.0	0.0006%	0.0260%	0.0006%	0.0261%	0.0006%	0.0260%
193.7	0.0006%	0.0263%	0.0006%	0.0263%	0.0006%	0.0263%
212.0	0.0006%	0.0290%	0.0005%	0.0291%	0.0006%	0.0290%
220.0	0.0006%	0.0317%	0.0006%	0.0318%	0.0006%	0.0317%
230.0	0.0012%	0.0291%	0.0012%	0.0292%	0.0012%	0.0291%
240.0	0.0005%	0.0331%	0.0005%	0.0333%	0.0005%	0.0331%
250.0	0.0006%	0.0421%	0.0006%	0.0423%	0.0006%	0.0421%
260.0	0.0053%	0.0498%	0.0053%	0.0500%	0.0053%	0.0498%

Table 3f.3.2.1-2: Unit 2 Limiting Void Fraction at Pump Inlet

Sump Temperature	Void Fraction (α) at Pump Inlet (%)					
	Cold Leg Recirculation		Containment Spray Recirculation		Hot Leg Recirculation	
°F	1-pump	2-pump	1-pump	2-pump	1-pump	2-pump
60.0	0.4641%	0.5788%	0.4630%	0.5825%	0.4660%	0.5788%
70.0	0.4293%	0.5355%	0.4283%	0.5389%	0.4310%	0.5355%
80.0	0.4023%	0.5019%	0.4013%	0.5051%	0.4039%	0.5019%
90.0	0.3817%	0.4764%	0.3808%	0.4795%	0.3833%	0.4764%
100.0	0.3668%	0.4580%	0.3659%	0.4610%	0.3683%	0.4580%
110.0	0.3175%	0.3956%	0.3168%	0.3979%	0.3186%	0.3956%
120.0	0.2807%	0.3491%	0.2801%	0.3509%	0.2816%	0.3491%
130.0	0.2516%	0.3125%	0.2511%	0.3140%	0.2523%	0.3125%
140.0	0.2159%	0.2675%	0.2155%	0.2687%	0.2164%	0.2675%
150.0	0.1957%	0.2423%	0.1954%	0.2432%	0.1962%	0.2423%
159.9	0.1840%	0.2276%	0.1837%	0.2284%	0.1844%	0.2276%
160.0	0.0429%	0.1337%	0.0429%	0.1342%	0.0430%	0.1337%
170.0	0.0372%	0.1210%	0.0372%	0.1214%	0.0373%	0.1210%
180.0	0.0327%	0.1108%	0.0327%	0.1111%	0.0328%	0.1108%
190.0	0.0306%	0.1088%	0.0306%	0.1092%	0.0307%	0.1088%
194.1	0.0301%	0.1090%	0.0300%	0.1093%	0.0301%	0.1090%
212.0	0.0294%	0.1170%	0.0293%	0.1174%	0.0294%	0.1170%
220.0	0.0304%	0.1267%	0.0303%	0.1272%	0.0305%	0.1267%
230.0	0.0268%	0.1062%	0.0268%	0.1066%	0.0269%	0.1062%
240.0	0.0275%	0.1290%	0.0275%	0.1296%	0.0276%	0.1290%
250.0	0.0327%	0.1643%	0.0326%	0.1652%	0.0328%	0.1643%
260.0	0.0423%	0.1434%	0.0423%	0.1440%	0.0424%	0.1434%

The above analysis is conservative since it neglects any dissolution of air downstream of the strainer. It also neglects the "salting-out" effect which states that the solubility of gases in water with electrolytes (e.g. boric acid) is less than in fresh water.

3f.3.2.2 Air Accumulation in Suction Box

A potential consequence of deaeration is the accumulation and coalescence of small air bubbles at the top of the strainer suction box. The accumulated air can be problematic as it can result in air binding of the RHR pumps if large air slugs are ingested and it can also result in a loss of driving head for the RHR pumps. Therefore, the potential for air accumulation was investigated (Reference A.104).

Salem Nuclear Generating Station Units 1 and 2
Docket Nos. 50-272 and 50-311
Generic Letter 2004-02
Updated Supplemental Response for Salem

The potential for air bubbles to accumulate at the top of the suction box is addressed using streamlines produced as part of the CFD analysis of the suction box created for the strainer head loss computation (Reference A.77). The CFD model is based on the Salem Unit 1 geometry which is symmetrically identical to the Unit 2 geometry; therefore, the CFD results are valid for both Unit 1 and Unit 2. Based on the streamlines shown in Figure 3f.3.2.2-1, there is a clear movement of water entering the sump pit from the diffuser of the z-shaped duct to the ECCS pump suction pipes, with velocities in the top region of the pit of 1 m/s or more. The streamline plots show the primary flow of water from the diffuser moving towards the rear wall of the pit and then down towards the pump suction pipes.

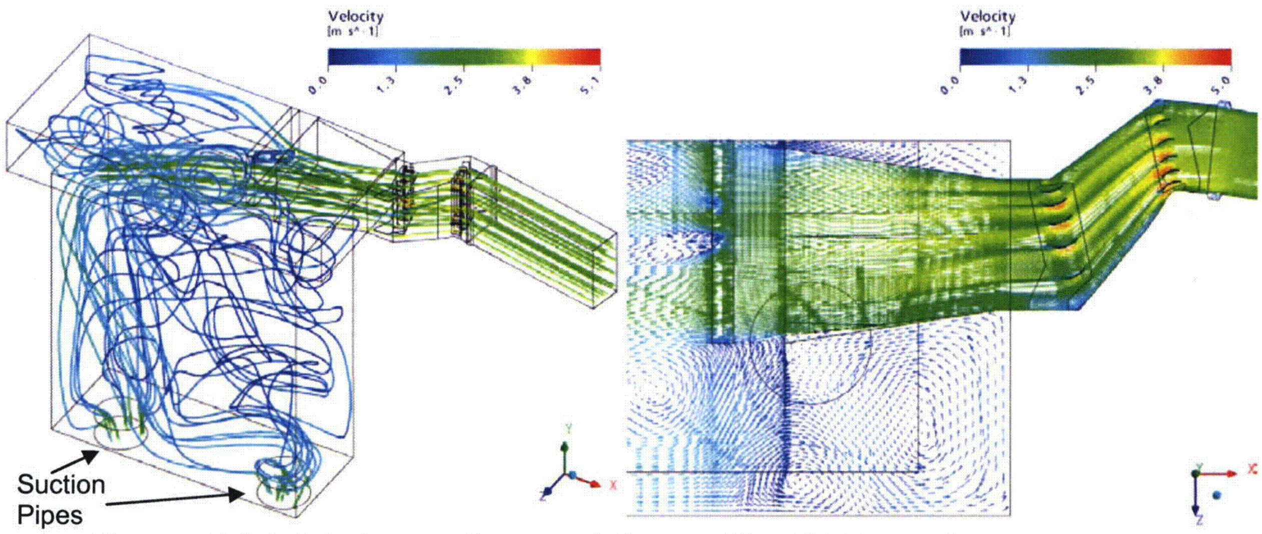

Figure 3f.3.2.2-1: Streamlines and Vector Plot (9000 gpm)

The CFD analyses also determined that the average velocity across both a horizontal plane near the top of the sump (not in the suction box) and a horizontal plane near the bottom of the sump (near the outlet pipes) is ~0.3 m/s for a 5110 gpm flow and ~0.5 m/s for a 9000 gpm flow. These velocities are much greater than the maximum upward velocity for air bubbles evolved in the debris bed.

The maximum upward air bubble velocity is the terminal velocity. The terminal velocity is computed by performing a force balance on a spherical bubble where the buoyancy force is offset by the gravity force and drag force (which is velocity dependent). For air bubbles from 10-100 μm in diameter, the maximum terminal velocities in the post-LOCA sump are on the order of $2x10^{-4}$ to 0.02 m/s, respectively (Reference A.104). Therefore, air bubbles would remain entrained in the downward flow. The bubble size is based on the maximum expected size of the interstitial spaces in a debris bed. Based on Figures 3f.3.2.2-2 and 3f.3.2.2-3 below, the interstitial spaces between fibers in a debris bed are 10-100 μm.

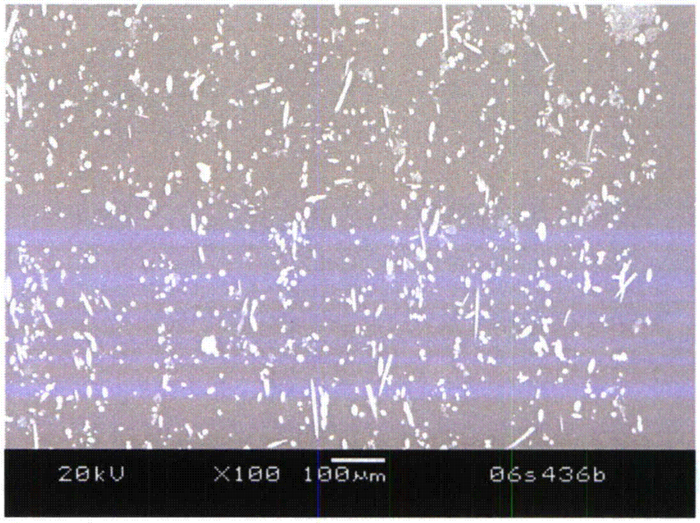

Figure 3f.3.2.2-2: SEM of NUKON Fiber Region in a Debris Bed

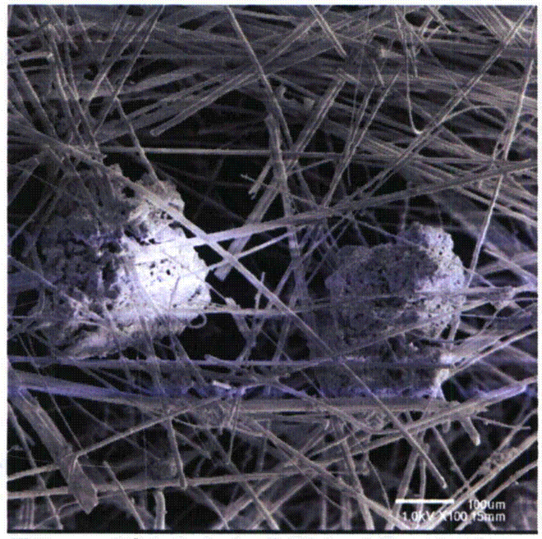

Figure 3f.3.2.2-3: SEM of Particulate Embedded in Fibrous Debris Bed

Figure 3f.3.2.2-2 is Figure 6.30 of NUREG/CR-6917 (Reference 43) and Figure 3f.3.2.2-3 is Figure VIII-1 of Appendix VIII to the NRC SE for NEI 04-07 (Reference 3). Figure 3f.3.2.2-2 is based on a debris bed which contained 1015 g/m^2 (0.21 lbm/ft^2) of NUKON fiber and a total debris loading of 1522 g/m^2 (0.31 lbm/ft^2) per Section 6.4 of NUREG/CR-6917. Figure 3f.3.2.2-3 is based on the tests documented in NUREG/CR-6874 (Reference 44); however, multiple debris loadings were tested and it is not clear which test the picture is based on. Per Table 2.1 of NUREG/CR-6874, NUKON fiber loadings of 0.023 and 0.046 ft^3/ft^2 were tested. Thus, the debris bed shown in Figure 3f.3.2.2-3 is either for 0.05 or 0.11 lbm/ft^2 of NUKON (based on an as-fabricated density of 2.4 lbm/ft^3).

The total fiber (NUKON, Kaowool, Anti-Sweat Fiberglass, and Latent) loading is 0.14 lbm/ft^2 for Unit 1 and 0.07 lbm/ft^2 for Unit 2 based on the minimum total fiber debris transported to the strainer (Reference A.104). Including the coating debris and latent particulate in Table 3e.6-1 results in an additional 0.15 lbm/ft^2 of particulate debris for Unit 1 and 0.14 lbm/ft^2 of particulate debris for Unit 2, resulting in total debris loadings of 0.29 and 0.21 lbm/ft^2 for Units 1 and 2, respectively. Thus, the total debris loading on the Salem strainers is similar to the debris loadings in the tests upon which Figures 3f.3.2.2-2 and 3f.3.2.2-3 are based. Therefore, the interstitial spaces in the Salem debris beds will most likely be smaller than 10-100 μm, which provides support for the air bubbles evolved in the debris bed being on the order of 10-100 μm.

It is recognized that bore holes may occur at low sump temperatures (<160°F) at which chemicals are present. Fewer interstitial spaces will exist in a bore hole than in the debris bed. However, bore holes will not result in completely clean strainer area as is evidenced in Figure 3f.4.2.3.4-4 of this response.

Therefore, air bubbles evolved in flow through bore holes would have a size similar to those evolved in the debris bed. These air bubbles would remain entrained in the downward flow in the suction box due to both the bubble size and the high velocity flow through the bore holes. Thus, air bubbles formed due to bore holes would not accumulate at the top of the suction box.

In addition to bubbles forming due to the pressure drop across the debris bed, bubbles may form within the strainer structure due to the component head loss (i.e. due to flow through the center channel, Z-duct, etc.) (Reference A.104). The size of bubbles formed inside the strainer is based on many factors, including the pressure drop, the flow velocity, and the quantity of nucleation points (e.g. very fine particulate and fiber) in the water (Reference 45). Higher pressure drops generally lead to larger bubble sizes.

In the tests described in Reference 45, water saturated with air at pressures of 2, 5, and 8 atm was subjected to pressure drops of approximately 1, 4, and 7 atm, respectively, to determine a bubble size distribution. For an air saturation pressure of 8 atm, the evolved bubbles ranged in size from 5 μm to 195 μm with roughly half of the total volume of air in bubbles 115 μm or larger. For an air saturation pressure of 2 atm, the evolved bubbles ranged in size from 5 μm to 170 μm with roughly half of the total volume of air in bubbles 95 μm or larger. At an air saturation pressure of 2 atm, only 4% of all the bubbles were larger than 70 μm since large bubbles contain much more air than small bubbles. The maximum strainer component (internals) pressure drop at Salem is 3.1 feet (0.1 atm) based on Table 3f.10.2-4 of this response. Given that the strainer component pressure drop is much less than the pressure drops tested in Reference 45, it is expected that the bubbles evolved inside the strainer would be much smaller than the bubbles observed in Reference 45.

Also, the nozzle used to create the pressure drop in the Reference 45 tests was designed to minimize the collisions between bubbles due to the turbulent (high Reynolds number) flow, thus minimizing the bubble size. The Salem strainers have very low flow rates compared to the flow rates from the Reference 45 tests, indicating that fewer bubble collisions would occur. This further supports the argument that the bubbles that form inside the strainer would be much smaller than those measured in the tests.

A separate study examined the effects of fine particles and fibers on bubble size. In champagne, bubbles are formed at the small residual fibers in the fluid (Reference 46). The pressure drop for champagne in a bottle following the popping of the cork is 6 atm. In Reference 46, very fine photography was used to determine the location of bubble formation and the size of the bubbles that formed. Most of the particles that acted as nucleation sites were cellulose fibers roughly 100 μm long and several micrometers (~10 μm) in diameter. This is comparable to the size and shape of the fine debris in the debris bed and flow where nucleation would occur at Salem. The initial bubble diameters found in the Reference 46 tests were between 14 and 31 μm. Since the debris on the strainer and in the flow will contain similarly sized fibers to those in champagne, it is expected that the evolved air bubbles inside the strainer would be similar in size to those which form in champagne.

Based on a comparison of the testing performed in the two studies described in References 45 and 46 to the Salem strainer conditions, it is expected that the size of the bubbles which could form inside the strainer would be in the range of 10 μm to 100 μm. Therefore, air bubbles evolved in flow inside the strainer would have a size similar to those evolved in the debris bed. These air bubbles would remain entrained in the downward flow in the suction box. Thus, air bubbles formed inside the strainer would not accumulate at the top of the suction box.

3f.4 Provide a summary of the methodology, assumptions, and results of prototypical head loss testing for the strainer, including chemical effects. Provide bases for key assumptions.

3f.4.1 CCI Test Apparatuses and Procedures

CCI has developed a number of test facilities which were used to perform strainer performance tests. The test facilities include a small vertical flow loop (small scale tests), a large pool type horizontal flow loop (large scale tests), and a horizontal flow Multi-Functional Test Loop (MFTL). Two MFTL configurations were used: one with a 1-sided strainer module and one with a 2-sided prototypical strainer module. All strainer head loss and bypass tests were performed with tap water. The test series which were undertaken for Salem in these facilities are:

- Small Scale Head Loss Tests (September 2005)
- Large Scale Head Loss and Bypass Tests (October 2005)

- 1-Sided MFTL Fiber Bypass Tests (March - April 2006)
- 1-Sided MFTL Head Loss Tests including Chemical Effects (December 2006 - January 2007)
- 2-Sided MFTL Head Loss Tests including Chemical Effects (February - June 2008)
- 2-Sided MFTL Fiber Bypass Tests (November - December 2008)

Prior to each test series, a test specification was developed by CCI. Deviations from the test specifications were noted in the test reports for each test.

Descriptions of each of these test loops are provided in the following sections; however, detailed descriptions are only provided for the tests which are used for the design basis strainer bypass and head loss. The small and large scale head loss tests were performed to develop preliminary strainer sizing requirements, while the design basis tests validated the sizing of the strainers. The design basis particulate bypass data is based on the 2005 large scale testing while the design basis fiber bypass data is based on the 2006 and 2008 MFTL testing. The design basis strainer head loss is based on the 2008 2-sided MFTL head loss testing.

3f.4.1.1 Small Scale Head Loss Tests (September 2005)

The small scale head loss tests were performed in September 2005 using CCI Test Specification Q.003.84 741 (Reference A.85). These tests measured the head loss across a six pocket strainer module installed in a vertical flow test loop. This orientation allowed minimal sedimentation and formed a fairly uniform debris bed. The tested fiber and particulate debris loads were greater than the design basis fiber and particulate debris load since the debris load was reduced after these tests were performed. Chemical effects were not considered in the small scale tests. This test series included 5 debris laden strainer head loss tests.

The results of the small scale tests are given in CCI Report 680/41132 (Reference A.86). Further discussion of the small scale tests is not provided as they are not part of the design basis strainer head loss.

3f.4.1.2 Large Scale Head Loss and Bypass Tests (October 2005)

The large scale head loss tests were performed in October 2005 using CCI Test Specification Q.003.84 745 (Reference A.65). These tests were used for preliminary strainer sizing and the head loss results are not part of the design basis strainer head loss. The results of the large scale tests are given in CCI Report 680/41128 (Reference A.65). Both full load and thin bed head loss tests were performed and the results indicated that a thin bed did not occur due to the non-uniformity of the debris bed. Chemical effects were not considered in the large scale tests. This test series included 4 debris laden strainer head loss tests.

The material bypass results from Tests 4 and 5 are used in the downstream effects component wear calculation (Reference A.18). Therefore, Tests 4 and 5 are described in the following subsections. There were no deviations from the test specification for these tests.

3f.4.1.2.1 Large Scale Test Loop Configuration (Reference A.65)

The large scale head loss tests were performed in a pool approximately 3 m long. A 120 pocket 2-sided strainer module is installed in the middle of the pool, although the top 30 pockets on each side are blocked off (60 total blocked pockets) in order to more closely simulate the height of the installed strainers. The flow orientation into the pockets was horizontal, which corresponds to the actual installation at Salem. This orientation simulated the flow conditions in a more realistic way than the small scale tests, including the effects of non-uniformity of the debris bed as is expected in case of LOCA in the plant. The pockets are representative of those installed at Salem, except that the pockets in the test loop are rotated 90° from those in the plant; i.e. the pockets in the test loop are 120 mm tall and 84 mm wide while the pockets in the plant are 84 mm tall and 120 mm wide. See Figure 3f.4.1.5.1-3 for basic geometry of a typical strainer pocket. The difference in orientation is not expected to impact test results since the pockets are otherwise geometrically identical (e.g. pocket length, perforation size, etc.) to the installation. The test module was placed on the pool floor which resulted in an effective height for the test assembly of approximately 23 inches while the overall height of the installed assembly is approximately 26 inches.

Flow was continuously recirculated in the test loop during the course of each test. The water from the strainer is returned to the test loop via a sparger upstream of the strainer module. The strainer differential pressure, flow rate, temperature, and turbidity were all measured with calibrated instruments.

The water height in each test was approximately 1.5 m. The large tests were run with room temperature water which ranged from 12-16°C (54-61°F).

A schematic of the test facility used for large scale testing is shown in Figure 3f.4.1.2.1-1.

Figure 3f.4.1.2.1-1: Sketch of Large Scale Test Loop

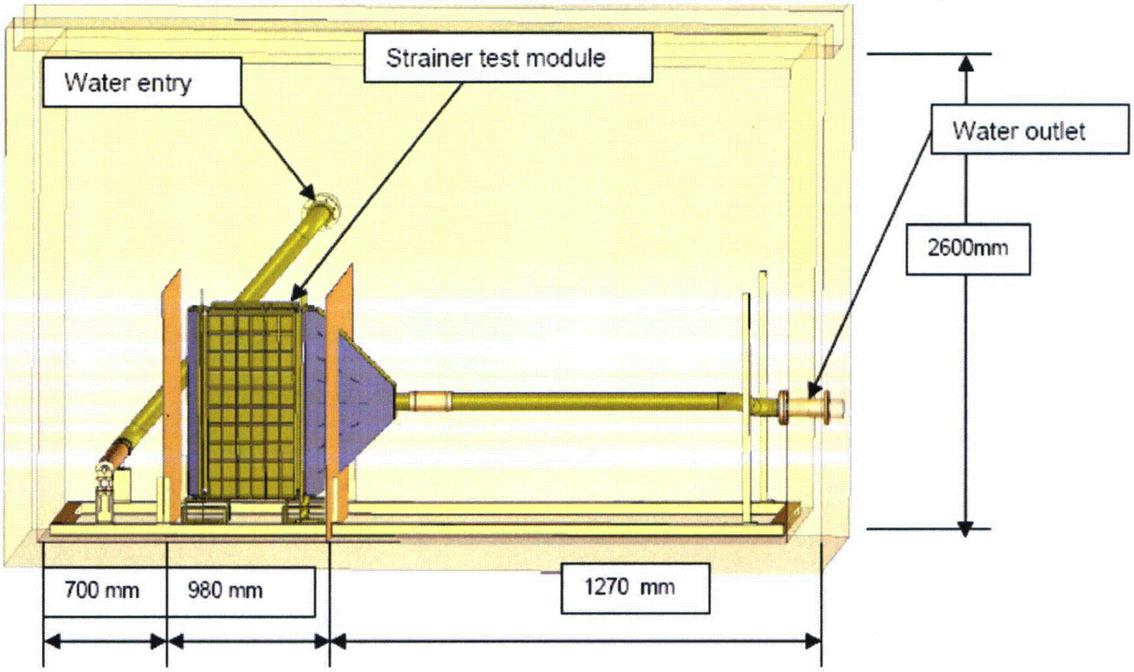

3f.4.1.2.2 Large Scale Test Scale Factor (Reference A.65)

The test scale factor is presented in Table 3f.4.1.2.2-1 below.

Table 3f.4.1.2.2-1: Large Scale Test Scale Factor

Tests	Modeled Strainer Area ft^2	Sacrificial Area ft^2	Equivalent Strainer Area ft^2	Test Module Strainer Area m^2	Scale Factor
4-5	4763	500	4263	8.55	46.3

The modeled strainer area was based on preliminary strainer sizing.

3f.4.1.2.3 Large Scale Test Flow Rates

All tests utilized an equivalent plant flow rate of 9960 gpm (Reference A.65), which is greater than the design maximum two pump flow rate of 8850 gpm (Reference A.14). This results in higher penetration velocities in the tests than would exist in the plant. The nominal (100%) strainer flow rate for Tests 4 and 5 was 48.8 m^3/h, but flow rates of 70%, 100%, 120%, and 140% of nominal were tested (Reference A.65).

3f.4.1.2.4 Large Scale Test Debris Load (Reference A.65)

The tested debris loads for Tests 4 and 5 are presented in Tables 3f.4.1.2.4-1 and 3f.4.1.2.4-2. The tested debris quantity was determined using both the test scale factor and the density of each insulation which was measured at the time the test was performed. Test 4 included enough fiber to form a thin bed and coatings debris. Test 5 was a full load test. The fiber was modeled as 50% NUKON and 50% Kaowool in each test.

Table 3f.4.1.2.4-1: Large Scale Test Debris Load

Debris Type	Quantity
RMI	1525 ft^2
Fiber (1/2 NUKON, 1/2 Kaowool)	1200 ft^3
Qualified epoxy coatings	25.5 ft^3
Unqualified epoxy coatings	0.5 ft^3
Latent particulate	1.01 ft^3
Latent fiber (1/2 NUKON, 1/2 Kaowool)	12.5 ft^3

Table 3f.4.1.2.4-2: Debris Quantity Added to Large Scale Test Loop

Test	Tested Debris Quantity (kg)			
	NUKON	Kaowool	Coatings	RMI
4	0.404	0.853	44.270	0
5	11.543	24.376	44.270	3.684

The tested fiber and particulate debris loads are greater than the design basis fiber and particulate debris load since the debris load was reduced after these tests were performed.

3f.4.1.2.5 Debris Preparation and Addition for Large Scale Tests (Reference A.65)

PSEG provided both NUKON and Kaowool to CCI for testing. The fibers were prepared in a similar manner to that described in Section 3f.4.1.5.7.1, except that the fibers were not baked for the large scale tests.

Qualified and unqualified coatings debris was modeled as stone flour. The justification for using stone flour as a surrogate is provided in Sections 3h.3 and 3h.4 of this response.

The debris is added near the sparger in the test pool. All debris (including RMI) is added to the test loop in a short amount of time.

3f.4.1.2.6 Bypass Measurements for Large Scale Tests (Reference A.65)

Bypass samples were taken from the beginning of each test at a rate of every 10 minutes for the first hour and every 30 minutes from 1 hour until the end of each test. The samples were taken from the line downstream of the strainer that was pumped through the turbidimeter. The tested flow rate results in a test loop turnover time of 4.2 hours (Reference A.65). The plant turnover time ranges from approximately 21 minutes to 145 minutes. The minimum time is calculated by dividing the minimum water volume inside the Reactor Containment (Reference A.21) by maximum ECCS pump flow rate (Reference A.14). Similarly, the maximum time is determined by dividing the maximum water volume inside the Reactor Containment by minimum ECCS pump flow rate (Reference A.4).

The material concentration in each sample was determined by passing the sampled water through two consecutive paper filters with a screen size of 8 microns and 0.45 microns, respectively. Afterwards the two filters were dried and weighed to determine the mass of the material in the sample. Using this information, the debris concentration in milligrams material per liter of water was determined for each sample.

3f.4.1.3 1-Sided MFTL Fiber Bypass Tests (March-April 2006)

The 2006 fiber bypass tests constitute part of the fiber bypass design basis; the other part is based on the 2008 fiber bypass tests. The purpose of the 2006 fiber bypass tests was to determine the fiber bypass characteristics of the strainer. Therefore, tests were performed with various debris loads and flow rates. A total of 9 tests were run. The parameters which differed between each test are outlined in the following subsections. These tests are referred to as "1-sided" since the strainer module in the test only had one side of pockets unlike the installed strainer which has pockets on two sides. The 2006 fiber bypass test results are used in the downstream effects component wear calculation (Reference A.18).

The 2006 fiber bypass tests were performed using CCI Test Specification Q.003.84 764 (Reference A.84) and the results are presented in CCI Test Report 680/41217 (Reference A.83). Deviations from the test specification are documented in the test report. The deviations did not impact the validity of the test results.

3f.4.1.3.1 1-Sided MFTL Configuration for Fiber Bypass Tests (References A.84 and A.83)

The 1-sided MFTL fiber bypass tests were performed in an open channel flume approximately 3 m long and 0.4 m wide (inner dimension). A 40 pocket 1-sided strainer module is installed at one end of the flume, although the top 20 pockets are blocked off in order to more closely simulate the height of the installed strainers (Reference A.84). The flow orientation into the pockets was horizontal. The pockets are representative of those installed at Salem, except that the pockets in the test loop are rotated 90° from those in the plant; i.e. the pockets in the test loop are 120 mm tall and 84 mm wide while the pockets in the plant are 84 mm tall and 120 mm wide (References A.84 and A.77). The difference in orientation is not expected to impact test results since the pockets are otherwise geometrically identical to the installation (e.g. pocket length, perforation size, etc.). The distance from the flume floor to the bottom row of pockets is approximately 1 inch, which is approximately the minimum height off the floor in the plant (Reference A.91). Flow was continuously recirculated in the test loop during the course of each test. The water from the strainer is returned to the test loop via a sparger upstream of the strainer module. The strainer differential pressure, flow rate, temperature, and water level were all measured with calibrated instruments.

A steel sheet was inserted into the test loop approximately 1 meter from the test module. This sheet was raised and lowered to create a flow disturbance on the bottom of the channel to keep the fibers suspended until they transported to the strainer. The water level was monitored during testing and the metal sheet was raised and lowered as needed to maintain the water level above the test pockets. Through the use of the steel plate, nearly all fiber added to the test loop transported to the test module.

The fibers which bypassed the strainer were collected on a 0.31 mm stainless steel mesh (Reference A.84). The mesh was placed upstream of the turbulence plate but downstream of the sparger location. The main return piping includes a bottom mounted extraction pipe which allowed samples of the debris laden bypass water to be taken to determine the fiber concentration as a function of time.

In order to more closely match the installed strainers, the water level was set between 3 and 6 inches above the top row of open pockets prior to each test (Reference A.84). This is similar to the minimum submergence above the strainers of 3 inches (Reference A.6). However, for Tests 7a and 8a, a higher water level was used due to the large flow velocity. The fiber bypass tests were run with room temperature water which ranged from 11-21°C (52-70°F) (Reference A.83).

A schematic of the test loop used for bypass testing is shown in Figure 3f.4.1.3.1-1. Note, however, that this figure does not contain the steel plate or the downstream bypass screen.

Figure 3f.4.1.3.1-1: Sketch of MFTL Test Loop with 1-Sided Test Module

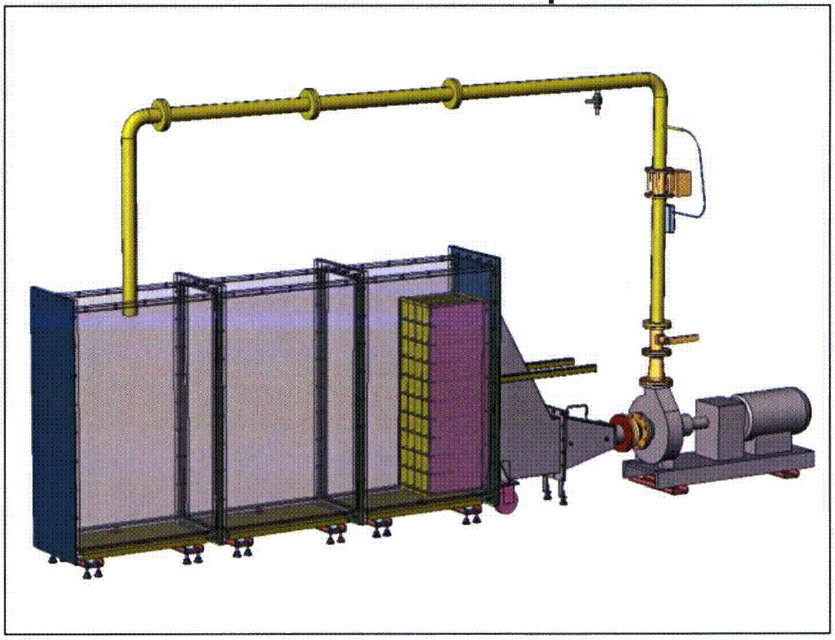

3f.4.1.3.2 1-Sided MFTL Scale Factor for Fiber Bypass Tests (Reference A.84)

Three different test scale factors were determined for the fiber bypass testing since three different strainer areas were utilized. The purpose of utilizing three strainer areas was to determine the impact of penetration velocity on bypass (flow was held constant in all tests). The scale factors utilized are presented in Table 3f.4.1.3.2-1 below.

Table 3f.4.1.3.2-1: 1-Sided MFTL Scale Factors for Fiber Bypass Tests

Tests	Modeled Strainer Area ft^2	Sacrificial Area ft^2	Equivalent Strainer Area ft^2	Test Module Strainer Area m^2 (ft^2)	Scale Factor
1-4, 9	5345	500	4845	2.49 (26.8)	180.8
5-6	2673	500	2173	2.49 (26.8)	81.1
7-8	1336	500	836	2.49 (26.8)	31.2

The tests which utilized the 180.8 scale factor are most similar to the installed strainer configuration which has an area of 4854 ft^2 for Unit 1 and 4656 ft^2 for Unit

2 (Reference A.77). The final area of the installed strainer was unknown at the time at which the fiber bypass tests were performed.

3f.4.1.3.3 1-Sided MFTL Flow Rates for Fiber Bypass Tests

All tests utilized an equivalent plant flow rate of 9000 gpm (Reference A.84), which is greater than the design maximum two pump flow rate of 8850 gpm (Reference A.14). This results in higher penetration velocities in the tests than would exist in the plant. The flume flow rates tested were 11.3, 25.2, and 65.5 m^3/h for scale factors of 180.8, 81.1, and 31.2, respectively.

3f.4.1.3.4 1-Sided MFTL Debris Loads for Fiber Bypass Tests (Reference A.84 and A.83)

The tested debris loads for each fiber bypass test are presented in Table 3f.4.1.3.4-1. All tests except Test 2 used only NUKON fiber. Test 2 used equal volumes of NUKON and Kaowool fiber. The tested debris quantity was determined using both the test scale factor and the density of each insulation which was measured at the time the test was performed.

Table 3f.4.1.3.4-1: 1-Sided MFTL Debris Loads for Fiber Bypass Tests

Test	Scale Factor	Modeled Debris Quantity (ft^3)		Tested Debris Quantity (kg)	
		NUKON	Kaowool	NUKON	Kaowool
1	180.8	1212.5	-	5.915	-
2	180.8	606.25	606.25	2.957	6.245
3a	180.8	212.5	-	1.027	-
4	180.8	112.5	-	0.560	-
5	81.1	212.5	-	2.30	-
6	81.1	112.5	-	1.21	-
7a	31.2	212.5	-	6.00	-
8a	31.2	112.5	-	3.18	-
9b	180.8	12.5	-	0.0623	-

3f.4.1.3.5 Debris Preparation and Addition for 1-Sided MFTL Fiber Bypass Tests (References A.83 and A.84)

PSEG provided both NUKON and Kaowool to CCI for testing. The fibers were prepared in a similar manner to that described in Section 3f.4.1.5.7.1, except that the fibers were not baked for the 1-Sided MFTL fiber bypass tests and that the fibers were leaf shredded (not hand cut) prior to being decomposed with water jet.

The fiber debris is introduced near the middle of the test flume which corresponds to a distance of approximately 1 m (3 ft) from the front face of the strainer. All fiber is added to the test loop within a short interval (Reference A.83).

3f.4.1.3.6 Bypass Determination (Reference A.84)

Each fiber bypass test was run for 6 hours. Bypass samples were taken starting after the first fibers were introduced into the test loop from a sample line upstream of the test pump. After the initial sample, samples were taken every 3 minutes beginning with the initiation of the test until 30 samples had been taken. After the 30th sample was taken, samples were taken every 30 minutes from hours 1 to 4. The samples were taken in 500 ml bottles. The tap was purged prior to taking each sample and the purged water was returned to the test loop in the bypass filter region (near the sparger). The tested flow rates result in test loop turnover times of ~6 minutes, ~3 minutes, and ~2 minute, with the longest turnover time corresponding to the lowest flow rate (References A.83 and A.84). These turnover times are all faster than in the plant. The plant turnover time ranges from approximately 21 minutes to 145 minutes. The minimum time is calculated by dividing the minimum water volume inside the Reactor Containment (Reference A.21) by maximum ECCS pump flow rate (Reference A.14). Similarly, the maximum time is determined by dividing the maximum water volume inside the Reactor Containment by minimum ECCS pump flow rate (Reference A.4).

The fiber concentration in each sample was determined by passing the sampled water through two consecutive paper filters with a screen size of 8 microns and 0.45 microns, respectively. Afterwards the two filters were dried and weighed to determine the mass of the material in the sample. Using this information, the debris concentration in milligrams material per liter of water was determined for each sample.

In addition to the mass of material in the samples, the mass of material on the bypass screen is determined. The dry weight of the bypass screen was recorded prior to and after each test. The difference in the two weights is the mass of material which bypassed the strainer, less the mass of material in the samples. The mass of material on the bypass screen was combined with the mass of material from the samples to determine the total mass of fiber bypass.

The calibrated scale used to determine bypass mass had a resolution of 0.001 kg.

3f.4.1.4 1-Sided MFTL Head Loss Tests (December 2006 – January 2007)

The 1-sided MFTL head loss tests were performed from December 2006 to January 2007 using CCI Test Specification Q.003.84 772 (Reference A.87). These tests were performed using the same horizontal flow flume configuration as was used for the 1-sided bypass tests described in Section 3f.4.1.3 of this response, but with a higher water level. Thus 20 pockets were utilized in the tests. Chemical effects were included in the 1-sided MFTL head loss tests. Also, the steel plate used to induce turbulence was only used for four of the tests. The chemical precipitates for these tests were generated in the test loop. This test series included 8 debris laden strainer head loss tests, 2 of which included chemical precipitates (neither included the steel plate used to induce turbulence). One of the chemical effects head loss tests was run for a total of 17 days.

The results of the 1-sided MFTL head loss tests were presented to the NRC during the October 2007 Salem GL 2004-02 audit (Reference A.78) and are also given in CCI Report 680/41352 (Reference A.88). Both full load and thin bed head loss tests were performed and the results indicated that the thin bed effect was not observed. Although the 1-sided MFTL head loss tests are not part of the strainer design basis, certain trends exhibited in the Unit 1 chemical effects head loss tests (i.e. channeling) substantiate why the design basis 2008 2-Sided MFTL Unit 1 chemical effects tests are valid even in the presence of more chemical precipitate than tested (see Section 3o.1.17d(ii) of this response). Therefore, details pertaining to the performance of the 1-sided Unit 1 chemical effects head loss Tests 5 and 6 are provided below.

3f.4.1.4.1 1-Sided MFTL Scale Factor for Unit 1 Chemical Effects Head Loss Tests (Reference A.87)

The scale factor utilized in the chemical effects head loss tests is presented in Table 3f.4.1.4.1-1 below. Only the scale factor for Unit 1 is presented as chemical effects testing was only performed for Unit 1 in the 1-sided MFTL.

Table 3f.4.1.4.1-1: 1-Sided MFTL Scale Factors for Unit 1 Tests

Tests	Modeled Strainer Area ft^2	Sacrificial Area ft^2	Equivalent Strainer Area ft^2	Test Module Strainer Area m^2 (ft^2)	Scale Factor
5 & 6	4854	500	4354	2.49 (26.8)	162.5

The modeled strainer area was based on final strainer sizing. The Unit 1 strainer has a total filtering surface area of 4854 ft^2 (Reference A.77).

3f.4.1.4.2 1-Sided MFTL Flow Rates for Unit 1 Chemical Effects Head Loss Tests (Reference A.87)

The Unit 1 chemical effects tests utilized an equivalent plant flow rate of 9000 gpm (Reference A.87), which is greater than the design maximum two pump flow rate of 8850 gpm (Reference A.14). This results in higher penetration velocities in the tests than would exist in the plant. The flume flow rate tested was 12.58 m^3/h for a scale factor of 162.5. The equivalent flow rate was also reduced to 5110 gpm during each of the Unit 1 chemical effects tests.

3f.4.1.4.3 1-Sided MFTL Non-Chemical Debris Loads for Unit 1 Chemical Effects Head Loss Tests (Reference A.87)

The tested debris loads for each Unit 1 chemical effects head loss test are presented in Table 3f.4.1.4.3-1.

Table 3f.4.1.4.3-1: 1-Sided MFTL Debris Loads for Unit 1 Chemical Effects Head Loss Tests (Reference A.87)

Debris Type	Modeled Debris Quantity (ft^3 or ft^2)[1]	Density (lbm/ft^3)	Mass (lbm)
Insulation			
NUKON	381	2.4	914
Kaowool	42	8.0	336
Generic Fiberglass[2]	48	6.0	288
Min-K	5.5	16.0	88
MRI[3,4]	938	490.0	77
Coatings			
Qualified	12.6	167.4	2109
Unqualified	0.5	167.4	84
Latent Debris			
Fiber	12.5	2.4	30
Particulate	1.0	167.4	167
Other			
Blanket fiber	1.0	86.5	87

1) All quantities are in given ft^3 except for MRI, which is given in ft^2.
2) Generic fiberglass was later determined to be Anti-Sweat Fiberglass.
3) MRI mass is computed using a foil thickness of 2 mil.
4) MRI was added at the end of Test 5 only, and was not included in Test 6.

The equivalent NUKON quantity for the tested NUKON, Kaowool, generic fiberglass, and blanket fiber is 675 ft^3 (based on the methodology presented in Section 3f.4.1.5.8 of this response).

Generic fiberglass and latent fiber were tested as NUKON. Blanket fiber was tested as Kaowool. Coatings and latent particulate were tested as stone flour. The tested debris loads were those provided in Table 3f.4.1.4.3-2.

Table 3f.4.1.4.3-2: 1-Sided MFTL Tested Debris Loads for Unit 1 Chemical Effects Head Loss Tests (Reference A.87)

Debris Type	Test 5 (kg)	Test 6 (kg)
NUKON	3.439	3.439
Kaowool	1.179	1.179
Min-K	0.246	0.246
MRI	0.214	0.0
Stone Flour	6.587	6.587

3f.4.1.4.4 1-Sided MFTL Chemical Debris Loads for Unit 1 Chemical Effects Head Loss Tests (Reference A.87)

Chemical precipitates for the 1-sided MFTL chemical effects head loss tests were generated using the CCI injection method. The CCI injection method added aqueous 36 wt% sodium aluminate and 38 wt% sodium silicate to the test loop, which was 2500 ppm as boron, to generate aluminum hydroxide and sodium aluminum silicate chemical precipitates. The equivalent quantity of dissolved chemicals and the equivalent quantity of chemical precipitates predicted to form in the post-LOCA sump are presented in Table 3f.4.1.4.4-1. Both the dissolved chemical and precipitate quantity were computed using WCAP-16530-NP (Reference 24).

Table 3f.4.1.4.4-1: 1-Sided MFTL Chemical Debris Loads for Unit 1 Chemical Effects Head Loss Tests (References A.4 and A.87)

Material	Mass (kg)
Dissolved Chemicals	
Calcium (Ca)	25.6
Silicon (Si) as SiO_2	255.4
Aluminum (Al)	46.1
Precipitates Predicted to Form	
Sodium Aluminum Silicate ($NaAlSi_3O_8$)	370.9
Aluminum Oxyhydroxide (AlOOH)	17.1
Total precipitate mass	388.0

In order to test the theoretical 100% quantity of dissolved chemicals, 3.941 kg of sodium aluminate solution and 5.613 kg of sodium silicate solution was required in the test loop (Reference A.87); however, the actual chemical quantities added differed slightly as they were calculated based on the actual test loop solution volume. Additional solution was proportionally added to test chemical quantities up to 140% of the nominal value (i.e. up to the equivalent of 543 kg of precipitate in the plant).

3f.4.1.4.5 Debris Preparation and Addition for 1-Sided MFTL Unit 1 Chemical Effects Head Loss Tests (Reference A.87)

PSEG provided both NUKON and Kaowool to CCI for testing. The fibers were prepared in a similar manner to that described in Section 3f.4.1.5.7.1.

The fiber debris is introduced directly in front of the strainer to facilitate debris transport. All fiber is added to the test loop within a short interval (Reference A.87).

Settled debris was not re-suspended via agitation during these tests.

3f.4.1.5 2-Sided MFTL Head Loss Tests (February-June 2008)

The 2008 chemical effects head loss testing constitutes the design basis head loss testing for the Salem strainers installed in Units 1 and 2. This testing was witnessed by the NRC Staff on April 20-25, 2008, and the NRC observations are documented in a trip report dated July 16, 2008 (ADAMS Accession No. ML081640193, Reference A.81). In this report, the NRC concluded that the test methods being employed by CCI were generally prototypical or conservative.

The design basis head loss is based on the following five tests (References A.75 and A.77).

- Test 1: Clean Strainer Head Loss Test
- Test 2: Unit 2 Thin Bed Head Loss Test
- Test 3-Repeat: Unit 1 Thin Bed Head Loss Test
- Test 5: Unit 1 Full Debris Load Chemical Effects Head Loss Test
- Test 6: Unit 2 Full Debris Load Chemical Effects Head Loss Test

Tests 2 and 3-repeat were run to determine if the installed strainers were susceptible to the thin bed effect, while Tests 5 and 6 determined the full debris load head loss.

This testing was performed using CCI Test Specifications Q.003.84 805 and Q.003.84 808 (References A.74 and A.89, respectively) and the results are documented in CCI Test Report 680/41465 (Reference A.75). Deviations from the test specification are documented in the test report. The deviations did not impact the validity of the design basis test results (Reference A.75).

3f.4.1.5.1 2-Sided MFTL Configuration

The MFTL testing was performed in an open channel flume approximately 3 m long and 0.4 m wide which can accommodate a maximum water depth of approximately 1.4 m (References A.74 and A.89). A 42 pocket strainer test module (2 sides which are each 3 pockets wide by 7 pockets tall) was placed near the middle of the flume. The strainer module was prototypical (i.e. based on the installed strainer design) and was manufactured specifically for the Salem testing. The module was approximately 0.36 m wide, which left a slight gap on either side. However, this gap was sealed (no flow from the upstream to downstream side of the strainer module) creating a configuration similar to the installed strainer. The bottom of the bottom pockets in the test module was approximately 61 mm above the flume floor. This height is consistent with the maximum strainer height off the floor in the plant and was selected to test the strainer at the minimum submergence. The test module had unperforated side and top plates and had perforated bottom plates, consistent with the installed strainers.

As in the plant, the water flow to the front side of the strainer was predominantly horizontal, whereas the flow to the rear side of the strainer had to flow over the top of the module and enter from the rear side. Ample distance (~ 2 meters) was provided upstream of the strainer module to ensure that flow into the front of the test module was horizontal. A steel divider plate was inserted in the flume 24 inches downstream of the strainer to simulate the containment liner in containment, which is approximately 24 inches behind the installed strainer.

For Tests 3-repeat, 5, and 6, a prototypical debris interceptor was installed in the test loop 12 inches upstream of the strainer module, similar to the debris interceptor installed in the plant (see Figures in Section 3e.4 of this response). In addition, for Tests 3-repeat, 5, and 6, a perforated plate from the bottom of the downstream face of the strainer to the flume floor was installed to block the flow of debris underneath the strainer, similar to the perforated plate installed in the plant. Neither the debris interceptor nor the perforated plate underneath the strainer module was included in Tests 1 and 2.

The water in the flume was continuously recirculated during the course of each test. The differential pressure, flow rate, water temperature, and water level were all measured with calibrated instruments. Figures 3f.4.1.5.1-1 and 3f.4.1.5.1-2 show the test flume as it was configured for the head loss tests. However, these figures do not include the following features: 1) debris interceptor included in Tests 3-repeat, 5, and 6, and 2) diffuser at the strainer outlet which was used for Tests 5 and 6.

Figure 3f.4.1.5.1-1: Picture of CCI MFTL with the 2-Sided Test Module (with chemical debris in the test loop)

Figure 3f.4.1.5.1-2: Sketch of the CCI MFTL with the 2-Sided Test Module

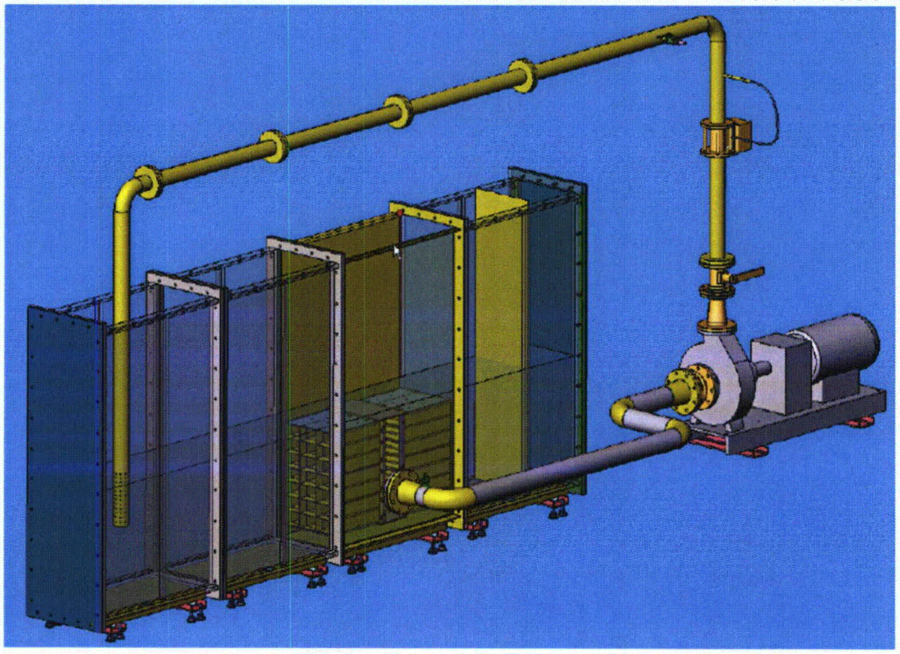

The pockets were each 84 mm tall, 120 mm wide, and 400 mm deep, which is the same size pocket in the same orientation as installed at Salem (References A.74 and A.89). The basic geometry of a typical strainer pocket are shown in Figure 3f.4.1.5.1-3. An array of these pockets forms a strainer cartridge.

Figure 3f.4.1.5.1-3: CCI Strainer Pocket

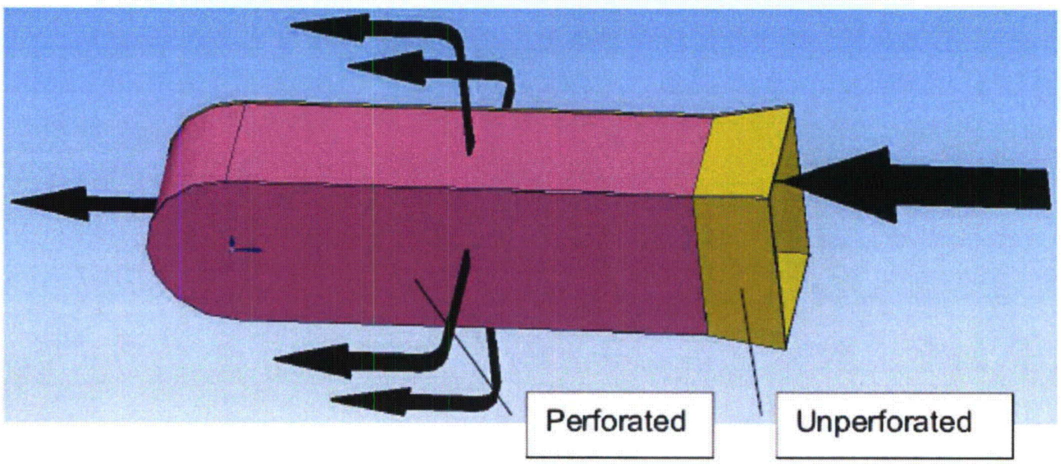

Based on the above information, the test strainer module is geometrically identical to the installed strainers (pocket size, pocket orientation, center channel size, etc.).

The tested configuration is considered geometrically similar, although not identical, to the installed configuration at Salem.

3f.4.1.5.2 2-Sided MFTL Water Level and Submergence

The minimum submergence in the plant is 3 inches (Reference A.6). All of the head loss tests were performed with a nominal strainer submergence of 7-8 cm (~3 inches). The water level was continuously adjusted during the tests to ensure that the strainer submergence was relatively constant (References A.74 and A.89).

For Tests 2 and 3-repeat, the water level was adjusted by draining the test loop following debris additions. The drained water was filtered and any debris removed was reintroduced to the test loop at the sparger location upstream of the strainer module.

For Tests 5 and 6, the water level during the non-chemical and chemical debris additions was adjusted by raising or lowering "water jugs" placed in the loop prior to the test (see Figure 3f.4.1.5.2-1). However, between the non-chemical and chemical debris additions, the water level was adjusted by draining the loop.

Figure 3f.4.1.5.2-1: Water Jugs (blue) in MFTL

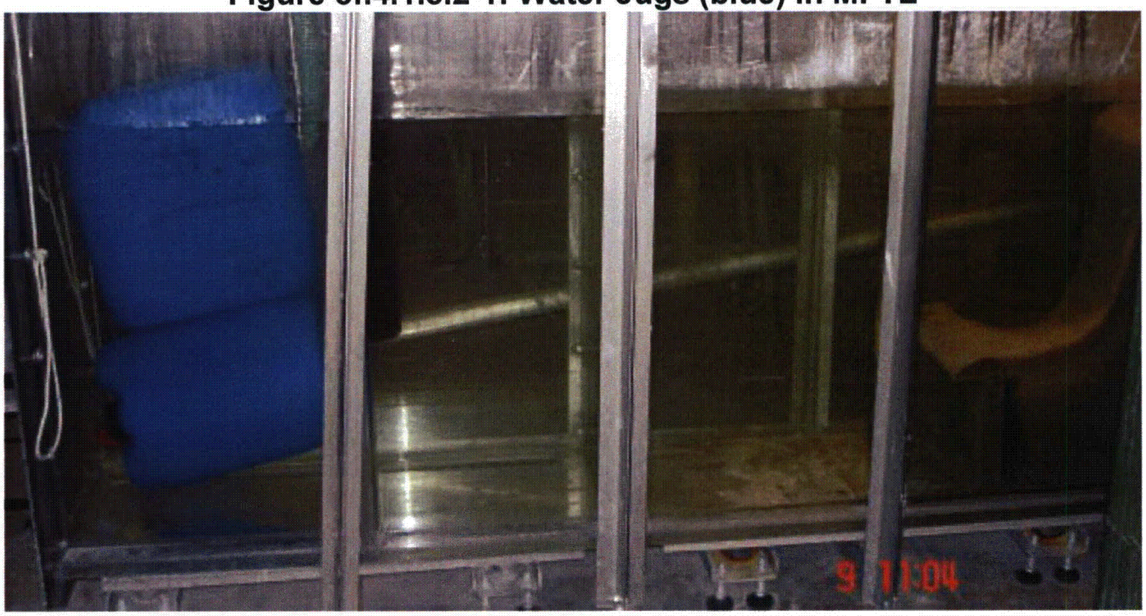

3f.4.1.5.3 2-Sided MFTL Water Temperature

Tests 1, 2 and 3-repeat were run with room temperature water. During these tests, the water temperature range was from 17 to 25°C (63 to 77°F) (Reference A.75).

Salem Nuclear Generating Station Units 1 and 2
Docket Nos. 50-272 and 50-311
Generic Letter 2004-02
Updated Supplemental Response for Salem

Tests 5 and 6 were run in a temperature controlled, heated test loop. The water was heated using welding pre-heater elements wrapped around the upper return pipe from the pump to the sparger. During these tests, the water temperature range was from 40 to 50°C (104 to 122°F) (Reference A.75).

3f.4.1.5.4 2-Sided MFTL Scale Factor

The test scale factor is described in Section 3o.1.19c(i) of this response and is presented in Table 3f.4.1.5.4-1 below.

Table 3f.4.1.5.4-1: 2-Sided MFTL Test Scale Factors

Tests	Unit	Modeled Strainer Area ft^2	Sacrificial Area ft^2	Equivalent Strainer Area ft^2	Test Module Strainer Area m^2	Scale Factor
3-repeat & 5	1	4854	500	4354	5.54	73.0
2 & 6	2	4656	500	4156	5.54	69.7

The modeled strainer area was based on final strainer sizing. The Unit 1 and Unit 2 strainers have a total filtering surface area of 4854 ft^2 and 4656 ft^2, respectively (Reference A.77).

3f.4.1.5.5 2-Sided MFTL Test Flow Rates

The maximum design basis flow rate through the strainer is 8850 gpm (Reference A.14). This is the maximum two pump flow rate for both Unit 1 and Unit 2. This flow rate was used as the basis for the flow rate for Tests 5 and 6. For Tests 2 and 3-repeat, 9000 gpm was conservatively used. The maximum single pump flow rate is 5110 gpm for Unit 1 and 4980 gpm for Unit 2. The single pump flow rates were not used for the design basis portion of the head loss tests. The two pump flow rates were scaled using the test scale factors in Table 3f.4.1.5.4-1 and result in the following test loop flow rates and bulk upstream velocities in the flume (References A.74 and A.89).

Table 3f.4.1.5.5-1: 2-Sided MFTL Test Flow Rates and Upstream Velocities

Test (Unit)	Scale Factor	Plant Flow Rate gpm	Plant Flow Rate m^3/h	Test Loop Flow Rate m^3/h	Bulk Upstream Velocity in Flume m/s (ft/s)
2 (U2)	69.7	9000	2044	29.33	0.027 (0.089)
3-repeat (U1)	73.0	9000	2044	28.00	0.026 (0.085)
5 (U1)	73.0	8850	2010	27.53	0.026 (0.085)
6 (U2)	69.7	8850	2010	28.84	0.027 (0.089)

The test module mimics a typical "slice" of the strainers installed at Salem. Therefore, the flow rates tested are typical of those which would be experienced in the plant and the flume flow rates did not require adjustment to account for the potential of a circumscribed flow condition.

The clean screen head loss tests were performed using flume flow rates from 0 to 132.3 m^3/h (Reference A.75). This corresponds to plant flow rates of 0 to ~42,500 gpm for Unit 1 and 0 to ~40,600 gpm for Unit 2.

At the tested flow rates the approximate test loop turnover time is 2.5 to 3 minutes (References A.74 and A.89). The test loop turnover time for 15 turnovers is approximately 40 to 45 minutes. The plant turnover time ranges from approximately 21 minutes to 145 minutes. The minimum time is calculated by dividing the minimum water volume inside the Reactor Containment (Reference A.21) by maximum ECCS pump flow rate (Reference A.14). Similarly, the maximum time is determined by dividing the maximum water volume inside the Reactor Containment by minimum ECCS pump flow rate (Reference A.4).

After all debris was added to the test loop, a flow sweep was performed to determine the head loss at different flow rates for Tests 3-repeat and Test 6. Flows from 80 to 120% of the nominal scaled 9000 gpm (Test 3-repeat) or 8850 gpm (Test 6) flow rate were included in the flow sweep in 10% increments.

3f.4.1.5.6 2-Sided MFTL Non-Chemical Debris Load

The tested non-chemical debris loads for the design basis head loss tests are provided in Tables 3f.4.1.5.6-1 to 3f.4.1.5.6-4 (References A.74 and A.89). The majority of the debris was added upstream of the strainer module, but some debris was added downstream of the strainer module, consistent with the transport analysis (see Sections 3e.1, 3e.2, and 3e.6 of this response). The transport analysis determined that during blowdown and washdown, some debris transports either to the top of the strainer modules or behind the strainer modules. For testing, the transported debris on top of and behind the strainer modules was added to the area behind the strainer module.

The "upstream" quantity in Tables 3f.4.1.5.6-1 through 3f.4.1.5.6-8 refers to the debris transported or added in front of the strainer. The "downstream" quantity refers to the debris transported or added to the area behind the strainer (between the strainer module and the containment liner).

Table 3f.4.1.5.6-1: Test 2 Debris Load (for Unit 2)

Type of Debris	Upstream Volume ft^3	Downstream Volume ft^3	Density lbm/ft^3	Upstream Mass lbm	Downstream Mass lbm
Insulation					
NUKON	21.9	1.4	2.4	52.56	3.36
Kaowool	31.5	3.5	8.0	252	28
Generic Fiberglass	43.5	3.5	6.0*	261	21
Min-K	22.7	1.8	16.0	363.2	28.8
Coating					
Qualified	11.8	0.8	167.4	1975.32	133.92
Unqualified	0.5	0.00	167.4	83.7	0
Latent Debris					
Fiber	9.4	3.1	2.4	22.56	7.44
Particulate	0.75	0.25	167.4	125.55	41.85

* Generic fiberglass was later determined to be anti-sweat fiberglass as documented in Section 3c.2 of this response.

Table 3f.4.1.5.6-2: Test 3-repeat Debris Load (for Unit 1)

Type of Debris	Upstream Volume ft^3	Downstream Volume ft^3	Density lbm/ft^3	Upstream Mass lbm	Downstream Mass lbm
Insulation					
NUKON	277.1	33.2	2.4	665.04	79.68
Kaowool	34.7	3.9	8.0	277.6	31.2
Fiberglas	41.6	3.4	3.9	162.24	13.26
Min-K	5.03	0.27	16.0	80.48	4.32
Coating					
Qualified	11.8	0.8	167.4	1975.32	133.92
Unqualified	0.5	0.00	167.4	83.7	0
Latent Debris					
Fiber	9.4	3.1	2.4	22.56	7.44
Particulate	0.75	0.25	167.4	125.55	41.85

Table 3f.4.1.5.6-3: Test 5 Debris Load (for Unit 1)

Type of Debris	Upstream Volume ft^3	Downstream Volume ft^3	Density lbm/ft^3	Upstream Mass lbm	Downstream Mass lbm
Insulation					
NUKON	207	29.4	2.4	496.8	70.56
Kaowool	29.2	3.9	8.0	233.6	31.2
Fiberglas	41.6	3.4	3.9	162.24	13.26
Min-K	5.03	0.27	16.0	80.48	4.32
Coating					
Qualified	10.7	0.8	167.4	1791.18	133.92
Unqualified	0.5	0.00	167.4	83.7	0
Latent Debris					
Fiber	9.4	3.1	2.4	22.56	7.44
Particulate	0.75	0.25	167.4	125.55	41.85

Table 3f.4.1.5.6-4: Test 6 Debris Load (for Unit 2)

Type of Debris	Upstream Volume ft^3	Downstream Volume ft^3	Density lbm/ft^3	Upstream Mass lbm	Downstream Mass lbm
Insulation					
NUKON	18.8	2.1	2.4	45.12	5.04
Kaowool	25.7	3.5	8.0	205.6	28
Fiberglas	43.5	3.5	3.9	169.65	13.65
Min-K	22.7	1.8	16.0	363.2	28.8
Coating					
Qualified	10.7	0.8	167.4	1791.18	133.92
Unqualified	0.5	0.00	167.4	83.7	0
Latent Debris					
Fiber	9.4	3.1	2.4	22.56	7.44
Particulate	0.75	0.25	167.4	125.55	41.85

During the course of the testing, analytical refinements were made to reduce the debris load. In addition, it was determined that the generic fiberglass tested in Test 2 (as NUKON) was actually anti-sweat fiberglass and thereafter was tested as such. The anti-sweat fiberglass at Salem is either Owens Corning Fiberglas or Johns Manville Micro-Lok HP (Reference A.14); Fiberglas was used for the testing. For all tests, qualified and unqualified coatings and latent particulate were modeled using stone flour (see Section 3f.4.1.5.7.3) and latent fiber was modeled as NUKON. The above debris quantities combined with the test scale factor resulted in the following debris quantities being added to the test loop for each test (References A.74, A.75, and A.89).

Table 3f.4.1.5.6-5: Test 2 Debris Added to Test Loop

Type of Debris	Upstream Mass kg	Downstream Mass kg	% of Debris Added Downstream %
NUKON	2.188	0.207	8.6%
Kaowool	1.640	0.182	10.0%
Fiberglas	-	-	-
Min-K	2.364	0.187	7.3%
Stone Flour	14.218	1.144	7.4%

Table 3f.4.1.5.6-6: Test 3-repeat Debris Added to Test Loop

Type of Debris	Upstream Mass kg	Downstream Mass kg	% of Debris Added Downstream %
NUKON	4.272	0.541	11.2%
Kaowool	1.723	0.194	10.1%
Fiberglas	1.008	0.082	7.5%
Min-K	0.500	0.027	5.1%
Stone Flour	13.571	1.092	7.4%

Table 3f.4.1.5.6-7: Test 5 Debris Added to Test Loop

Type of Debris	Upstream Mass kg	Downstream Mass kg	% of Debris Added Downstream %
NUKON	3.226	0.485	13.1%
Kaowool	1.451	0.194	11.8%
Fiberglas	1.008	0.082	7.5%
Min-K	0.500*	0.027	5.1%
Stone Flour	12.427	1.092	8.1%

* 0.575 kg Min-K actually added to test loop (Reference A.75)

Table 3f.4.1.5.6-8: Test 6 Debris Added to Test Loop

Type of Debris	Upstream Mass kg	Downstream Mass kg	% of Debris Added Downstream %
NUKON	0.440	0.081	15.5%
Kaowool	1.338	0.182	12.0%
Fiberglas	1.104	0.089	7.5%
Min-K	2.364	0.187	7.3%
Stone Flour	13.020	1.144	8.1%

The total debris quantity added to the test loop was further subdivided into smaller portions as described in the debris addition subsection below (3f.4.1.5.11).

3f.4.1.5.7 2-Sided MFTL Debris Preparation and Surrogates for Testing

3f.4.1.5.7.1 NUKON, Kaowool, Anti-Sweat Fiberglass, and Latent Fiber

Both NUKON insulation and latent fiber were tested as NUKON which was provided by PSEG (References A.14, A.74, and A.89). PSEG purchased the NUKON from Performance Contracting Inc. (PCI) and had it sent to CCI. Thus a surrogate was not used for NUKON insulation debris. The use of NUKON as a surrogate for latent fiber is consistent with the SE for NEI 04-07 (Reference 2) which states that a bulk density of 2.4 lbm/ft^3 (the density of NUKON) can be assumed for latent fiber. For Test 2 only, NUKON was used to represent generic fiberglass. However, the mass of NUKON added to represent generic fiberglass was based on a bounding density of 6 lbm/ft^3, which is much greater than the 2.4 lbm/ft^3 density of NUKON (Reference 2).

Kaowool insulation was tested as Kaowool which was provided by PSEG. PSEG purchased the Kaowool through PCI and had it sent to CCI (References A.14, A.74, and A.89). Thus a surrogate was not used for Kaowool insulation debris. The Kaowool purchased had a 4 lbm/ft^3 density, which was less than that used in the plant (8 lbm/ft^3 per Reference A.14). However, since the tested quantity was based on the generated volume and installed density, this did not impact the tests.

Anti-sweat fiberglass insulation, which is either Owens Corning Fiberglas or Johns Manville Micro-Lok HP, was tested as Owens Corning Fiberglas which was provided by PSEG. PSEG purchased the Fiberglas from Owens Corning and had it sent to CCI. The bulk density of Fiberglas ranges from 3.7-3.9 lbm/ft^3 while the bulk density of Micro-Lok HP ranges from 4.0 to 5.1 lbm/ft^3 depending on the pipe diameter and insulation thickness (References A.1 and A.14). Considering 50% of each type of anti-sweat insulation, the average bulk density is 4.0 lbm/ft^3. Testing was based on a bulk density of 3.9 lbm/ft^3, which is slightly less than the overall bulk density. This discrepancy is considered negligible with respect to the overall debris load, especially given the margins documented in Section 3f.4.1.5.8 of this Response. Fiberglas was used as a surrogate for Micro-Lok HP insulation.

The preparation of the NUKON and Kaowool fiber debris is described in the steps below (References A.74 and A.89). Fiberglas preparation followed the same preparation methodology, except that Fiberglas was not baked since it is not installed on hot piping in the plant. All fibers were conservatively prepared as fines, although the transport analysis indicates that some small pieces of NUKON, Kaowool, and anti-sweat fiberglass also transport to the strainer in addition to the fines (see Section 3e.6 of this response). Testing of small piece fiber debris as fines is conservative as pieces are more likely to disrupt the formation of a uniform debris bed, or settle, which would result in lower strainer head losses.

The fiber debris preparation sequence consists of:

- The fibers were freed from the jacketing (if jacketed).
- Then the fibers were baked by placing them in an oven with a regulated temperature of 250°C for 24 hours. The baking was meant to simulate the exposure of fiber insulation in the plant to hot surfaces such as the steam generator, pressurizer, and piping. This step does not apply to Fiberglas preparation.
- The fibers were hand cut into pieces approximately 50 mm x 50 mm.
- The dry material was weighed.
- The fibers were split into batches of 3 to 4 dm^3 (0.1 to 0.14 ft^3).
- Each batch was soaked in ~2 liters of water (½ gal) until the fiber appeared saturated.
- The fiber pieces were decomposed by a high pressure water jet with a capacity of 100 bar and with the jet a distance of ± 0.05 m to the water surface. Each fiber batch was blasted for approximately 4 minutes.
- Water added during fiber decomposition with the water jet was not drained as some of the fiber fines would be lost.
- It was ensured by visual means that the insulation was decomposed in the water into fine pieces with no clumps of fibers remaining intact and individual fiber pieces smaller than 8 mm.
- Several batches could be mixed together to a main batch (portion) according to the test description.

The fiber debris preparation method used is consistent with that proposed by the NEI as an industry standard (Reference 50).

In the tests, NUKON and Kaowool were mixed together into the same fiber slurry while Fiberglas was mixed in a separate slurry.

Figure 3f.4.1.5.7.1-1 shows photographs of the prepared NUKON/Kaowool fines (left) and prepared Fiberglas fines (right).

Figure 3f.4.1.5.7.1-1: Prepared Fiber Debris

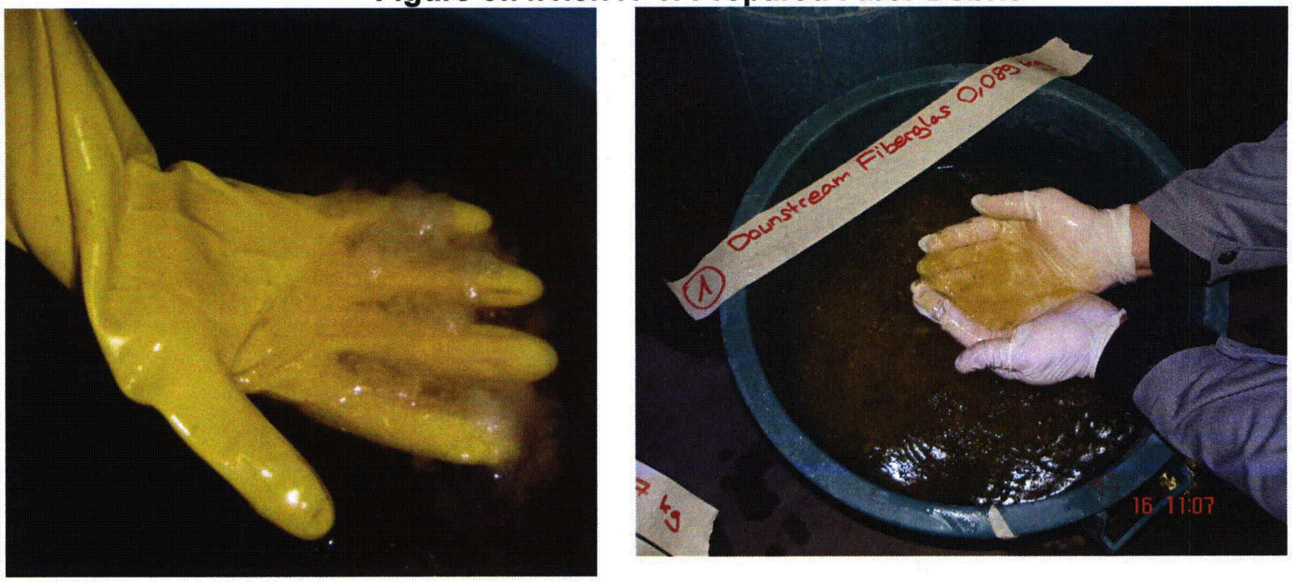

CCI measured the size distribution of fiber fines in both a NUKON/Kaowool slurry and a Fiberglas slurry and obtained the following results (Reference A.75).

Table 3f.4.1.5.7.1-1: Fiber Fines Size Distribution in NUKON/Kaowool Slurry

Size Class	1	2	3	4
Fiber length	< 0.5 mm	0.5 – 1 mm	1 – 2 mm	> 2 mm
Fraction	48%	34%	13%	5%

Table 3f.4.1.5.7.1-2: Fiber Fines Size Distribution in Fiberglas Slurry

Size Class	1	2	3	4
Fiber length	< 2 mm	2 – 5 mm	5 – 10 mm	> 10 mm
Fraction	34%	38%	21%	7%

3f.4.1.5.7.2 Min-K

In the head loss tests, Min-K insulation was tested as Min-K Flex BL21811-16, F182, which was provided by PSEG (References A.14, A.74, and A.89). PSEG purchased the Min-K from Thermal Ceramics and had it sent to CCI. Thus a surrogate was not used for Min-K insulation debris. The density of the Min-K installed at Salem could not be verified; therefore, the maximum Min-K density of 16 lbm/ft^3 was used. The Min-K insulation was reduced to powder form (fines) by hand crushing for the tests. Testing Min-K debris as fines is consistent with the transport analysis (see Section 3c.4 and 3e.4 of this response). Once in powder form, the Min-K added to water to form a slurry. Sometimes the Min-K was mixed with stone flour.

3f.4.1.5.7.3 Coatings and Latent Particulate

The qualified and unqualified epoxy coatings and latent particulate were modeled using stone flour (Refs. A.74 and A.89). The justification for the use of stone flour as a surrogate for coatings is provided in Sections 3h.3 and 3h.4 of this response. Section 3h.4 presents the size distribution and specific surface area for stone flour and states that the specific surface area corresponds to an average particle size less than 10 microns. Thus, stone flour is fine debris. Testing unqualified and qualified epoxy coatings and latent particulate as fines was consistent with the transport analysis (see Section 3h.2 of this response) and the NRC SE for NEI 04-07 (Reference 3). The stone flour was added to water to form a slurry. Sometimes the stone flour was mixed with Min-K.

The guidance in the SE for NEI 04-07 (Reference 3) indicates that latent particulate has a density of 168.6 lbm/ft^3. This is similar to stone flour which has a density of 2680 kg/m^3 (167.4 lb/ft^3) (References A.74 and A.89). The guidance in the SE for NEI 04-07 also states that a suitable size distribution for latent particulate would be 28% from 500 μm to 2 mm, 35% from 75 to 500 μm, and 37% less than 75 μm. Since the use of smaller particulate is generally conservative, the use of stone flour as a surrogate for latent particulate was considered acceptable.

3f.4.1.5.8 2-Sided MFTL Tested Debris Compared to Analytically Determined Debris at Strainer

The tested debris quantity at the sump strainer for Tests 5 and 6 is compared to the limiting (i.e. Break S1 for NUKON and Break S10 for qualified coatings) quantity analytically determined by the debris generation and transport analyses (References A.1 and A.2) in Tables 3f.4.1.5.8-1 and 3f.4.1.5.8-2. The difference between the tested quantity and the analytically determined quantity is operational margin as documented in Reference A.2.

The debris quantity in Tests 2 and 3-repeat is not compared to the analytically determined quantity since the purpose of those tests was to determine if the strainer was susceptible to the thin bed effect. The design basis head loss tests are Tests 5 and 6, as documented in Section 3f.4.2.3 of this response.

Table 3f.4.1.5.8-1: Comparison of Analytically Determined Transported Debris Quantity to Tested Debris Quantity for Test 5

Debris Type	Units	Transport Analysis Values		Strainer Vendor Test Values	
		In Front of Strainer	Top/Back of Strainer	In Front of Strainer	Back of Strainer
Insulation (U1)					
NUKON	[ft^3]	212.4	20.1	207	29.4
Kaowool	[ft^3]	19.3	2.2	29.2	3.9
Anti-Sweat Fiberglass	[ft^3]	13.0	1.1	41.6	3.4
Min - K	[ft^3]	0.0	0.0	5.03	0.27
MRI	[ft^2]	1476	903	N/A (Note 1)	N/A (Note 1)
Qualified Coatings	[ft^3]	5.3	0.3	10.7	0.8
Unqualified Coatings	[ft^3]	1.89	0.0	0.5	0.0
Latent Debris					
Fiber	[ft^3]	12.5	0.0	9.4	3.1
Particulate	[ft^3]	1.0	0.0	0.75	0.25
Lead Blanket Covers					
Fiber[3]	[ft^3]	3.0			
Silicone Rubber	[ft^3]	0.03			
Foreign Materials					
Labels / Placards	[ft^2]	573		667 (Note 2)	

Table 3f.4.1.5.8-2: Comparison of Analytically Determined Transported Debris Quantity to Tested Debris Quantity for Test 6

Debris Type	Units	Transport Analysis Values		Strainer Vendor Test Values	
		In Front of Strainer	Top/Back of Strainer	In Front of Strainer	Back of Strainer
Insulation (U2)					
NUKON	[ft^3]	0.0	0.0	18.8	2.1
Kaowool	[ft^3]	24.3	2.7	25.7	3.5
Anti-Sweat Fiberglass	[ft^3]	13.6	1.1	43.5	3.5
Min - K	[ft^3]	15.1	0.8	22.7	1.8
MRI	[ft^2]	1776	1087	N/A (Note 1)	N/A (Note 1)
Transco RMI	[ft^2]	280	115	N/A (Note 1)	N/A (Note 1)
Qualified Coatings	[ft^3]	5.3	0.3	10.7	0.8
Unqualified Coatings	[ft^3]	1.21	0.0	0.5	0.0
Latent Debris[3]					
Fiber	[ft^3]	12.5	0.0	9.4	3.1
Particulate	[ft^3]	1.0	0.0	0.75	0.25
Lead Blanket Covers					
Fiber[3]	[ft^3]	3.4			
Silicone Rubber	[ft^3]	0.04			
Foreign Materials					
Labels / Placards	[ft^2]	525		667 (Note 2)	

Notes for Tables 3f.4.1.5.8-1 and 3f.4.1.5.8-2

1) RMI was not tested as discussed in Section 3f.4.1.5.9.1 of this response.
2) A 500 ft^2 sacrificial area is accounted for in the test scaling per Section 3f.4.1.5.4 of this response which is appropriate for 667 ft^2 of foreign materials at the strainer assuming a 25% reduction in foreign material area to account for overlap per References 3 and A.2.
3) The fiber value is the equivalent quantity of uncompressed NUKON for the fiberglass component of the lead blanket covers (Reference A.2).

Based on the results in Sections 3f.4.2.3.4 and 3f.4.2.3.5 of this response for Tests 5 and 6, respectively, approximately 60% of the total debris added to the test flume transported to the front side of the strainer (including the debris interceptor and flume floor) while approximately 40% transported to the top or rear of the strainer. This indicates that a significant amount of debris transports over the top of the strainer since only 5-16% of the tested debris was added to the test loop in back of the strainer based on Tables 3f.4.1.5.6-7 and 3f.4.1.5.6-8. Therefore, when determining the how much margin is available for a given debris type, the total analytically determined debris quantity can be compared to the total tested debris quantity.

Furthermore, to obtain a more useful quantification of operational margin, all fiber insulation quantities are converted into an equivalent NUKON quantity.

Strainer blockage is a volumetric phenomenon. Therefore, in order to determine a quantity of NUKON equivalent to a given quantity of a different type of fiber insulation (Type X), the total volume of fibers of Type X on the strainer needs to be determined. Then, the uncompressed volume of NUKON which contains the same volume of Type X fibers can be computed. The uncompressed volume of NUKON is the equivalent quantity of NUKON for fiber Type X.

For a given quantity of fiber debris, the volume of fibers is determined as follows:

$$V_X = Q_X \cdot \frac{c_X}{\rho_X} \qquad \text{(Eq. 3f.4.1.5.8-1)}$$

Where:

V_X	volume of fibers within a given quantity of Type X debris (ft^3)
Q_X	uncompressed volume of Type X debris (ft^3)
c_X	as-fabricated density of Type X insulation (lbm/ft^3)
ρ_X	material (i.e. fiber) density for fibers in Type X insulation (lbm/ft^3)

The equivalent quantity of NUKON (N) debris is then determined as follows:

$$Q_N = V_X \cdot \frac{\rho_N}{c_N} \qquad \text{(Eq. 3f.4.1.5.8-2)}$$

Combining Equations 3f.4.1.5.8-1 and 3f.4.1.5.8-2 results in the following equation for determining the equivalent quantity of NUKON for a given quantity of Type X insulation.

$$Q_N = Q_X \cdot \frac{c_X}{c_N} \cdot \frac{\rho_N}{\rho_X} \qquad \text{(Eq. 3f.4.1.5.8-3)}$$

Based on Table 3-2 of NEI 04-07 (Reference 2), the guidance in the SE for NEI 04-07 (Reference 3), and the plant specific information presented in Section 3c.2 of this Response and Reference A.2, the following as-fabricated and material densities are used for NUKON, anti-sweat fiberglass, and Kaowool.

Table 3f.4.1.5.8-3: Fiber Properties Used to Determine Equivalent NUKON

Fiber Type	As-Fabricated Density (lbm/ft^3)	Material (Fiber) Density (lbm/ft^3)
NUKON	2.4	159
Owens-Corning Fiberglas	4.0	159
Kaowool	8.0	160

Operational margin is available for all tested debris types in case additional debris is discovered or added in containment. The operational margin is determined based on the generated, transported, and tested debris quantities. When determining operational margin, the qualified and unqualified coatings are combined. Similarly, the Min-K is combined with the silicone rubber component of lead blanket covers as the silicone rubber is expected to be detrimental to head loss. Qualified and unqualified coatings are combined since strainer blockage is a volumetric phenomenon, and the volume of coatings debris generated is the same as the coatings volume on the strainer; i.e. compression factors do not need to be accounted for as with fiber insulation. The operational margins are established to also envelope the chemical effects analysis.

3f.4.1.5.9 2-Sided MFTL Untested Debris Types

3f.4.1.5.9.1 Reflective Metal Insulation (RMI/MRI)

CCI's experience has shown that larger pieces of debris have the potential to disrupt thin bed formation during testing. Therefore, RMI/MRI was not used during Tests 2 and 3-repeat since these tests were investigating the thin bed effect (References A.75 and A.89).

The use of RMI in the 1-sided MFTL chemical effects testing had no effect on the head loss when added upon test conclusion (Reference A.88). The same tests demonstrated that including RMI in the full debris load has a beneficial effect on head loss; i.e. inclusion of RMI in the full debris load resulted in a lower head loss than testing without RMI added to the full debris load. Although RMI fines are expected to transport to the strainer and disrupt the debris bed, RMI/MRI was conservatively not included in the full debris loads used for the Tests 5 and 6 (References A.75 and A.74).

3f.4.1.5.9.2 Epoxy Coatings as Chips (Instead of as Particulate)

For plants that cannot substantiate formation of a thin fiber bed, the NRC position is that assumptions related to coatings characterization be realistically conservative based upon the plant-specific susceptibilities and data identified by the licensee, or that a default area equivalent to the area of the sump-screen openings be used for coatings size (Reference 3). As documented in Section 3.f.4.1.5.11 of this response, the fiber bed thickness is greater than the typical thin bed thickness of 1/8 inch for Unit 1 and Unit 2. Therefore, both Units can substantiate at least a thin bed; and testing with coatings as chips was not performed. Additionally, CCI's experience through numerous tests of different clients is that head loss tests with stone flour (particulates) in lieu of paint chips results in higher head losses and as such are more conservative (Reference A.67).

Therefore, the use of particulates instead of chips for epoxy coatings in the tests is conservative.

3f.4.1.5.10 2-Sided MFTL Chemical Precipitate Debris Load

The tested chemical precipitate debris load is described in detail in Sections 3o.1.17d(ii) and 3o.1.21d(i) of this response.

Chemical precipitate preparation is described in detail in Section 3o.1.12d(i) of this response. The WCAP-16530-NP precipitate generator method is used. For this method, the precipitates are generated outside the test loop prior to being added to the test loop.

Section 3o.1.15d(ii) provides the results of the 1-hour settled volume tests. All precipitates used in the testing met their 1-hour settled volume criteria when near field settlement is not credited.

3f.4.1.5.11 2-Sided MFTL Debris Addition

The debris was prepared as described in Section 3f.4.1.5.7 of this response and then split into portions corresponding to various theoretical bed thicknesses (References A.74 and A.89). The size and the order of addition of the portions was dependent on the test being run.

Test 2 was the Unit 2 thin bed test which was run using the draft NRC head loss test guidance issued on September 27, 2007 (Reference 35). Per this NRC thin bed test guidance, very fine fiber debris (NUKON and Kaowool) was added to the flowing test loop in portions equivalent to ~1/16 inch theoretical fiber thickness on the strainer (Reference A.89). The fiber portions were added until a thin fiber bed was visually verified on the strainer module using an underwater camera. Once a thin fiber bed was verified, 100% of the particulate debris load (Min-K and stone flour) was added to the test loop. After the head loss due to the thin bed fiber quantity and particulate stabilized, the remainder of the fiber was added to the test loop in portions equivalent to ~1/16 inch theoretical fiber thickness on the strainer. The total theoretical fiber thickness on the strainer for Test 2 was slightly greater than 0.5 inches.

Test 3-repeat was the Unit 1 thin bed test which was run using the revised NRC head loss test guidance issued on March 28, 2008 (Reference 36). Per this NRC thin bed test guidance, 100% of the particulate debris load (Min-K and stone flour) was added to the flowing test loop prior to adding any fiber debris. Once all particulate debris was added, very fine fiber debris (NUKON, Kaowool, and Fiberglas) was added to the test loop in portions equivalent to ~1/16 inch theoretical fiber thickness on the strainer (Reference A.89). After enough fiber was added to ensure that the thin bed fiber thickness was surpassed (~1/2 inch theoretical fiber thickness), the fiber portions increased in size. The total theoretical fiber thickness on the strainer for Test 3-repeat was slightly greater than 1.1 inches.

Tests 5 and 6 were the Unit 1 and 2 full load chemical effect head loss tests, respectively. Both of these tests utilized the revised NRC head loss test guidance issued on March 28, 2008 (Reference 36). Fiber and particulate additions were alternated throughout the course of each test. For Test 5, very fine fiber portions equivalent to ~1/16 inch theoretical fiber thickness on the strainer were added until the theoretical fiber thickness on the strainer was ~1/2 inch, after which slightly larger portions were added (Reference A.74). For Test 6, all fiber portions were very fine and equivalent to ~1/16 inch theoretical fiber thickness on the strainer (Reference A.74). The particulate portion sizes were chosen to attempt to capture a thin bed head loss, if one were to occur. The total theoretical fiber thicknesses on the strainer for Tests 5 and 6 were slightly greater than 0.9 and 0.3 inches, respectively. Following the addition of all fiber and particulate debris, chemical precipitate debris was added in Tests 5 and 6.

Upstream debris was introduced at the sparger approximately 1.5 meters from the strainer (References A.74, A.75, and A.89), except for the Test 2 particulate which was added at 0.5 meters from the strainer face. Downstream debris was introduced approximately 0.5 meters downstream of the rear strainer face. Fiber and particulate debris were added in separate portions (never mixed together) in slurry form. During the debris addition sequences, the fiber and particulate slurries were periodically mixed/re-suspended in the debris preparation buckets to break-up and prevent debris agglomeration prior to addition to the test loop (Reference A.75).

All debris was added very slowly into the test loop at the water surface. During the debris addition, water from the loop was used to help dilute/agitate the debris in the addition bucket to prevent clumping or agglomeration. This was done by dipping the addition bucket into the loop and then slowly raising it while tilted allowing the fines to release into the flume. The addition bucket was dipped slowly to prevent waves or turbulence in the loop. After each debris addition, the loop was checked for sedimentation and was agitated as necessary. The slow addition of debris in this manner along with agitation ensured that non-prototypical sedimentation, agglomeration and deposition of debris did not occur during debris addition (Reference A.75).

Figure 3f.4.1.5.11-1 shows underwater photos taken during a test (flume was flowing) which show how debris (fiber and particulate) accumulates on the strainer. The photo on the left was taken with less debris than the photo on the right. Both photos were taken during the same test. The debris accumulates on each surface of a pocket until the pocket becomes full. The debris accumulation is relatively uniform, but slightly more debris accumulates on the lower surface of the pocket.

3f.4.1.5.11-1: Debris Accumulation on Strainer (Underwater Photos)

During these tests, the fiber fines were prepared by CCI as described below and in Section 3f.4.1.5.7.1 of this response. The mass of the individual portions of fiber was less than 0.5 kg per bucket. Each fiber portion was prepared using a high pressure water jet until between 40 to 45 liters of water was in each bucket. This resulted in a maximum concentration of approximately 11 to 12.5 grams per liter fiber fines. As the water and fiber slurry was added to the loop in individual dip buckets its concentration was further diluted with water in the loop. Additionally, as the water/fiber slurry was transferred from the preparation bucket to the loop, filtered water collected near the sparger was taken from the loop and added to the preparation bucket. This practice further reduced the fiber concentration in the preparation buckets (Reference A.75).

Similar to the fiber preparation, the particulate debris was first mixed into a water and particulate slurry. Just as with the fiber slurry, the particulate was diluted further within the individual dip buckets as the particulate was added to the loop. Also, filtered water collected near the sparger was taken from the loop and added to the preparation bucket to continually reduce particulate concentration (Reference A.75).

Salem Nuclear Generating Station Units 1 and 2
Docket Nos. 50-272 and 50-311
Generic Letter 2004-02
Updated Supplemental Response for Salem

After the stability criterion (discussed in Section 3f.4.1.5.13 of this response) was reached with all non-chemical debris in the test loop for Tests 5 and 6, the chemical precipitate was added (Reference A.74). The chemical precipitates were added to the test loop using a transfer pump. Each precipitate portion was added in 20 minutes or less. A total of 4 precipitate portions (3 sodium aluminum silicate portions and 1 aluminum oxyhydroxide portion) were added during each test. A minimum of 4 hours elapsed between chemical portion additions to the test loop. The water level was adjusted during each chemical portion addition to maintain the appropriate submergence.

Figures 3f.4.1.5.11-2 through 3f.4.1.5.11-6 show typical fiber, particulate, and chemical precipitate additions, respectively.

Figure 3f.4.1.5.11-2: Typical Fiber Addition Upstream of Strainer

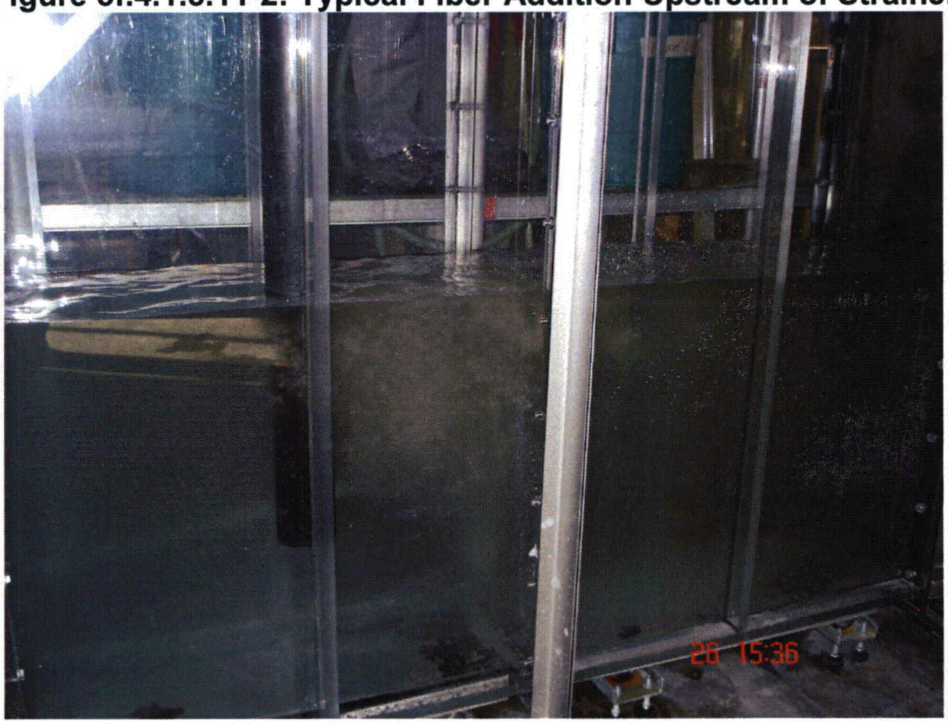

Figure 3f.4.1.5.11-3: Typical Fiber Addition Downstream of Strainer

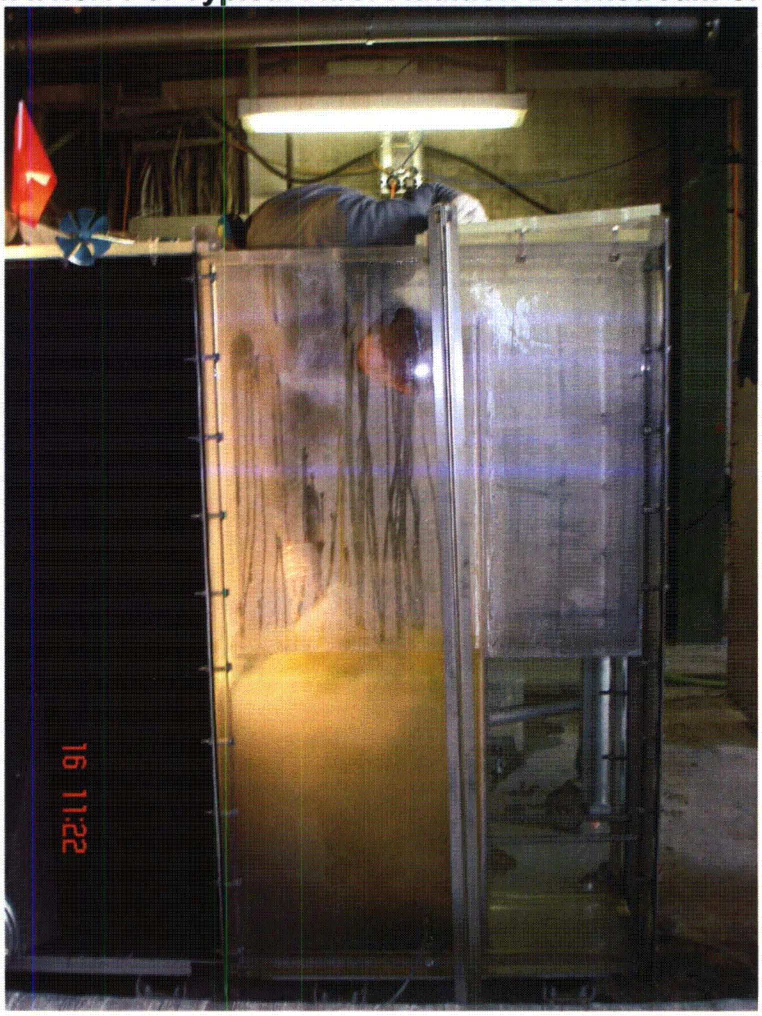

Figure 3f.4.1.5.11-4: Typical Particulate Addition Upstream of Strainer

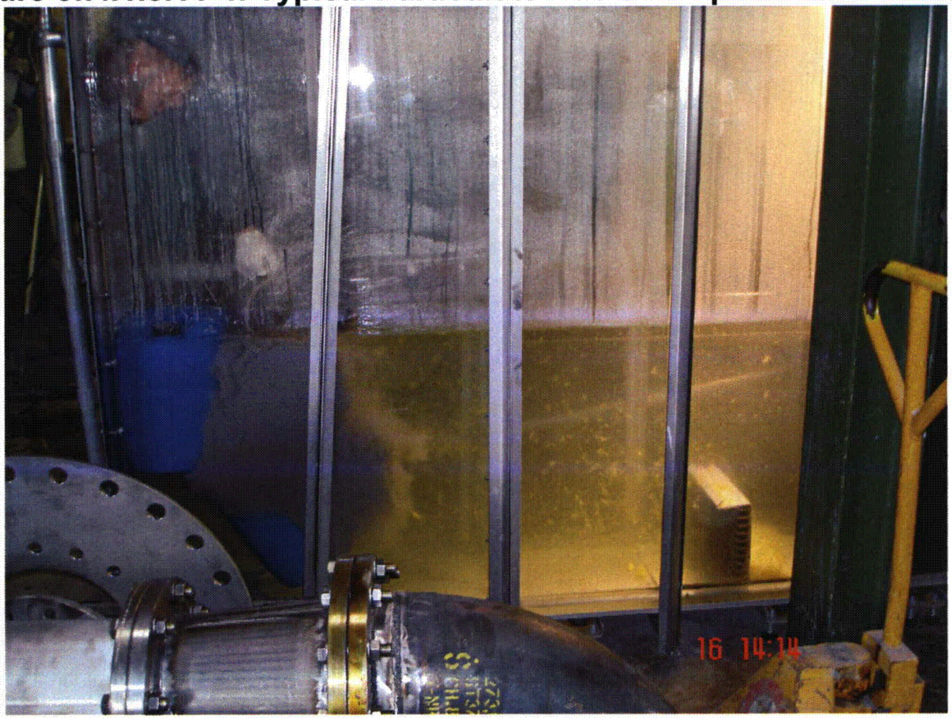

Figure 3f.4.1.5.11-5: Typical Particulate Addition Downstream of Strainer

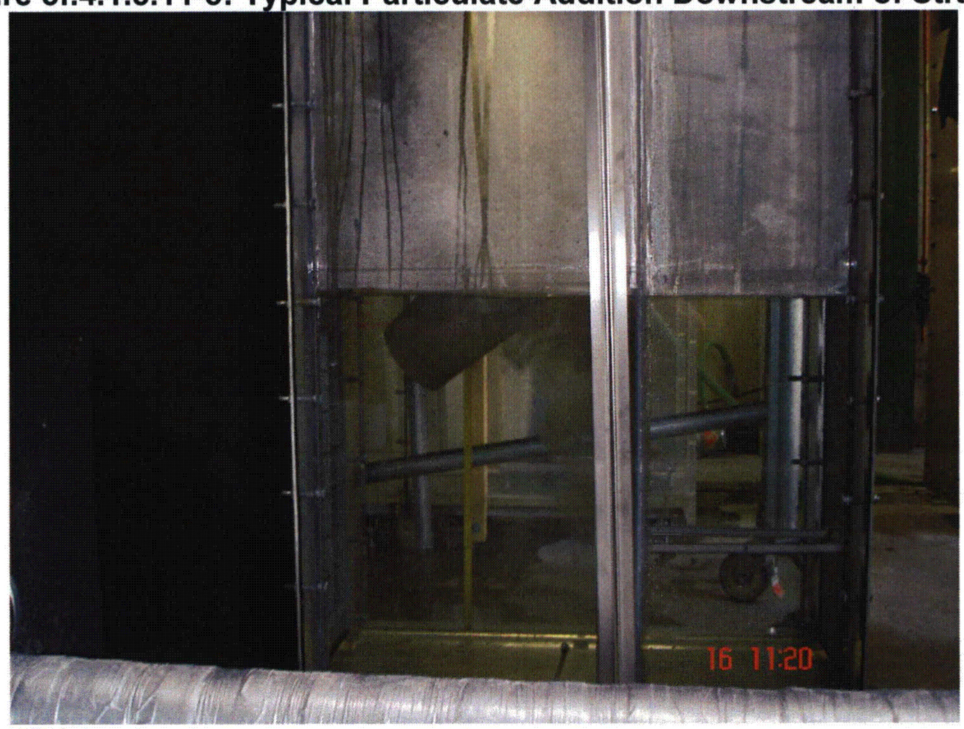

Figure 3f.4.1.5.11-6: Typical Chemical Precipitate Addition

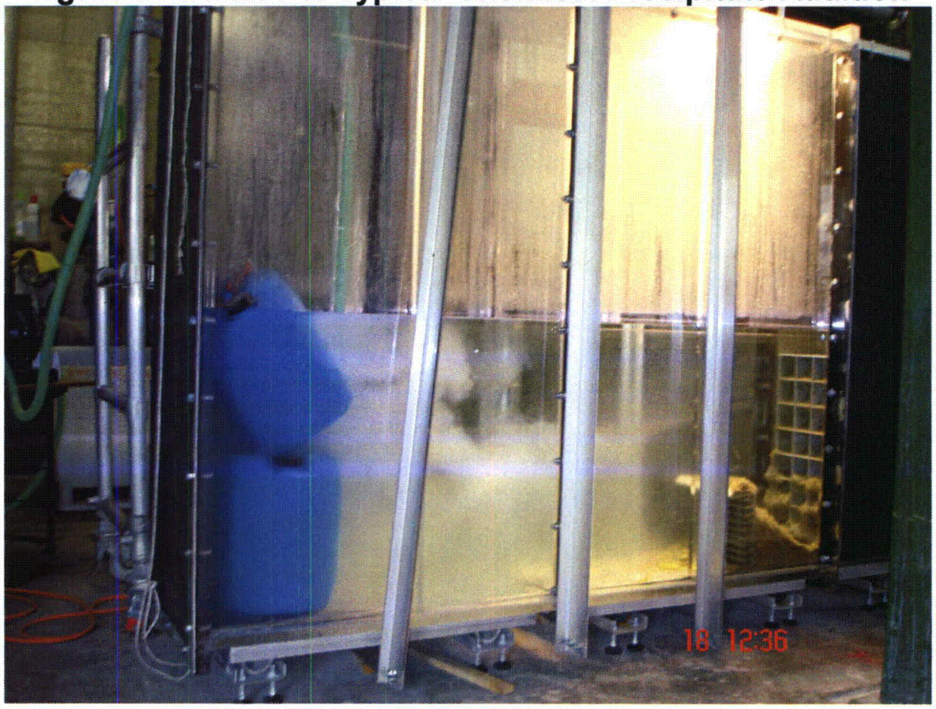

3f.4.1.5.12 2-Sided MFTL Debris Agitation

During and after each debris addition, the loop was checked for sedimentation both upstream and downstream of the strainer. Per the CCI Test Engineer's judgment, sedimentation on the loop floor was agitated and re-suspended using one of two methods (References A.74 and A.89):

1) A short burst from propeller style drill bit was used in the sedimentation area to re-suspend debris, or

2) A squeegee approximately the width of the flume was used to move fiber and particulate away from the either the upstream side of the debris interceptor or downstream side of the strainer. Once the debris was moved away from the strainer or debris interceptor, the debris was agitated with the propeller style drill bit or a squeegee was used to "lift" the debris off the floor. Note, for Test 2 (which did not include the debris interceptor), debris was moved away from the upstream side of the strainer. Also, Test 2 utilized a paddle style pole instead of a squeegee, but the functionality was similar.

Using either method, the debris bed was not disrupted. Agitation Method 1 was only used further than 30 cm from the strainer face and was never directed or angled towards the strainer. Furthermore, only agitation Method 2 was used on the downstream side of the strainer with the exception of during the Test 3-repeat particulate addition. During Test 3-repeat, the debris on the downstream side of the strainer was agitated with the propeller style drill bit when only particulate was in the test loop. On the downstream side of the strainer, debris further than 10 cm from the strainer face was agitated. For tests which included the debris interceptor, the debris between the debris interceptor and front face of the strainer was not agitated.

During or after debris agitations there were no visual or pressure drop indicators that the debris bed was adversely affected. Each agitation re-suspended the targeted fiber fines and particulate evenly throughout the height and width of the test flume. Agitating the debris resulted in a conservatively even debris distribution as it provided more opportunity for fiber fines to remain as single fibers and maximize the potential to distribute along the clean pocket surface area.

3f.4.1.5.13 2-Sided MFTL Stability Criteria / Test Termination Criteria

For Test 2, small fiber portions were added until a thin fiber bed was verified on the strainer as discussed in Section 3f.4.1.5.11 of this response, and then 100% of the particulate load was added to the test loop. After the particulate addition and all subsequent fiber additions, the head loss was allowed to stabilize. The stability criterion used for this test was ±1% head loss change for 30 continuous minutes (Reference A.89).

For Test 3-repeat, 100% of the particulate load was added to the test loop followed by small fiber portions as discussed in Section 3f.4.1.5.11 of this response. After each fiber addition, the head loss was allowed to stabilize. The stability criterion used was ±1% head loss change for 30 continuous minutes (Reference A.89). However, the stability criterion following the last fiber addition was ±1% head loss change for 60 continuous minutes. For the flow sweep performed in this test, the head loss stability criterion was ±1% change for 30 continuous minutes (Reference A.89).

For Tests 5 and 6, the stability criterion following non-chemical and chemical debris addition was ±1% head loss change for 60 continuous minutes (or a minimum of 4 hours following debris addition) while the stability criterion during the flow sweep in Test 6 was ±2% head loss change for 30 continuous minutes (Reference A.74). These stability and termination criteria are also discussed in Sections 3f.4.2.3 and 3o.1.16d(i) of this response.

The stability criteria could be bypassed at the discretion of the test engineer in all tests. However, this was not necessary since the stability criteria were met as explained in Section 3f.4.2.3 of this response.

3f.4.1.5.14 2-Sided MFTL Debris Sedimentation

The debris in various locations in the test loop was collected and placed in separate individual marked containers (References A.74 and A.89). The containers were placed side by side and the percentage of debris which in each location was estimated and recorded. At a minimum the fraction of debris in each of the following locations was determined:

- In the upstream (front) strainer pockets
- In the downstream (rear) strainer pockets
- On the flume floor upstream of the strainer module
- On the flume floor downstream of the strainer module

The sedimentation results are provided in Section 3f.4.2.3 of this response.

3f.4.1.6 2-Sided MFTL Fiber Bypass Tests (November-December 2008)

The 2008 fiber bypass tests constitute part of the fiber bypass design basis; the other part is based on the 2006 fiber bypass tests. The purpose of the 2008 fiber bypass tests was to confirm that the results of the 2006 fiber bypass tests were conservative when the fiber debris preparation included baking the fibers (the fibers used in 2006 were not baked). The 2008 fiber bypass test results substantiate the bypass values used in the downstream effects component wear calculation (Reference A.18) and are used in the fuel deposition calculation (Reference A.13). A total of 3 tests were run. These tests are referred to as "2-sided" since the strainer module in the 2008 tests utilized the prototypical strainer module used for the 2008 head loss tests. The three tests run were:

Test 1: Composite Test (bounding fiber debris quantity from both Units 1 and 2)
Test 2: Unit 2 Full Fiber Debris Load
Test 3: Latent Fiber Only

The 2008 fiber bypass tests were performed using CCI Test Specification Q.003.84 808 (Reference A.89) and the results are presented in CCI Test Report 680/41465 (Reference A.75). Deviations from the test specification are documented in the test report. The deviations did not impact the validity of the test results.

3f.4.1.6.1 2-Sided MFTL Configuration for Fiber Bypass Tests (Reference A.89)

The 2-sided MFTL fiber bypass tests were performed using the same test loop configuration as the 2-sided MFTL head loss tests described in Section 3f.4.1.5.1. The only modification made to the test loop for the fiber bypass tests was that a fiber bypass screen was added to the test loop. The fibers which bypassed the strainer were collected on a 0.31 mm stainless steel mesh (Reference A.89). The mesh was placed downstream of the sparger location. The horizontal return piping includes a side (horizontal) mounted extraction tap which allowed samples of the debris laden bypass water to be taken to determine the fiber concentration as a function of time.

The water level in the tests was continuously monitored to maintain a minimum submergence of approximately 7-8 cm (Reference A.89), similar to the 2-sided MFTL head loss tests. This is similar to the minimum submergence above the strainers of 3 inches (Reference A.6). The water level was adjusted by draining the test loop following debris additions. The drained water was filtered and any debris removed was reintroduced to the test loop. The fiber bypass tests were run with room temperature water which ranged from 15-20°C (52-70°F) (Reference A.75).

3f.4.1.6.2 2-Sided MFTL Scale Factor for Fiber Bypass Tests (Reference A.89)

The 2-sided MFTL fiber bypass tests all conservatively utilized the Unit 2 scale factor of 69.7 from the 2-sided MFTL head loss tests (see Section 3f.4.1.5.4 of this response) (Reference A.89). The Unit 2 scale factor was chosen since it results in higher penetration velocities than the Unit 1 scale factor (73.0).

3f.4.1.6.3 2-Sided MFTL Flow Rates for Fiber Bypass Tests (Reference A.89)

All bypass tests utilized a flow rate of 8850 gpm (Reference A.89), which is the same as the design maximum two pump flow rate (Reference A.14).

3f.4.1.6.4 2-Sided MFTL Debris Loads for Fiber Bypass Tests (Reference A.89)

The tested debris loads for each fiber bypass test are presented in Tables 3f.4.1.6.4-1 and 3f.4.1.6.4-2 (Reference A.89). The tested debris quantity was determined using both the test scale factor and the density of each insulation. Test 1 was run using the maximum fiber debris quantity from both Unit 1 and Unit 2 with margin added; hence it was a "composite" test. Test 2 was based on the Unit 2 fiber debris quantity plus margin. Test 3 was a latent fiber only test. Latent fiber was modeled as NUKON.

Table 3f.4.1.6.4-1: 2-Sided MFTL Fiber Bypass Test Debris Loads

Type of Debris	Upstream Volume	Downstream Volume	Density	Upstream Mass	Downstream Mass
	ft^3	ft^3	lbm/ft^3	lbm	lbm
Test 1					
NUKON	235	33.8	2.4	564	81.12
Kaowool	32.6	4.4	8.0	260.8	35.2
Fiberglas	50.5	4.1	3.9	196.95	15.99
Latent Fiber	9.4	3.1	2.4	22.56	7.44
Test 2					
NUKON	18.8	2.1	2.4	45.12	5.04
Kaowool	25.7	3.5	8.0	205.6	28
Fiberglas	43.5	3.5	3.9	169.65	13.65
Latent Fiber	9.4	3.1	2.4	22.56	7.44
Test 3					
Latent Fiber	9.4	3.1	2.4	22.56	7.44

Table 3f.4.1.6.4-2: 2-Sided MFTL Fiber Bypass Debris Added to Test Loop

Type of Debris	Test 1		Test 2		Test 3	
	Upstream Mass	Downstream Mass	Upstream Mass	Downstream Mass	Upstream Mass	Downstream Mass
	kg	kg	kg	kg	kg	kg
NUKON	3.818	0.576	0.440	0.081	0.147	0.048
Kaowool	1.697	0.229	1.338	0.182		
Fiberglas	1.282	0.104	1.104	0.089		

3f.4.1.6.5 Debris Preparation, Addition, and Agitation for 2-Sided MFTL Fiber Bypass Tests (Reference A.89)

PSEG provided NUKON, Kaowool, and Fiberglas to CCI for testing (Reference A.89). The fibers were prepared in the same manner as that described in Section 3f.4.1.5.7.1. The fiber debris was introduced to the test flume in the same manner as for the 2-sided MFTL head loss tests (see Section 3f.4.1.5.11 of this response) (Reference A.89). All fiber was added approximately 1.5 meters upstream of the strainer module. After each fiber addition, the test loop was checked for sedimentation and agitated if necessary using the same techniques described in Section 3f.4.1.5.12 of this response for the 2-sided MFTL head loss tests.

The fiber debris preparation method used is consistent with that proposed by the NEI as an industry standard (Reference 50).

3f.4.1.6.6 Bypass Determination (Reference A.89)

Each fiber bypass test was run for 6 hours. Bypass samples were taken starting after the first fibers were introduced into the test loop from a sample line downstream of the strainer in the horizontal return line (Reference A.89). After the initial sample, samples were taken every 3 minutes beginning with the initiation of the test until 15 samples had been taken. After the 15th sample was taken, a sample was taken at 1 hour and then samples were taken every 30 minutes until the end of the test. The samples were taken in 500 ml bottles. The tap was purged prior to taking each sample and the purged water was returned to the test loop in the bypass filter region (near the sparger). As stated in Section 3f.4.1.5.5, the approximate test loop turnover time is 2.5 to 3 minutes.

The mass of material on the bypass screen was determined in the same manner as in the 2006 1-sided MFTL tests. The dry weight of the bypass screen was recorded prior to and after each test. The difference in the two weights is the mass of material which bypassed the strainer, less the mass of material in the samples (Reference A.89). The calibrated scale used to determine bypass mass was accurate to the 0.0001 kg place (Reference A.75).

3f.4.2 Strainer Bypass and Head Loss Test Results

The test results from the large scale bypass tests, the 2006 and 2008 fiber bypass tests, and the 2-sided MFTL head loss tests are presented in this section.

3f.4.2.1 Large Scale Material (Fiber and Particulate) Bypass Test Results

As discussed in Section 3f.4.1.2 of this response, the head loss tests performed in the large scale test loop are not used for the design basis strainer head loss. However, the bypass results from Tests 4 and 5 in large scale test loop (Reference A.65) are used in the downstream effects component wear calculation (Reference A.18) to determine the particulate removal efficiency. The bypass results presented as concentration of material (fiber and particulate) downstream of the strainer from Tests 4 and 5 are presented in Table 3f.4.2.1-1.

Salem Nuclear Generating Station Units 1 and 2
Docket Nos. 50-272 and 50-311
Generic Letter 2004-02
Updated Supplemental Response for Salem

Table 3f.4.2.1-1: Bypass Results from Large Scale Tests 4 and 5

Test 4		Test 5	
Time	Downstream Material Concentration (ppm)	Time	Downstream Material Concentration (ppm)
9:40	3320	12:10	664
9:50	2498	12:20	292
10:00	2040	12:30	232
10:10	1720	12:40	128
10:20	1354	12:50	86
10:30	1272	13:00	82
10:40	1108	13:10	46
11:10	894	13:40	42
11:40	704	14:10	14
12:10	598	14:40	34
12:40	532	15:10	52
13:10	390	15:40	8.2
		16:10	<1

3f.4.2.2 Fiber Bypass Test Results

The results from both the 2006 and 2008 fiber bypass tests are provided in the following sections. The results from the 2006 fiber bypass tests bound the results from the 2008 fiber bypass tests.

3f.4.2.2.1 2006 1-Sided MFTL Fiber Bypass Tests

The results of the 2006 fiber bypass results are presented in Figures 3f.4.2.2.1-1 through 3f.4.2.2.1-2 (Reference A.83). These figures present the bypass per strainer area as a function of both fiber added to the test loop and penetration velocity. The penetration velocity is based on the total strainer area. For these tests all fibers added to the test loop transported to strainer.

Figure 3f.4.2.2.1-1: Bypass as a Function of Fiber Mass Added to Test

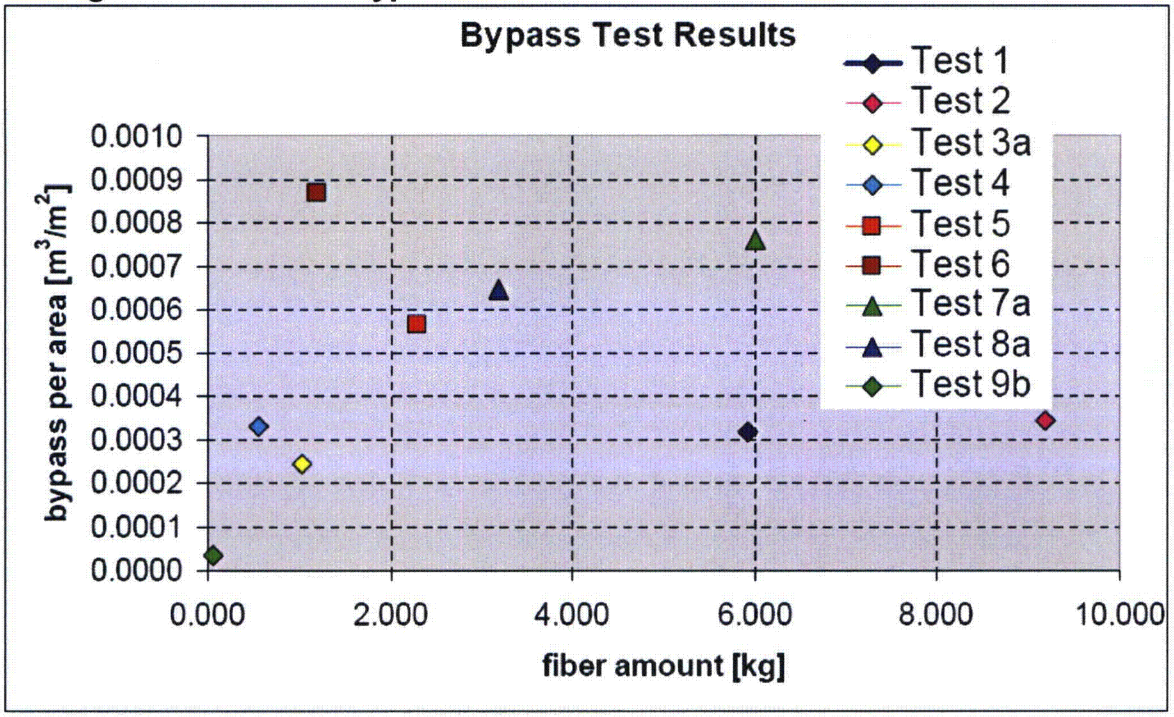

Figure 3f.4.2.2.1-2: Bypass as a Function of Penetration Velocity

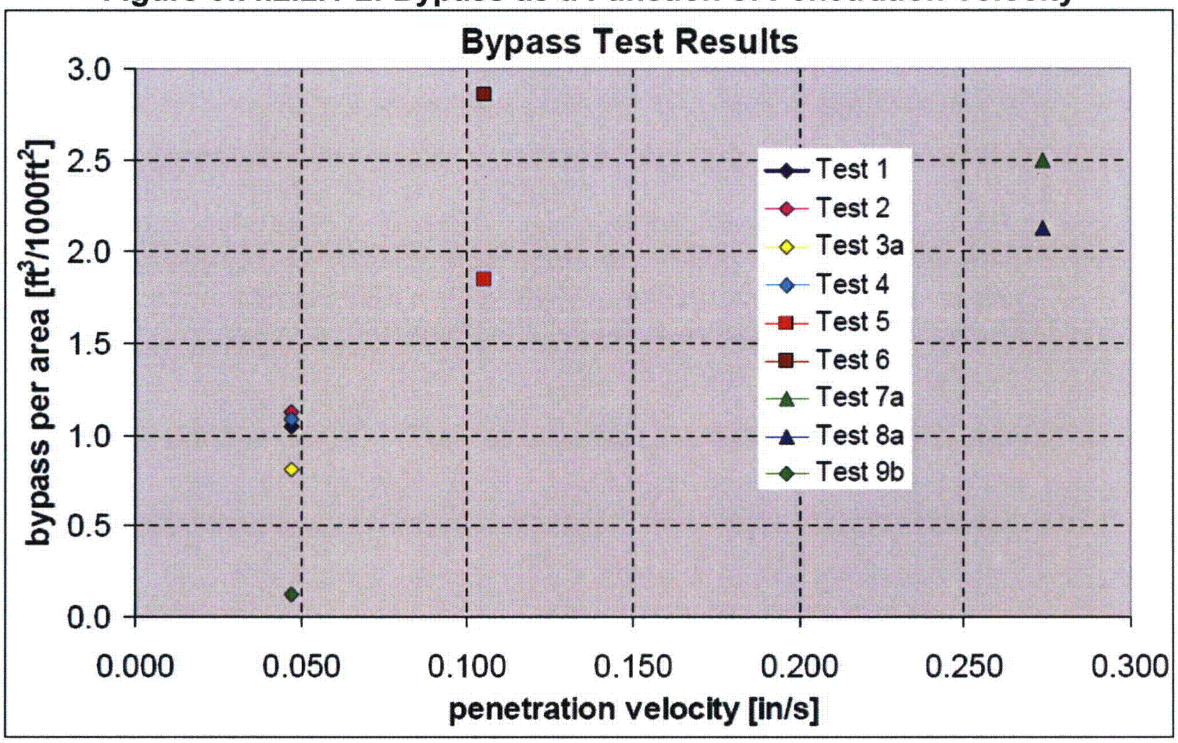

Based on the above figures, the following conclusions are made (Reference A.83):

- Once the strainer becomes saturated with fiber, an increase in the upstream fiber quantity does not result in a higher amount of fiber bypass. Therefore, the quantity of fiber bypass is not proportional to the amount of upstream fiber and bypass cannot be characterized as a percentage of upstream material.
- The bypass volume is proportional to the penetration velocity and each penetration velocity has its own bypass value. The bypass quantity increases with the flow rate / penetration velocity.
- The bypass volume is proportional to the strainer area.

Although none of the tests in this test series were identical, some level of repeatability in the tests was shown (Reference A.83). Tests 1, 2, 3a, and 4 are all based on the same strainer area and flow rate and while the tests had different debris quantities added to the test loop, the bypass volume per area value of all four tests was approximately 1 ft^3/1000 ft^2.

Tests 1, 2, 3a, 4, and 9b were based on a strainer area of 5345 ft^2, while Tests 5 and 6 were based on a strainer area of 2673 ft^2 and Tests 7a and 8a were based on a strainer area of 1336 ft^2 (Reference A.84). Therefore, the results of Tests 1, 2, 3a, 4, and 9b are the most applicable to the installed Unit 1 and Unit 2 strainers which have areas of 4854 ft^2 and 4656 ft^2 , respectively (Reference A.77). The other tests (5-8a) were only used to develop the general fiber bypass trends noted above. For conservatism, the downstream effects wear calculation (Reference A.18) used the results of Tests 1-4, and excluded Test 9 since the strainer was not saturated in Test 9 and therefore had a much lower fiber bypass value.

The transient fiber concentration downstream of the strainer was also measured for one test (Reference A.83). The results are shown in Figure 3f.4.2.2.1-3.

Figure 3f.4.2.2.1-3: Transient Downstream Fiber Concentration

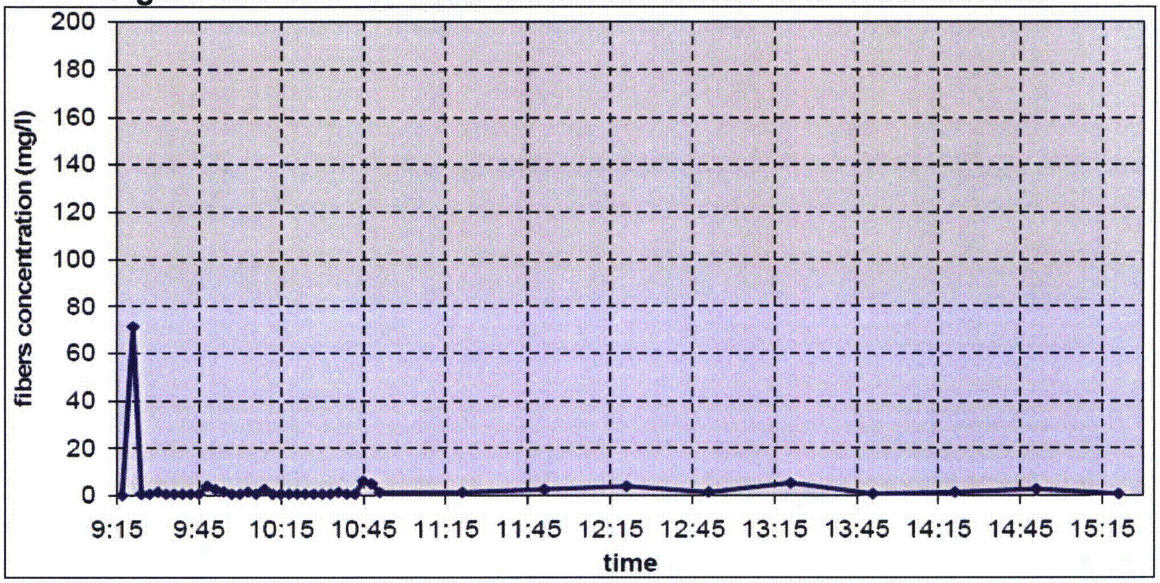

In addition to measuring the bypass mass, the size of the bypassed fibers was also measured for one test (Reference A.83). The size distribution of bypassed fibers is shown in Table 3f.4.2.2.1-1. It shows that the majority (~90%) of the fiber bypass is less than 1.0 mm long.

Table 3f.4.2.2.1-1: Bypass Fiber Size Distribution

Size Class	Fiber Size	Fraction
Class 1	0.1 to 0.5 mm	63.1 %
Class 2	0.5 to 1.0 mm	27.3 %
Class 3	1.0 to 2.0 mm	8.2 %
Class 4	> 2.0 mm	1.4 %

3f.4.2.2.2 2008 2-Sided MFTL Fiber Bypass Tests

The 2008 fiber bypass tests were run to confirm that the information from the 2006 fiber bypass tests was conservative. The primary difference between the two tests was that the fiber preparation methods in the 2008 tests included baking the fibers, while the 2006 tests did not bake the fibers (References A.84 and A.89). Also, the 2008 tests included three fiber types in the upstream fiber mixture (NUKON, Kaowool, and Fiberglas) while the 2006 tests were run primarily with NUKON only. In addition, the 2008 tests were run with a Salem specific 2-sided test module while the 2006 tests were run with a 1-sided test module (References A.84 and A.89).

The results of the 2008 tests are plotted along with the relevant data (Tests 1, 2, 3a, 4, and 9b) from the 2006 tests in Figures 3f.4.2.2.2-1 through 3f.4.2.2.2-2 (Reference A.75). The other 2006 tests are not included since they utilized much higher penetration velocities than would exist in the plant with the installed strainer configuration. These figures demonstrate that the 2006 fiber bypass test data bounds the data obtained in the 2008 tests.

Figure 3f.4.2.2.2-1: Bypass per Strainer Area Based on Uncompressed Upstream Fiber Volume

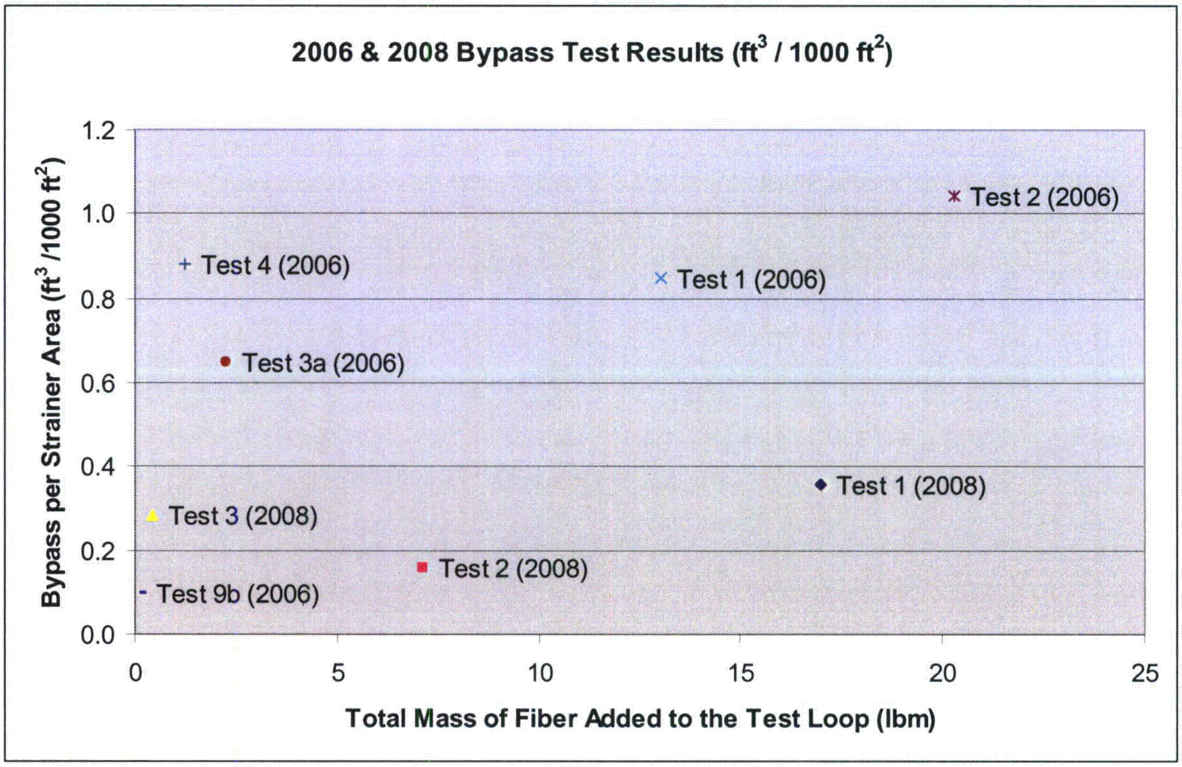

Figure 3f.4.2.2.2-2: Bypass per Strainer Area Based on Upstream Fiber Mass

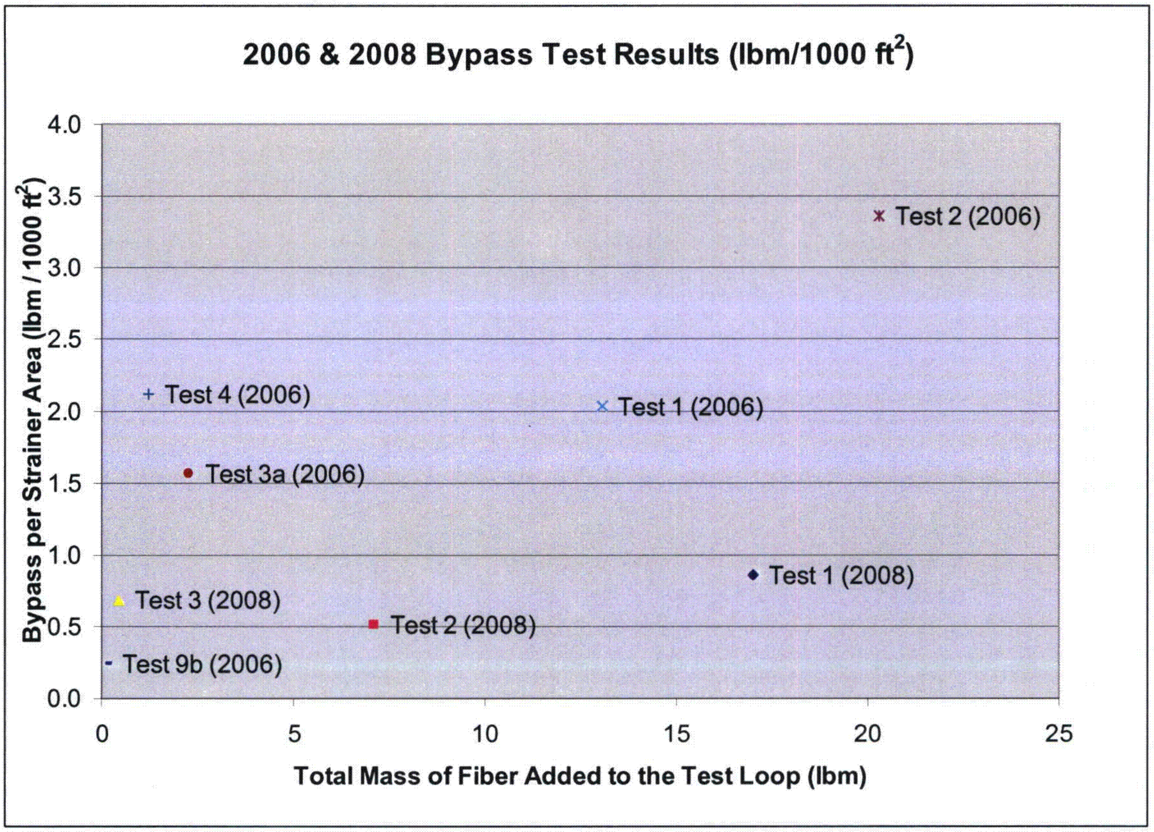

In addition to measuring the bypass mass, the size of the bypassed fibers was also measured for each 2008 test (Reference A.75). The size distribution of bypassed fibers is shown in Table 3f.4.2.2.2-1. It shows that the majority (> 90%) of the fiber bypass is less than 1.5 mm long. These results are comparable to the 2006 tests.

Table 3f.4.2.2.2-2: Bypass Fiber Size Distribution

Size Class	Fiber Size	Test 1	Test 2	Test 3
Class 1	0.1 to 0.5 mm	26 %	26 %	46 %
Class 2	0.5 to 1.0 mm	39 %	39 %	34 %
Class 3	1.0 to 1.5 mm	28 %	28 %	15 %
Class 4	> 1.5 mm	7 %	7 %	5 %

3f.4.2.3 2008 2-Sided MFTL Head Loss Tests (Reference A.75)

The results of the 2-sided MFTL head loss tests performed in 2008 are presented in this section. Each test is discussed separately. These are the same tests which were witnessed by the NRC from April 20 through April 25, 2008 (Reference A.81).

3f.4.2.3.1 Test 1: Clean Strainer Head Loss Test

Test 1 was performed on February 25, 2008. The pressure trace for Test 1 is provided below (Reference A.75). The pressure trace shows the relationship between flow rate and head loss for a clean strainer.

Figure 3f.4.2.3.1-1: Test 1 Pressure Trace (February 25, 2008)

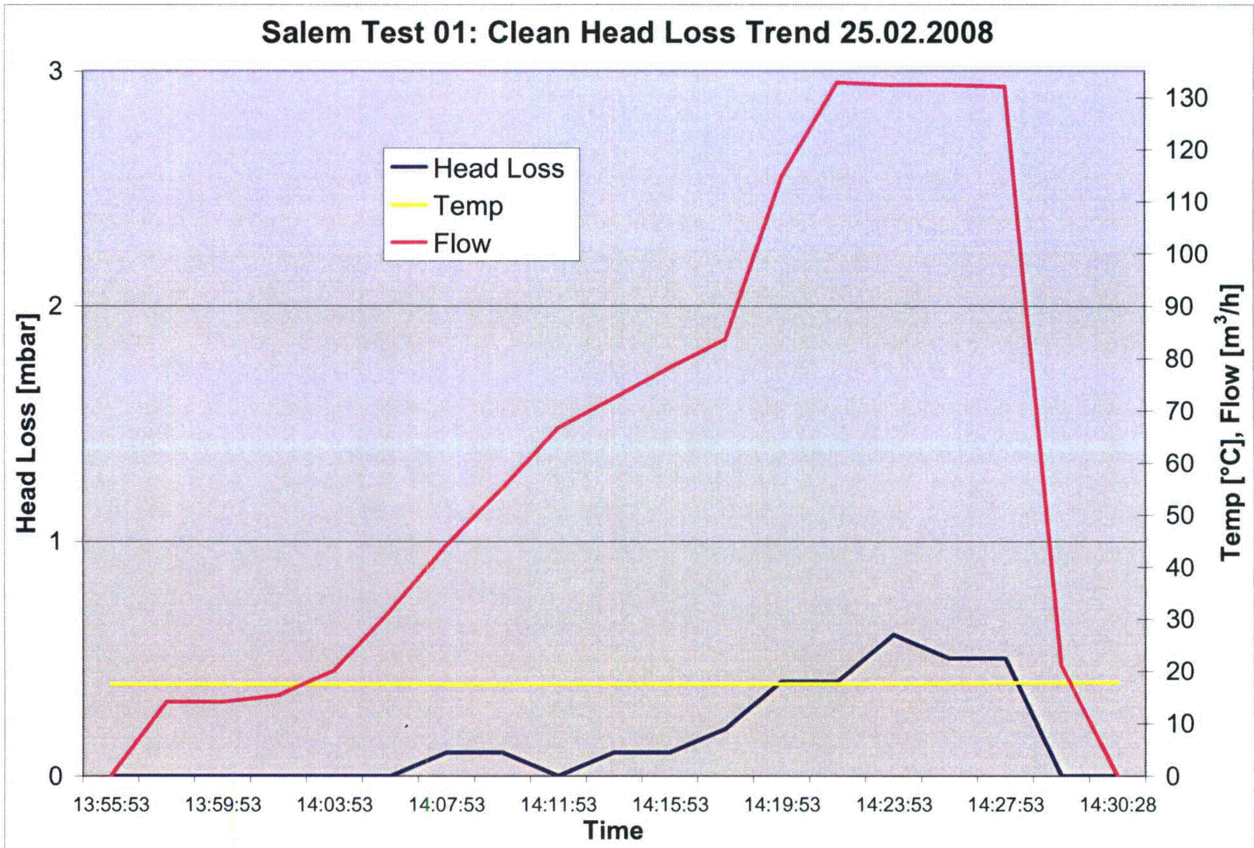

The head loss of the clean strainer was approximately 0.1 mbar at a nominal flow of 8850 gpm (27 to 28 m^3/h) and the maximum head loss of 0.5 mbar was observed at greater than 400% of nominal flow. Therefore, it can be concluded that the clean strainer head loss due to the perforated plate is negligible. Vortices were not observed at any of the flow rates tested with a strainer submergence of approximately 3 inches (Reference A.75).

3f.4.2.3.2 Test 2: Unit 2 Thin Bed Head Loss Test

Test 2 was performed from February 26 to March 3, 2008. This test employed the September 2007 NRC thin bed effect testing guidance (Reference 35). The pressure trace for Test 2 is shown below (Reference A.75).

Figure 3f.4.2.3.2-1: Test 2 Pressure Trace (February 26 - March 3, 2008)

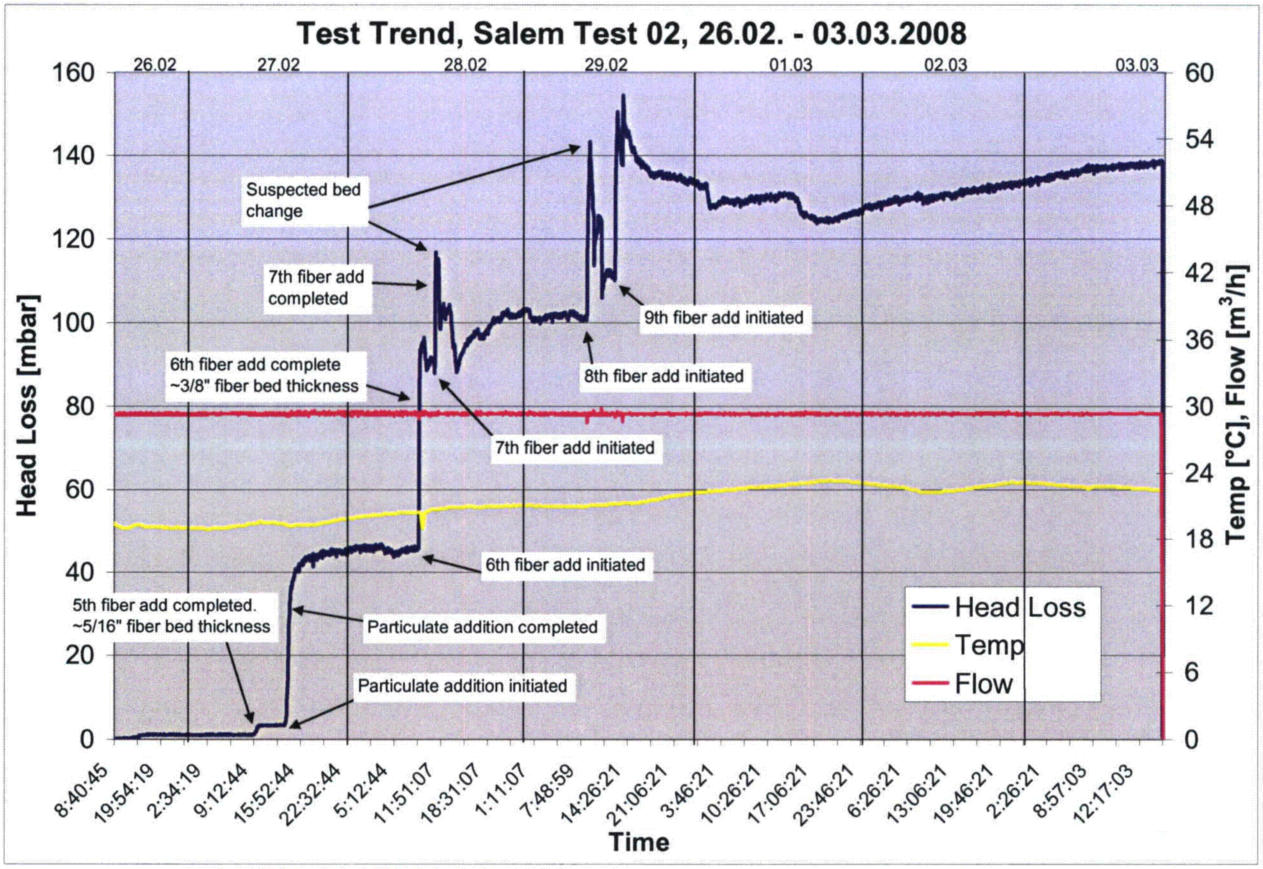

The maximum stability achieved following addition of 100% of the particulate was 1.3% change in head loss over 30 minutes. The maximum stability achieved following addition of 100% of the debris was 0.5% change in head loss over 60 minutes. No bore holes were visibly observed in the test. The pressure spikes on February 28 and 29 were due to bed readjustments following fiber additions.

The maximum head loss with 100% debris in the test loop was 154.4 mbar at a temperature of 21.3°C (70°F) and an equivalent flow rate of 9000 gpm. This is less than the Test 6 (Unit 2 full load head loss test) maximum head loss of 242.2 mbar at a temperature of 47.6°C (118°F) and an equivalent flow rate of 8850 gpm with the 100% non-chemical debris bed (see Section 3f.4.2.3.5 of this response). The difference between the Test 2 and 6 head losses is actually larger than 88 mbar (=242.2-154.4) since Test 6 was run with a heated test loop and the corresponding head loss in a room temperature test loop would have been greater due to the difference in viscosities. Test 6 also utilized an 8850 gpm equivalent flow rate compared to the Test 2 equivalent flow rate of 9000 gpm. Thus, it was concluded that the Unit 2 strainer design basis head loss should be based on the full load head loss test and not the thin bed effect head loss test to be conservative.

Furthermore, no thin bed effect was observed in Test 2. This was evident based on the head loss increase after 100% particulate addition. When temperature scaling is taken into account the head loss increase is not considered substantial enough to be representative of the thin bed effect.

The quantity of debris at various locations in the test apparatus is documented below. Very little debris settled on the floor in front of either side of the strainer module.

- Debris in front (upstream) strainer pockets 41.4%
- Debris in rear (downstream) strainer pockets 41.4%
- Debris on flume floor upstream of strainer module 8.6%
- Debris on flume floor downstream of strainer module 8.5%

3f.4.2.3.3 Test 3-repeat: Unit 1 Thin Bed Head Loss Test

Test 3-repeat was performed from April 1 to 3, 2008. This test employed the March 2008 NRC thin bed effect testing guidance (Reference 36) in which 100% of the particulate debris was added at the beginning of the test followed by small fiber portions. The pressure trace for Test 3 is shown below (Reference A.75).

Salem Nuclear Generating Station Units 1 and 2
Docket Nos. 50-272 and 50-311
Generic Letter 2004-02
Updated Supplemental Response for Salem

Figure 3f.4.2.3.3-1: Test 3-repeat Pressure Trace (April 1 - 3, 2008)

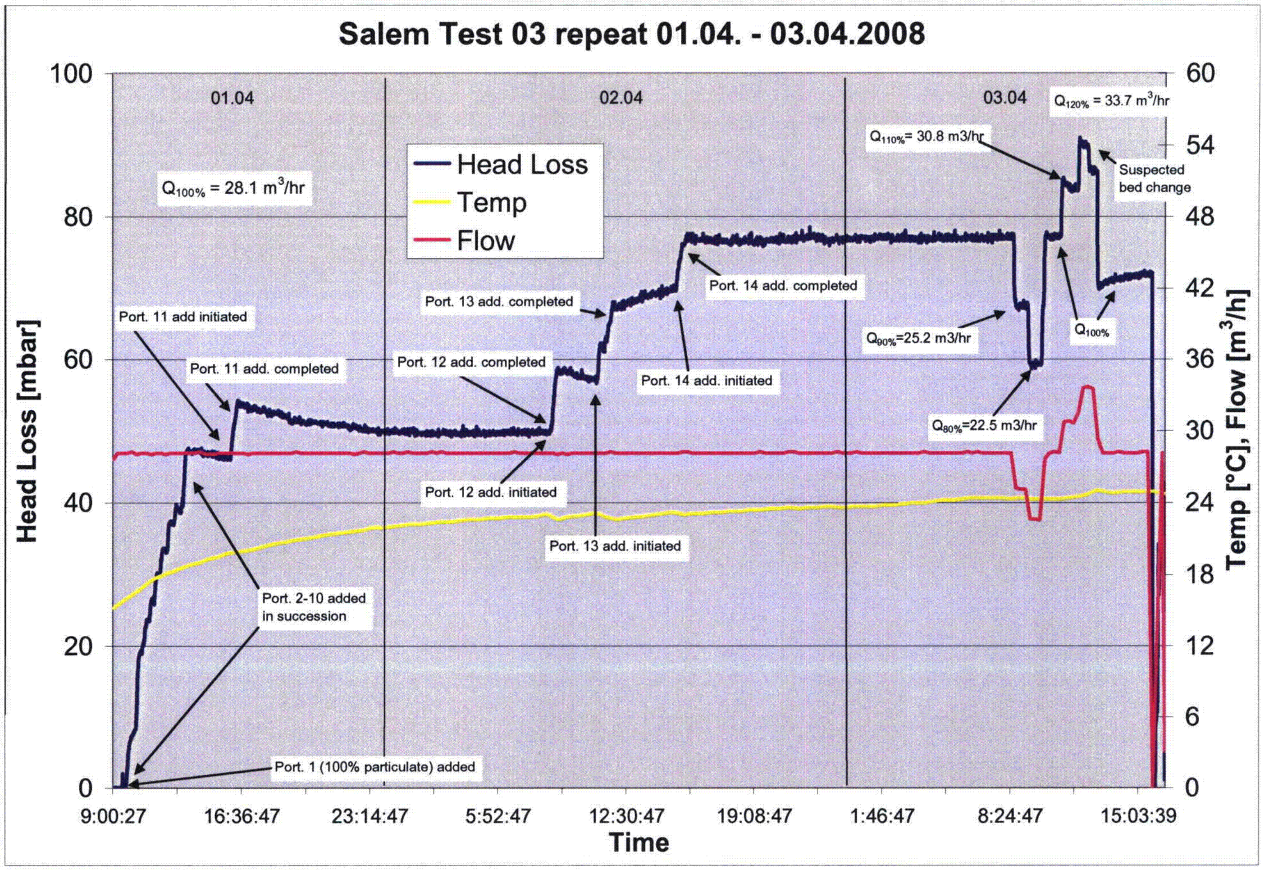

The maximum stability achieved following addition of 100% of the debris was 0.6% change in head loss over 60 minutes. No bore holes were visibly observed in the test. At the end of the test, the pump was stopped for 10 minutes and then restarted to determine if vortices would form upon restart due to potential clean strainer windows which could have formed when air was released from solution following the pump stop. Upon restart with a strainer submergence of approximately 3 inches, no vortices or air ingestion were observed.

The maximum head loss (prior to the flow sweep) with 100% non chemical debris in the test loop was 78.5 mbar at a temperature of 23.6°C (74°F) and an equivalent flow rate of 9000 gpm. Although there was a steady increase in head loss at the beginning of the test while fiber portions 2-10 were added (total theoretical fiber bed thickness of ~0.6 inches (Reference A.89)), none of the head loss increases were very large. Thus, it is concluded that the Unit 1 strainer is not susceptible to the thin bed effect and that the full load head loss test (Test 5) is the appropriate test to use to determine the design basis strainer head loss.

The quantity of debris at various locations in the test apparatus is documented below. Very little debris settled on the floor in front of either side of the strainer module.

- Debris in and on front (upstream) strainer pockets = 49.8%
- Debris in rear (downstream) strainer pockets = 26.8%
- Debris on flume floor between the debris interceptor and the front face of the strainer and underneath the strainer module = 21.1%
- Debris on flume floor downstream of strainer module = 1.9%
- Debris on top of strainer = 0.4%
- Debris on flume floor upstream of on debris interceptor = ~0%

3f.4.2.3.4 Test 5: Unit 1 Full Debris Load Chemical Effects Head Loss Test

Test 5 was performed from June 4 to 12, 2008. The pressure trace for Test 5 is shown below (Reference A.75).

Figure 3f.4.2.3.4-1: Test 5 Pressure Trace (June 4 - 12, 2008)

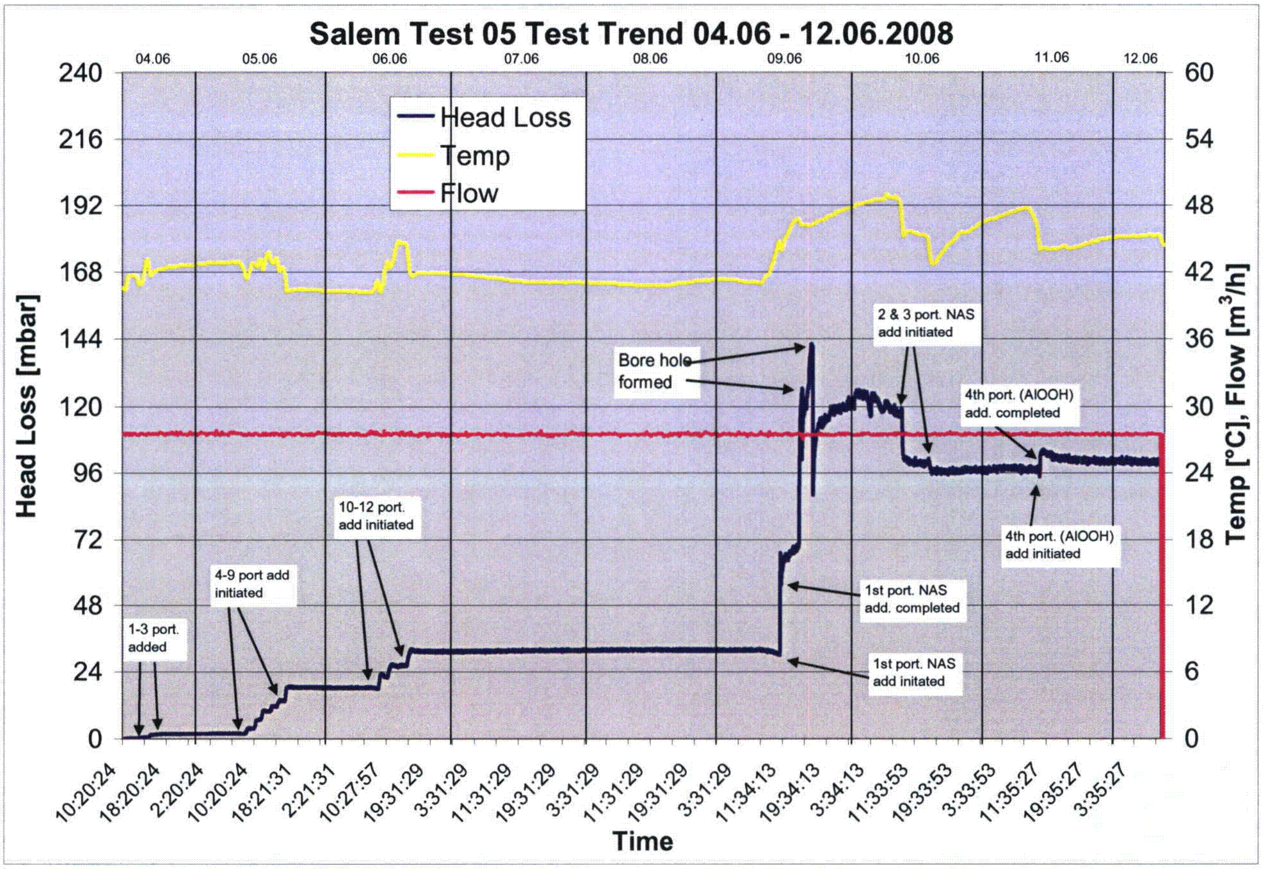

The maximum stability achieved following addition of 100% of the non-chemical debris was 1.3% change in head loss over 60 minutes while the maximum stability achieved following addition of 100% of the non-chemical and chemical debris was 0.9% change in head loss over 60 minutes.

Bore holes were not observed in the non-chemical debris bed. The non-chemical debris bed is shown in Figures 3f.4.2.3.4-2 and 3f.4.2.3.4-3. However, bore holes did form in the debris bed following the first chemical precipitate addition. The debris bed on the front of the strainer following the first chemical addition is shown in Figure 3f.4.2.3.4-4. The debris bed on the back of the strainer during draindown (100% chemicals added) is shown in Figure 3f.4.2.3.4-5.

The maximum head loss with 100% non-chemical debris in the test loop was 32.5 mbar at a temperature of 41°C (106°F) and an equivalent flow rate of 8850 gpm. The maximum head loss with 100% non-chemical and chemical debris in the test loop was 142.0 mbar at a temperature of 46.2°C (115°F) and an equivalent flow rate of 8850 gpm. The maximum head loss with 100% non-chemical and chemical debris occurred prior to the largest head loss drop due to formation of a bore hole.

At the end of the test, the pump was stopped for 10 minutes and then restarted to determine if vortices would form upon restart due to potential clean strainer windows which could have formed when air was released from solution following the pump stop. Upon restart with a strainer submergence of approximately 3 inches, no vortices or air ingestion were observed.

The quantity of debris at various locations in the test apparatus is documented below. Very little debris settled on the floor in front of either side of the strainer module.

- Debris in front (upstream) strainer pockets 40.8%
- Debris in rear (downstream) strainer pockets 29.9%
- Debris on flume floor upstream of and on debris interceptor 1.0%
- Debris on flume floor between debris interceptor and front of strainer 4.8%
- Debris underneath strainer 14.4%
- Debris on flume floor downstream of strainer module 2.1%
- Debris on top of strainer 7.0%

It is noted the Unit 1 thin bed test (Test 3-repeat) described in Section 3f.4.2.3.3 of this response appeared to have a significantly higher maximum head loss (78.5 mbar) than the maximum Unit 1 non-chemical full load head loss (32.5 mbar) for Test 5 (described in this Section). However, the maximum non-chemical head loss for Test 3-repeat was actually comparable to that observed in Test 5, as described below. Therefore, use of the full load test for chemical effects testing was appropriate.

Test 3-repeat used a debris load and flow rate that were greater than those used for Test 5. Furthermore, Test 3-repeat utilized room temperature water, while the Test 5 utilized a heated test loop. The impact of each of these factors is discussed below.

The total debris loads for Test 3-repeat and Test 5 are provided in Tables 3f.4.1.5.6-2/3/6/7 of this response. These are the debris loads at which the maximum head loss values were recorded. The differences in the debris loads for the two tests are presented in Table 3f.4.2.3.4-1.

Table 3f.4.2.3.4-1: Comparison of Test 3-repeat and Test 5 Debris Loads

Debris Type	Test 3-repeat (Thin Bed Test) Quantity ft^3	Test 5 (Full Load Test) Quantity ft^3	% Difference* %
NUKON	310	236	31%
Kaowool	39	33	18%
Qualified Coatings	12.6	11.5	9.6%

* *The % difference is based on the full load test.*

Test 3-repeat included more debris than the design basis debris load which was used for Test 5. This is acceptable, though, since the thin bed test was used to demonstrate a trend (i.e. that the thin bed effect was not experienced on a complex strainer).

A more appropriate comparison of head losses is the Test 5 full load head loss to the head loss after the addition of Portion 12 in the Test 3-repeat thin bed test (see Figure 3f.4.2.3.3-1 of this response). The Test 5 full load theoretical bed thickness was 0.90 inches, and theoretical bed thickness after Portion 12 in Test 3-repeat was 0.86 inches. The Test 3-repeat head loss after the addition of Portion 12 was ~58 mbar (see Figure 3f.4.2.3.3-1 of this response). The Test 3-repeat thin bed head loss after the addition of Portion 14, which corresponded to a theoretical bed thickness of 1.12 inches, was 78.5 mbar.

In addition, the Test 5 maximum non-chemical head loss was measured at 106°F, while the Test 3-repeat maximum head loss was measured at 74°F. The ratio of water viscosities at 74°F to 106°F is 1.45; thus, the Test 3-repeat thin bed head loss of 58 mbar at 74°F is equivalent to 40 mbar at 106°F. Furthermore, Test 3-repeat utilized a flow rate of 9000 gpm, not the design two pump flow rate of 8850 gpm. This reduces the equivalent Test 3-repeat thin bed head loss of 40 mbar to 39 mbar.

Although 39 mbar (Test 3-repeat equivalent maximum head loss) is greater than 32.5 mbar (Test 5 maximum non-chemical head loss), it also does not account for the ~10% more qualified coatings (~5% more coatings overall) in Test 3-repeat. The impact of the additional coatings in Test 3-repeat is considered to offset the addition of 75 g more Min-K to the Test 5 full load test than specified (see Table 3f.4.1.5.6-7 of this response). The additional coatings in Test 3-repeat resulted in 1.1 kg more stone flour being added to the test loop than in the Test 5, which is significantly more than 75 g.

Thus, the head losses measured for the Unit 1 thin bed and full load tests were very comparable. In addition, previous Unit 1 testing which used the 1-Sided MFTL configuration (see Section 3f.4.1.4 of this response) indicated that the thin bed effect was not observed. Furthermore, the Unit 2 thin bed and full load tests which used the 2-Sided MFTL configuration (described in Sections 3f.4.2.3.2 and 3f.4.2.3.5 of this response, respectively) also indicated that the thin bed effect was not observed. Based on the equivalence of the Test 3-repeat thin bed and Test 5 full load head losses, along with CCI's experience of their strainer not exhibiting the thin bed effect, the Unit 1 full load test (Test 5) was the appropriate test to use as the basis for the Unit 1 chemical effects head loss.

Figure 3f.4.2.3.4-2: Test 5 Non-Chemical Debris Bed on Front of Strainer

Figure 3f.4.2.3.4-3: Test 5 Non-Chemical Debris Bed on Back of Strainer

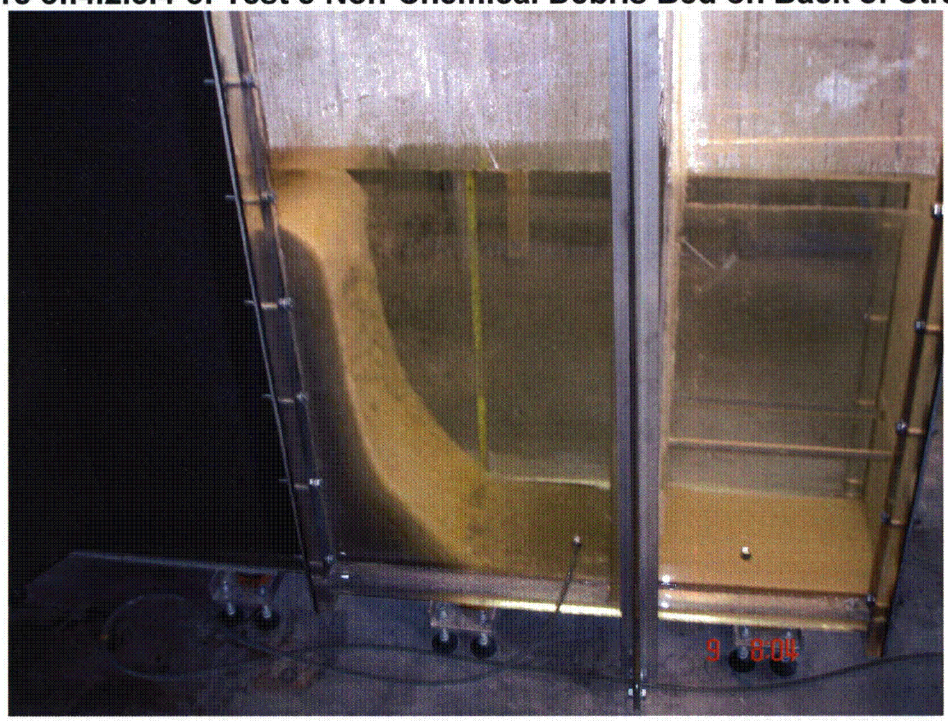

Salem Nuclear Generating Station Units 1 and 2
Docket Nos. 50-272 and 50-311
Generic Letter 2004-02
Updated Supplemental Response for Salem

Figure 3f.4.2.3.4-4: Test 5 Debris Bed After First Chemical Portion (Underwater Photo of Front of Strainer Showing Bore holes)

Figure 3f.4.2.3.4-5: Test 5 Debris Bed After All Chemical Portions During Draindown

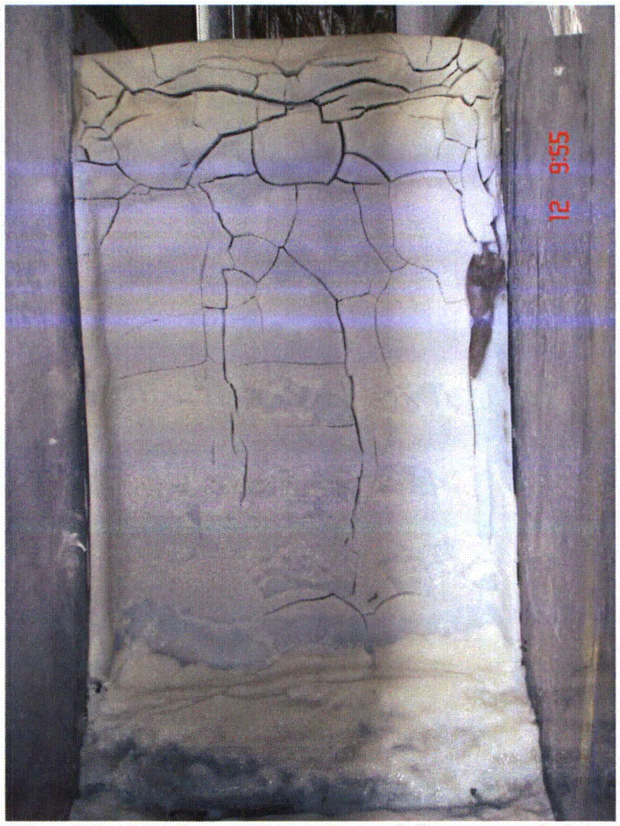

3f.4.2.3.5 Test 6: Unit 2 Full Debris Load Chemical Effects Head Loss Test

Test 6 was performed from June 16 to 24, 2008. The pressure trace for Test 6 is shown below (Reference A.75).

Figure 3f.4.2.3.5-1: Test 6 Pressure Trace (June 16 - 24, 2008)

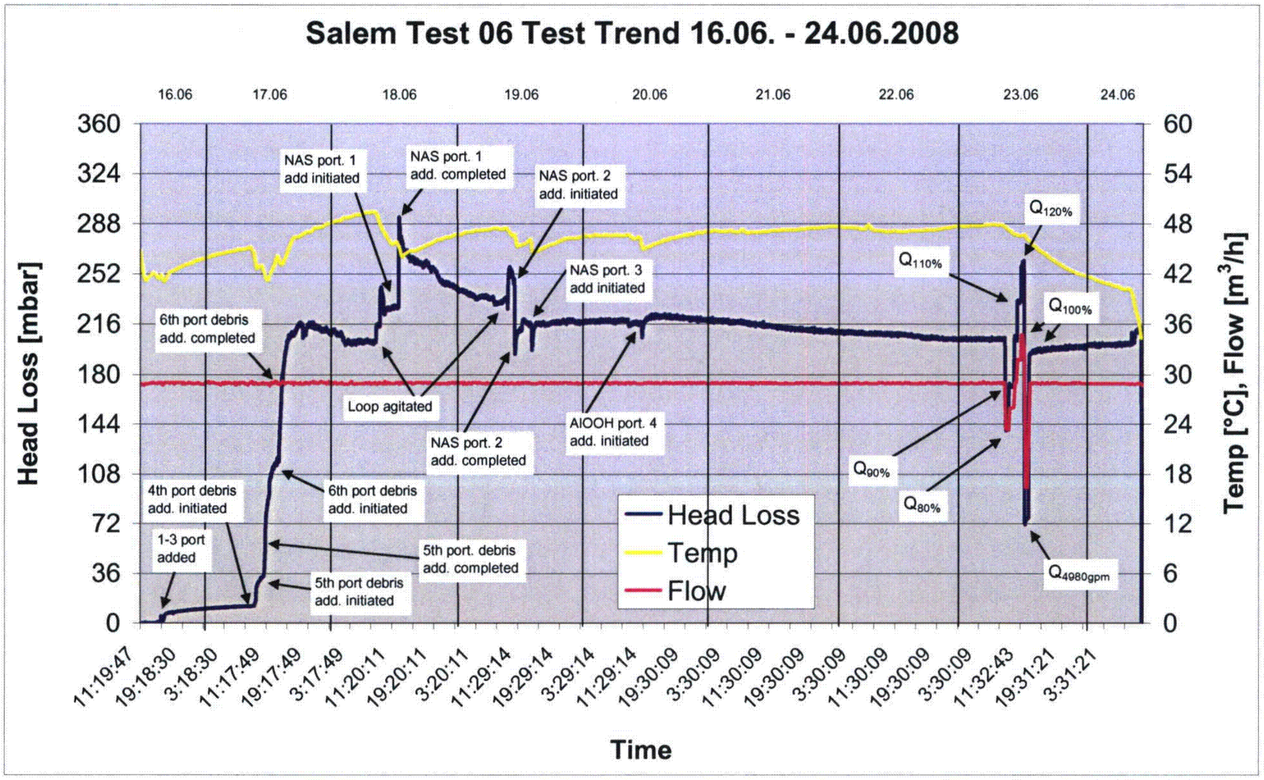

The maximum stability achieved following addition of 100% of the non-chemical debris was 0.7% change in head loss over 60 minutes while the maximum stability achieved following addition of 100% of the non-chemical and chemical debris was 0.3% change in head loss over 60 minutes.

Bore holes were not observed in the non-chemical debris bed. The non-chemical debris bed is shown in Figures 3f.4.2.3.5-2 and 3f.4.2.3.5-3. However, bore holes did form in the debris bed following the first chemical precipitate addition. The bore holes were not as visually apparent as in Test 5 (see Figure 3f.4.2.3.4-4) since the Unit 2 debris load is much less than the Unit 1 debris load and therefore the pockets were not as full in Test 6. The debris bed on the front and back of the strainer during draindown (100% chemicals added) is shown in Figures 3f.4.2.3.5-4 and Figure 3f.4.2.3.5-5.

The maximum head loss with 100% non-chemical debris in the test loop was 242.2 mbar at a temperature of 47.6°C (118°F) and an equivalent flow rate of 8850 gpm. The maximum head loss with 100% non-chemical and chemical debris in the test loop was 292.5 mbar at a temperature of 45.0°C (113°F) and an equivalent flow rate of 8850 gpm. The maximum head loss with 100% non-chemical and chemical debris occurred prior to formation of a bore hole.

At the end of the test, the pump was stopped for 10 minutes and then restarted to determine if vortices would form upon restart due to potential clean strainer windows which could have formed when air was released from solution following the pump stop. Upon restart with a strainer submergence of approximately 3 inches, no vortices or air ingestion were observed.

The quantity of debris at various locations in the test apparatus is documented below. Very little debris settled on the floor in front of either side of the strainer module.

- Debris in front (upstream) strainer pockets = 43.9%
- Debris in rear (downstream) strainer pockets = 38.8%
- Debris on flume floor upstream of debris interceptor = 0.6%
- Debris on debris interceptor = 0.5%
- Debris on flume floor between debris interceptor and front of strainer = 3.8%
- Debris underneath strainer = 11.7%
- Debris on flume floor downstream of strainer module = 0.8%
- Debris on top of strainer (not measured, but minimal (Reference A.75))

Figure 3f.4.2.3.5-2: Test 6 Non-Chemical Debris Bed on Front of Strainer (Underwater Photo)

Figure 3f.4.2.3.5-3: Test 6 Non-Chemical Debris Bed on Back of Strainer

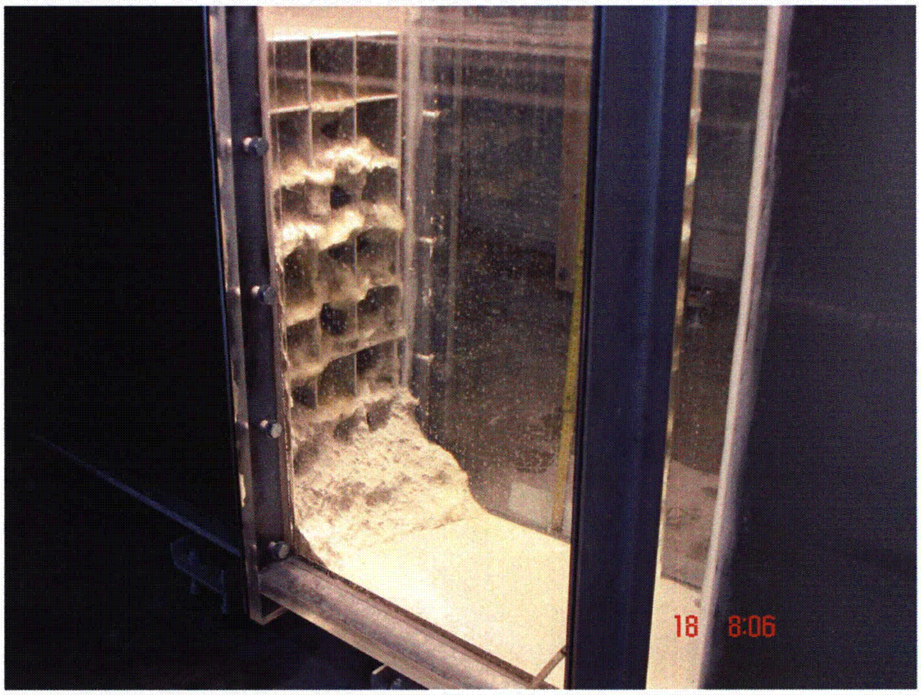

Figure 3f.4.2.3.5-4: Test 6 Debris Bed After All Chemical Portions During Draindown

Figure 3f.4.2.3.5-5: Test 6 Debris Bed After All Chemical Portions During Draindown

3f.4.2.4 2006-2007 Non-Design Basis 1-Sided MFTL Head Loss Tests (Reference A.88)

The results of the 1-Sided MFTL Unit 1 chemical effects head loss tests performed in 2006-2007 are presented in this section. Each test is discussed separately. These tests are not design basis tests due to concerns with debris preparation and observed settling in the tests (References A.71 and A.78). However, certain trends exhibited in these tests (i.e. channeling / bore holes) help to substantiate why the design basis 2008 2-Sided MFTL Unit 1 chemical effects tests are valid even in the presence of more chemical precipitate than tested (see Section 3o.1.17d(ii) of this response). Note, the terms channeling and bore holes describe the same phenomenon and are used interchangeably herein.

3f.4.2.4.1 Non-Design Basis Test 5: Unit 1 Full Debris Load Chemical Effects Head Loss Test

Non-design basis Test 5 was performed from December 19, 2006, to January 1, 2007. The pressure trace for the first ~32 hours of non-design basis Test 5 is shown below (Reference A.88). All non-chemical and chemical debris was added within this time period.

Figure 3f.4.2.4.1-1: Non-Design Basis Test 5 Pressure Trace (December 20-21, 2006)

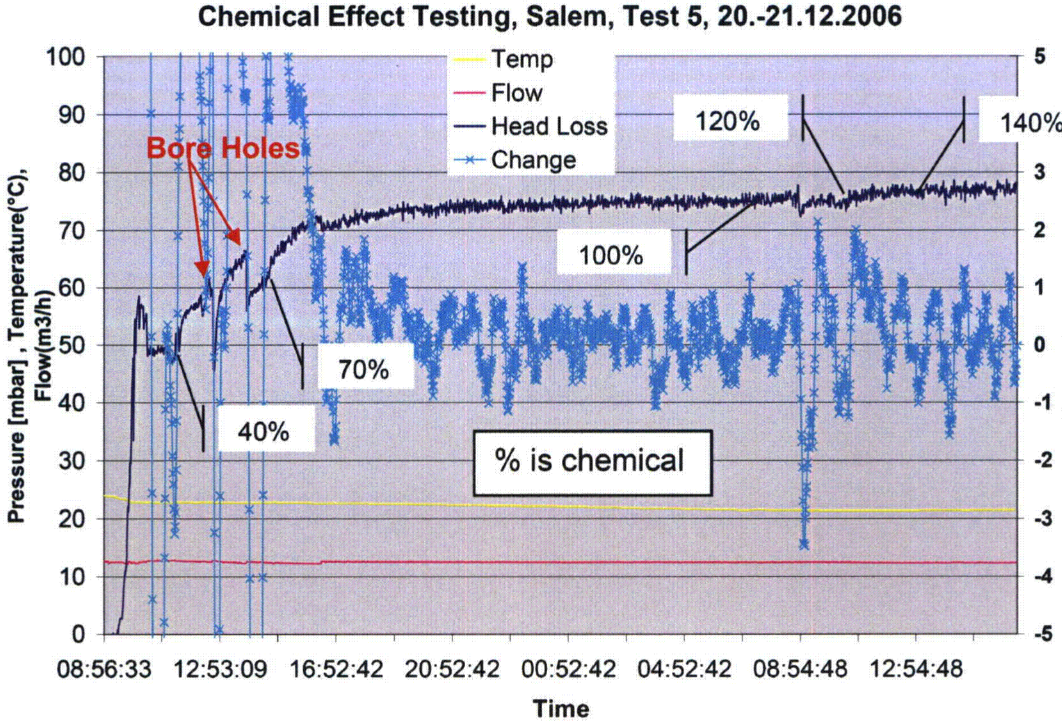

Bore holes were not observed in the non-chemical debris bed. However, bore holes did form in the debris bed following the first chemical precipitate addition.

The maximum head loss with 100% non-chemical debris in the test loop was 49 mbar at a temperature of 22.8°C (73°F) and an equivalent flow rate of 9000 gpm. The maximum head loss with 100% non-chemical and chemical debris in the test loop was 75 mbar at a temperature of 21.4°C (71°F) and an equivalent flow rate of 9000 gpm. The maximum head loss with 100% non-chemical and 140% chemical debris in the test loop was 77 mbar at a temperature of 21.5°C (71°F) and an equivalent flow rate of 9000 gpm. Approximately 80% of all debris settled on the floor in front of the strainer module.

3f.4.2.4.2 Non-Design Basis Test 6: Unit 1 Full Debris Load Chemical Effects Head Loss Test

Non-design basis Test 6 was performed from January 8-10, 2007. The pressure trace for non-design basis Test 6 is shown below (Reference A.88).

Figure 3f.4.2.4.2-1: Non-Design Basis Test 6 Pressure Trace (January 8-10, 2007)

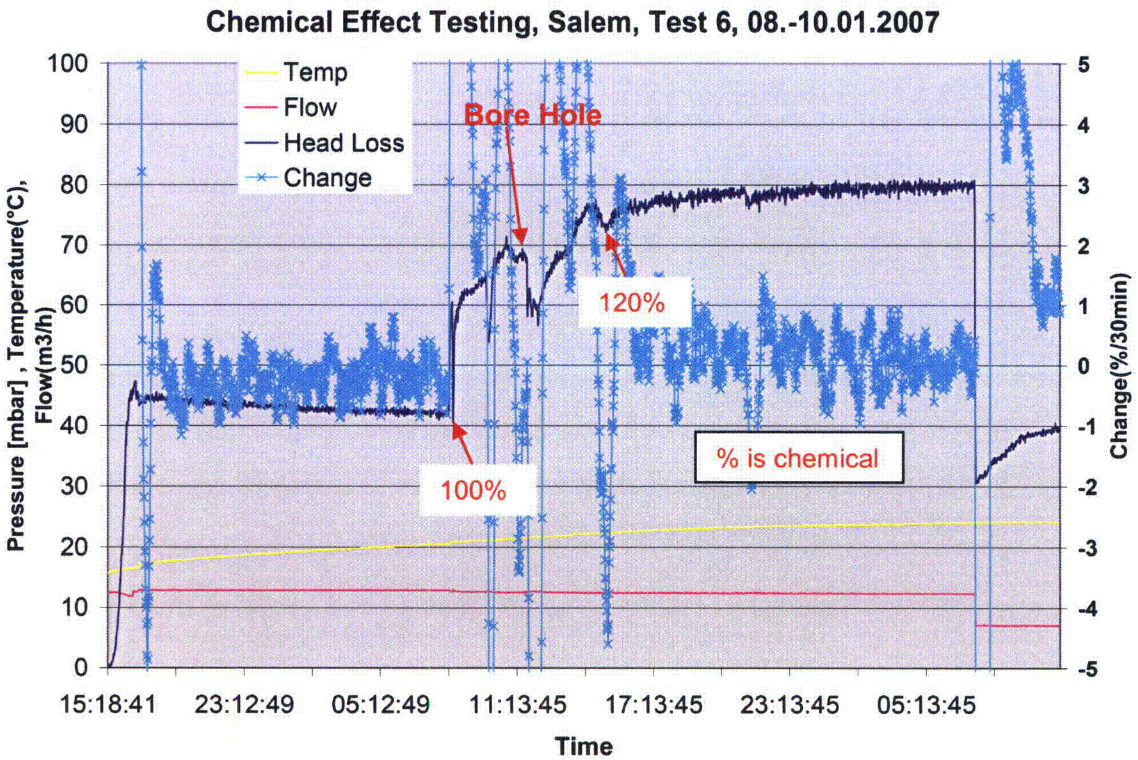

Bore holes were not observed in the non-chemical debris bed. However, a bore hole did form in the debris bed following the first chemical precipitate addition.

The maximum head loss with 100% non-chemical debris in the test loop was 42 mbar at a temperature of 20.6°C (69°F) and an equivalent flow rate of 9000 gpm. The maximum head loss with 100% non-chemical and chemical debris in the test loop was 75.5 mbar at a temperature of 22.3°C (72°F) and an equivalent flow rate of 9000 gpm. The maximum head loss with 100% non-chemical and 120% chemical debris in the test loop was 80 mbar at a temperature of 24.0°C (75°F) and an equivalent flow rate of 9000 gpm. Additional chemical (140% of total) was added, but at a reduced flow rate. Approximately 80% of all debris settled on the floor in front of the strainer module.

3f.5 Address the ability of the design to accommodate the maximum volume of debris that is predicted to arrive at the screen.

The design basis strainer head loss is based on Tests 5 and 6 of the 2008 2-Sided MFTL chemical effects head loss testing. The configuration used for this testing is described in Section 3f.4.1.5.1 of this response. The tested strainer module is a representative "slice" of the long train of modules in the plant, including the debris interceptor. Therefore, the accumulation of debris on this slice is representative of the debris accumulation which would occur in the plant, including the debris which enters the pockets and which is deposited in front of, underneath, and behind the module. In Tests 5 and 6, the only debris which did not transport over the debris interceptor was the debris which became lodged in the grating.

The scaled debris loads for Tests 5 and 6 are both based on plant debris loads greater than the maximum quantity of debris which is predicted to transport over the debris interceptor (see Sections 3e and 3f.4.1.5.8 of this response). Therefore, the strainer design is able to accommodate the maximum volume of debris that is predicted to arrive at the strainer.

3f.6 Address the ability of the screen to resist the formation of a "thin bed" or to accommodate partial thin bed formation.

The Unit 1 and Unit 2 strainers are not susceptible to thin bed formation (Reference A.75) as explained in Sections 3f.4.2.3.2 and 3f.4.2.3.3 of this response.

3f.7 Provide the basis for the strainer design maximum head loss.

The basis for the strainer design maximum head loss (maximum allowable head loss) is provided in Section 3g.16 of this response. The maximum allowable head loss is based on both the hydraulic allowable head loss and the structural allowable head loss. The hydraulic allowable head loss is based on the difference between the net positive suction head available (NPSHa) and net positive suction head required (NPSHr) for the RHR pumps during recirculation including the effects of void fraction at the pump inlet. The structural allowable head loss is based on the limiting component in the strainer installation. The limiting component is the suction box which can sustain head losses up to 16.94 ft (Reference A.77) as discussed in Section 3k.3 of this response.

The minimum partial pressure of air in containment prior to an accident is 10.1 psia for Unit 1 and 10.18 psia for Unit 2 (Reference A.3). The saturation temperatures corresponding to 10.1 psia and 10.18 psia are 193.7°F and 194.1°F, respectively.

The use of the minimum initial partial pressure of air in containment prior to an accident is discussed in the Section 3g.13 and 3g.15 responses. The minimum water level used is discussed in the Section 3g.1 and 3g.8 responses. The suction piping hydraulic losses are discussed in the Section 3g.4 response. The pump flow rates and NPSHr values used are discussed in the Section 3g.1, 3g.3, and 3g.16 responses.

3f.8 Describe significant margins and conservatisms used in the head loss and vortexing calculations.

The basis of the GL 2004-02 evaluation is the methodology in NEI-04-07 and its associated SER. This methodology is regarded as having a substantial degree of conservatism in all its steps and assumptions. This methodology is used for break selection, break modeling, debris generation, debris transport, and allowable head loss.

The conservatisms and margins in the clean strainer head loss calculation are addressed in Section 3f.9 of this response.

The conservatisms and margins in the strainer debris head loss calculation are addressed in Section 3f.10 of this response.

The conservatisms and margins in the vortexing calculation are addressed in Section 3f.3 of this response.

3f.9 Provide a summary of the methodology, assumptions, bases for the assumptions, and results for the clean strainer head loss calculation.

The Salem strainer consists of a train of two sided modules each with ten or fifteen columns and seven rows of pockets made of perforated plate per side. The Unit 1 strainer has 23 ten column modules and 1 fifteen column module while the Unit 2 strainer has 22 ten column modules and 1 fifteen column module. The train of modules is connected by a central duct into which all of the filtered water flows. This central flow channel ends with a z-shaped duct that is connected to a suction box which covers the inlets to the ECCS suction pipe inlets (Reference A.77). The head loss through the train of strainer modules is dependent on the flow distribution among the individual modules. The flow distribution is in turn dependent on the head loss through the debris bed. When the strainers are clean, the majority of the flow enters the central duct in the first few modules closest to the suction box. When the strainers are laden with debris, the flow is much more evenly distributed among the modules (Reference A.77).

The head loss through the strainer modules is separated into several parts as shown in Figure 3f.9-1 (Reference A.77). These head losses are itemized below.

Figure 3f.9-1: Head Losses in the Train of Strainer Modules

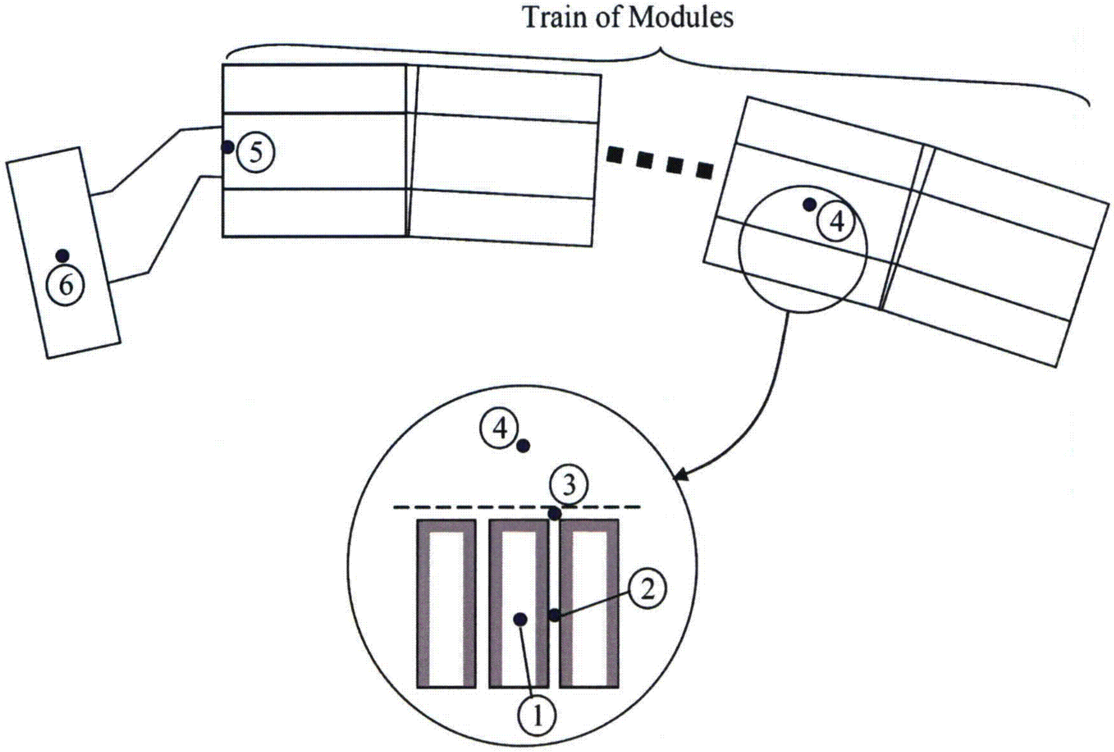

a. The head loss between points 1 and 2 is the head loss across the strainer pocket. When the strainer is clean, this head loss is dominated by the hydraulic resistance of the perforated plate. This resistance is determined using correlations for perforated plates from The Handbook of Hydraulic Resistance, Reference 30. When the strainer is laden with debris, the head loss between points 1 and 2 is dominated by the hydraulic resistance of the debris bed. The debris bed resistance is determined using the results of the strainer vendor head loss tests (Reference A.75) as discussed in Section 3f.10 of this response.

b. The head loss between points 2 and 3 occurs in the narrow channels that exist between the strainer pockets. Typically, the flow here is in the transition region between laminar and turbulent flow. The head loss in the narrow channels is determined as if it were pipe flow with a conservative Moody friction factor of 0.04 found in Reference 30.

c. The head losses between points 3 and 4 and between points 4 and 5 are calculated with two different methodologies. In the first methodology, the central duct of the train of strainer modules is treated as a series of converging tees with straight flow along the central duct and branch flow entering the side of the duct from each module. Head loss correlations for converging tees from Reference 30 are used to determine the hydraulic resistance for the central duct and side entrance of each module.

   In the second methodology, the head loss of the central duct is treated as a linearly increasing flow along a square duct. The head loss is determined using pipe flow equations from Reference 30 and a conservative Moody friction factor of 0.04. There are also flow restrictions between each module where the central duct temporarily narrows. The hydraulic resistance of these restrictions is determined using head loss correlations for a thick edged orifice found in Reference 30.

   The maximum head loss found using either methodology is applied to the central duct of each strainer module individually in the head loss analysis.

d. The head loss between points 5 and 6 has been determined at two different flow rates using the Computational Fluid Dynamics code CFX-10 (Reference A.77, Appendix A). At 5110 gpm, the head loss of the z-duct and strainer box was determined to be 0.583 ft. At 9000 gpm, the head loss was determined to be 1.844 ft.

The hydraulic resistance correlations outlined in items a through c were determined for each module in the strainer train under both clean strainer conditions and a range of debris bed head losses. These resistance correlations were solved simultaneously to determine the flow distribution among the strainer modules and the head loss of each module. The head loss through the z-duct and suction box is dependent solely on flow rate and is not influenced by the flow distribution among the modules. A correlation was developed that determines the total head loss of the strainer module components as a function of the debris bed head loss. This strainer component head loss correlation was used to determine the component portion of the total strainer head loss at various sump temperatures and flow rates (see Section 3f.10 of this response).

When the strainer is clean (i.e. no debris bed), the Unit 1 and Unit 2 strainer trains behave similar to one another since their first few modules closest to the suction box are identical. With a clean strainer, the head loss through the strainer train and into the suction box was determined to be 2.88 feet at the two pump operation flow rate of 8850 gpm (Reference A.77).

When the strainer is laden with debris and the flow among the strainer modules is evenly distributed, the head loss through the strainer modules (i.e. the head loss due to the strainer internals/components, not the debris bed) reaches an asymptotic value as the debris head loss is increased. For Unit 1, the maximum head loss due to the strainer components when the strainer is laden with debris is 1.02 feet at the single pump operation flow rate of 5110 gpm and 3.08 feet at the two pump operation flow rate of 8850 gpm. For Unit 2, the maximum head loss due to the strainer components when the strainer is laden with debris is 0.97 feet at the single pump operation flow rate of 4980 gpm and 3.09 feet at the two pump operation flow rate of 8850 gpm (Reference A.77).

3f.10 Provide a summary of the methodology, assumptions, bases for the assumptions, and results for the debris head loss analysis.

This section includes discussions of both the debris head loss analysis and the total strainer head loss analysis.

3f10.1 Debris Head Loss Analysis

The Unit 1 and Unit 2 debris bed head loss analyses are based Tests 5 and 6, respectively, of the 2008 head loss tests performed in the 2-Sided MFTL. These tests are described in Section 3f.4.1.5 of this response. The results of these tests are provided in Sections 3f.4.2.3.4 and 3f.4.2.3.5, respectively. Since the head loss testing was performed prototypically, the measured test head losses are the same as those expected in the plant.

For both Tests 5 and 6, bore holes did not form in the debris bed prior to the addition of chemical precipitates (Reference A.75). Therefore, the debris head loss analysis is performed differently for the non-chemical debris bed and the debris bed with chemical precipitates.

For the debris bed without bore holes (non-chemical debris load), the maximum measured debris bed head loss is scaled for both velocity and viscosity (temperature) using the NUREG/CR-6224 head loss correlation (References 8 and A.77). The viscosity scaling conservatively accounts for the potential increase in the sump pool viscosity due to the presence of dissolved chemicals using viscosity data from Integrated Chemical Effects Test (ICET) 1 (Reference 38). The increase in sump viscosity is based on Figure 35 of Reference 38. Considering that the maximum viscosity measurements between Days 11 through 14 of ICET 1 were measured with a fouled viscosimeter, the mean viscosity over the test duration, 0.514 E-6 m^2/s, is used to determine the increase in sump viscosity. This is acceptable since the viscosity was relatively constant throughout the test. The increase in sump viscosity is obtained by comparing the mean measured value to the kinematic viscosity of pure water at 140°F (60°C), 0.474 E-6 m^2/s. Thus, the sump viscosity could increase by a factor of 1.084 [0.514 / 0.474] (Reference A:77). The impact of chemicals on viscosity decreases with increasing temperature based on a comparison of the viscosities reported in Figures 35 (60°C) and Figure 36 (23°C) of Reference 38. Thus, it is conservative to use the viscosity data for 60°C (140°F) for temperatures above 60°C.

Thus, the maximum measured debris head loss prior to the addition of chemicals is scaled as follows (Reference A.77).

$$HL_{Tsump} = HL_{test} \cdot \frac{Q_{plant}}{Q_{test}} \cdot \frac{\mu_{Tsump} \cdot C_{chem}}{\mu_{Ttest}}$$

Where:

HL_{Tsump}	debris head loss at a given sump temperature
HL_{test}	debris head loss measured in the test
Q_{plant}	flow rate in the plant
Q_{test}	flow rate upon which the test was based (8850 gpm)
μ_{Tsump}	water viscosity at the sump temperature
μ_{Ttest}	water viscosity in the test loop when the head loss was measured
C_{chem}	factor by which the viscosity is increased, 1.084

In Test 5 for Unit 1, the maximum head loss observed prior to the addition of chemical precipitates was 32.5 mbar (1.09 ft) at a temperature of 41.3°C (106°F). In Test 6 for Unit 2, the maximum head loss observed prior to the addition of chemical precipitates was 242.2 mbar (8.1 ft) at a temperature of 47.6°C (118°F). The scaling of these values to different sump temperatures is presented in Section 3f.10.2 in Tables 3f.10.2-1 through 3f.10.2-4.

For the debris bed with bore holes (non-chemical and chemical debris load), the measured debris bed head loss is not scaled for either velocity or viscosity (Reference A.77). Instead, the maximum head loss measured in the test when chemical precipitates were present was conservatively applied to all flow conditions where bore holes are expected (i.e. when chemical precipitates are present).

In Test 5 for Unit 1, the maximum head loss prior to observing the bore hole which lead to the largest pressure drop was 142.0 mbar (4.75 ft) at a temperature of 46.2°C (115°F) following the addition of the first of four chemical precipitate portions. This was the highest head loss observed during Test 5. Thus, the Unit 1 debris head loss is 4.75 feet for all conditions where chemical precipitates are present.

In Test 6 for Unit 2, the maximum head loss prior to observing bore holes was 292.5 mbar (9.78 ft) at a temperature of 45.0°C (113°F) following the addition of the first of four chemical precipitate portions. This was the highest head loss observed during Test 6. Thus, the Unit 2 debris head loss is 9.78 feet for all conditions where chemical precipitates are present.

The maximum sump temperature at which chemical precipitates form is 160°F as described in Section 3o.1.21d(i).

The debris head loss analysis is conservative since the tested non-chemical debris bed is based on the quantity of debris expected after 30 days of fiber erosion. At a sump temperature of 160°F, approximately one-half of the 30 day fiber erosion quantity has transported to the strainer. The quantity of non-chemical debris tested also was greater than that expected to be generated and transported to the strainer as documented in Section 3f.4.1.5.8 of this response. Furthermore, the debris bed head loss with chemical precipitates is based on the maximum head loss observed with chemical precipitates, which occurs prior to bore hole formation (with less than the total chemical precipitate debris load) as documented in Section 3o.1.17d(ii) of this response.

3f.10.2 Total Strainer Head Loss Analysis

The total strainer head loss is the sum of the component head loss presented in Section 3f.9 and the debris head loss presented in Section 3f.10.1 of this response (Reference A.77). The component head loss is a function of the debris head loss, which in turn is a function of the sump temperature. The total head loss for the one and two pump operating scenarios for Unit 1 and Unit 2 is presented in Tables 3f.10.2-1 through 3f.10.2-4.

Note that the total component head loss in Tables 3f.10.2-1 through 3f.10.2-4 is not always the exact sum of the z-duct and train head losses due to truncation errors, but is within ±0.01 ft. Similarly, the total head loss is not always the exact sum of the total component and debris bed head losses, but is within ±0.01 ft.

Table 3f.10.2-1: Unit 1 Total Strainer Head Loss for 1 Pump Flow

T_{sump} °F	$HL_{z\text{-}duct}$ ft	HL_{train} ft	$HL_{component,tot}$ ft	HL_{debris} ft	HL_{total} ft
60	0.58	0.44	1.02	4.75	5.77
70	0.58	0.44	1.02	4.75	5.77
80	0.58	0.44	1.02	4.75	5.77
90	0.58	0.44	1.02	4.75	5.77
100	0.58	0.44	1.02	4.75	5.77
110	0.58	0.44	1.02	4.75	5.77
120	0.58	0.44	1.02	4.75	5.77
130	0.58	0.44	1.02	4.75	5.77
140	0.58	0.44	1.02	4.75	5.77
150	0.58	0.44	1.02	4.75	5.77
160	0.58	0.44	1.02	4.75	5.77
170	0.58	0.40	0.98	0.40	1.37
180	0.58	0.39	0.98	0.37	1.34
190	0.58	0.39	0.97	0.35	1.32
193.7	0.58	0.39	0.97	0.34	1.31
212	0.58	0.38	0.96	0.30	1.27
220	0.58	0.38	0.96	0.29	1.25
230	0.58	0.38	0.96	0.27	1.23
240	0.58	0.38	0.96	0.26	1.21
250	0.58	0.37	0.95	0.25	1.20
260	0.58	0.37	0.95	0.23	1.18

Table 3f.10.2-2: Unit 2 Total Strainer Head Loss for 1 Pump Flow

T_{sump} °F	$HL_{z\text{-}duct}$ ft	HL_{train} ft	$HL_{component,tot}$ ft	HL_{debris} ft	HL_{total} ft
60	0.56	0.42	0.97	9.78	10.75
70	0.56	0.42	0.97	9.78	10.75
80	0.56	0.42	0.97	9.78	10.75
90	0.56	0.42	0.97	9.78	10.75
100	0.56	0.42	0.97	9.78	10.75
110	0.56	0.42	0.97	9.78	10.75
120	0.56	0.42	0.97	9.78	10.75
130	0.56	0.42	0.97	9.78	10.75
140	0.56	0.42	0.97	9.78	10.75
150	0.56	0.42	0.97	9.78	10.75
160	0.56	0.42	0.97	9.78	10.75
170	0.56	0.41	0.97	3.21	4.17
180	0.56	0.41	0.97	2.99	3.96
190	0.56	0.41	0.97	2.80	3.76
194.1	0.56	0.41	0.97	2.73	3.69
212	0.56	0.41	0.97	2.44	3.41
220	0.56	0.41	0.96	2.33	3.30
230	0.56	0.41	0.96	2.21	3.17
240	0.56	0.41	0.96	2.10	3.06
250	0.56	0.41	0.96	1.99	2.96
260	0.56	0.41	0.96	1.90	2.86

Table 3f.10.2-3: Unit 1 Total Strainer Head Loss for 2 Pump Flow

T_{sump} °F	$HL_{z\text{-}duct}$ ft	HL_{train} ft	$HL_{component,tot}$ ft	HL_{debris} ft	HL_{total} ft
60	1.78	1.30	3.08	4.75	7.83
70	1.78	1.30	3.08	4.75	7.83
80	1.78	1.30	3.08	4.75	7.83
90	1.78	1.30	3.08	4.75	7.83
100	1.78	1.30	3.08	4.75	7.83
110	1.78	1.30	3.08	4.75	7.83
120	1.78	1.30	3.08	4.75	7.83
130	1.78	1.30	3.08	4.75	7.83
140	1.78	1.30	3.08	4.75	7.83
150	1.78	1.30	3.08	4.75	7.83
160	1.78	1.30	3.08	4.75	7.83
170	1.78	1.11	2.89	0.69	3.58
180	1.78	1.10	2.88	0.64	3.52
190	1.78	1.08	2.86	0.60	3.46
193.7	1.78	1.07	2.86	0.58	3.44
212	1.78	1.04	2.83	0.52	3.35
220	1.78	1.03	2.81	0.50	3.31
230	1.78	1.01	2.80	0.47	3.27
240	1.78	1.00	2.78	0.45	3.23
250	1.78	0.98	2.76	0.43	3.19
260	1.78	0.96	2.75	0.41	3.15

Table 3f.10.2-4: Unit 2 Total Strainer Head Loss for 2 Pump Flow

T_{sump} °F	$HL_{z\text{-}duct}$ ft	HL_{train} ft	$HL_{component,tot}$ ft	HL_{debris} ft	HL_{total} ft
60	1.78	1.31	3.09	9.78	12.87
70	1.78	1.31	3.09	9.78	12.87
80	1.78	1.31	3.09	9.78	12.87
90	1.78	1.31	3.09	9.78	12.87
100	1.78	1.31	3.09	9.78	12.87
110	1.78	1.31	3.09	9.78	12.87
120	1.78	1.31	3.09	9.78	12.87
130	1.78	1.31	3.09	9.78	12.87
140	1.78	1.31	3.09	9.78	12.87
150	1.78	1.31	3.09	9.78	12.87
160	1.78	1.31	3.09	9.78	12.87
170	1.78	1.29	3.07	5.70	8.77
180	1.78	1.29	3.07	5.31	8.39
190	1.78	1.29	3.07	4.97	8.04
194.1	1.78	1.29	3.07	4.84	7.91
212	1.78	1.28	3.07	4.34	7.41
220	1.78	1.28	3.06	4.15	7.21
230	1.78	1.28	3.06	3.93	6.99
240	1.78	1.28	3.06	3.72	6.78
250	1.78	1.27	3.06	3.54	6.60
260	1.78	1.27	3.05	3.37	6.43

Where:

$HL_{z\text{-}duct}$ head loss through the z-duct and suction box (from 5 to 6 in Figure 3f.9-1)

HL_{train} head loss through the strainer center channel (from 2 to 5 in Figure 3f.9-1)

$HL_{component,tot}$ sum of HL_{zduct} and HL_{train} (from 2 to 6 in Figure 3f.9-1)

HL_{debris} debris head loss (from 1 to 2 in Figure 3f.9-1)

HL_{total} sum of $HL_{component,tot}$ and HL_{debris} (from 1 to 6 in Figure 3f.9-1)

The results from these tables are graphically presented along with the strainer hydraulic and structural allowable head loss in Figures 2, 5, 8, and 11 in Section 3g.14 of this response.

3f.11 State whether the sump is partially submerged or vented (i.e., lacks a complete water seal over its entire surface) for any accident scenarios and describe what failure criteria in addition to loss of net positive

suction head (NPSH) margin were applied to address potential inability to pass the required flow through the strainer.

The Salem Unit 1 and 2 sump enclosures and strainer trains are fully submerged with more than 3 inches of water cover at the time of switch over to recirculation operation. There are no vents or vent paths.

3f.12 State whether near-field settling was credited for the head-loss testing and, if so, provide a description of the scaling analysis used to justify near-field credit.

The design basis head loss testing does not credit near-field settling.

The design basis strainer head loss testing was performed used the 2-Sided MFTL. The physical configuration of the MFTL for these tests is described in Section 3f.4.1.5.1 of this response. The approach velocity field scaling was prototypical as the test configuration with the "slice" of the strainer train was representative of the corresponding "slice" in the plant as discussed in Section 3f.4.1.5.5 of this response. Thus, any settling which occurred in the test would also occur in the plant. However, debris upstream of the debris interceptor and downstream of the strainer back face in the test flume was agitated to re-suspend the debris as discussed in Section 3f.4.1.5.12 of this response.

The majority (>98%) of debris added to the test loop during the design basis tests transported over the debris interceptor and over 70% of the debris transported to the strainer pockets (see Sections 3f.4.2.3.4 and 3f.4.2.3.5 of this response). The debris which did not transport to the pockets ended up in one of the following locations: between the debris interceptor and the front face of the strainer, underneath the strainer, on top of the strainer, or on the flume floor adjacent to the back face of the strainer. Debris accumulation in any of these locations is considered prototypical since the test configuration, flow rate, and debris load were prototypical or conservative.

Furthermore, the tested and installed strainers both have perforated bottom plates which tend to cause some debris to transport under the strainer. Once the space underneath the strainer is filled, the flow through the bottom plate will still draw some debris towards the areas on the floor both in front of and behind the strainer. In addition, any attempt to agitate debris directly adjacent to the strainer faces would have a detrimental impact on the debris bed formed in the strainer pockets.

3f.13 State whether temperature/viscosity was used to scale the results of the head loss tests to actual plant conditions. If scaling was used,

provide the basis for concluding that boreholes or other differential-pressure induced effects did not affect the morphology of the test debris bed.

The scaling of the debris bed head loss with temperature/viscosity is presented in Section 3f.10 of this response. As discussed in Section 3f.10, the head loss through the non-chemical debris bed was scaled using viscosity since no bore holes were observed in the non-chemical debris bed. This head loss is utilized at high sump temperatures where chemical precipitates may not be present (see Section 3o.1.21d(i).

However, bore holes were observed following the addition of chemical precipitates to the non-chemical debris bed. Therefore, the head loss at low sump temperatures where chemical precipitates may be present does not utilize viscosity scaling.

3f.14 State whether containment accident pressure was credited in evaluating whether flashing would occur across the strainer surface, and if so, summarize the methodology used to determine the available containment pressure.

The flashing evaluation is documented in Reference A.77 and is repeated below. The flashing evaluation was performed using post-LOCA containment pressure and sump water temperature response curves for both a Double Ended Pump Suction (DEPS) LOCA scenario with maximum safeguards and no recirculation spray and a DEPS LOCA scenario with minimum safeguards and no recirculation spray. These response curves are for a Salem Unit 2 LOCA with the replacement steam generator and are provided in Appendix A of WCAP-16503-NP (Reference A.5).

As stated in the response to Section 3g.14, the analyses in WCAP-16503-NP (Reference A.5) are performed using assumptions which maximize the global containment pressure and temperature response due to design basis mass and energy release events. For example, the LOCA analyses assume maximum temperatures for both the RWST and the ultimate heat sink. However, sufficient margin is available such that flashing will not occur under any circumstance.

Flashing will not occur provided the pressure in the sump water is greater than saturation pressure of the water. The pressure in the water is equal to the containment pressure plus the submergence head less the head loss across the strainer. Therefore, flashing can be precluded provided the total strainer head loss (HL) is less than the difference between the sum of the containment pressure head

(h_{ctmt}) and submergence head (h_{sub}) and the saturation pressure of the sump water ($h_{v,sump}$); i.e. $HL < h_{ctmt} + h_{sub} - h_{v,sump}$ (Reference A.77). The submergence head is 97.8 mm (3.85 inches) based on the as-built strainer. This analysis is shown below for both the DEPS minimum and maximum safeguards LOCA analyses.

Table 3f.14-1: Allowable Strainer Head Loss to Preclude Flashing for DEPS LOCA with Minimum Safeguards

Time Post-LOCA	s	1.75E+03	4.00E+03	5.00E+04	5.00E+05	5.00E+06	9.00E+06
Containment Pressure	psig	39.99	26.93	23.89	7.57	2.68	2.32
	Pa	3.757E+05	2.857E+05	2.647E+05	1.522E+05	1.185E+05	1.160E+05
Sump Temperature	°F	257.8	248.2	183.3	132.4	110.3	107.1
Sump Saturation Pressure	Pa	2.352E+05	1.992E+05	5.573E+04	1.637E+04	8.878E+03	8.095E+03
Allowable Strainer Head Loss	Pa	1.414E+05	8.733E+04	2.099E+05	1.368E+05	1.105E+05	1.088E+05
	ft	47.28	29.21	70.20	45.75	36.96	36.39

Table 3f.14-2: Allowable Strainer Head Loss to Preclude Flashing for DEPS LOCA with Maximum Safeguards

Time Post-LOCA	s	1.60E+03	3.50E+03	5.00E+04	1.10E+05	7.70E+05	5.00E+06
Containment Pressure	psig	34.37	22.70	11.89	8.35	4.86	2.41
	Pa	3.370E+05	2.565E+05	1.820E+05	1.576E+05	1.335E+05	1.166E+05
Sump Temperature	°F	233.6	219.3	140.1	123.1	120.2	114.0
Sump Saturation Pressure	Pa	1.533E+05	1.170E+05	2.000E+04	1.273E+04	1.175E+04	9.872E+03
Allowable Strainer Head Loss	Pa	1.846E+05	1.404E+05	1.629E+05	1.458E+05	1.227E+05	1.077E+05
	ft	61.74	46.96	54.48	48.75	41.02	36.01

Since all of the above allowable strainer head loss values are much greater than the structural head loss limit of 16.94 ft (Section 3f.7 of this response and Reference A.77), flashing will not occur either in the debris bed or downstream of the strainer. In addition, since the elevation difference between the minimum submergence level and pump inlet is 34 feet and the pump suction line loss is less than 5 feet, flashing will not occur at the pump inlet (Reference A.77). Therefore, the void fraction due to flashing is zero both downstream of the strainer and at the pump inlet.

Based on the flashing evaluation above, the minimum margin available prior to flashing for the strainer head loss early in the transient is approximately 12 feet based on the structural allowable limit. Similarly, the minimum margin available prior to flashing for the strainer head loss later in the recirculation phase is approximately 19 feet with a containment pressure of 2.4 psig and a sump temperature of 114°F. This margin would be reduced by approximately 5 feet if the containment pressure were 0 psig.

Therefore, it is concluded that flashing will not occur, even if a more conservative LOCA pressure response were used. Thus, the void fraction due to flashing in the debris bed, downstream of the strainer, and at the pump inlet is zero.

3g. Net Positive Suction Head (NPSH)
The objective of the NPSH section is to calculate the NPSH margin for the ECCS and CSS pumps that would exist during a loss-of-coolant accident (LOCA) considering a spectrum of break sizes.

Note: In Section 3g below, various numerical values are provided that are made applicable to Salem Units 1 and 2. There could be a slight difference between the two Units, however the conservative value is made applicable to both Units.

For both Salem Units, the RHR pumps are the only ECCS pumps taking suction directly from the containment sump during recirculation. Therefore, to ensure that the ECCS system has adequate flow, the NPSH available must be greater than the NPSH required for the RHR pumps. The charging and safety injection pumps take suction from the discharge of the RHR pumps during recirculation. The CS pumps do not operate during recirculation.

Since final GL 2004-02 testing had not been completed at the time of the February 2008 response, the NPSH calculation, common to both Salem Unit 1 and 2, was updated in two phases.

The first phase, documented in the February 2008 response, concluded that the new strainer configuration is operable under the previous design basis, which assumed that the strainers would be 50% blocked with debris. The NPSH calculation methodology used for this phase was the same as that used for the pre GL 2004-02 ECCS sump screen. In accordance with the Salem UFSAR Appendix 3A, for conservatism, no credit was taken for containment air pressure in determining ECCS pump NPSHa.

The second phase, documented in this response, verifies that the new strainer configuration is operable under the GL 2004-02 design basis. However, with the requirements for the new strainer configuration, the methodology described in Appendix 3A is too conservative. Therefore, Salem requested and the NRC approved (Amendment Nos. 285 and 268) changes to the licensing basis that allow the use of the minimum partial pressure of air in the containment atmosphere prior to a LOCA to calculate the NPSHa (Reference A.9).

The current (phase 2) NPSH calculation uses the results of the chemical head loss testing at the CCI vendor facility (Reference A.75). Following the NRC approved changes to the licensing basis (Amendment Nos. 285 and 268), the NPSH calculation credits the initial partial pressure of air in the containment. The containment pressure is then the greater of either the initial partial pressure of air or the vapor pressure of the sump water. The NPSHa is then the static head plus the containment pressure minus the vapor pressure of the sump water minus the suction piping friction losses and strainer head loss.

3g.1) Provide applicable pump flow rates, the total recirculation sump flow rate, sump temperature(s), and minimum containment water level.

The RHR pump flow rates vary depending on the pump configuration and the ECCS mode of operation. Since each RHR pump has its own suction line from the ECCS containment sump, the pump suction line losses can be based on the single pump flow rates. However, since the suction is through a single strainer train, the strainer head loss values for both single and dual RHR pump operating conditions were considered.

NPSHa values were determined using the maximum single pump flow rate for each operating condition, as this results in the maximum head loss through the RHR suction pipe. Table 3g-1 shows the maximum flow rates for a single train of RHR (Reference A.41).

Table 3g-1: Maximum Flow Rates (Single Train of RHR)

Mode	**Maximum Pump Flow Rate [gpm] (Reference A.41)**
Cold Leg Recirculation (Unit 1)	5,110
Cold Leg Recirculation (Unit 2)	4,900
Recirculation Containment Spray (Unit 1)	4,850
Recirculation Containment Spray (Unit 2)	4,850
Hot Leg Recirculation (Unit 1)	4,980
Hot Leg Recirculation (Unit 2)	4,980

A flow rate of 5,110 gpm can only be achieved on Salem Unit 1 when one RHR pump is operating and additional flow is through the idle pump piping. The configuration consists of the operating RHR pump injecting via all four cold legs. A flow rate of 5,110 gpm is the highest single RHR pump flow rate for Salem Unit 1 and a flow rate of 4,980 gpm is the highest single RHR pump flow rate for Salem Unit 2.

In the case when both RHR pumps are running, the total flow is split between the two pumps. The NPSH calculation (Reference A.41) shows the maximum suction flow rates from the containment sump during the recirculation alignment of two RHR pumps for Salem Unit 1 and 2. These flow rates are shown in Table 3g-2. The combined flow rate of Trains A and B, 8,850 gpm, was used to determine the maximum strainer head loss for dual pump operation.

Table 3g-2: Maximum Flow Rates for Units 1 & 2 (Two Trains of RHR)

Mode	Maximum Pump Flow Rate [gpm] (Reference A.41)
Cold Leg Recirculation (Train A)	4,425
Cold Leg Recirculation (Train B)	4,425
Recirculation Containment Spray (Train A)	4,563
Recirculation Containment Spray (Train B)	4,287
Hot Leg Recirculation (Train A)	4,425
Hot Leg Recirculation (Train B)	4,425

Revision 3 of Westinghouse Calculation WCAP-16503-NP (Reference A.5) contains the sump water temperature profiles. The DEPS minimum safeguards LOCA scenario for Salem Unit 2 with replacement steam generators yields the harshest long-term temperature and pressure transients. For this case, the maximum sump structural temperature is 264°F at 1500 seconds, which is before recirculation begins.

The sump screen has an upper hydraulic design temperature of 260°F, which is higher than the calculated sump water temperature during recirculation phase; however, the screen is also designed to withstand sump water temperatures up to 264 °F.

The minimum sump water level at switchover to recirculation is 80.83 ft (80 feet 10 inch). This is the minimum water level based on the total channel uncertainty of the new sump level instruments, which were installed specifically for indicating sufficient water level for switchover to recirculation. The minimum water level (80.83 ft) is used to determine the NPSH for cold leg recirculation scenarios; however, the water level for the recirculation containment spray and hot leg recirculation alignments, which occur later in the accident transient, is 81.67 ft (81 feet 8 inches) (Reference A.41).

The new instruments maintain the setpoint of 80 feet 11 inches, but have an uncertainty of 0.75 inch, conservatively rounded to ± 1 inch. Therefore, 80 feet 10 inch is the minimum water level at ECCS switchover to recirculation. Salem confirmed via calculation S-C-CAN-MDC-2061 (Reference A.21) that this level is reached prior to recirculation. Response 3g.8 describes in further detail the calculated minimum flood level.

3g.2) Describe the assumptions used in the calculations for the above parameters and the sources/bases of the assumptions.

Addressed under response 3g.1 above.

3g.3) Provide the basis for the required NPSH values, e.g., three percent head drop or other criterion.

NPSHr is a function of the design of the RHR pumps and the flow rate at which they operate. These values are based on the RHR pump operating curves provided with the pumps and verified by the pump vendor. The actual values for each pumping configuration are listed in section 3g.16.

3g.4) Describe how friction and other flow losses are accounted for.

The RHR line loss values were not directly affected by the modification of the sump strainer. In the pre GL 2004-02 NPSH calculation, the line losses were determined according to the maximum single pump flow rates for each configuration. These suction line losses are increased to account for the increased post-LOCA sump water viscosity due to chemical effects. The increase in sump water viscosity causes the frictional pressure drop through the suction piping to increase. However, it does not cause an increase in component (e.g. valves, tees, etc.) pressure drops since the pressure drop is due primarily to form losses, not friction. The increase in water viscosity is based on the viscosity data recorded as part of ICET #1, documented in Sections 4.5.5 and 4.5.6 of NUREG/CR-6914, Volume 2. ICET #1 utilized a sodium hydroxide (NaOH) buffer environment with NUKON fiber debris and is considered representative of Salem. The viscosity of clean water is based on 260°F water (at saturation pressure) for high temperature conditions and 60°F water (at atmospheric pressure) for low temperature conditions. The worst case between the two water temperatures is used in the suction line loss computation of the allowable strainer head loss.

3g.5) Describe the system response scenarios for LBLOCA and SBLOCAs.

The Refueling Water Storage Tank (RWST) provides borated water which is injected into the Reactor Coolant System (RCS) through the Emergency Core Cooling System (ECCS) pumps or sprayed into containment for containment heat removal and pressure control during the injection phase of Loss of Coolant Accident (LOCA) (Reference A.21).

Salem Nuclear Generating Station Units 1 and 2
Docket Nos. 50-272 and 50-311
Generic Letter 2004-02
Updated Supplemental Response for Salem

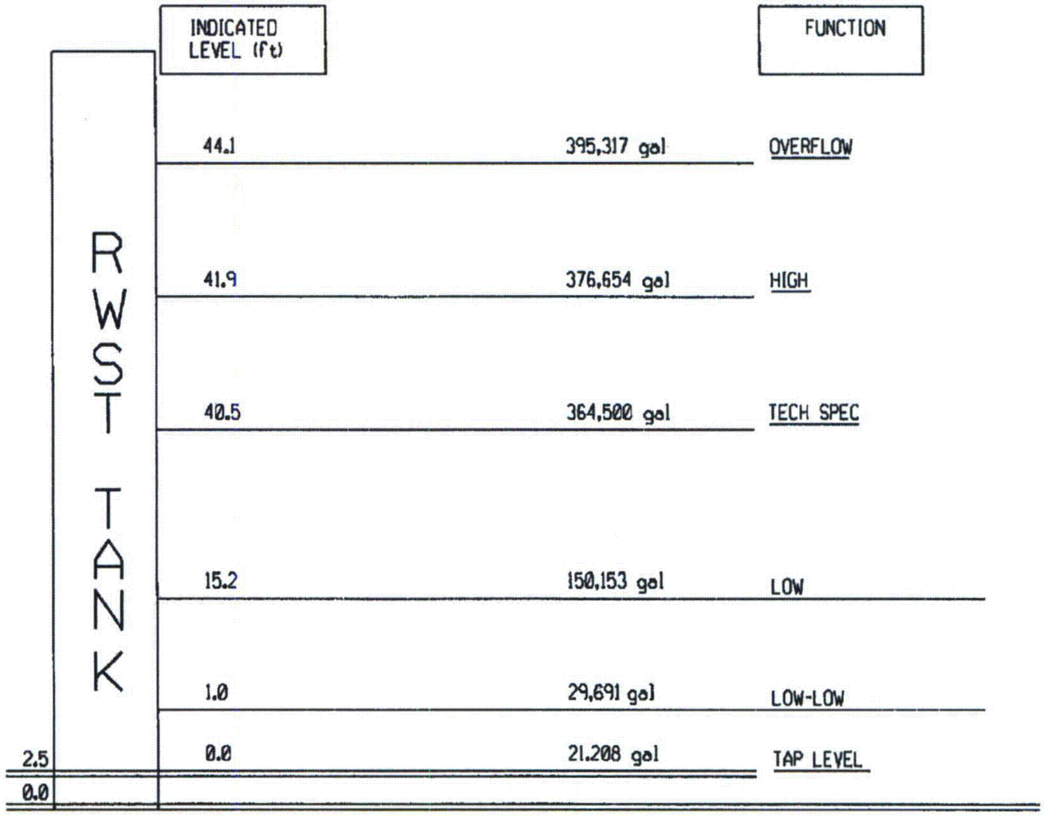

Figure 3g.5-1: Salem Unit 1 RWST Setpoints

The above figure shows the Salem Unit 1 RWST setpoints (Reference A.121). The Salem Unit 2 RWST setpoints values are equal to or slightly greater than the Unit 1 values. The values provided below are for Unit 1.

The RWST level instrumentation is used to monitor level during normal and accident conditions. The high level alarm alerts the operator that the high level is reached to avoid overfilling the tank. The low level alarm indicates that there is sufficient volume in containment to allow operators to switch from injection phase to recirculation phase. The low-low level alarm indicates that the tank is empty.

An automatic Safety Injection (SI) signal is initiated via the Engineered Safety Features (ESF) System when any of the following occur: 1) low pressurizer pressure, 2) high containment pressure, 3) high steam line differential pressure between any two steam generators, 4) high steam line flow in two of four lines coincident with either low T_{avg} or low steam line pressure, and 5) manual actuation.

The SI signal starts the Centrifugal Charging pumps, the Safety Injection (SI) Pumps, and the Residual Heat Removal (RHR) Pumps. These pumps inject to the RCS cold legs, taking suction from the RWST. The initial injection of borated water from the RWST to the RCS is referred to as the ECCS injection phase. The Containment Spray (CS) pumps start automatically when containment pressure reaches the initiation setpoint. The CS pumps take suction from the RWST through a different line than the ECCS suction and discharge to the containment ring header.

The RWST level is monitored by two separate level transmitters during normal and post-accident conditions. Additionally, alarms are provided for "RWST high", "RWST low", and "RWST low-low" water level. The low level alarm setpoint is set high enough to ensure a sufficient volume is available to allow operators the time to switch from injection to recirculation phase before level decreases to the low-low level setpoint. The level setpoints are established considering instrument uncertainty.

When the RWST level reaches its low-level alarm at 15.2 feet, procedural guidance directs operators to initiate switchover to the recirculation phase. One of the first steps the operator needs to verify is that adequate sump level exists (>62%) for transfer to recirculation operation. There are two level switches in each unit that provide control room indication when the containment flood level is greater than 62% which is equivalent to Elevation 80 feet 11 inches which is the minimum required indicated level for transfer to recirculation (Reference A.21).

Due to design differences between Salem Unit 1 and Salem Unit 2 there is a slightly different strategy for system swap over to recirculation operation.

For Unit 1, once adequate sump inventory has been verified for the swap over to the recirculation phase, the following actions are taken: The operators will stop the RHR pumps and manually reconfigure the pump suctions from the RWST to the recirculation sump. After the manual realignment of the pump suction is completed, the RHR pumps are restarted in accordance with the EOPs and recirculate the containment sump water to the RCS cold legs and provide suction to the Charging and SI pumps. One RHR pump also provides recirculation containment spray flow to one ring header. This alignment is referred to as cold leg recirculation.

The Unit 2 procedure is similar to Unit 1. Once RWST low level alarm is reached and the required containment flood level is verified, operators arm a semi-automatic swap over system. This semi-automatic swap over system realigns the RHR pump suctions from the RWST to the recirculation sump. The RHR pumps run continuously during the swap over and are not stopped (unlike Unit 1). The remainder of the transition process is similar to that of Salem Unit 1 and controlled by emergency operating procedures.

For both Salem Units, continuing with the establishment of cold leg recirculation, a single containment spray pump remains in service with its suction aligned to the RWST until a low-low level alarm is received. The containment spray pump is then stopped. This is the point at which maximum available inventory from the RWST has been transferred to containment (not accounting for any manual makeup initiated by the operating crew). Approximately 120,000 gallons of additional inventory is injected into containment from the time of receiving the low-level alarm until the low-low level alarm is received.

The cold leg recirculation occurs for approximately 14 hours for Unit 1 and 6.5 hours for Unit 2. Upon completion of the cold leg recirculation, EOPs will guide the operators into transitioning to hot leg recirculation. In hot leg recirculation the discharge of SI pumps is realigned from the RCS cold legs to the RCS hot legs to suppress any residual boiling and dissolve boric acid that may have deposited at the core outlet.

If the RWST reaches the low level (15.2 feet level above the level tap) and the required containment flood level is not reached, then the operator continues to drawdown from the RWST until either the required containment flood level (80 feet 11 inches) is reached or the RWST low-low water level alarm is reached. During this period, the control room operator uses various combinations of ECCS pumps in accordance with EOPs. However, all the operating ECCS and CS pumps taking suction from the RWST are stopped when the RWST reaches the low-low alarm level.

At Salem, the plant operators are trained to complete switchover from injection phase to recirculation phase within the minimum time available from RWST low level to low-low level. This condition is based on maximum flow of the ECCS pumps in a maximum safeguard scenario. The pump configuration, flow rates, and minimum time to low-low level are discussed in VTD 323585 for Unit 1 (Reference A.105) and VTD 323001 for Unit 2 (Reference A.106).

During a postulated LOCA, operators at Salem use several Emergency Operating Procedures (EOPs) during various phases of LOCA. Following is a brief description of the EOPs that could be entered if the RWST gets depleted and the minimum containment flood level is not achieved.

- Per EOP-LOCA-1 (Loss of Reactor Coolant, References A.107 and A.108) flow from the RWST continues until the RWST low level alarm is reached which corresponds to RWST level of 15.2 feet.
- When the RWST low level alarm is reached, EOP-LOCA-3 (Transfer to Cold Leg Recirculation, References A.109 and A.110) is entered. One of the first steps in this EOP is to verify that adequate sump level exists (80 feet 11 inches) for transfer to recirculation operation. If adequate water level exists then switchover to recirculation operation is initiated.
- If inadequate water level exists for recirculation operation, then EOP-LOCA-5 (Loss of Emergency Recirculation, References A.111 and A.112) is entered. Under this EOP, the ECCS injection from the RWST continues until either the required containment flood level (80 feet 11 inches) is reached or the RWST low-low water level alarm is reached (i.e. pumps are not stopped when RWST low level is reached).
- Under EOP-LOCA-5, if the RWST level reaches the low-low level alarm setpoint and the required containment flood level is not reached, then all the operating ECCS and CS pumps that take suction from RWST are stopped.
- EOP-LOCA-5 provides various steps that would add makeup to the RWST to extend its time available as a viable suction source and to minimize the RWST outflow, thereby extending the time core cooling can be provided by the RWST. One of the alternate suction sources would be providing borated water from the Reactor Makeup Water Control System by taking suction from the Boric Acid Storage Tank mixed with the water from Primary Water Storage Tank and using the centrifugal charging pumps and normal charging lines to inject water into the RCS.

The above describes the response of the ECCS system to a Large Break LOCA (LBLOCA).

The difference between a LBLOCA and a Small Break LOCA (SBLOCA) is the size of the break. The drain down time for the RWST is extended for the SBLOCA since the RCS pressure remains above the RHR pump shutoff head.

The SBLOCA scenario is controlled by EOP-LOCA-2 (References A.114 and A.115). Depending on the size of the break, the RCS may stabilize at a pressure value where RHR may not inject into the RCS. The break size is such that the CS system will not be required. For a SBLOCA, the outflow from the RWST may be low enough that the plant may be stabilized before the need to transition to the recirculation phase. The small break LOCA with elevated RCS pressure is not limiting in terms of RWST drain down times. Finally, SBLOCA produces a fraction of the debris generated by a LBLOCA.

3g.6) Describe the operational status for each ECCS and CSS pump before and after the initiation of recirculation.

Addressed in section 3g.5.

3g.7) Describe the single failure assumptions relevant to pump operation and sump performance.

The Salem ECCS per UFSAR Section 6.3.1.4 is designed to tolerate a single active failure during the short-term immediately following an accident (injection phase) or to tolerate a single active or passive failure during the long-term (recirculation phase) following an accident (Reference A.21).

The Salem EOPs are constructed to account for these potential single failures. EOPs provide guidance for events dealing from the total loss of off-site power to a single active or passive failure of an ECCS component in conjunction with the loss of off-site power. The containment sump strainer screens are designed and analyzed to remain operational during a design basis LOCA.

The RHR pumps stop taking suction from the RWST once the RWST low level, which corresponds to an RWST level of 15.2 feet, is reached provided the required containment level is reached. This condition ensures that there is adequate strainer submergence.

RHR pump operation at the RWST low-low level setpoint, which corresponds to an RWST level of 1.0 feet, is a very unlikely scenario. During a LOCA, water from the RWST will be directed into the RCS through the ECCS pumps to provide core cooling or sprayed into containment for containment heat removal and pressure control. The water pumped from the RWST will collect on the containment floor and mix with that discharged from the postulated large break in the RCS piping raising the containment flood level.

The RWST could reach the low-low alarm level coincident with the containment sump level indication (in control room) not meeting the minimum required level for transfer to recirculation if a RWST pipe break occurs outside the Reactor Containment or containment flood level indication malfunctions.

The first possibility requires a break in the RCS pressure boundary and another break in the RWST piping outside the Reactor Containment during the injection phase. This is not a credible accident; assuming two simultaneous breaks is outside the Salem design and licensing basis per single failure criteria.

There are two redundant level switches installed inside the Reactor Containment. In addition to the level switches there are two separate level transmitters that provide the containment flood level. Therefore, simultaneous failure of two redundant level switches is outside the design and licensing basis of Salem Units.

3g.8) Describe how the containment sump water level is determined.

A minimum containment flood level was determined based on an accounting of available water sources and subtracting entrapped water not available for containment flooding (Reference A.21). The water sources and water entrapped are determined on a mass basis and then converted to volume based on the density of the sump water. The flood level is the net water volume available for flooding divided by the net floor area.

The minimum water level was determined by accounting for entrapped water in the following locations:

- Reactor Cavity and Reactor Coolant Drain Tank Pit – Water enters this area either from flowing over the 9 inch curb that surrounds the openings on 81 feet Elevation or from containment spray falling through the annular space around the reactor. Flow through the annular space is assumed to be equal to the percentage of the containment spray falling on the control rod drive missile barrier.
- Sumps, Trenches and Piping – The containment sump, elevator pit, outer annulus trench, 16 inch drain piping and 12 inch drain piping are all conservatively assumed to be filled before ECCS switchover.
- Containment Air Space – A maximum containment net free volume is assumed to maximize the water vapor entrapped in the containment atmosphere following a LOCA and, therefore, minimizes the water available for flooding of the containment floor.
- Refueling Cavity – Using plant drawings, the refueling cavity area and containment area are conservatively estimated to determine the portion of containment spray water that is entrapped in the refueling cavity.
- Condensation – A maximum heat sink surface area is assumed to maximize the water entrapped due to the condensation layer and therefore minimizes the water available for flooding of the containment floor. The heat sink surface temperature is conservatively assumed to be equal to the initial containment temperature throughout the transient.
- RCS Reflood – The maximum RCS volumes at full reactor power are assumed during reflooding. An RCS temperature of 100°F is assumed for the liquid reflooding and a minimum containment pressure is assumed for

the vapor reflooding of the RCS. This is conservative, because it maximizes the mass of water entrapped in the RCS reflood and therefore minimizes the water available for flooding of the containment floor.
- Spray Water Droplets in the Containment Atmosphere – The analysis utilizes the terminal velocities of droplets and the falling distance from the highest spray ring elevation to the containment floor.
- Containment Spray Piping – Volume of CS piping filled during injection phase of LOCA.

To minimize the flood level, making the NPSH calculation conservative, the following minimum water sources were used:

- The minimum RWST water volume available for switchover to recirculation was determined based on the difference between the minimum level allowed by the Technical Specifications (TS) and the Low Level Alarm setpoint (207,800 gal for Salem Unit 1 and 204,500 gal for Salem Unit 2).
- The minimum RCS volume at full reactor power is 12,020 ft^3 for Unit 1 and Unit 2.
- The minimum volume of one accumulator is 6,223 gallons for both Unit 1 and Unit 2, resulting in a total accumulator volume of 24,892 gallons for all four accumulators per unit.
- The minimum net vapor available in the containment air space at the start of the LOCA is 2571 lbm or 2,619,849 ft^3.
- The Spray Additive Tank (SAT) is not considered to contribute to the water available for flooding.

The minimum flood level calculation evaluated two cases to verify the required flood level at the time of ECCS switchover is met. Both cases assume that a break occurs in the immediate vicinity of the Reactor Cavity opening on 81 feet Elevation, with the cavity filling prior to water flowing to the containment annulus, where it is available for recirculation operation.

Case 1 considers a break large enough to allow RCS blowdown but not large enough to allow the total ECCS flow to drain from the break (i.e., the ECCS pumps are able to keep the entire RCS full). For Case 2, the break considered is large enough to allow complete blowdown of the RCS and partially refill the RCS from the RWST (i.e., the ECCS injection flow drains from the break as fast as the ECCS pumps inject).

These two cases are considered to be the bounding cases for determining the minimum containment water level at the time the RWST reaches its low level alarm point. Initial filling of the reactor cavity is conservative because it limits the amount of water available to flood the containment floor, which is then available for recirculation operation.

If the required minimum water level elevation can be met under this condition, the required minimum containment flood level for recirculation operation will be met under all other conditions. This is because the reactor cavity cannot begin to fill until the flood level exceeds the cavity curb elevation of 81 feet 9 inches which is in excess of the minimum water level required for recirculation operation. Flooding to the containment at this elevation exceeds the required elevation at ECCS switchover; therefore, there is no need to consider cases with weir flow into the pit.

The calculated minimum containment flood level at the time the RWST reaches its low level alarm point is greater than the required water level of 80 feet 10 inches for adequate strainer submergence and ECCS recirculation operation, except for Case 1. For the Case 1 scenario, EOPs are currently in place to address this situation (Section 8.1 of Reference A.21).

Based on these EOPs, if adequate water level does not exist for switching to recirculation operation at the time the RWST reaches it low level alarm, then injection from the RWST will continue until the RWST low-low level set point is reached. The calculation confirmed that the minimum containment flood level required for ECCS recirculation operation 80 feet 10 inches is reached prior to the RWST reaching its low-low level alarm point. Therefore, for the purposes of the NPSH calculation, the flood level was revised to 80 feet 10 inches for the cold leg recirculation mode (Section 8.1 of Reference A.21).

An evaluation was also performed to determine the containment flood level if the RCS pressure does not drop low enough to actuate injection from the accumulators. The minimum containment flood level analysis was modified such that injection from the accumulators was not credited. Per Technical Specification 3.5.1 the accumulator contained volume is between 6223 gallons and 6500 gallons. Therefore, the evaluation conservatively used 6500 gallons of water per accumulator with a total volume of 26,000 gallons.

The containment flood level without crediting the accumulators is determined below for Salem Unit 1. Since the differences between the two units are very small, this evaluation is also applicable to Salem Unit 2. The information provided below is from Reference A.21 unless otherwise noted.

RWST volume to reach containment flood level of 80 feet 11 inches = 264,380 gallons

Volume in each accumulator = 6500 gallons (Reference A.10)
Water in four accumulators = 26,000 gallons

Based on the minimum flood level calculation, injected volume at RWST low level alarm (with accumulator injection) = 207,800 gallons

For conservatism, the RCS inventory is neglected and 207,800 gallons are assumed on the floor at the RWST low level.

Containment flood volume at RWST low level alarm (without accumulator injection) = 207,800 -26,000 = 181,800 gallons

Water volume between Elevation 80 feet 11 inches and RWST low level alarm = 264,380 – 181,800 = 82,580 gallons

RWST low level alarm location from the RWST level tap = 15.2 feet (note, the level tap is the location from where the RWST level is measured and is used for the control room alarms)

RWST volume per foot = 8483.2 gallons/feet
RWST low-low level alarm above level tap = 1 foot

Calculated water level in feet below low level alarm = 82,580/8483.2 = 9.8 feet
RWST level above level tap = 15.2 – 9.8 = 5.4 feet
RWST level above low-low level alarm = 5.4 – 1.0 = 4.4 feet

Based on the above evaluation, the minimum containment flood level will not be reached when the RWST low level alarm is reached. Per the EOPs, the operators would continue to draw down the RWST until the required containment flood level is reached. This evaluation shows that the minimum containment flood level will be reached prior to reaching the RWST low-low level alarm with a margin of 4.4 feet of RWST level even with not crediting the accumulators discharging into the containment floor. Therefore, there is no concern with adequate submergence even if the inventory from all of the accumulators is not credited.

3g.9) Provide assumptions that are included in the analysis to ensure a minimum (conservative) water level is used in determining NPSH margin.

Addressed under response 3g.8 above.

3g.10) Describe whether and how the following volumes have been accounted for in pool level calculations: empty spray pipe, water droplets,

condensation and holdup on horizontal and vertical surfaces. If any are not accounted for, explain why.

All items have been accounted for as described in response 3g.8 above.

3g.11) Provide assumptions (and their bases) as to what equipment will displace water resulting in higher pool level.

The minimum flood level calculation conservatively did not include the volume of equipment in containment that would displace water, as this would increase the water level. However, the volume of equipment is accounted for in a separate calculation to determine the maximum water level in containment (Reference A.10).

3g.12) Provide assumptions (and their bases) as to what water sources provide pool volume and how much volume is from each source.

Addressed under response 3g.8 above.

3g.13) If credit is taken for containment accident pressure in determining available NPSH, provide description of the calculation of containment accident pressure used in determining the available NPSH.

Containment accident pressure is not credited in determining the available NPSH. However, the pre-accident partial pressure of air in containment is credited in determining the available NPSH for sump temperatures where the vapor pressure of sump water is less than the partial pressure of air in containment during normal operation. The approach in which the pre-accident air pressure is credited in determining the available NPSH is described in detail in the methodology section of Calculation S-C-RHR-MDC-1711 (Reference A.41).

This approach constituted a change to the Salem licensing basis. Therefore, PSEG submitted LAR S07-05 (Reference A.8) to the NRC, which was approved by the NRC on November 15, 2007 (Reference A.9). The approval was documented in Amendments 285 and 268 for Salem Unit 1 and 2, respectively (Reference A.9).

The pre-accident air pressure in containment is determined in Calculation S-C-CAN-MDC-2144 (Reference A.3). This calculation computes the minimum partial pressure of air in containment, which could exist prior to an accident. To conservatively minimize the partial pressure of air, the Technical Specification minimum normal operating containment total pressure –1.5 psig (air plus water vapor) is used as an input. Instrument uncertainty is also accounted for.

The relative humidity is assumed to be 100% and the containment is assumed to be at its TS maximum normal operating temperature (120°F) to maximize the contribution of the water vapor partial pressure to the total pressure.
Once the partial pressure of air is determined using these assumptions, it is further reduced by assuming that the air is cooled to the minimum containment temperature (60°F) during normal operating conditions. The use of these assumptions results in a conservative pre-accident partial pressure of air for use in the NPSH analysis.

The minimum partial pressure of air in containment during normal operation is 10.1 psia for Salem Unit 1 and 10.18 psia for Salem Unit 2. The pre-accident air pressure is credited for NPSH determination for sump water temperatures less than 193.7°F for Salem Unit 1 and less than 194.1°F for Salem Unit 2. At these temperatures the pre-accident air pressure is equal to the sump water vapor pressure for the corresponding Unit.

3g.14) Provide assumptions made which minimize the containment accident pressure and maximize the sump water temperature.

Containment accident pressure is not credited in determining the available NPSH. However, the following assumptions were used to minimize the pre-accident partial pressure of air in containment in the determination of available NPSH. These assumptions are documented in Calculation S-C-CAN-MDC-2144 (Reference A.3) and are provided in Section 3g.13.

- The containment temperature is assumed to be at the maximum value, 120°F, allowed by the TS.
- The relative humidity in the containment is assumed to be 100%.
- The containment pressure is reduced by assuming that the containment temperature reduces from its maximum value to the minimum temperature, 60 °F.
- Initial containment pressure is reduced to account for instrument uncertainty.

The following assumptions were used for maximizing sump water temperature. These assumptions are documented in WCAP-16503-NP, Rev. 3 (Reference A.5).

- The ultimate heat sink temperature was assumed to be at its maximum value for the duration of the event.
- One RHR and one CCW heat exchanger were used, representing a loss of a safeguard train.

- RWST water temperature was assumed to be maximum, 100°F.

Revision 3 of Westinghouse Calculation WCAP-16503-NP contains the sump water temperature profiles to be used for Salem Unit 1 and 2. The Double Ended Pump Suction (DEPS) minimum safeguards LOCA scenario for Salem Unit 2 Replacement Steam Generators yields the harshest long-term temperature and pressure transients. For this case, the maximum sump temperature is 264°F at 1500 seconds, which is before recirculation begins at 1748 seconds.

At the onset of recirculation, the maximum sump temperature is 258°F. Therefore, for conservatism, the sump screen was designed to an upper limit hydraulic design temperature of 260°F, and was designed to withstand sump water temperatures up to 264 °F.

Containment accident pressure is not credited in determining the available NPSH. However, the pre-accident partial pressure of air is utilized in determining the available NPSH. See the preceding response (3g.13) for the assumptions used in the determination of the pre-accident air pressure in containment.

The NPSH available is computed as a function of sump water temperature, not as a function of time. However, to determine the NPSH available at a specific time post-LOCA, the post-LOCA sump water temperature profiles provided in WCAP-16503-NP (Reference A.5) are used.

The analyses in WCAP-16503-NP (Reference A.5) are performed using assumptions which maximize the global containment pressure and temperature response to design-basis mass and energy release events.

The sump water temperature responses for all Unit 1 and Unit 2 scenarios modeled in WCAP-16503-NP (Reference A.5) were compared and the most limiting scenario (highest sump water temperature) was determined to be Salem Unit 2 RSG and a DEPS break with minimum safeguards and no recirculation containment spray. The sump water temperature profile is provided in Figure A.6.3-6 of WCAP-16503-NP and is repeated in the response to Item 3o.1.3d(i).

3g.15) Specify whether the containment accident pressure is set at the vapor pressure corresponding to the sump liquid temperature.

For determining the NPSHa in the NPSH calculation, the assumption that the containment pressure is equal to the vapor pressure of the sump fluid was overly conservative. PSEG requested and the NRC approved the change request (Amendment Nos. 285 and 268, Reference A.9) to the methodology that allows the use of the minimum partial pressure of air in the containment atmosphere prior to a LOCA in determining the NPSHa.

The containment accident pressure is set equal to the sump water vapor pressure for sump water temperatures greater than 193.7°F for Salem Unit 1 and greater than 194.1°F for Salem Unit 2, where the vapor pressure of water in the sump is greater than the partial pressure of air (Reference A.41). Below this sump water temperature, the pre-accident partial pressure of air and the sump water vapor pressure are both included in the determination of NPSH available.

3g.16) Provide the NPSH margin results for pumps taking suction from the sump in recirculation mode.

Based on the information above, the results from the NPSH calculation (Reference A.41) are shown in Table 3g-3. The smallest NPSH margin for any of the cases is 1.1 feet of water. This case is Salem Unit 2 with hot leg recirculation and single pump operation. The results show that sufficient NPSH available exists for the RHR pumps even when considering the impact of any potential air evolution as the sump fluid passes through the debris bed/strainer.

The void fraction (α_p) at the pump inlet in per cent by volume was used to compute a β multiplier for the NPSH required in accordance with Appendix A of Regulatory Guide 1.82, Revision 3 (e.g. $NPSH_{required,adjusted}$ for α_p<2% = $NPSH_{required}$ x β where β = 1+0.50*α_p) (Reference 4). The maximum void fraction for all cases is less than 0.6%, while the maximum void fraction for the limiting margin cases is 0.1% (Reference A.104).

Salem Nuclear Generating Station Units 1 and 2
Docket Nos. 50-272 and 50-311
Generic Letter 2004-02
Updated Supplemental Response for Salem

Table 3g-3: NPSH Results

Mode	Flow Rate (gpm)	Strainer Head Loss (ft)	NPSHa (ft)	NPSHr (ft)	α_p at Minimum Limiting Margin (%)	NPSHr Adjusted (ft)	NPSH Margin (ft)	Structural Margin[3] (ft)	Limiting Margin (ft)
Cold Leg Recirculation (Note 1)									
U1 –One Pump	5110	1.31	26.6	25.0	0.0006	25.01	1.6	15.6	1.6
U2 –One Pump	4900	3.69	24.8	22.8	0.0301	23.14	1.6	13.3	1.6
U1 –Two Pump	4425	3.44	26.0	18.8	0.0263	19.05	7.0	13.5	7.0
U2 –Two Pump	4425	7.91	21.6	18.8	0.1090	19.82	1.7	9.0	1.7
Containment Spray Recirculation (Note 2)									
U1 –One Pump	4850	1.31	28.1	22.0	0.0006	22.01	6.1	15.6	6.1
U2 –One Pump	4850	3.69	25.7	22.0	0.0300	22.33	3.4	13.3	3.4
U1 –Two Pump	4563	3.44	26.6	19.8	0.0263	20.06	6.5	13.5	6.5
U2 –Two Pump	4563	7.91	22.1	19.8	0.1093	20.88	1.2	9.0	1.2
Hot Leg Recirculation (Note 1)									
U1 –One Pump	4980	1.31	27.8	24.0	0.0006	24.01	3.8	15.6	3.8
U2 –One Pump	4980	3.69	25.4	24.0	0.0301	24.36	1.1	13.3	1.1
U1 –Two Pump	4425	3.44	26.9	18.8	0.0263	19.05	7.8	13.5	7.8
U2 –Two Pump	4425	7.91	22.4	18.8	0.1093	19.82	2.6	9.0	2.6

* Values based on spreadsheet computations are rounded.

(1) The maximum flow through a single pump during two pump operation is 4425 gpm for cold leg and hot leg recirculation. The total flow through the strainer is 8850 gpm.

(2) The maximum flow through a single pump during two pump operation is 4563 gpm for containment spray recirculation. The total flow through the strainer is 8850 gpm.

(3) The structural margin is computed based on the strainer head loss and the strainer structural limit of 16.94 feet.

Plots of NPSH margin, structural margin and limiting margin are shown on the following pages. The limiting cases for Unit 1 and Unit 2 with one or two pump modes of operation are shown. For single pump operation, the limiting margin occurs during cold leg recirculation (Figures 1-3) while for Unit 2 the limiting margin occurs during hot leg recirculation (Figures 4-6). For two pump operation, the limiting margin for Units 1 (Figures 7-9) and 2 (Figures 10-12) occurs during containment spray recirculation. For each limiting configuration three figures are shown. First, the NPSH margin is shown for each of the cases. Second, the structural margin for the strainer is shown. Third, the limiting margin is shown.

The NPSH margin is shown for each limiting configuration in Figures 1, 4, 7, and 10. Each figure has three sump temperature dependent plots. First the NPSHa is shown. The NPSHa is calculated two different ways. For low sump temperatures, where the vapor pressure of water is less than the initial partial pressure of air, the NPSHa is calculated using Equation 3g.16-1. For high sump temperatures, where the vapor pressure of water is greater than the initial partial pressure of air, the NPSHa is calculated using Equation 3g.16-2 (Reference A.41). The temperature that is the cutoff for using Equation 3g.16-2 instead of 3g.16-1 is 193.7°F for Unit 1 and 194.1°F for Unit 2. Note: see Section 3g.13 of this response for more discussion on the determination of the initial partial pressure of air.

$NPSHa = h_{air} - h_{vp} + h_{st} - h_f$ Equation 3g.16-1

$NPSHa = h_{st} - h_f$ Equation 3g.16-2

Where (See Reference A.41 for more explanation of these parameters):

- h_{air} Minimum partial pressure of air during normal conditions (ft)
- h_{vp} Vapor pressure of water at the given sump temperature (ft)
- h_{st} Static head of water above the pump (ft)
- h_f Friction and form losses in suction piping and strainers (ft)

Second the NPSHr is shown. The NPSHr for the RHR pumps includes the impact of void fraction at the pump inlet and is also taken from the NPSH calculation (Reference A.41). Lastly, the NPSH margin is shown. The NPSH margin is the difference between the NPSHa and the NPSHr.

The structural margin is shown for each limiting configuration in Figures 2, 5, 8, and 11. Each figure has three sump temperature dependent plots. First the structural limit is shown. The structural limit is 16.94 feet of water, per the Strainer Head Loss Calculation (Reference A.77). Second the strainer head loss is shown. The strainer head loss is presented in the Strainer Head Loss Calculation (Reference A.77), and is summarized in Attachment 10.6 of the NPSH calculation

Salem Nuclear Generating Station Units 1 and 2
Docket Nos. 50-272 and 50-311
Generic Letter 2004-02
Updated Supplemental Response for Salem

(Reference A.41). The data show that the strainer head loss is constant for sump temperatures less than 160°F, where chemical precipitates may form (see Section 3o.1.21d(i) of this response), and is temperature dependent at higher sump temperatures. Details of the determination of the strainer head loss are provided in Section 3f.10 of this response. Lastly, the structural margin is shown. The structural margin is the difference between the structural limit and the strainer head loss.

The limiting margin is shown in Figures 3, 6, 9, and 12. The limiting margin is the lesser of the NPSH margin and the structural margin at each temperature. Each figure shows the NPSH margin and the structural margin and highlights the limiting margin.

Figure 1: NPSH Available and Margin
Unit 1 Cold Leg Recirculation - Single Pump Operation